



รายงานวิจัยฉบับสมบูรณ์

โครงการ การสังเคราะห์และการประเมินฤทธิ์ทางชีวภาพของสารในกลุ่มลาเมตลารินและ
อนุพันธ์ที่มีการปรับเปลี่ยนทางโครงสร้าง

โดย ดร. พูนศักดิ์ พลอยประดิษฐ์ สถาบันวิจัยจุฬาภรณ์

สนับสนุนโดยสำนักงานกองทุนสนับสนุนการวิจัย

(งานวิจัยยังไม่เสร็จสมบูรณ์ โปรดอย่านำไปอ้างอิง)

15 สิงหาคม 2554

รายงานวิจัยฉบับสมบูรณ์

โครงการ การสังเคราะห์และการประเมินฤทธิ์ทางชีวภาพของสารในกลุ่มลาเมตลาโรนและ
อนุพันธ์ที่มีการปรับเปลี่ยนทางโครงสร้าง

ดร. พูนศักดิ์ พลอยประดิษฐ์ (หัวหน้าโครงการ) สถาบันวิจัยจุฬาภรณ์

สนับสนุนโดยสำนักงานกองทุนสนับสนุนการวิจัย

(ความเห็นในรายงานนี้เป็นของผู้วิจัย สกว. ไม่จำเป็นต้องเห็นด้วยเสมอไป)

Abstract

Some lamellarin analogs with structural modifications have been successfully prepared via the method developed in our laboratory with some modifications for some steps. The resulting analogs provided important information for the establishment of structure-activity relationships (SARs). It was found that the hydroxy groups at C7, C8, and C20 play some critical roles for the anticancer activity while the orthogonal aromatic ring as well as its substituents also play some roles, perhaps less critical, for the overall activity. Through collaborations, the drug likeness of some lamellarin analogs was assessed while quantitative structure-activity relationship (QSAR) of some lamellarins and their anticancer activity against two breast cancer cell lines (hormone-dependent and hormone-independent) was established via comparative molecular field analysis (CoMFA) and comparative molecular similarity index analysis (CoMSIA).

Two complementary methods of generating *ortho*-quinone methides (*o*-QMs) and mediating their [4+2]-cycloaddition reactions to provide the corresponding chromans have been successfully developed using *p*-toluene sulfonic acid immobilized on silica (PTS-Si) or PtCl₄. A relatively wider range of the *o*-QM precursors as well as the olefins could be utilized with the reactions using PtCl₄ although the diastereoselectivity from such reactions was lower than that obtained from those using PTS-Si. In addition, the intermediacy of Pt(IV)-stabilized *o*-QM has been proposed and supported by some spectroscopic means.

บทคัดย่อ

สารอนุพันธ์ในกลุ่มลามลลารินที่มีโครงสร้างแตกต่างไปจากสารผลิตภัณฑ์ธรรมชาติได้ถูกสังเคราะห์ขึ้นจากกระบวนการที่กลุ่มวิจัยได้พัฒนาขึ้น โดยอาจมีการปรับเปลี่ยนรายละเอียดในการดำเนินการสังเคราะห์จากการศึกษาความสัมพันธ์ระหว่างโครงสร้างและฤทธิ์ด้านมะเร็งพบว่าหมู่ไฮดรอกซีที่ตำแหน่ง 7 8 และ 20 มีความสำคัญมาก ในขณะที่ผลจากวงโรมาติกที่ตั้งฉากรวมทั้งหมู่แทนที่อื่นๆบนวงดังกล่าวมีความสำคัญน้อยกว่าแต่ไม่สามารถตัดทิ้งได้ทั้งหมด ทั้งนี้ได้นำผลการศึกษาในเบื้องต้นไปใช้ในการประเมินคุณสมบัติทางยาของสารในกลุ่มนี้โดยได้ทำการวิจัยร่วมกับ ดร.มนทกานต์ จิตต์แจ้ง จากสถาบันวิจัยจุฬาภรณ์ นอกจากนี้ยังได้วิจัยร่วมกับ รศ.ดร.สุภา หารหนองบัว จากมหาวิทยาลัยเกษตรศาสตร์ในการใช้แบบจำลองทางคณิตศาสตร์มาแสดงความสัมพันธ์เชิงโครงสร้างและฤทธิ์ด้านมะเร็งฤทธิ์ของสารในกลุ่มลามลลารินที่มีต่อเซลล์มะเร็งเต้านมสองชนิดคือชนิดที่มีการตอบสนองและชนิดที่ไม่มีการตอบสนองต่อฮอร์โมนเอสโตรเจน โดยใช้ระเบียบวิธีแบบ CoMFA และ CoMSIA

กลุ่มวิจัยยังได้ศึกษาและพัฒนากระบวนการสังเคราะห์สารที่มีโครงสร้างของวงโครแมนเป็นองค์ประกอบหลักโดยมีออร์โธควิโนนเมไธด์เป็นสารมัธยันต์สำคัญ และใช้กรดพาราโทลูอินซัลโฟนิคบนซิลิกา (PTS-Si) หรือแพลตตินัมคลอไรด์เป็นรีเอเจนต์ พบว่าสามารถใช้แพลตตินัมคลอไรด์กับสารตั้งต้น หรือสารพันธะคู่ที่เข้าทำปฏิกิริยาที่มีความหลากหลายทางโครงสร้างมากกว่า ถึงแม้ว่าผลิตภัณฑ์ที่เกิดขึ้นจากปฏิกิริยาที่ใช้แพลตตินัมคลอไรด์จะมีความเฉพาะเจาะจงทางสเตอริโอเคมีที่ลดลงบ้างก็ตาม ทั้งนี้ยังได้ทำการศึกษาเชิงลึกทางด้านกลไกการเกิดปฏิกิริยาที่ใช้แพลตตินัมคลอไรด์เป็นตัวเร่งปฏิกิริยาและพบว่าอาจจะมีสารมัธยันต์ที่มีความเสถียรจากการที่แพลตตินัม(IV)ช่วยเข้าจับกับออร์โธควิโนนเมไธด์ที่เกิดขึ้น

รายงานวิจัยฉบับสมบูรณ์

โครงการ “การสังเคราะห์และการประเมินฤทธิ์ทางชีวภาพของสารในกลุ่มลาเมลลารินและอนุพันธ์ที่มีการปรับเปลี่ยนทางโครงสร้าง”

สรุปผลการดำเนินงาน

ในส่วนของการวิจัยสังเคราะห์สารในกลุ่มลาเมลลารินนั้น ผู้วิจัยได้ศึกษาการประเมินฤทธิ์ทางชีวภาพ โดยเน้นฤทธิ์ต้านมะเร็งและได้ทำการศึกษาค้นคว้าความสัมพันธ์ระหว่างโครงสร้างและฤทธิ์ต้านมะเร็ง พบว่า หมู่ไฮดรอกซี (hydroxy groups) ที่ตำแหน่ง 7 8 และ 20 บนโครงสร้างของลาเมลลารินมีความสำคัญต่อฤทธิ์ต้านมะเร็ง ในขณะที่ผลของหมู่ไฮดรอกซีที่ตำแหน่งอื่นๆ ต่อฤทธิ์ต้านมะเร็งมีความสำคัญน้อยกว่า แต่มีความสำคัญเช่นกัน ทั้งนี้ยังได้ทำการปรับเปลี่ยนโครงสร้างโดยการตัดหมู่เอโรมาติกที่ไม่ได้เป็นส่วนหนึ่งของระบบเพนตะไซคลิกที่เป็นโครงสร้างหลักของลาเมลลาริน และพบว่าฤทธิ์ต้านมะเร็งลดลงอย่างมีนัยสำคัญ

นอกเหนือไปจากงานวิจัยทางด้านลาเมลลารินแล้วผู้วิจัยยังได้ศึกษาและพัฒนากระบวนการสังเคราะห์สารในกลุ่มโครแมน (chroman) ที่มีรายงานเกี่ยวกับฤทธิ์ทางชีวภาพที่น่าสนใจโดยศึกษาการนำสารมัธยันต์ที่มีความว่องไวในการเข้าทำปฏิกิริยาเคมี คือออร์โธควิโนนเมไธด์ (*ortho*-quinone methide) มาทำปฏิกิริยาการปิดวงแบบ [4+2] หรือที่รู้จักกันว่าเป็นแบบ hetero Diels-Alder กับสารประกอบที่มีพันธะคู่บางชนิด ซึ่งกลุ่มวิจัยสามารถประยุกต์ใช้กรดบวัญภาคของแข็ง (ซิลิกา) และเกลือของโลหะบางชนิด เช่นแพลตตินั่มคลอไรด์ ในการเปลี่ยนสารตั้งต้นให้เกิดเป็นออร์โธควิโนนเมไธด์ และในการเกิดปฏิกิริยาการปิดวงดังกล่าวได้อย่างมีประสิทธิภาพ ให้ผลิตภัณฑ์ในปริมาณสูงและมีความเฉพาะเจาะจงทางสเตอริโอเคมีที่ดีมาก นอกจากนี้ยังได้ทำการศึกษาเชิงลึกด้านกลไกของกระบวนการทางเคมีที่เกี่ยวข้องกับการเกิดออร์โธควิโนนเมไธด์ และปฏิกิริยาการปิดวงแบบ [4+2] ภายใต้สภาวะการใช้กรดบวัญซิลิกา และแพลตตินั่มคลอไรด์

โดยรวมกลุ่มงานได้ตีพิมพ์ผลงานวิจัยในวารสารนานาชาติทั้งสิ้น 8 บทความ

- 1) Chemistry, A European Journal (IF = 5.476) จำนวน 1 บทความ*
- 2) Journal of Organic Chemistry (IF = 4.002) จำนวน 1 บทความ*
- 3) Marine Drugs (IF = 3.471) จำนวน 1 บทความ
- 4) ChemMedChem (IF = 3.306) จำนวน 1 บทความ*
- 5) European Journal of Medicinal Chemistry (IF = 3.193) จำนวน 1 บทความ
- 6) Tetrahedron (IF = 3.011) จำนวน 2 บทความ*
- 7) Monatshefte für Chemie (IF = 1.356) จำนวน 1 บทความ

*เป็น corresponding author ของผลงานวิจัยตีพิมพ์นี้ (5 บทความ)

ค่า impact factor (IF) ของปีล่าสุด (2010) ผลงานวิจัยมีผลรวมค่า impact factor ทั้งสิ้น 26.826 (ค่าเฉลี่ย impact factor = 3.353 ต่อ 1 บทความ)

นอกจากนี้ยังได้เสนองานวิจัยในที่ประชุมนานาชาติ 6 ครั้ง และที่ประชุมในประเทศ 2 ครั้ง

Complete Research Report

Synthesis and Biological Evaluations of Structurally-modified Lamellarins and Their Derivatives

Executive Summary

We have investigated the lamellarins and their analogs following the successful development of their convergent syntheses. Structure-activity relationships have been performed to obtain some preliminary data to establish the structural requirements for potent anticancer activity. It was found that the hydroxy groups at C7, C8, and C20 played some key roles in the anticancer activity while those at other positions appeared less critical. However, it was determined from this study that the orthogonal aromatic ring, while carrying less critical oxygenated substituents, was required for optimal anticancer property. Both partial and complete deletion of this ring or its oxygenated substituents resulted in lower anticancer potency of the corresponding analogs.

In addition to the work in the area of lamellarins, we have successfully developed a highly efficient synthesis of the chroman framework via the intermediacy of a highly reactive species, namely the *ortho*-quinone methide (*o*-QM). Acids on solid supports such as silica as well as transition metal salts (e.g. platinum(IV) chloride) were found to be effective in mediating the generation of the *o*-QM and the subsequent [4+2]-cycloaddition reactions with some properly activated olefins. The hetero-Diels-Alder reactions furnished the corresponding chromans in good to excellent yields as well as good to excellent diastereoselectivities. Moreover, detailed mechanistic understanding of the generation of the *o*-QMs and their subsequent cyclization both in the presence of acid on silica and platinum(IV) chloride was also investigated.

Overall, during the grant period of 3 years (2008-2011), this research program produced 8 publications in the peer-reviewed journals as shown below.

- 1) Chemistry, A European Journal (IF = 5.476): 1 article*
- 2) Journal of Organic Chemistry (IF = 4.002): 1 article*
- 3) Marine Drugs (IF = 3.471): 1 article
- 4) ChemMedChem (IF = 3.306): 1 article *
- 5) European Journal of Medicinal Chemistry (IF = 3.193): 1 article
- 6) Tetrahedron (IF = 3.011): 2 articles *
- 7) Monatshefte für Chemie (IF = 1.356): 1 article

*denoting corresponding author for these articles (5 articles)

Latest values of impact factor (IF; 2010) were used. These 8 articles totaled IF values of 26.826, with an average IF of 3.353 per published article.

The research work was also presented internationally 6 times and nationally twice.

เนื้อหางานวิจัย

Introduction

As a continuation of our interest in the lamellarins, we have made a number of analogs aiming to reduce the molecular volume of the resulting compounds since most of the natural lamellarins possess rather high molecular volumes and masses. With established efficient synthesis, a relatively large number of structurally diversified analogs could be made to establish structure-activity relationships, with an emphasis on anticancer property. By applying position-to-position comparisons, the importance of each position can be discerned. A classical “deletion” strategy was anticipated to shed some light on the requirements for good anticancer potency for the lamellarin skeleton.

In addition to the lamellarins which are natural products derived from marine organisms with potent anticancer property, we have been interested in developing some efficient synthetic methods for chromans. The chroman, or benzopyran, is an important core structure in a number of natural compounds exhibiting interesting biological activities including anticancer, antioxidant, anti-inflammatory, antimicrobial, anxiolytic, and myorelaxant properties. With our interest in the use of solid-supported reagents in organic synthesis, we anticipated that some solid-supported acids could be utilized to generate a highly reactive intermediate—the *ortho*-quinone methide (*o*-QM), which, upon reacting with appropriately activated olefins, would furnish the corresponding chroman via the [4+2]-cycloaddition reactions. It was foreseen also that a catalytic process utilizing some metal salts/complexes to mediate both the generation and the cycloaddition reactions would complement the use of solid-supported acids.

Objectives

During the third year of our program, based on the anticancer property of the reported lamellarins against hormone-dependent T47D and hormone-independent MDA-MB-231 breast cancer cell lines, quantitative structure-activity relationship (QSAR) was performed using CoMFA and CoMSIA to generate predictive models for compounds in the lamellarin family. In addition, we continued to study the synthesis of other structurally diverse lamellarin analogs which contained “deleted” moieties around the lamellarin skeleton.

For the chroman synthesis, following our work in both the intermolecular and intramolecular [4+2]-cycloaddition reactions of the *o*-QMs, we have now focused on establishing the scope of this reaction with differently substituted *o*-QM precursors and olefins. In addition, we investigated the use of metal salts/complexes in mediating this reaction. The differences in the reaction profiles of the two processes using either (1) immobilized *p*-toluene sulfonic acid (PTS-Si) or (2) PtCl₄ prompted us to investigate the mechanistic aspects of this reaction.

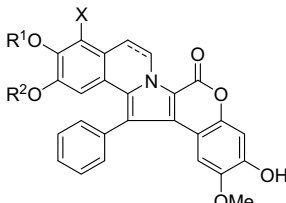
Results and Discussion

Lamellarins

Using our established synthetic methods developed for the lamellarin framework, we have been able to prepare a relatively large number of the lamellarin analogs with different patterns of substituents on the aromatic rings around the pyrroloisoquinoline lactone core. We anticipated that, by using the point-to-point comparison strategy, each pair of the analogs with only one difference could provide some preliminary structure-activity relationships (SARs) which were included in the first year report. Our study has shown that the hydroxy groups at C7, C8, and C20 play some critical roles in the cytotoxicity against cancer cell lines under current investigation. In addition, the lamellarin compounds with unsaturation between C5 and C6 are generally more cytotoxic towards most cancer cell lines.

In contrast to the distinct effects shown by the groups at the positions discussed above, the effects from the substituents on the orthogonal aromatic ring as well as the ring itself have not been clearly delineated. Thus, it was the aim of our research program to prepare analogs with different substitution patterns on the aromatic ring as well as those containing other smaller groups in place of the orthogonal aromatic ring. It was anticipated that, if the orthogonal aromatic ring is not very critical for the cytotoxicity against cancer cell lines, this may serve as a suitable starting point for further modifications to incorporate other groups which may provide desirable pharmacological parameters such as aqueous solubility enhancement. Table 1 and 2 summarize the results of our preparation of these analogs.

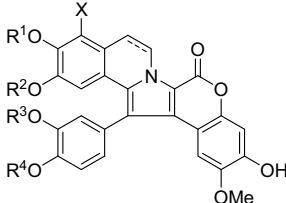
Table 1. Yields (%) of the steps for the preparation of unnatural lamellarin analogs with modified F-rings.



The chemical structure shows a complex polycyclic core consisting of a pyrroloisoquinoline lactone system. It features a benzene ring fused to a pyrrole ring, which is further fused to an isoquinoline ring system. A lactone ring is attached to the isoquinoline core. Various substituents are indicated: X on a benzene ring, R¹O and R²O on another benzene ring, and a hydroxyl group (OH) and a methoxy group (OMe) on a third benzene ring.

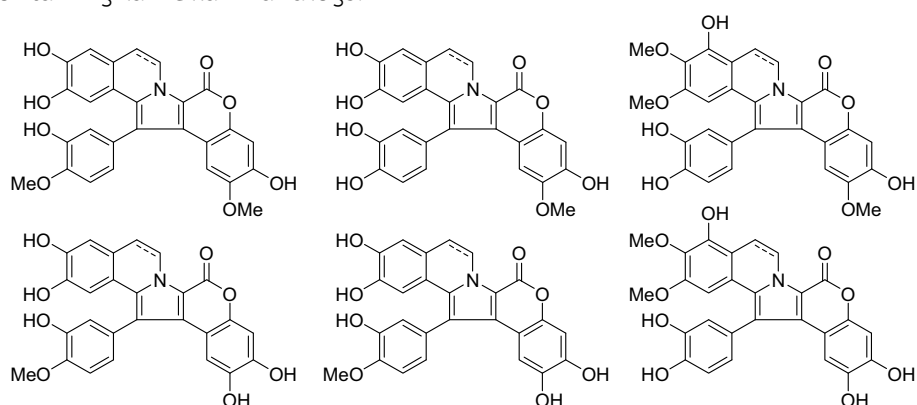
X	R ¹	R ²	Grob	H ₂ /Lactonization	acetylation	DDQ	deacetylation
H	OMe	OMe	79	88	100	100	87
H	OH	OMe	52	62	97	74	65
H	OMe	OH	52	72	80	97	71
OMe	OMe	OMe	67	76	100	100	92

Table 3. Yields (%) of the steps for the preparation of the C13- and C14-modified unnatural lamellarin analogs.



X	R ¹	R ²	R ³	R ⁴	Grob	H ₂ /Lac	acetylation	DDQ	deacetylation
H	OH	OMe	OMe	H	36	79	84	95	95
H	OH	OMe	H	OMe	62	65	99	94	99
H	OH	OMe	OH	H	48	76	99	98	62
H	OH	OMe	H	OH	60	90	90	95	96
OH	OMe	OMe	OMe	H	46	72	100	93	93
OH	OMe	OMe	H	OMe	43	71	100	88	82
OH	OMe	OMe	OH	H	43	81	100	94	85
OH	OMe	OMe	H	OH	67	67	100	96	91

A few members of the catechol-containing lamellarin analogs were also naturally-occurring but their syntheses have not been reported. These analogs, due to their increased number of the hydroxy groups, were expected to possess higher aqueous solubility. With some slight modifications to our current syntheses developed for the lamellarin framework, we were able to prepare some of these catechol-containing analogs albeit in yields in the range (10-60%) lower than those of other analogs. Some problems we have encountered during the syntheses were related to the relatively labile nature of the catechol moiety towards oxidation to the corresponding quinone. Shown below are the structures of the catechol-containing lamellarin analogs.

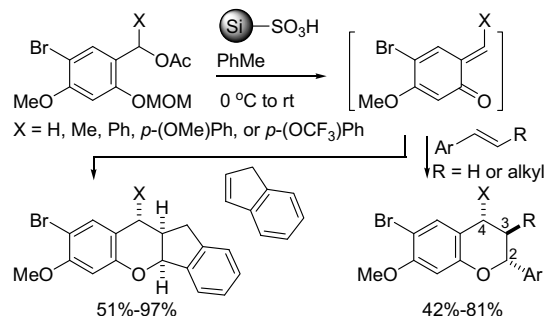


Most recently, through collaboration with Dr. Montakarn Chittchang, we have investigated the drug likeness of the lamellarins. In addition, through collaboration with Associate Professor Supa Hannongbua, we have constructed predictive models by performing correlations between structures and anticancer activity using comparative

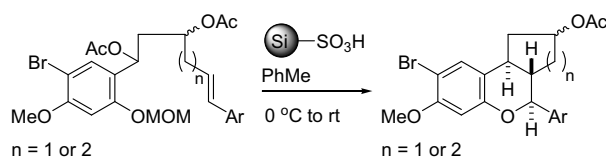
molecular field analysis (CoMFA) and comparative molecular similarity index analysis (CoMSIA) techniques. We have focused on the correlations between 25 lamellarins and their anticancer activity against two types of human breast cancer cell lines (hormone-dependent T47D and hormone-independent MDA-MB-231).

ortho-Quinone methides

Due to the wide array of biological activities of the compounds possessing a chroman core, its efficient synthesis, especially for the 2-arylchroman, would contribute to the progress of the benzopyran field. The chroman can be formed via the [4+2]-cycloaddition reactions of the *ortho*-quinone methide (*o*-QM) with appropriately activated olefins. Our interest in the use of solid-supported acids such as *p*-toluene sulfonic acid immobilized on silica (PTS-Si) in organic synthesis has led us first to explore the use of acids to initiate the generation of *o*-QM from the appropriate precursors as well as mediate the subsequent cycloaddition reactions. The results showed that the use of PTS-Si is superior to the use of other acids for both purposes. The use of PTS-Si allowed for a simple and efficient method to generate *o*-QM under mild conditions (e.g. at 0 °C to room temperature). The conditions were also compatible with a relatively wide range of the properly activated olefins such as styrene derivatives. With a substituent at the benzylic position, the reactions provided the corresponding chroman products in moderate to good yields and moderate to excellent diastereoselectivities between C2 and C4.

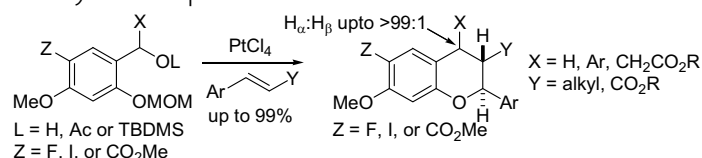


We have also successfully developed similar sequence for the intramolecular generation of the *o*-QM and the subsequent hetero-Diels-Alder reaction using PTS-Si. Such reactions would provide some interesting tricyclic core structures commonly found in a number of natural chroman-containing products. This convergent approach towards the tricyclic structures was efficient and robust for modifications on other moieties of the precursors. Overall, the reactions provided the tricyclic structures in good to excellent yields and good to excellent diastereoselectivities.

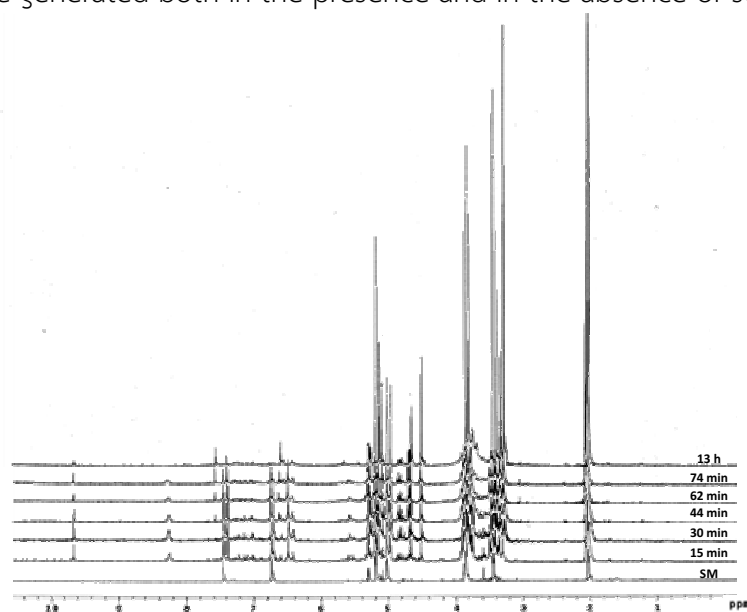


Despite the advantages of employing PTS-Si for the chemistry of *o*-QM, the reactions required equimolar amount of the acid. In addition, the scope of substrates was rather limited as both bromine atom (Br) and a methoxy group were both required at the respective positions on the aromatic ring as shown above. Thus, another method, preferably catalytic, with a wide range of compatibility to the functional groups present either on the *o*-QM precursors or the olefins was desirable.

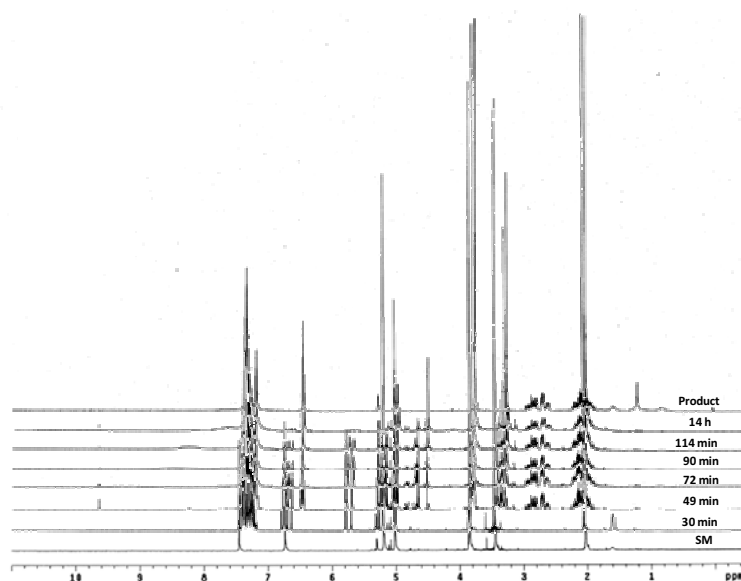
Metal salts/complexes have been utilized in a number of reactions in organic synthesis. The metal centers are known to stabilize some highly reactive intermediates including *o*-QMs. However, it has not been reported whether any of the metals can stabilize a “free” *o*-QM. Through experimentation, it was found that PtCl₄ could effectively and catalytically generate *o*-QMs from a wide range of the *o*-QM precursors as well as mediate the subsequent cycloaddition reactions with a wide range of olefins including the non-styrene compounds. Both intermolecular and intramolecular reactions utilizing PtCl₄ as a catalyst were successfully developed.



Due to the successful development of using catalytic amount of PtCl₄ for both generating the *o*-QM and mediating the [4+2]-cycloaddition reactions, we decided to perform the NMR studies of the reactions using PtCl₄. From the studies, it could be proposed that some transient reactive species were generated, which then reacted with styrene, to generate the corresponding chroman. It should be noted that similar reactive intermediates were generated both in the presence and in the absence of styrene.

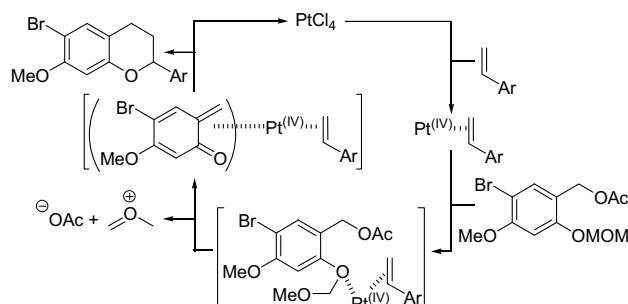


In the absence of styrene



In the presence of styrene

Our experiment provided an evidence of a Pt-stabilized “free” *ortho*-QM species which could still react with styrene to generate the chroman product. A proposed mechanism is shown below.



Knowledge from this part of our research program in the *ortho*-quinone methide chemistry will be useful for the synthesis of other complex natural products containing the chroman core.

Experimental

Detailed experimental procedures can be found for each published article as either a Supporting Information or Supplementary Material.

Research Output (over 3 years: June 2008-July 2011)

1) **Total Impact Factor: 26.826 for 8 articles. Average IF/article: 3.353**

Chemistry, A European Journal (5.476)	1 article
Journal of Organic Chemistry (4.002)	1 article
Marine Drugs (3.471)	1 article
ChemMedChem (3.306)	1 article
European Journal of Medicinal Chemistry (3.193)	1 article
Tetrahedron (3.011)	2 articles
Monatshefte für Chemie (1.356)	1 article

2) **6 International Meetings**

3) **2 Local Meetings**

International Publication

- 1) Radomkit, S.; Sarnpitak, P.; Tummatorn, J.; Batsomboon, P.; Ruchirawat, S.; **Ploypradith, P.** Pt(IV)- and Au(III)-Catalyzed Generation of *o*-Quinone Methides and [4+2]-Cycloaddition Reactions. *Tetrahedron* **2011**, *67*, 3904-3914.
- 2) Thipnate, P.; Chittchang, M.; Thasana, N.; Saparpakorn, P.; **Ploypradith, P.**; Hannongbua, S. Exploring the Molecular Basis for Selective Cytotoxicity of Lamellarins against Human Hormone-dependent T47D and Hormone-independent MDA-MB-231 Breast Cancer Cells. *Monatsh Chem* **2011**, *142*, 97-109.
- 3) Chittchang, C.; Gleeson, M. P.; **Ploypradith, P.**; Ruchirawat, S. Assessing the Drug-likeness of Lamellarins, a Marine Derived Natural Product Class with Diverse Oncological Activities. *Eur. J. Med. Chem.* **2010**, *45*, 2165-2172.
- 4) Tummatorn, J.; Ruchirawat, S.; **Ploypradith, P.** A Convergent General Strategy for the Functionalized 2-Aryl Cycloalkyl-fused Chromans: Intramolecular Hetero Diels—Alder (HDA) Reactions of *ortho*-Quinone Methides (*o*-QMs). *Chem. Eur. J.* **2010**, *16*, 1445-1448.
- 5) Batsomboon, P.; Phakhodee, W.; Ruchirawat, S.; **Ploypradith, P.** Generation of *ortho*-Quinone Methides by *p*-TsOH on Silica and Their Hetero-Diels—Alder Reactions with Styrenes. *J. Org. Chem.* **2009**, *74*, 4009-4012.
- 6) Tangdenpaisal, K.; Sualek, S.; Ruchirawat, S.; **Ploypradith, P.** Factors Affecting Orthogonality in the Deprotection of 2,4-Di-Protected Aromatic Ethers Employing Solid-Supported Acids. *Tetrahedron* **2009**, *65*, 4316-4325.
- 7) Chittchang, M.; Batsomboon, P.; Ruchirawat, S.; **Ploypradith, P.** Cytotoxicities and Structure-Activity Relationships of Natural and Unnatural Lamellarins towards Cancer Cell Lines. *ChemMedChem* **2009**, *4*, 457-465.

- 8) Baunbæk, D.; Trinkler, N.; Ferandin, Y.; Lozach, O.; **Ploypradith, P.**; Ruchirawat, S.; Ishibashi, F.; Iwao, M.; Meijer, L. Anticancer Alkaloid Lamellarins Inhibit Protein Kinases. *Mar. Drugs* **2008**, *6*, 514-527.

International Meetings

- 1) Tummatorn, J.; Batsomboon, P.; Radomkit, S.; Sarnpitak, P.; Ruchirawat, S.; **Ploypradith, P.** Use of Solid-Supported Reagents in Organic Synthesis. Pure and Applied Chemistry Conference 2010 (PACCON 2010), Ubon Ratchathani, Thailand, **2010**.
- 2) Sarnpitak, P.; Radomkit, S.; Batsomboon, P.; Ruchirawat, S.; **Ploypradith, P.** Metal-catalyzed Generations of *ortho*-Quinone Methides and Their Intermolecular Cycloaddition Reactions. 5th International Conference in Cutting-Edge Organic Chemistry in Asia (ICCEOCA-5), Hsinchu, Taiwan, 2010.
- 3) Tummatorn, J.; Radomkit, S.; Sarnpitak, P.; Batsomboon, P.; Ruchirawat, S.; **Ploypradith, P.** Use of Immobilized *p*-TsOH on Silica and Metal Salts/Complexes in the Generations of *ortho*-Quinone Methides and Their Formal [4+2]-Cycloaddition Reactions. Presymposium of the 5th International Conference in Cutting-Edge Organic Chemistry in Asia (ICCEOCA-5), Khaosiang, Taiwan, **2010**.
- 4) **Ploypradith, P.**; Tummatorn, J.; Batsomboon, P.; Radomkit, S.; Ruchirawat, S. *Ortho*-Quinone Methides Generated by *p*-TsOH on Silica and Their [4+2]-Cycloaddition Reactions with Styrenes. 4th International Conference in Cutting-Edge Organic Chemistry in Asia (ICCEOCA-4), Bangkok, Thailand, **2009**.
- 5) **Ploypradith, P.**; Tangdenpaisal, K.; Sualek, S.; Kagan, R. K.; Bertoni, D. R.; Guzman, V.; Ruchirawat, S. Solid-Supported Reagents in the Synthesis of Lamellarins and Deprotection of Aromatic Ethers. 3rd International Conference in Cutting-Edge Organic Chemistry in Asia (ICCEOCA-3), Hangzhou, China, **2008**.
- 6) **Ploypradith, P.** Solid-Supported Acids as Mild and Versatile Reagents for the Deprotection of Aromatic Ethers. Contemporary Organic Synthesis Symposium, UK-Thailand Partners in Science, National Science and Technology Development Agency (NSTDA), Pathumthani, Thailand, **2008**.

Local Meetings

- 1) **Ploypradith, P.** Development of Synthetic Methodology for Chromans via [4+2] Cycloaddition Reactions of *ortho*-Quinone Methides. The 36th Congress on Science and Technology of Thailand (STT 36), Bangkok, **2010**.
- 2) **Ploypradith, P.** Lamellarin Synthesis via Conventional and Solid-supported Reagents. The Science Forum 2008, Chulalongkorn University, Bangkok, **2008**.

Appendix

1) Reprints of research articles

Chemistry, A European Journal	1 article
Journal of Organic Chemistry	1 article
Marine Drugs	1 article
ChemMedChem	1 article
European Journal of Medicinal Chemistry	1 article
Tetrahedron	2 articles
Monatshefte für Chemie	1 article

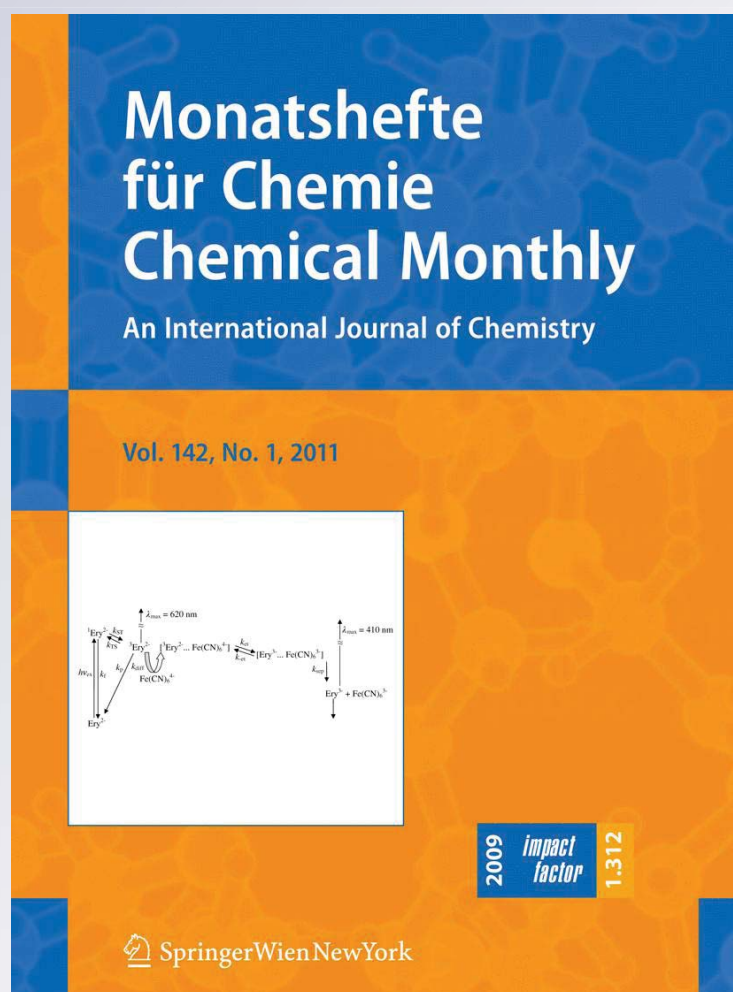
2) First page and abstract of meetings (8 items)

Exploring the molecular basis for selective cytotoxicity of lamellarins against human hormone-dependent T47D and hormone-independent MDA-MB-231 breast cancer cells

**Monatshefte für Chemie -
Chemical Monthly**
An International Journal of
Chemistry

ISSN 0026-9247
Volume 142
Number 1

Monatsh Chem (2010)
142:97-109
DOI 10.1007/s00706-010-0409-
y



Your article is protected by copyright and all rights are held exclusively by Springer-Verlag. This e-offprint is for personal use only and shall not be self-archived in electronic repositories. If you wish to self-archive your work, please use the accepted author's version for posting to your own website or your institution's repository. You may further deposit the accepted author's version on a funder's repository at a funder's request, provided it is not made publicly available until 12 months after publication.

Exploring the molecular basis for selective cytotoxicity of lamellarins against human hormone-dependent T47D and hormone-independent MDA-MB-231 breast cancer cells

Poonsiri Thipnate · Montakarn Chittchang ·
Nopporn Thasana · Patchreenart Saparpakorn ·
Poonsakdi Ploypradith · Supa Hannongbua

Received: 5 May 2010 / Accepted: 7 August 2010 / Published online: 5 November 2010
© Springer-Verlag 2010

Abstract The common structural requirements for cytotoxicity of lamellarins against two human breast cancer cell lines were determined using comparative molecular field analysis (CoMFA) and comparative molecular similarity indices analysis (CoMSIA) techniques. Twenty lamellarins were selected to serve as the training set, whereas another group of six compounds were used as the test set. The best CoMFA and CoMSIA models for both cell lines yielded satisfactory predictive ability with r_{cv}^2 values in the range of 0.659–0.728. Additionally, the contour maps obtained from both the CoMFA and CoMSIA models agreed well with the experimental results and may be used in the design of more potent cytotoxic compounds for human breast cancers. Both analyses not only suggested structural requirements of various substituents around the lamellarin skeleton for their cytotoxic activity against both human breast cancer cell lines but also revealed the molecular basis for the differences between the saturated and unsaturated D-rings of the lamellarins.

Keywords QSAR · CoMFA · CoMSIA · Lamellarins · Human breast cancer · Cytotoxicity

P. Thipnate · P. Saparpakorn · S. Hannongbua (✉)
Department of Chemistry, Faculty of Science, Kasetsart
University (KU), Chatuchak, Bangkok 10900, Thailand
e-mail: fscisph@ku.ac.th

P. Thipnate · P. Saparpakorn · S. Hannongbua
Center of Nanotechnology, Kasetsart University (KU),
Chatuchak, Bangkok 10900, Thailand

M. Chittchang · N. Thasana · P. Ploypradith
Chulabhorn Research Institute and Chulabhorn Graduate
Institute, Vibhavadee-Rangsit Highway, Laksi,
Bangkok 10210, Thailand

Introduction

Lamellarins (Fig. 1) are marine-derived polyaromatic pyrrole alkaloids that have been isolated from different sources, such as ascidians, molluscs, and sponges [1–11]. To date, more than 30 lamellarins have been isolated, many of which exhibit interesting biological activities. For example, lamellarin α 20-sulfate is a potential candidate for human immune-deficiency virus (HIV) treatments as it can inhibit HIV-1 integrase in vitro [12, 13]. On the other hand, nonsulfated lamellarins appear to possess potent cytotoxic activity against cancer cells [14], especially lamellarin D, which has been receiving a lot more attention than all the other compounds in this series. Their cancer cytotoxicity has been attributed to the finding that lamellarin D is an effective stabilizer of human topoisomerase I–DNA covalent complexes, and thus capable of stimulating DNA cleavage [15, 16]. More recently, lamellarin D has also been demonstrated to induce apoptosis as well as to disrupt the inner transmembrane potential of mitochondria, which is a novel pharmacological target for anticancer chemotherapy [17–21]. Additionally, lamellarin D and some other lamellarins have shown potent inhibition of various protein kinases [22]. Nontoxic doses of some lamellarins, especially lamellarin I, can also reverse multidrug resistance (MDR) of cancer cells by inhibiting P-glycoprotein (P-gp)-mediated drug efflux with a 9–16 times higher MDR modulating potency than that of verapamil [23].

Even though lamellarins D, K, and M are usually classified among the most cytotoxic molecules in the lamellarin series, structure–activity relationship studies of lamellarins for their cytotoxicity towards cancer cell lines have exclusively focused on lamellarin D and its derivatives. Generally, lamellarins with a C5–C6 double bond are more

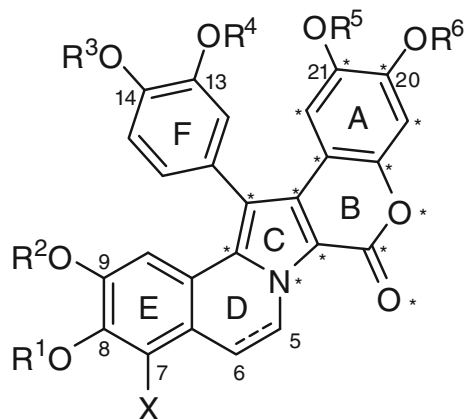


Fig. 1 Core structure of the lamellarins, in which the common atoms used for three-dimensional (3D) quantitative structure–activity relationship (QSAR) matching alignments are denoted by *asterisks*

cytotoxic than those bearing a C5–C6 single bond. However, some exceptions have been observed with lamellarin M, which is roughly equally cytotoxic to its saturated counterpart, lamellarin K, whereas lamellarin M-triacetate is actually much less cytotoxic than its corresponding analogue in the saturated series, lamellarin K-triacetate [23, 24]. For the substituents on the lamellarin core, it appears that the hydroxyl groups at the C8 and C20 positions of lamellarin D are important structural requirements, while the hydroxyl group at C14 and the two methoxy groups at C13 and C21 are not necessary for cytotoxic activity [25, 26]. Employing a systematic approach based on a large number of lamellarins and cancer cell lines, our recent findings not only substantiate the significant contributions of the C5–C6 olefin moiety as well as the hydroxyl groups at C8 and C20, but also demonstrate the importance of the C7 hydroxyl group for the first time [29].

Computational chemistry has been used to verify and explain these experimental findings. Molecular models of the ternary complex formed between topoisomerase I–DNA with a lamellarin D molecule fully intercalating into the DNA duplex have been created using the AutoDock 3.0 docking program and studied using nanosecond molecular dynamics simulations in aqueous solution [15, 26]. The results confirm that the C8 and C20 hydroxyl groups on the lamellarin core are the major determinants of both the topoisomerase I cleavable complex stabilization and the cytotoxic action. In contrast, there is no clear explanation for the functional role of the C5–C6 double bond, which when present in the quinoline D-ring tends to make the compounds more cytotoxic than those having a C5–C6 single bond. In more recent findings, a small number of structurally different lamellarins have been successfully used to generate 3D pharmacophore mapping for the cytotoxicity of lamellarins against human hormone-

dependent T47D breast cancer cell. Four-dimensional (4D) quantitative structure–activity relationship (QSAR) and 3D pharmacophore were built and investigated for this cytotoxicity using only 26 lamellarins [28]. However, no explanation for the difference between C5–C6 double and single bond was found in this work.

In our previous studies, these 26 natural and unnatural lamellarins were synthesized using our published synthetic routes [29] and tested for their cytotoxicity against 11 cancer cell lines [27]. The prominent selectivity observed with certain lamellarins towards human hormone-dependent T47D and hormone-independent MDA-MB-231 breast cancer cells has prompted us to further investigate the possible underlying reasons. With the inclusion of two unnatural compounds (dehydrolamellarins J and Y), a total of ten pairs of lamellarins, each of which only differ in the presence of either a saturated or an unsaturated D-ring (Tables 1, 2), were used to explore their potential differences in steric, electrostatic, hydrophobic, and hydrogen-bond interactions in detail.

The questions addressed in the present study are not only what causes the different cytotoxicity of saturated and unsaturated quinoline D-ring lamellarins, but also why lamellarins show different cytotoxicity in both breast cancer cells. Therefore, 3D-QSAR methods were employed to understand the mechanism of the interactions between ligands and an unknown receptor. In order to use these methods, the physicochemical properties of 26 lamellarin molecules were represented in the form of molecular fields, which could then be effectively correlated with their cytotoxic activity using partial least-squares (PLS) regression analysis [30–32]. Additionally, comparative molecular field analysis (CoMFA) [31] and comparative molecular similarity indices analysis (CoMSIA) [30, 32] techniques were applied to examine the molecular basis for the differences between the lamellarins containing a saturated D-ring and those with a C5–C6 double bond. The common structural requirements for their cytotoxic activity against both human breast cancer cell lines were also determined.

Results and discussion

Twenty-six lamellarins used in this study can be classified into two groups that differ mainly in the nature of the C5–C6 bond in the D-ring. Eleven compounds with a saturated D-ring in Table 1 (excluding lamellarin G and the acetate-containing derivatives) contain exactly the same substituents as their corresponding analogues with a C5–C6 double bond in Table 2, e.g., lamellarins C and B, lamellarins E and X, etc. Most of the compounds used in this study were naturally occurring lamellarins, except the two unnatural

Table 1 Structure and cytotoxic activity of lamellarins with a saturated D-ring

Lamellarin	Substituent group							-log IC_{50}	
	X	OR ¹	OR ²	OR ³	OR ⁴	OR ⁵	OR ⁶	T47D	MDA-MB-231
C	OMe	OMe	OMe	OH	OMe	OMe	OH	5.11	5.08
E	OH	OMe	OMe	OMe	OH	OMe	OH	5.28	5.47
F	OH	OMe	OMe	OMe	OMe	OMe	OH	5.34	5.44
G	H	OH	OMe	OMe	OH	OH	OMe	5.07	4.83
I	OMe	OMe	OMe	OMe	OMe	OMe	OH	5.02	5.07
J	H	OH	OMe	OMe	OMe	OMe	OH	4.89	5.13
K	OH	OMe	OMe	OH	OMe	OMe	OH	7.04	6.40
L	H	OH	OMe	OMe	OH	OMe	OH	5.36	5.75
T	OMe	OMe	OMe	OMe	OH	OMe	OH	4.88	5.06
U	H	OMe	OMe	OMe	OH	OMe	OH	4.99	5.35
Y	H	OMe	OH	OMe	OH	OMe	OH	5.14	4.10
χ	H	OH	OMe	OH	OMe	OMe	OH	5.42	5.32
K triacetate	OAc	OMe	OMe	OAc	OMe	OMe	OAc	5.18	5.33
U diacetate	H	OMe	OMe	OMe	OAc	OMe	OAc	5.10	5.46
χ triacetate	H	OAc	OMe	OAc	OMe	OMe	OAc	5.54	5.18

Table 2 Structure and cytotoxic activity of lamellarins with an unsaturated D-ring

Lamellarin	Substituent group							-log IC_{50}	
	X	OR ¹	OR ²	OR ³	OR ⁴	OR ⁵	OR ⁶	T47D	MDA-MB-231
B	OMe	OMe	OMe	OH	OMe	OMe	OH	6.74	5.35
D	H	OH	OMe	OH	OMe	OMe	OH	10.10	6.40
M	OH	OMe	OMe	OH	OMe	OMe	OH	8.02	6.95
N	H	OH	OMe	OMe	OH	OMe	OH	9.22	6.22
W	OMe	OMe	OMe	OMe	OH	OMe	OH	5.37	5.29
α	H	OMe	OMe	OMe	OH	OMe	OH	6.23	5.41
X	OH	OMe	OMe	OMe	OH	OMe	OH	8.25	7.12
ε	OH	OMe	OMe	OMe	OMe	OMe	OH	8.26	6.59
ζ	OMe	OMe	OMe	OMe	OMe	OMe	OH	7.05	5.33
Dehydrolamellarin J	H	OH	OMe	OMe	OMe	OMe	OH	10.01	6.41
Dehydrolamellarin Y	H	OMe	OH	OMe	OH	OMe	OH	7.10	6.19

dehydrolamellarins J and Y, as well as three acetate-containing derivatives, which were also included in order to investigate the effect of acetylation on the cytotoxic activity of lamellarins. After aligning all lamellarins by using matching alignment, their orientations are represented in Fig. 2. It was shown that the overall planarity of the fused ring system (A through E) could be achieved only in the lamellarins containing a C5–C6 double bond (unsaturated D-ring), while those with a C5–C6 single bond in the D-ring were not planar, as the substituents on the E-ring (e.g., C7, C8, and C9) were spatially displaced. All structures in Fig. 2 were used for calculations of CoMFA and CoMSIA analysis in further analysis.

The cytotoxicity of lamellarins containing either a saturated or an unsaturated D-ring against T47D and MDA-MB-231 human breast cancer cell lines are presented in Tables 1 and 2 as the negative logarithm of the 50% inhibition concentration (IC_{50}) values previously reported by Chittchang et al. [27] except those of the three acetate-containing compounds. Interestingly, lamellarins with a C5–C6 single bond exhibited comparable cytotoxic activity towards both cell lines, with IC_{50} values of the same order of magnitude (Table 1). On the other hand, it is clearly demonstrated in Table 2 that all of the compounds with an unsaturated D-ring were significantly more cytotoxic to the hormone-dependent T47D cell line. Overall, lamellarins D

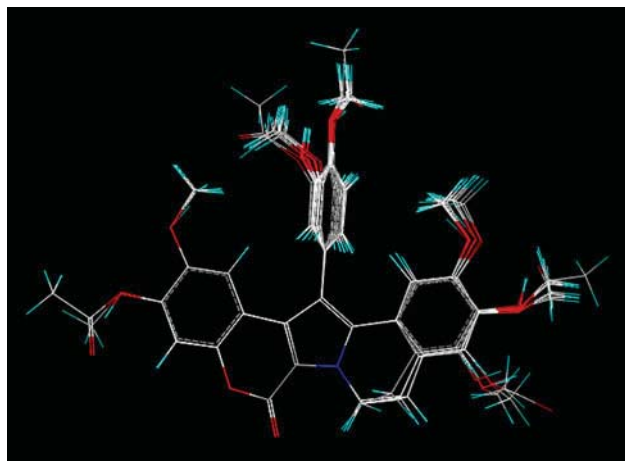


Fig. 2 Structure of lamellarins, obtained from 3D-QSAR matching alignments

and X were the most potent cytotoxic compounds against the T47D and MDA-MB-231 cell lines, respectively.

CoMFA and CoMSIA for cytotoxicity of lamellarins against T47D cells

CoMFA and CoMSIA models

Table 3 summarizes various parameters associated with the CoMFA models obtained by calculating the steric and electrostatic interactions between the aligned lamellarin molecules with each probe atom, which were subsequently correlated with their cytotoxic activity to identify the important interactions determining the cytotoxicity of lamellarins. All the models indicated that the changes in the steric interactions accounted for approximately two-thirds of the changes in the cytotoxic activity of lamellarins towards T47D cells, and the remaining 33–34% was contributed by the electrostatic interactions. Among the three

CoMFA models for the T47D cell line, namely models 1–3 in Table 3, model 1, calculated using a sp^3 carbon as the probe atom, yielded the highest predictive ability, as indicated by the r_{cv}^2 (or q^2) value. However, based on the F value and the $r_{test\ set}^2$, model 2 appeared to be the best CoMFA model of the T47D cell line. Other statistical parameters were comparable among the three models.

To further explore whether other types of interactions also play an important role in determining the cytotoxic activity of lamellarins in both cell lines, CoMSIA was also performed, and five models were generated using different combinations of steric (St), electrostatic (El), hydrophobic (Hyd), H-bond donor (Hd), and H-bond acceptor (Ha) field types, as shown in Table 4. However, only models 7 and 8 yielded acceptable predictive ability, as indicated by r_{cv}^2 values of >0.6 . Additionally, whenever the hydrogen-bond donor and/or acceptor fields were included, i.e., models 9–13, the r_{cv}^2 values were significantly decreased. These findings suggest that only the steric, electrostatic, and hydrophobic fields are important for the predictive ability of the model derived for breast cancer cell lines.

Model 8 was derived from model 7 upon the exclusion of lamellarin J with the lowest activity in the training set, resulting in a model with improved r_{cv}^2 as well as a lower standard error of estimation (s). Hence, model 8 was selected as the best CoMSIA model for T47D cells. All the CoMSIA models indicated that steric interactions accounted for approximately $<12\%$ of the changes in the cytotoxic activity of lamellarins, whereas the major contributions actually came from the electrostatic and hydrophobic fields.

The predictive ability of the selected CoMFA and CoMSIA models was determined using six lamellarin compounds as the test set. The CoMFA model was first considered, and the $-\log IC_{50}$ values predicted using

Table 3 Summary of CoMFA results for T47D and MDA-MB-231 cell lines

Model ^a	Probe atom	noc ^b	r_{cv}^2 ^c	S-PRESS ^d	r^2 ^e	s ^f	F ^g	Steric contribution	$r_{test\ set}^2$
1	sp^3 C(+1)	6	0.717	1.143	0.963	0.414	56.144	66.0	0.466
2	sp^3 O(+1)	6	0.659	1.255	0.965	0.405	58.959	66.9	0.628
3	H(+1)	6	0.672	1.231	0.965	0.403	59.581	66.7	0.570
4	sp^3 C(+1)	6	0.661	0.498	0.977	0.129	92.967	67.6	0.408
5	sp^3 O(+1)	6	0.728	0.447	0.981	0.117	114.66	68.1	0.364
6	H(+1)	6	0.685	0.481	0.974	0.138	81.624	66.3	0.405

^a Model 1–3 for T47D cell line and model 4–6 for MDA-MB-231 cell line

^b The optimum number of components

^c Cross-validated correlation coefficient

^d Uncertainty of the prediction

^e Conventional correlation coefficient

^f Standard error of estimation

^g F value

Table 4 Summary of CoMSIA results for T47D and MDA-MB-231 cell lines

Model ^a	Field type	noc. ^b	r_{cv}^2	S-PRESS	r^2	s	F	Contributions	$r_{test\ set}^2$
7	St + El + Hyd	5	0.623	1.271	0.923	0.575	33.541	St = 11.8 El = 45.7 Hyd = 42.5	0.918
8 ^c	St + El + Hyd	6	0.662	1.271	0.960	0.436	48.321	St = 11.6 El = 45.8 Hyd = 42.6	0.894
9	St + El + Hd	1	-0.090	1.907	0.325	1.500	8.688	St = 0.059 El = 0.302 Hd = 0.639	-
10	St + El + Ha	1	-0.080	1.898	0.229	1.604	5.344	St = 0.082 El = 0.420 Ha = 0.498	-
11	St + El + Hyd + Hd	5	0.489	1.480	0.900	0.655	25.153	St = 5.0 El = 25.6 Hyd = 27.8 Hd = 41.6	-
12	St + El + Hyd + Ha	5	0.548	1.393	0.913	0.611	29.324	St = 8.0 El = 33.9 Hyd = 34.3 Ha = 23.8	-
13	All	5	0.429	1.565	0.885	0.703	21.497	St = 4.2 El = 21.8 Hyd = 25.5 Hd = 37.2 Ha = 11.3	-
14	St + El + Hyd	6	0.608	0.536	0.954	0.184	44.956	St = 10.5 El = 48.3 Hyd = 41.1	0.595
15 ^d	St + El + Hyd	6	0.674	0.445	0.952	0.171	39.651	St = 10.2 El = 49.9 Hyd = 39.8	0.582
16	St + El + Hd	6	0.131	0.798	0.954	0.184	44.670	St = 0.058 El = 0.302 Hd = 0.633	-
17	St + El + Ha	1	-0.167	0.786	0.228	0.639	5.323	St = 0.077 El = 0.402 Ha = 0.521	-
18	St + El + Hyd + Hd	6	0.547	0.576	0.964	0.164	57.245	St = 5.0 El = 24.8 Hyd = 20.6 Hd = 49.6	-
19	St + El + Hyd + Ha	6	0.424	0.650	0.939	0.211	33.540	St = 7.6 El = 32.9 Hyd = 29.0 Ha = 30.6	-

Table 4 continued

Model ^a	Field type	noc. ^b	r_{cv}^2	S-PRESS	r^2	s	F	Contributions	$r_{test\ set}^2$
20	All	6	0.458	0.630	0.957	0.177	48.572	St = 4.1 El = 19.0 Hyd = 18.7 Hd = 44.4 Ha = 13.8	–

St steric; El electrostatic; Hyd hydrophobic, Hd H-bond donor; Ha H-bond acceptor

^a Model 7–13 for T47D cell line and model 14–20 for MDA-MB-231 cell line

^b The optimum number of components

^c Elimination of lamellarin J

^d Elimination of lamellarin Y

model 2 were plotted against the experimentally determined values (Fig. 3a). The prediction results were satisfactory for most of the compounds in the test set with the exception of lamellarin α . Exclusion of this compound from the test set significantly improved the $r_{test\ set}^2$ value for model 2 to 0.985. Similarly, the selected CoMSIA model 8 was also validated, and the results are presented in Fig. 3b. The model appeared to overestimate the $-\log IC_{50}$ values of lamellarin α and lamellarin M, while the predicted value of lamellarin K was lower than the experimental $-\log IC_{50}$ value. Nevertheless, CoMFA model 2 could be used to predict the cytotoxic activity of most lamellarins in the test set towards T47D cells.

CoMFA and CoMSIA contour maps

CoMFA and CoMSIA contour maps were created using the best CoMFA and CoMSIA models for each cell line, as shown in Figs. 4 and 5. The resulting contours on these maps not only highlight the key structural features correlated with the biological activity of the molecules considered but also provide detailed understanding of the binding pockets. Green and yellow regions represent areas where steric bulk enhanced and diminished biological activity, respectively. On the other hand, blue and red contours represent regions where electropositive and electronegative groups were associated with cytotoxicity, respectively. To avoid any ambiguity due to contour overlap, all contours are displayed in transparent style. Additionally, lamellarin D and lamellarin X, which were the most active molecules against T47D and MDA-MB-231 cell lines, respectively, were used as the reference molecules in the corresponding contour maps.

Interestingly, Fig. 4a clearly shows several steric and electrostatic contours generated using CoMFA model 2 for the T47D cell line. For the pentacyclic core, all contours were concentrated around the two rightmost D- and E-rings (Fig. 4a). There were green and blue regions near the C9

group. Red contours also occupy the space between the oxygen atom of the methoxy group at C9 and the hydroxyl group at C8. These suggest that oxygen atoms at C8 and C9 were important for cytotoxic activity. The steric and electropositive group at C9 might play an important role for activity. Considering two pairs of lamellarins (lamellarin Y compared with lamellarin U and dehydrolamellarin Y compared with lamellarin α), it was shown that the cytotoxic activity of the lamellarins was decreased when the C9 hydroxy group was replaced by a methoxyl group, which is somewhat different from the green contour of the predictive model. The reason for this is that both lamellarin U and lamellarin α were solely employed in the test set. Interesting contours in the E-ring were blue contours at the hydrogen atom and methyl group at C7, and a red contour located around the oxygen atom at C7. These might indicate that occupancy of the hydroxyl and methoxyl group was more cytotoxic than a hydrogen atom at this position. This result supports the pronouncement of Chittchang et al. [27] that substitution of the hydrogen atom at C7 with a hydroxyl group significantly increased the cytotoxicity of unsaturated lamellarins.

In terms of the orthogonal ring or F-ring, a large green contour was found virtually covering this ring. This finding suggests that the orthogonal ring of lamellarin could be essential for activity. Additionally, a red contour was found near an oxygen atom and an acetate group at C14 of the lamellarin. This contour showed that the oxygen atom and acetate group at C14 might be important for activity. The blue contour regions between C13 and C21 groups suggested that some electropositive groups in these areas might be advantageous for activity.

Finally, a yellow contour appeared behind the plane of the molecule near the C5–C6 double bond, while blue and green contours occupy the space around the D-ring. The yellow contour shows sterically unfavored areas near the C5–C6 double bond. This prediction, along with the superior cytotoxicity of the lamellarins containing a C5–C6

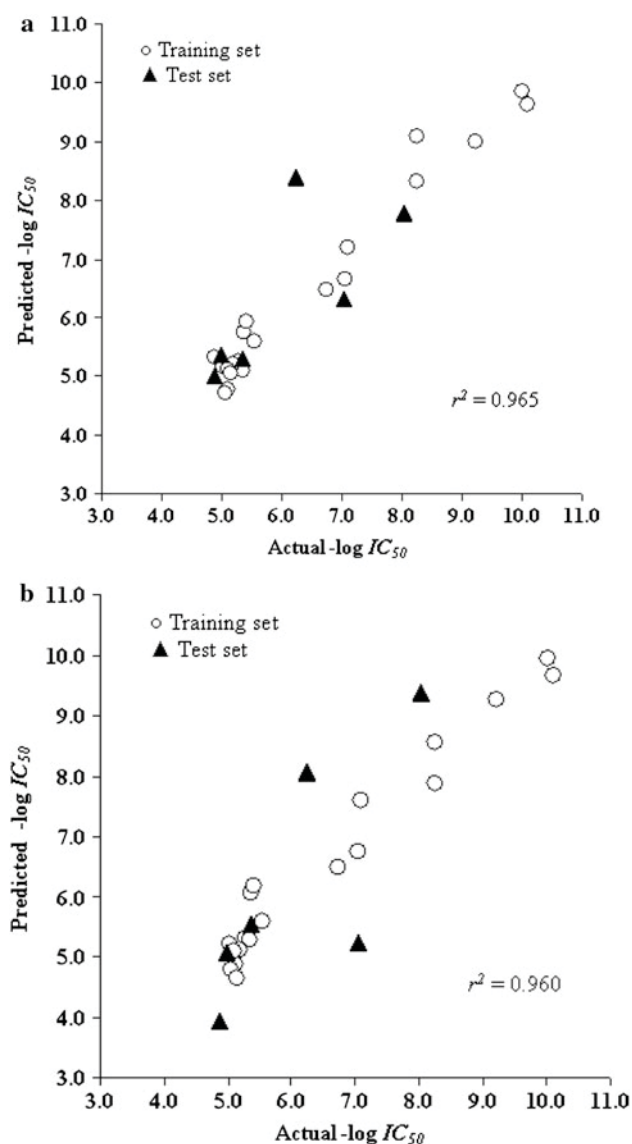


Fig. 3 Plot of predicted versus actual cytotoxic activity of lamellarins towards T47D cells. Predicted values were obtained from non-cross-validated CoMFA model 2 (a) and CoMSIA model 8 (b) for all compounds in both the training (*open circle*) and test (*filled triangle*) sets

double bond (Tables 1, 2), suggests that these compounds assume a structure that could fit into the binding pocket better than their counterparts with a single bond. It was observed in our preliminary molecular modeling studies that the lamellarins with a saturated D-ring were twisted, whereas the presence of the C5–C6 double bond leads to a more planar molecule that is likely to intercalate into the topoisomerase I–DNA complex more easily [27]. The blue and green contours result from the twisted bond of unsaturated lamellarins which cannot align at the same position as shown in Fig. 2.

In addition to the steric and electrostatic fields considered in CoMFA, CoMSIA helps to define the

contribution of the explicit hydrophobic interactions to the binding affinity of lamellarins, as shown in Fig. 5. Orange and white contours indicate areas where the presence of hydrophobic groups is associated with increase and decrease of biological activity, respectively. Since CoMSIA steric and electrostatic contours were shown in more detail than those of the CoMFA models at some positions, all three field contributions are discussed. The steric and electrostatic contours from the best CoMSIA model for the T47D cell line are shown in Fig. 5a. There was a green region at C9 and a white region near the oxygen atom at C9. Both contours indicated that the oxygen atom at this position was essential for potent cytotoxic activity. The presence of steric (yellow contour near the hydrogen atom), electrostatic (blue contour near the hydrogen atom and methyl group, and red contour near the oxygen atom), and hydrophobic (white contour) fields at C8 revealed that a nonsteric electropositive group around this area was required for better activity. The suggestion has been reported by Ishibashi et al. [25] and Chittchang et al. [27] that a hydroxyl group at C8 of lamellarin D is an important structural requirement for activity.

Furthermore, yellow and green contours near the hydroxyl and methoxyl group at C7 led to the idea that a bulky group at this position would increase activity, but the size of this group should not be too large. Additionally, there was a blue region near the hydroxyl and methoxyl group at C7, a red region located around the oxygen atom at C7, and a white region at C7. These might indicate that a steric electron-donating oxygen-containing group such as hydroxyl or methoxyl group would be beneficial for cytotoxicity. These findings support the work of Chittchang et al. [27] that replacement of the hydroxyl group at C7 by a methoxy group decreases the cytotoxic activity of unsaturated lamellarins. More hydrophobic fields (white, orange, and red contours) were found around the C5–C6 bond. The white contour appeared at CH₂ around the C5–C6 bond. The orange and red contours were located around the C5–C6 bond. Both contours could not play any important role in activity. These fields were shown around this area because of the difference in planarity between the lamellarins containing C5–C6 single and double bond, which could not align into the same plane. These results also confirm that the structural requirement relied more on the double rather than the single bond. The red contours located between the oxygen atom of C13 and C14 positions and near the carbonyl of the acetate group around C20 revealed the importance of the oxygen atom at these areas for cytotoxicity. The two green regions located at C13 and C21 suggest that the substituents at these positions should be bulky groups.

Fig. 4 Stereoviews of steric and electrostatic standard deviation \times coefficient contour maps, obtained from CoMFA model 2 for T47D cytotoxicity (a) and CoMFA model 5 for MDA-MB-231 cytotoxicity (b). Lamellarins D and X are presented inside the fields of the T47D and MDA-MB-231 CoMFA contour maps, respectively, in ball-and-stick display style. Sterically favored and unfavored areas are shown by *green* and *yellow* regions, respectively. Electropositive and electronegative areas are shown by *blue* and *red* regions, respectively

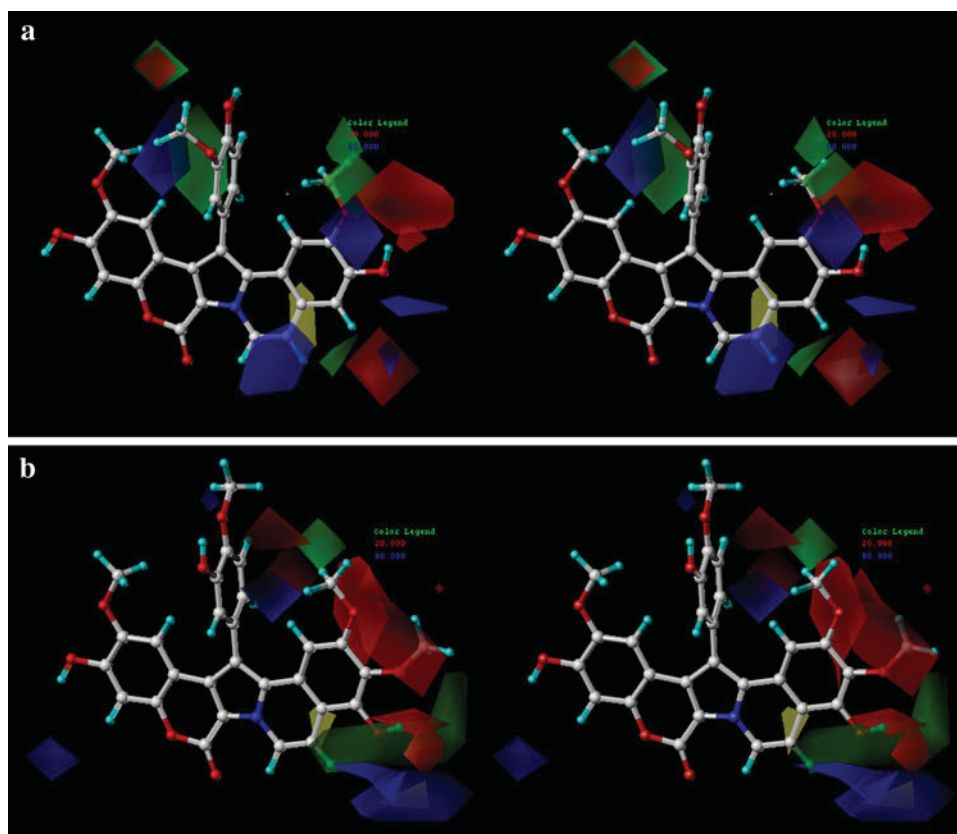
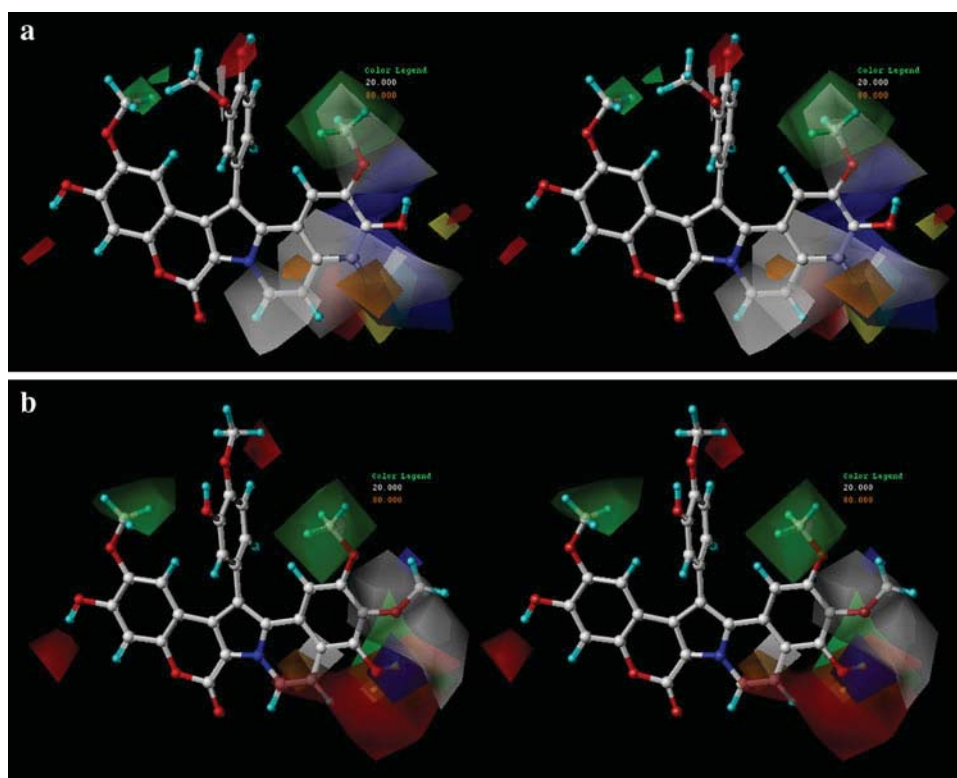


Fig. 5 Stereoviews of steric, electrostatic, and hydrophobic standard deviation \times coefficient maps, obtained from CoMSIA model 8 for T47D cytotoxicity (a) and CoMSIA model 15 for MDA-MB-231 cytotoxicity (b). Lamellarins D and X are presented inside the fields of the T47D and MDA-MB-231 CoMFA contour maps, respectively, in ball-and-stick display style. Sterically favored and unfavored areas are shown by *green* and *yellow* regions, respectively. Electropositive and electronegative areas are shown by *blue* and *red* regions, respectively. Hydrophobically favored and unfavored areas are shown by *orange* and *white* regions, respectively



CoMFA and CoMSIA for the cytotoxicity of lamellarins against MDA-MB-231 cells

CoMFA and CoMSIA models

The CoMFA and CoMSIA models for the MDA-MB-231 cell line were generated using the same compounds in the training and test sets as those used for the T47D cell line. The statistical parameters associated with CoMFA models 4–6 for the MDA-MB-231 cell line are shown in Table 3. Apparently, model 5 obtained using an sp^3 oxygen as the probe atom yielded not only the highest predictive ability with an r_{cv}^2 value of 0.728 but also the highest F value. Even though the other statistical parameters were not significantly different among the three models, model 5 still appeared to be the best CoMFA model for the MDA-MB-231 cell line, which indicated that steric interactions were the major factor, contributing approximately 68% of the changes in cytotoxic activity of lamellarins towards MDA-MB-231 cells.

With the sequential additions of the hydrophobic and hydrogen-bonding interactions, seven CoMSIA models (models 14–20) were subsequently constructed for the MDA-MB-231 cell line, as shown in Table 4. Based on the r_{cv}^2 values, the models involving only the steric, electrostatic, and hydrophobic fields, i.e., models 14 and 15, showed good predictive ability. Model 15 resulted from the exclusion of lamellarin Y with the lowest cytotoxic activity in the training set for model 14, giving rise to a significantly increased r_{cv}^2 value, even though the conventional r^2 and $r_{test\ set}^2$ values for both models were not significantly different. Thus, model 15 was chosen as the best CoMSIA model for the MDA-MB-231 cell line. The contributions from steric, electrostatic, and hydrophobic interactions were determined to be 10.2%, 49.9%, and 39.8%, respectively, similar to the values obtained from the CoMSIA model 8 for the T47D cell line.

The correlations between the actual $-\log IC_{50}$ data of lamellarins against the MDA-MB-231 cell line and the values predicted based on CoMFA model 5 and CoMSIA model 15 are shown in Fig. 6a and b, respectively. In the case of CoMFA model 5 (Fig. 6a), lamellarin L was the only compound in the test set for which the predicted cytotoxicity deviated from the actual value by more than one log unit, and the exclusion of this compound significantly increased the $r_{test\ set}^2$, from 0.364 to 0.612. A similar degree of deviation was also observed for the $-\log IC_{50}$ value of lamellarin α predicted using CoMSIA model 15 (Fig. 6b). Nevertheless, these results indicated that both CoMFA model 5 and CoMSIA model 15 could be used to predict the cytotoxicity of lamellarins towards the MDA-MB-231 cell line.

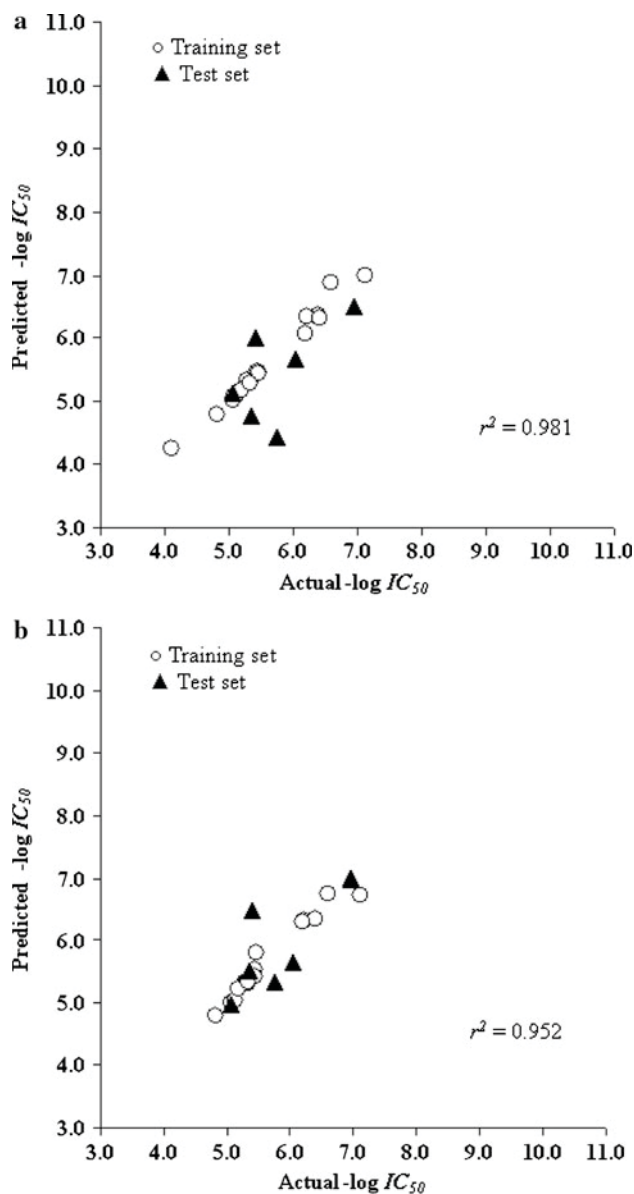


Fig. 6 Plot of the predicted versus actual cytotoxic activity of lamellarins against MDA-MB-231 cells. The predicted values were obtained from non-cross-validated CoMFA model 5 (**a**) and CoMSIA model 13 (**b**) for the compounds in both the training (*open circle*) and test (*filled triangle*) sets

CoMFA and CoMSIA contour maps

The steric and electrostatic maps of the CoMFA analysis for the MDA-MB-231 cell line are presented in Fig. 4b. Blue and green regions were found around hydroxy and methoxy groups at C9, and red regions located near the oxygen atom at C8 and C9. These might indicate that a steric electropositive group at C9 would increase cytotoxicity. However, there were only two lamellarins (Y and dehydrolamellarin Y) which have a hydroxyl group at C9. Hence, this might suggest only that the oxygen atom at C8

and C9 and an electropositive group at C9 would play an important role in increasing cytotoxic activity. The green, yellow, and blue contours near the hydroxyl group at C7 showed that the C7 area preferred a steric electropositive group, but it should not be too large. These results were supported by the experimental data reported in Tables 1 and 2. Lamellarins K, E, F, M, X, and ϵ with the hydroxyl group at C7 were more cytotoxic against MDA-MB-231 cell line than were lamellarins C, T, I, B, W, and ζ , respectively. Moreover, this result supports the conclusion of Chittchang et al. [27], as shown in the CoMSIA analysis for the T47D cell line. There was a yellow contour located behind the plane of the D-ring near the C5–C6 bond. This revealed the importance of a double bond at C5–C6 to enhance the MDA-MB-231 cytotoxic activity, similar to case of T47D activity. The red contours near the oxygen atom at C14 suggest that the oxygen atom at C14 would play an important role in increasing cytotoxic activity. The blue contour near C20 indicates that occupancy of an electropositive group at this position would help cytotoxic activity.

The steric, electrostatic, and hydrophobic contour maps of the CoMSIA model for the MDA-MB-231 cell line are displayed in Fig. 5b. Green and blue contours were found near C9. Additionally, a white region was found between C8 and the oxygen atom at C9. From these results it can be concluded that an electropositive group at C9 enhances cytotoxic activity. There were green contours between C7 and C8, yellow and blue contours at C7, and red contours around C7 and the C5–C6 bond. These suggest that a steric group disfavoring hydrophobic interactions at C8 is preferred. However, there were only two pairs of lamellarins for which direct comparison of the effect of substituting the hydroxyl group at C8 by a methoxy group could be made (lamellarin L compared with lamellarin U and lamellarin N compared with lamellarin α). Three of them (L, U, and α) were in the test set. At C7, a steric electron-donating oxygen-containing group which was not too large might be required to increase activity. Thus, the finding of CoMSIA analysis at C7 for the MDA-MB-231 cell line confirms the structure–activity relationship (SAR) result from the report of Chittchang et al. [27]. Both hydrophobic fields (white and orange contours) were found near the C5–C6 bond. The importance of an oxygen atom was also shown near the acetate group at C14 and C20 by red regions. The final contour is the green region at C21, representing the methoxyl group at this position.

Common structural requirement of lamellarins as a binding pocket of the T47D compared with the MDA-MB-231 cell lines

In summary, the T47D and MDA-MB-231 receptor binding site models are proposed as shown in Fig. 7a and b,

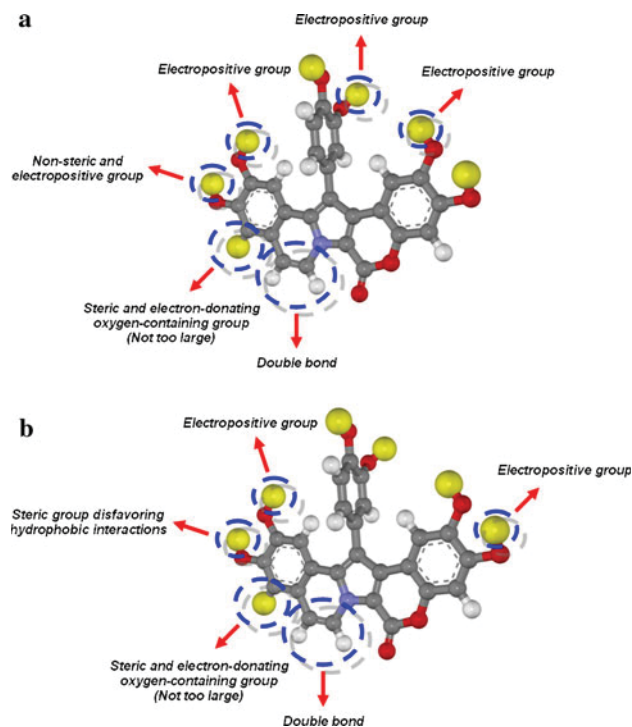


Fig. 7 Structural requirements of lamellarins for (a) T47D and (b) MDA-MB-231 receptor binding site obtained from combination of the CoMFA and CoMSIA contour maps

respectively. By using the combination of CoMFA and CoMSIA results, the structural requirement of lamellarins at the binding pockets of both cell lines are shown by common carbon atoms of the lamellarin skeleton. Figure 7a reveals that the double bond at C5–C6, the electropositive groups at C9, C13, and C21, a nonsteric electropositive group at C8, and a steric electron-donating oxygen-containing group at C7 are required for cytotoxic activity. Based on Fig. 7, the 3D-QSAR analysis revealed that the common structure of lamellarins around the binding pocket for both cell lines was similar in many positions, e.g., at C7, C9, and the C5–C6 bond. More importantly, this method showed some different structural requirements of the lamellarin skeleton for both cell lines, such as a nonsteric electropositive group at C8 in case of T47D cells. For the MDA-MB-231 cell line, on the other hand, the C8 area seemed to require a steric group disfavoring hydrophobic interactions. Additionally, the electropositive groups at C13 and C21, which appear crucial in case of the T47D cell line, were not important for the MDA-MB-231 cell line. The presence of an electropositive group at C20 may be important in case of the MDA-MB-231 cell line, but such an inclusion did not show any significant cytotoxicity for the T47D cell line. The requirement of a steric group disfavoring hydrophobic interactions at C8 may account for the potent cytotoxic activity of lamellarins M,

X, and ϵ against the MDA-MB-231 cell line, as shown in Table 2.

The importance of the substitution on F- and E-rings of lamellarin has been discussed in 4D-QSAR analysis using the same data set [28]. Overall, 4D-QSAR models found that the formation of an intermolecular hydrogen bond and the hydrophobic interactions for substituents on the E-ring most strongly modulated cytotoxicity towards T47D. Especially the 3D pharmacophore site near C8 and C9 from the 4D-QSAR model of a high-activity data set is seemingly distinguished from the 4D-QSAR model of the overall data set. A hydrophobic substituent on the F-ring can also increase cytotoxicity against the T47D cell line. 3D-QSAR analysis can also reveal some interesting structural requirements of lamellarins at C7, C8, C9, and C13, as shown in Fig. 7a. However, previous 4D-QSAR analysis cannot depict the different cytotoxicity of lamellarins containing saturated and unsaturated D-rings. The yellow contour near the C5–C6 double bond confirms that the binding pocket site prefers the unsaturated D-ring lamellarins over saturated D-ring lamellarins.

Conclusions

The 3D-QSAR methods CoMFA and CoMSIA were applied to lamellarins for cytotoxicity against T47D and MDA-MB-231 breast cancer cells. Lamellarins with saturated and unsaturated D-rings which bear different planarity at D- and E-ring structures were the focus. Satisfactory CoMFA and CoMSIA models were derived, and the obtained results revealed that these powerful 3D-QSAR methods can be used to handle even small data sets consisting of two groups of different types of geometries. As there is no information about the target structure for both cell lines, CoMFA and CoMSIA analyses provided more details about the steric, electrostatic, and hydrophobic field requirements of lamellarins for breast cancer cytotoxicity. In addition, the CoMSIA contour maps showed good correlation with those obtained by CoMFA. Based on CoMFA and CoMSIA contour maps, the results can discriminate the structural requirements between T47D and MDA-MB-231 cytotoxicity by common carbon atoms of the lamellarin skeleton such as at C8, C13, C20, and C21. Interestingly, different structural requirements of lamellarins at C8 may play an important role in the different cytotoxicity against the two cell lines. In the T47D cell line, 3D-QSAR contours highlight the importance of the F-ring at C13 for cytotoxicity; on the other hand, this did not occur in contour maps around this region for the MDA-MB-231 cell line. The contour maps of both cell lines suggest the necessity of the A-ring at C21 for cytotoxicity against the T47D cell line, but the importance of the A-ring for

cytotoxicity against the MDA-MB-231 cell line is clearly shown at C20.

Moreover, the 3D-QSAR results revealed specific structural requirements of the lamellarins for their cytotoxic activity towards two breast cancer cell lines, including a steric electropositive oxygen-containing group at C7, and an electropositive group at C9. Especially, the significance of the C5–C6 double bond was also found. Hence, 3D-QSAR is a useful method to explore the specific structural requirements between both types of human breast cancer cells and also as a guideline to design more effective inhibitors from lamellarins. These are not only helpful for more detailed understanding of the interactions of lamellarin derivatives upon binding to an unknown receptor, but are also applicable to a small lamellarin data set.

Methods

Lamellarin compounds and cytotoxicity assays

The 26 lamellarins used in this study (Tables 1, 2) were synthesized and purified as described previously [29]. All compounds were solubilized in dimethyl sulfoxide (DMSO) and tested for their cytotoxic activity against T47D and MDA-MB-231 cell lines as previously reported [27]. Briefly, the cells were incubated in 96-well microplates at 37 °C for 48 h with serial dilutions of the test compounds, positive control (etoposide), or negative control (DMSO). The number of surviving cells in each well was determined using crystal violet staining to obtain the IC_{50} value, defined as the concentration that inhibits cell growth by 50% after 48 h of continuous exposure to each test compound. The values thus obtained were then transformed by calculating their negative logarithm (i.e., $-\log IC_{50}$), which is a standard notation to make very small numbers fit into a more comprehensible range; larger values indicate more potent cytotoxicity.

Alignment rules, CoMFA and CoMSIA calculations

Lamellarin molecules were separated into two groups. The first group, consisting of 20 compounds, served as the training set. On the other hand, six compounds comprising the test set were chosen at random to include structurally diverse molecules possessing a wide range of cytotoxic activity against both cell lines, namely lamellarins α , K, L, M, T, and U. The starting geometries of all 26 lamellarin structures were fully optimized at the HF/3-21G level using the GAUSSIAN 03 program [33]. The partial atomic charges required for calculations of electrostatic interactions were subsequently computed using the Gasteiger-

Hückel method in the SYBYL 7.0 program (Tripos, L.P., St. Louis, MO, USA). Molecular alignments were then carried out using the matching method also available in the SYBYL software. The common structure used for matching alignments involves the atoms constituting the A-, B-, and C-rings, as denoted with asterisks in Fig. 1. Additionally, the most active molecule with respect to each cell line, i.e., lamellarin D for T47D and lamellarin X for MDA-MB-231 cells, was used as the template for alignments.

To calculate the CoMFA and CoMSIA descriptor fields, a cubic lattice was first generated around each lamellarin molecule based on its molecular volume, and a grid spacing of 2 Å was used to ensure that the grid extended by 4.0 Å beyond the molecular dimensions in all directions. In addition to an sp³ carbon atom with a +1 charge, which is the default probe atom in SYBYL, an sp³ oxygen atom with a -1 charge and a hydrogen atom with a +1 charge were also used as additional probe atoms for CoMFA calculations in this study, and these atoms were placed at each lattice point. On the other hand, the steric and electrostatic fields of each aligned lamellarin were generated based on their Lennard–Jones and Coulomb potentials, respectively. The interactions between these three-dimensional fields with each probe atom were then calculated using the CoMFA standard scaling technique, in which the minimum sigma value was set at 8.4 kJ/mol, and an energy cutoff value of 125 kJ/mol was selected to not only speed up the analysis but also reduce the amount of noise. All the calculated data were then put into a CoMFA table.

In CoMSIA, five similarity indices (including steric, electrostatic, hydrophobic, H-bond donor, and H-bond acceptor descriptors) were computed for each lamellarin molecule using the same cubic lattice employed for the CoMFA calculations, as well as the default carbon probe atom with 1 Å radius and +1 charge. The hydrophobic, H-bond donor, and H-bond acceptor fields were established more than generally potentials (Lennard–Jones and Coulomb) in CoMFA analysis. The relative contributions of the different fields were generated during this analysis. The three-dimensional properties of lamellarins determined using either CoMFA or CoMSIA were then correlated with their cytotoxic activity against each cell line using partial least-squares (PLS) regression analysis, and various 3D-QSAR models were subsequently derived.

The predictive ability of the derived 3D-QSAR models was evaluated by leave-one-out (LOO) cross-validation, and is expressed in terms of r_{cv}^2 (also called q^2), which is defined as shown in Eq. 1.

$$r_{cv}^2 = (SSY - PRESS)/SSY, \quad (1)$$

where SSY represents the variance of the cytotoxic activity of molecules around the mean value, and PRESS is the

prediction error sum of squares derived from the leave-one-out method. In contrast, the uncertainty of the prediction (S-PRESS) is defined as shown in Eq. 2.

$$S-PRESS = [PRESS/(n-k-1)]^{1/2}, \quad (2)$$

where n is the number of compounds used in the study, and k is the number of PLS components.

For all models, a maximum number of components was first used and subsequently decreased until an optimal number was obtained when the resulting cross-validated r_{cv}^2 differed from the previous value by <0.05. The optimal number of components was then used to perform non-cross-validated analyses. Briefly, the conventional correlation coefficient, r^2 , was calculated based on the 20 compounds in the training set. The CoMFA and CoMSIA models with r^2 value higher than 0.6 were subsequently validated by evaluating the correlations between the observed and predicted cytotoxic activities of the compounds in the test set, as indicated by the $r_{test\ set}^2$ values.

Acknowledgments This work would not have been possible without generous support from the Chulabhorn Research Institute (CRI), the Chulabhorn Graduate Institute (CGI), Phetchaburi Rajabhat University (PBRU), the Kasetsart University (KU) Graduate School, and the Commission on Higher Education (CHE). The Thailand Research Fund (TRF) is gratefully acknowledged for research grants (RTA5080005 to S.H., BRG5180013 to P.P., RMU4980048 to N.T., and DBG5180015 to M.C.). Moreover, the authors would like to thank the National Center of Excellence in Petroleum, Petrochemicals, and Advanced Materials, KU Research and Development Institute (KURDI), Laboratory for Computational and Applied Chemistry (LCAC) and the computing centre of KU, the Center of Nanotechnology KU, NANOTEC Center of Excellence at KU, and the Large Scale Research Laboratory of the National Electronics and Computer Technology (NECTEC) for computing and research facilities.

References

- Andersen RJ, Faulkner DJ, He CH, Van Duyne GD, Clardy J (1985) *J Am Chem Soc* 107:5492
- Carroll AR, Bowden BF, Coll JC (1993) *Aust J Chem* 46:489
- Davis RA, Carroll AR, Pierens GK, Quinn RJ (1999) *J Nat Prod* 62:419
- Ham J, Kang H (2002) *Bull Korean Chem Soc* 23:163
- Krishnaiah P, Reddy VLN, Venkataramana G, Ravinder K, Srinivasulu M, Raju TV, Ravikumar K, Chandrasekar D, Ramakrishna S, Venkateswarlu Y (2004) *J Nat Prod* 67:1168
- Lindquist N, Fenical W, Van Duyne GD, Clardy J (1988) *J Org Chem* 53:4570
- Reddy MVR, Faulkner DJ, Venkateswarlu Y, Rao MR (1997) *Tetrahedron* 53:3457
- Reddy SM, Srinivasulu M, Satyanarayana N, Kondapi AK, Venkateswarlu Y (2005) *Tetrahedron* 61:9242
- Urban S, Butler MS, Capon RJ (1994) *Aust J Chem* 47:1919
- Urban S, Capon RJ (1996) *Aust J Chem* 49:711
- Urban S, Hobbs L, Hooper JNA, Capon RJ (1995) *Aust J Chem* 48:1491
- Reddy MVR, Rao MR, Rhodes D, Hansen MST, Rubins K, Bushman FD, Venkateswarlu Y, Faulkner DJ (1999) *J Med Chem* 42:901

13. Ridley CP, Reddy MVR, Rocha G, Bushman FD, Faulkner DJ (2002) *Bioorg Med Chem* 10:3285
14. Fan H, Peng J, Hamann MT, Hu JF (2008) *Chem Rev* 108:264
15. Facompre M, Tardy C, Bal-Mahieu C, Colson P, Perez C, Manzanares I, Cuevas C, Bailly C (2003) *Cancer Res* 63:7392
16. Vanhuysse M, Kluza J, Tardy C, Otero G, Cuevas C, Bailly C, Lansiaux A (2005) *Cancer Lett* 221:165
17. Costantini P, Jacotot E, Decaudin D, Kroemer G (2000) *J Natl Cancer Inst* 92:1042
18. Debatin KM, Poncet D, Kroemer G (2002) *Oncogene* 21:8786
19. Dias N, Bailly C (2005) *Biochem Pharmacol* 70:1
20. Kluza J, Gallego MA, Loyens A, Beauvillain JC, Sousa-Faro JMF, Cuevas C, Marchetti P, Bailly C (2006) *Cancer Res* 66:3177
21. Mayer AMS, Gustafson KR (2008) *Eur J Cancer* 44:2357
22. Baunbaek D, Trinkler N, Ferandin Y, Lozach O, Ploypradith P, Rucirawat S, Ishibashi F, Iwao M, Meijer L (2008) *Mar Drugs* 6:514
23. Quesada AR, Garcia Gravalos MD, Fernandez Puentes JL (1996) *Br J Cancer* 74:677
24. Bailly C (2004) *Curr Med Chem Anticancer Agents* 4:363
25. Ishibashi F, Tanabe S, Oda T, Iwao M (2002) *J Nat Prod* 65:500
26. Marco E, Laine W, Tardy C, Lansiaux A, Iwao M, Ishibashi F, Bailly C, Gago F (2005) *J Med Chem* 48:3796
27. Chittchang M, Batsomboon P, Ruchirawat S, Ploypradith P (2009) *ChemMedChem* 4:457
28. Thipnate P, Liu J, Hannongua S, Hopfinger AJ (2009) *J Chem Inf Model* 49:2312
29. Ploypradith P, Petchmanee T, Sahakitpichan P, Litvinas ND, Ruchirawat S (2006) *J Org Chem* 71:9440
30. Bohm M, Sturzebecher J, Klebe G (1999) *J Med Chem* 42:458
31. Cramer RD III, Patterson DE, Bunce JD (1988) *J Am Chem Soc* 110:5959
32. Klebe G, Abraham U, Mietzner T (1994) *J Med Chem* 37:4130
33. Frisch MJ, Trucks GW, Schlegel HB, Scuseria GE, Robb MA, Cheeseman JR, Montgomery JA Jr, Vreven T, Kudin KN, Burant JC, Millam JM, Iyengar SS, Tomasi J, Barone V, Mennucci B, Cossi M, Scalmani G, Rega N, Petersson GA, Nakatsuji H, Hada M, Ehara M, Toyota K, Fukuda R, Hasegawa J, Ishida M, Nakajima T, Honda Y, Kitao O, Nakai H, Klene M, Li X, Knox JE, Hratchian HP, Cross JB, Bakken V, Adamo C, Jaramillo J, Gomperts R, Stratmann RE, Yazyev O, Austin AJ, Cammi R, Pomelli C, Ochterski JW, Ayala PY, Morokuma K, Voth GA, Salvador P, Dannenberg JJ, Zakrzewski VG, Dapprich S, Daniels AD, Strain MC, Farkas O, Malick DK, Rabuck AD, Raghavachari K, Foresman JB, Ortiz JV, Cui Q, Baboul AG, Clifford S, Cioslowski J, Stefanov BB, Liu G, Liashenko A, Piskorz P, Komaromi I, Martin RL, Fox DJ, Keith T, Al-Laham MA, Peng CY, Nanayakkara A, Challacombe M, Gill PMW, Johnson B, Chen W, Wong MW, Gonzalez C, Pople JA (2004) *Gaussian 03*. Gaussian Inc., Wallingford



Original article

Assessing the drug-likeness of lamellarins, a marine-derived natural product class with diverse oncological activities

Montakarn Chittchang^{a,b,*}, M. Paul Gleeson^{a,c}, Poonsakdi Ploypradith^{a,b}, Somsak Ruchirawat^{a,b}^a Laboratory of Medicinal Chemistry, Chulabhorn Research Institute, 54 Moo 4, Vibhavadee-Rangsit Highway, Laksi, Bangkok 10210, Thailand^b Chemical Biology Program, Chulabhorn Graduate Institute and the Center for Environmental Health, Toxicology and Management of Chemicals, 54 Moo 4, Vibhavadee-Rangsit Highway, Laksi, Bangkok 10210, Thailand^c Department of Chemistry, Faculty of Science, Kasetsart University, 50 Phaholyothin Road, Chatuchak, Bangkok 10900, Thailand

ARTICLE INFO

Article history:

Received 1 November 2009

Received in revised form

18 January 2010

Accepted 20 January 2010

Available online 28 January 2010

Keywords:

Lamellarins

Lipophilicity

Drug-likeness

Physicochemical profiling

In silico descriptors

Principal components analysis (PCA)

ABSTRACT

Natural products currently represent an underutilized source of leads for the pharmaceutical industry, especially when one considers that almost 50% of all drugs were either derived from such sources or are very closely related. Lamellarins are a class of natural products with diverse biological activities and have entered into preclinical development for the treatment of multidrug-resistant tumors. Although these compounds demonstrated good cell penetration, as observed by their low μM activity in whole cell models, they have not been extensively profiled from a physicochemical point of view, and this is the goal of this study.

For this study, we have determined the experimental logP values of a set of 25 lamellarins, given it is the single most important parameter in determining multiple ADMET parameters. We also discuss the relationship between this natural product class, natural product derivatives in development and on the market, oral marketed drugs, as well as drug molecules in development, using a range of physicochemical parameters in conjunction with principal components analysis (PCA). The impact of this systematic analysis on our ongoing medicinal chemistry strategy is also discussed.

© 2010 Elsevier Masson SAS. All rights reserved.

1. Introduction

Natural products currently represent an underutilized source of leads for the pharmaceutical industry due to the current dominance of high throughput screening (HTS) lead generation processes. Even if identified from alternative cell based models, their often unknown mode of action makes biological characterization and structure-activity relationship (SAR) expansion difficult using the favored *in vitro* assays. Coupled with their often low abundance in nature, or complex structures posing synthetic challenges, mean the progression of natural products in a modern development cascade is limited. Despite these hurdles, natural products, or molecules derived from natural products, represent ~50% of all drugs coming to market over the last 2 decades [1], which appears to add weight to arguments that naturally derived molecules are inherently better tolerated in the body than synthetically derived molecules [2–4].

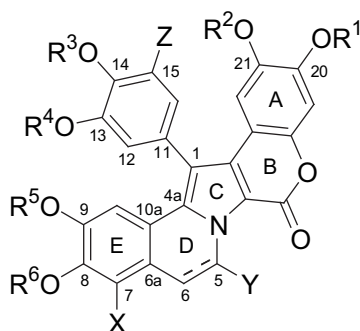
Lamellarins are a class of marine-derived natural products isolated from mollusks [5], ascidians [6–13], and marine sponges [14,15]. The majority of naturally-occurring lamellarins contain the same pentacyclic 2-pyrrolo(dihydro)isoquinoline lactone core, and only differ in the nature of the C5–C6 bond in the D-ring, as well as the substitution pattern on each ring (Table 1). Lamellarins have been the focus of considerable scientific research due to their diverse biological activities [16,17], demonstrating cytotoxic activities and multidrug resistance (MDR) reversal in a number of cancer cell lines [18–25], as well as being confirmed inhibitors of HIV-1 integrase [19,21], a number of kinases [26], and topoisomerase I [22–24]. Recognition of the biological potential of this compound class can be found in recent reports of lamellarins entering into preclinical development for the treatment of multidrug-resistant tumors [27–32].

Key to the success of any clinical candidate is their absorption, distribution, metabolism, excretion, and toxicity (ADMET) characteristics, and these are known to depend heavily on their overall molecular properties, in particular lipophilicity (logP), molecular weight (MWT), ionization state, as well as the number of H-bond donors and acceptors [33–35]. However, as with most natural products, lamellarins are not particularly drug-like in the conventional sense (although these compounds demonstrated good cell

* Corresponding author at: Laboratory of Medicinal Chemistry, Chulabhorn Research Institute, 54 Moo 4, Vibhavadee-Rangsit Highway, Laksi, Bangkok 10210, Thailand. Tel.: +66 2 574 0622; fax: +66 2 574 2027.

E-mail address: montakarn@cri.or.th (M. Chittchang).

Table 1
Structures of lamellarins in group 1 and group 2.



Group 1 (with a C5–C6)	Group 2 (with a C5=C6)	Substituents									
		OR ¹	OR ²	Z	OR ³	OR ⁴	OR ⁵	OR ⁶	X	Y	
Lamellarin A ^a	–	OH	OMe	H	OH	OMe	OMe	OMe	OMe	OMe	OH
Lamellarin C	Lamellarin B	OH	OMe	H	OH	OMe	OMe	OMe	OMe	OMe	H
Lamellarin χ	Lamellarin D	OH	OMe	H	OH	OMe	OMe	OMe	OH	H	H
Lamellarin E	Lamellarin X	OH	OMe	H	OMe	OH	OMe	OMe	OMe	OH	H
Lamellarin F	Lamellarin ϵ	OH	OMe	H	OMe	OMe	OMe	OMe	OMe	OH	H
Lamellarin G	–	OMe	OH	H	OMe	OH	OMe	OH	OH	H	H
–	Lamellarin H ^d	OH	OH	H	OH	OH	OH	OH	OH	H	H
Lamellarin I	Lamellarin ζ	OH	OMe	H	OMe	OMe	OMe	OMe	OMe	OMe	H
Lamellarin J	Dehydrolam J ^b	OH	OMe	H	OMe	OMe	OMe	OMe	OH	H	H
Lamellarin K	Lamellarin M	OH	OMe	H	OH	OMe	OMe	OMe	OMe	OH	H
Lamellarin L	Lamellarin N	OH	OMe	H	OMe	OH	OMe	OH	OH	H	H
Lamellarin S ^a	–	OH	OH	H	OH	OH	OMe	OH	OH	H	H
Lamellarin T	Lamellarin W	OH	OMe	H	OMe	OH	OMe	OMe	OMe	OMe	H
Lamellarin U	Lamellarin α	OH	OMe	H	OMe	OH	OMe	OMe	OMe	H	H
Lamellarin V ^a	–	OH	OMe	H	OMe	OH	OMe	OMe	OMe	OMe	OH
Lamellarin Y	Dehydrolam Y ^b	OH	OMe	H	OMe	OH	OH	OMe	OMe	H	H
Lamellarin Z ^a	–	OMe	OH	H	OH	OH	OMe	OH	H	H	
Lamellarin β^a	–	OH	OH	H	OMe	OH	OH	OH	H	H	
Lamellarin γ^a	–	OH	OMe	OMe	H	OMe	OMe	OMe	OMe	OH	H
–	Lamellarin ϕ^a	OH	OMe	H	OH	OMe	OH	OMe	OMe	OMe	H
Dihydrolam η^b	Lamellarin η	OH	OMe	H	OMe	OMe	OMe	OMe	OMe	H	H

^a Synthesis in progress.

^b Unnatural lamellarins.

penetration, as observed by their low μM activity in whole cell models [25], but a number of them showed poor solubility under assay conditions). As a class, they have not been extensively profiled from a physicochemical point of view, and this is the goal of this study.

In this study, we experimentally determined logP values of 25 lamellarins synthesized in our laboratory since it is the single most important parameter affecting multiple ADMET parameters [35]. It is also one of the most difficult molecular properties to predict *in silico*. Given the importance of maintaining logP values in the range of oral drugs (~ 2.5) [36–38], we also investigated the structure–logP relationships of lamellarins and the validity of *in silico* methods. We subsequently assessed the relationship between this natural product class, natural product derivatives in development and on the market, oral marketed drugs, as well as drug molecules in development. Principal components analysis (PCA), in conjunction with computed and experimental molecular properties, was used for this purpose.

2. Results and discussion

2.1. Measured and predicted logP values of lamellarins

The results obtained from our experimental and theoretical efforts are given in Table 2. In Table 3, we summarize the results

further, listing the mean, standard deviation, minimum, and maximum obtained for 25 synthesized lamellarins from each logP method. We also report the root mean square error (RMSE) and a number of line of best fit statistics (r^2 , slope, intercept, and standard error (SE)) to allow for a meaningful inter-comparison of the values, both in terms of their absolute predictions and correlation with experimental data. See the [Supplementary Material and reference \[39\]](#) for more details regarding the statistics used here.

The mean experimental logP value for the 25 lamellarins tested here was 3.66. The standard deviation of data set was 0.71 log unit, with only one compound having a logP value > 5 putting the set in a reasonable area of logP space. However, not all calculation methods predicted the lamellarins as a class to have moderate lipophilicity. The most popular lipophilicity calculators, AlogP, ACD LogP, and ClogP, performed worst, predicting mean logP values of 5.11, 4.99, and 4.65, respectively. Their root mean square errors were therefore found to be large at 1.64, 1.57, and 1.15 log units, respectively. The best prediction was obtained from the OpenEye implementation of xlogP, displaying a mean value for the set of only 0.09 log unit from the experimental mean and the smallest RMSE of 0.44. Surprisingly, the three xlogP based methods used here, OE-xlogP, MI-xlogP, FAF-xlogP, showed predictions that varied considerably, displaying mean logP values of the set at 3.75, 4.16, and 4.23, respectively, with RMSEs of 0.44, 0.62, and 0.85, respectively. These variations arise from the subtle difference in the way

Table 2
Experimentally determined and calculated logP values of lamellarins.

Lamellarin	Experimental logP values (HPLC Method)	Calculated logP Values						
		MI-xlogP	OE-xlogP	FAF-xlogP	ACD LogP	ClogP	CSlogP	AlogP
Lamellarin A ^a	–	3.40	3.14	3.33	4.02	3.17	3.66	4.78
Lamellarin C	4.02 ± 0.001	4.06	3.69	3.80	5.32	4.39	3.91	5.38
Lamellarin B	4.93 ± 0.001	4.64	4.25	4.57	4.61	4.72	3.93	4.94
Lamellarin χ	2.78 ± 0.003	3.57	2.87	3.96	4.85	4.28	3.77	5.17
Lamellarin D	3.45 ± 0.001	4.15	3.43	4.74	4.14	4.76	3.79	4.73
Lamellarin E	3.14 ± 0.002	3.78	2.95	3.61	4.87	3.96	3.65	5.15
Lamellarin X	3.75 ± 0.001	4.36	3.51	4.38	4.16	4.38	3.67	4.71
Lamellarin F	3.49 ± 0.002	4.09	3.69	3.66	5.49	4.43	3.91	5.38
Lamellarin ε	4.10 ± 0.001	4.67	4.25	4.44	4.78	4.85	3.93	4.94
Lamellarin G	2.63 ± 0.002	3.57	2.87	3.96	4.84	4.28	3.77	5.17
Lamellarin H ^a	–	3.22	1.20	5.06	3.07	3.88	3.00	4.05
Lamellarin I	4.33 ± 0.002	4.36	4.43	3.85	6.02	4.87	4.17	5.60
Lamellarin ζ	5.19 ± 0.003	4.94	4.99	4.62	5.32	5.19	4.19	5.16
Lamellarin J	3.07 ± 0.002	3.87	3.61	4.01	5.55	4.75	4.04	5.39
Dehydrolam J	3.69 ± 0.004	4.45	4.17	4.79	4.85	5.24	4.06	4.95
Lamellarin K	3.15 ± 0.005	3.78	2.95	3.61	4.79	3.96	3.65	5.15
Lamellarin M	3.79 ± 0.004	4.36	3.51	4.38	4.08	4.38	3.67	4.71
Lamellarin L	2.74 ± 0.001	3.57	2.87	3.96	4.93	4.28	3.77	5.17
Lamellarin N	3.37 ± 0.007	4.15	3.43	4.74	4.22	4.76	3.79	4.73
Lamellarin S ^a	–	2.95	1.39	4.18	4.08	3.70	3.25	4.72
Lamellarin T	3.99 ± 0.005	4.06	3.69	3.80	5.40	4.39	3.91	5.38
Lamellarin W	4.83 ± 0.006	4.64	4.25	4.57	4.69	4.72	3.93	4.94
Lamellarin U	3.31 ± 0.007	3.87	3.61	4.01	5.69	4.75	4.04	5.39
Lamellarin α	3.98 ± 0.004	4.45	4.17	4.79	4.99	5.12	4.06	4.95
Lamellarin V ^a	–	3.40	3.14	3.33	4.10	3.17	3.66	4.78
Lamellarin Y	2.59 ± 0.005	3.57	2.87	3.96	4.93	4.28	3.77	5.17
Dehydrolam Y	3.21 ± 0.002	4.15	4.74	3.43	4.22	4.76	3.79	4.73
Lamellarin Z ^a	–	3.26	2.13	4.07	4.59	3.85	3.51	4.94
Lamellarin β^a	–	2.95	1.38	4.18	4.02	3.70	3.25	4.72
Lamellarin γ^a	–	4.48	3.47	3.93	5.42	4.78	3.91	5.38
Lamellarin ϕ^a	–	4.33	3.51	4.38	4.08	4.38	3.67	4.71
Dihydrolam η	3.65 ± 0.001	4.18	4.35	4.07	6.32	5.22	4.30	5.62
Lamellarin η	4.33 ± 0.004	4.76	4.91	4.84	5.61	5.59	4.32	5.18

^a Synthesis in progress. Used in the *in silico* profiling exercises only.

each method is implemented in practice. For example, the OpenEye has implemented a variant of xlogP, which utilizes a 2D approach rather than 3D, neglects the internal hydrogen bond term, and corrects subtle atom-type inconsistencies, with performance comparable to the original version [40]. The logP method implemented in ChemBioDraw Ultra, CSlogP, performed moderately well, with a mean predicted logP of 3.91 and an RMSE of 0.66.

While it is important to be able to accurately benchmark the lipophilicity of a given chemotype, it may be acceptable if a prediction method correlates well with the experimental parameter, even if the absolute values are not well predicted, potentially proving useful for SAR rationalization. Should a particular series be consistently under or over predicted, it may also be

possible to correct the absolute value to give results closer to the expected value. This we can assess using linear regression (Table 3). The line of best fit results showed that MI-xlogP ($r^2 = 0.83$), rather than OE-xlogP ($r^2 = 0.62$), correlated better with experimental logP values. The lower prediction error of the latter method is due to the fact that the un-regressed slope and intercept (Table 3) are closer to the line of unity than the former, but correcting all methods to remove any prediction bias, revealed that MI-xlogP would perform better than OE-xlogP. The line of best fit standard error, which can be considered as being analogous to the RMSE associated with the $Y = X$ line (see Supplementary Material Table S1), was 0.30 log unit, compared to 0.44 for OE-xlogP. The lower prediction error was because MI-xlogP was intrinsically better correlated with the experimental logP of the lamellarins. However, it was predicted with a greater bias than OE-xlogP, as can be seen from the slope and intercept in Table 3. Note while correcting the ACD LogP, ClogP, and AlogP values dramatically lowered their overall error, it was almost comparable to the standard deviation of the data, indicating they are still of limited utility.

To assess the value of corrected logP predictions further, we performed a leave-one out (LOO) cross-validation exercise for the two best performing methods: MI-xlogP and OE-xlogP. In this procedure, each compound was left out in turn and subsequently predicted using the line of best fit equation obtained from the other compounds. From the LOO results, we found that MI-xlogP displayed an r^2 of 0.80 and an SE of 0.32, compared to an r^2 of 0.54 and an SE of 0.49 for OE-xlogP, respectively, suggesting such an approach could have predictive potential. However, while correcting a prediction for a given series may be advantageous in the short term, care should be taken since such relationships have a tendency

Table 3
Summary of the experimental and theoretical logP results. Reported are the mean, minimum (Min) and maximum (Max) logP values for 25 synthesized lamellarins obtained from each method, as well as the standard deviation (SD) and the root mean square error (RMSE). Also given is the correlation coefficient obtained from the line of best fit between the experimental and theoretical logP measures, along with the corresponding slope, intercept, and standard error (SE).

ID	Mean	Min	Max	SD	RMSE	r^2 (slope/intercept/SE)
Experimental logP	3.66	2.59	5.19	0.71	–	–
MI-xlogP	4.16	3.57	4.94	0.40	0.62	0.83 (1.61/–3.02/0.30)
OE-xlogP	3.75	2.87	4.99	0.65	0.44	0.62 (0.86/0.44/0.44)
FAF-xlogP	4.23	3.61	4.84	0.42	0.85	0.19 (0.73/0.57/0.65)
ACD LogP	4.99	4.08	6.32	0.59	1.57	0.02 (0.16/2.85/0.71)
ClogP	4.65	3.96	5.59	0.41	1.15	0.29 (0.93/–0.68/0.61)
CSlogP	3.91	3.65	4.32	0.20	0.66	0.27 (1.89/–3.74/0.61)
AlogP	5.11	4.71	5.62	0.27	1.64	0.00 (–0.13/4.30/0.72)

to break down as more compounds in the series are synthesized, with markedly different functional groups or dramatic changes to the scaffold, leading them away from the so called model space [41,42].

2.2. Effects of structural modifications on logP

Apart from the correction factors for intramolecular interactions, the logP increments assigned for various atoms or fragments form the fundamental basis of most currently available calculation methods. As a result, the deviations between the calculated and measured logP values are partly governed by the reliability of those atomic and fragmental values which, in turn, depends on the methods and the classes of compounds from which these values have been derived. Additionally, a key problem with most logP software packages is that they typically assume almost constant logP increments associated with related substituent changes, even though equivalent substitutions at different positions can have dramatically different effects [43–46].

Since at least five of the currently available logP calculators did not appear applicable to lamellarins, a possible source of disparities between the calculated and experimental logP values of these compounds was investigated. The systematically diversified substitution patterns of the lamellarins used in this study enabled us to determine the logP increments resulting from various structural modifications around the lamellarin core. Those determinations were performed using the matched molecular pairs analysis [47] by comparing the logP values of any two lamellarin structures that differ only in each structural component being considered. The results are reported as the Δ logP values in Table 4.

The first structural modification considered was the conversion of the C5–C6 bond to a double bond. Interestingly, our HPLC determinations demonstrated that the introduction of a C5–C6 double bond into the D-ring of a lamellarin molecule consistently increased the logP value by an average of +0.70 log unit (Table 4). In contrast, the logP increments applied by various calculators for changing the C5–C6 bond to an olefin moiety widely ranged from only +0.02 log unit in CSlogP to –0.71 and +0.78 log unit in ACD LogP and FAF-xlogP, respectively.

Such a significant increase in the chromatographic logP values upon the introduction of the C5–C6 olefin is not likely to solely result from the modification of a particular bond which, theoretically, induces minimal changes in molecular weight, molecular volume, and polar surface area. However, the geometry of

lamellarin molecules is constrained to be more planar in the presence of the C5–C6 double bond [22,25]. This molecular planarity enhances intermolecular stacking interactions, which has been demonstrated to significantly increase lipophilicity of some compounds [48].

In contrast, all but two software programs consistently predicted a decrease in the logP values, albeit to different extents, of these compounds upon hydroxylation at either C5 or C7, as well as methoxylation at C7. Such predictions are conceivable since these oxygen-containing functional groups are capable of hydrogen bonding with water molecules. However, HPLC determinations demonstrated a relatively small decrease in the experimental logP values by –0.20 log unit upon hydroxylation at the C7 position (Table 4). On the contrary, substitution of the hydrogen atom at the C7 position with a methoxy group actually led to a substantial increase (by +0.77 log unit) in the experimental logP values.

These observations suggest that, when attached to the pentacyclic core structure of lamellarins, the oxygen atom in either a hydroxy group or a methoxy group becomes less accessible to interact with water molecules than when present in smaller compounds. Nonetheless, when C7 is hydroxylated, the H-bond donor property of the resulting aromatic OH group still remains to interact with water, leading to a small decrease in the logP values of lamellarins upon C7-hydroxylation. In contrast, methoxylation at the C7 position results in an aromatic ether, which is considered as an exceptionally poor H-bond acceptor [47,49]. As a result, the overall increase in the logP values experimentally observed upon C7-methoxylation was probably due to the hydrophobic interactions between the methyl component and the chromatographic stationary phase.

Another series of structural modifications investigated in this study involve methylation of various hydroxy groups around the lamellarin core. An increase in the logP values was observed for this transformation, as expected from both the removal of an H-bond donor and the increased hydrophobic interactions through the methyl group. Most of the logP calculators used in this study tend to predict very similar logP increments for this type of modifications at various positions (Table 4). Interestingly, our experimental results clearly indicated that the logP values of lamellarins were remarkably increased upon methylation of the hydroxy groups at C7, C8, or C9 positions on the pentacyclic lactone core. In contrast, a smaller effect was observed in the case of the same modification at either C13 or C14 residing on the aromatic ring orthogonal to the core structure.

Table 4
Effects of structural modifications on the logP values for the key lamellarin substitution positions.

Transformation	Pairs	Δ logP (log unit)							
		Experimental logP	MI-xLogP	OE-xlogP	FAF-xlogP	ACD LogP	ClogP	CSlogP	AlogP
C5–C6 → C5=C6	12	+0.70 ± 0.11	+0.58	+0.56	+0.78	–0.71	+0.41	+0.02	–0.44
5-H → 5-OH	2	^a	–0.66	–0.55	–0.47	–1.30	–1.23	–0.25	–0.60
7-H → 7-OH	4	–0.20 ± 0.04	–0.09	–0.66	–0.41	–0.83	–0.77	–0.39	–0.24
7-H → 7-OMe	4	+0.77 ± 0.10	+0.19	+0.08	–0.22	–0.30	–0.38	–0.13	–0.01
7-OH → 7-OMe	6	+0.98 ± 0.14	+0.28	+0.74	+0.19	+0.53	+0.39	+0.26	+0.23
8-OH → 8-OMe	4	+0.60 ± 0.03	+0.31	+0.74	+0.05	+0.77	+0.41	+0.27	+0.23
9-OH → 9-OMe	2	+0.75 ± 0.04	+0.30	+0.74	+0.05	+0.77	+0.42	+0.27	+0.22
13-OH → 13-OMe	8	+0.34 ± 0.01	+0.31	+0.74	+0.05	+0.62	+0.47	+0.26	+0.23
14-OH → 14-OMe	6	+0.29 ± 0.04	+0.30	+0.74	+0.05	+0.70	+0.47	+0.26	+0.22
20-OH → 20-OMe	1	^a	+0.31	+0.74	–0.11	+0.51	+0.15	+0.26	+0.22
8-OMe, 9-OH → 8-OH, 9-OMe	2	+0.16 ± 0.01	0.00	0.00	0.00	0.00	0.00	0.00	0.00
13-OMe, 14-OH → 13-OH, 14-OMe	6	–0.05 ± 0.03	0.00	0.00	0.00	+0.08	0.00	0.00	0.00
14-OMe, 15-H → 14-H, 15-OMe	1	^a	+0.39	–0.22	+0.27	–0.07	+0.35	0.00	0.00
20-OH, 21-OMe → 20-OMe, 21-OH	1	–0.11 ^b	0.00	0.00	0.00	–0.09	0.00	0.00	0.00

^a Pair(s) not available for experimental determination.

^b SD not determined as only one matched pair of lamellarins were available for comparison.

These findings suggest that similar substituents located on the orthogonal ring of lamellarins exhibit different physicochemical properties from those on the pentacyclic core. However, this is not unexpected given their distinctly different degrees of flexibility. In contrast, the two substituents located at C13 and C14 are more comparable in their physicochemical nature, considering that switching the hydroxy and methoxy groups between these two positions causes minimal changes in both the calculated and experimentally determined logP values (Table 4). All these findings demonstrate that not only the chemical nature, but also the position, of substituents could affect the lipophilicity of the molecules, as previously reported for smaller compounds [43–46].

In addition to the positional dependency, the experimental logP increments upon each modification were examined separately for the two groups of lamellarins (see Table 1), and then compared using *t*-test with unequal variances. Interestingly, no statistically significant ($p > 0.05$) differences were observed for any particular modifications in these two series of compounds, except for C7 substituent modifications. The logP increments for lamellarins in groups 1 and 2 were as follows: (a) -0.17 ± 0.01 vs. -0.23 ± 0.00 ($p = 0.049$) upon C7-hydroxylation, (b) $+0.68 \pm 0.00$ vs. $+0.86 \pm 0.01$ ($p = 0.018$) for C7-methoxylation, and (c) $+0.85 \pm 0.02$ vs. $+1.10 \pm 0.03$ ($p = 0.002$) for C7-OH methylation. These results provide additional evidence that the C7 substituents in these two series of compounds must be oriented differently, as predicted by our previously reported molecular modeling studies [25].

In summary, even though some of the logP increments used by certain software programs coincide with the values experimentally obtained for lamellarins in this study, most of them significantly deviate. This could be one of the reasons for the discrepancies between the calculated and experimental logP values of these compounds. Additional analogs with more diverse substitution patterns would be required to allow for the reliable estimation of the logP values of lamellarins. Nevertheless, the Δ logP values determined for each structural modification around the lamellarin core can be used to predict the lipophilicity of certain lamellarin analogs from the experimental logP values of their parent compounds.

2.3. Lamellarins vs. drugs, natural products, and compounds in development

The importance of benchmarking compounds to known areas of chemical space is evident from many publications in the area, including: Proudfoot et al. [50], who assessed the evolution of oral drugs over time; Oprea et al. [51], who compared drugs, candidates, lead-like and pub-like compounds; Wenlock et al. [52], who assessed the relationship between drugs and candidates in different stages of development; Ritchie et al. [53], who compared the relationship between inhaled, intranasal, and oral drugs; as well as O'Shea et al. [54], who assessed the overlap between antibacterials and a literature derived data set.

In this section, we compared the lamellarin chemotype to a set of relevant drug data sets from literature in order to understand the differences and devise the most effective way of developing this chemotype into one with more drug-like properties. To this end, we have compared the lamellarin molecules to other natural product derivatives in development and on the market, to oral marketed drugs, as well as to molecules in drug development. The comparison was performed using a range of fundamental physicochemical parameters, in conjunction with multivariate PCA (Fig. 1) and univariate statistical methods (Table 5).

The PCA based model of chemical space described 80% of the total variation in the data set analyzed, with component 1 describing the largest portion of information at 49%, followed by

14% by component 2, 10% by component 3, and 7% by component 4. This means that the descriptors used here have a high degree of correlation. To aid comprehension, we briefly explain how to interpret Fig. 1. Components 1 and 2 collectively described 63% of the total variation, and the molecular significance of the location of compounds on the scores plot (Fig. 1a) can be understood by considering the corresponding loadings plot (Fig. 1b). Descriptors with a large positive loading on the X-axis of Fig. 1b, such as MWT, have larger values for compounds with positive loadings on the scores plot (Fig. 1a), such as lamellarins, and smaller values for compounds with negative loadings. In contrast to MWT, the values of ABS have a negative loading on Fig. 1b so are thus inversely correlated with MWT (*i.e.*, decrease as MWT increases). This means lamellarins have lower ABS scores than oral drugs, but higher molecular weight. Finally, descriptors, such as MWT, PSA, and LIPINSKI, have comparable loadings on the X-axis of Fig. 1b, meaning they are highly correlated with each other.

Thus, we can relate the PCA components in a relatively crude way to aid interpretation: component 1 primarily separates large molecules (those with +ve coefficients on the X-axis of Fig. 1a) from smaller ones (–ve coeff.), component 2 separates basic molecules (+ve coeff.) from acidic molecules (–ve coeff.), component 3 separates lipophilic (–ve coeff.) from hydrophilic molecules (+ve coeff), and component 4 separates chiral (–ve coeff.) from achiral molecules (+ve coeff.). Analysis of Fig. 1 shows that lamellarins as a class occupy a position towards the edge of drug-like chemical space, as defined by the two most important components (Fig. 1a). While lamellarins occupy a central position on component 2 due to their lack of ionizable functionality, their size related characteristics result in them being located at the edge of component 1, and thus, oral drug space. On the components 3 and 4 (Fig. 1c), lamellarins occupy a more central position due in part to their reasonable lipophilicity and due to the lack of a chiral center, respectively.

However, lamellarins as a class do not have particularly extreme properties when compared to natural product treatments, either on the market or in development (note that 26% of these compounds are not shown in Fig. 1 as they have a loading > 9 on component 1), which suggests they still represent a good starting point for a lead optimization campaign, given their diverse oncological activities. For example, while the mean MWT of lamellarins at 522 Da is above the Lipinski cut-off, that of natural products in development is 712 Da, and 568 Da for those compounds on the market (Table 5). In addition, the mean logP for lamellarins is 3.4 log units, almost 1 log unit higher than oral drugs, and 2 log units higher than natural product drugs. However, the mean number of H-bond donors and acceptors are low, 2.7 and 1.1, respectively, suggesting there is considerable scope to increase the polarity of the molecules and reduce the logP further.

In recent years, a number of modifications by others have been made to the lamellarin skeleton, aiming to increase the polarity of these compounds. Most recently, the conjugation of lamellarin D with poly(ethylene) glycol (PEG) has been undertaken to address the physicochemical properties of lamellarins [55,56]. However, such conjugations, while potentially providing groups which increase aqueous solubility, inevitably increase molecular weight, molecular volume, and the number of H-bond donors/acceptors of the PEG-lamellarin adducts, pushing the molecules further from drug-like chemical space. From our physicochemical profiling exercise, we believe an approach is required to move the lamellarins towards a more optimal area of physicochemical parameter space that in conjunction will allow us to explore wider SAR space. To this end, we are virtually assessing synthetic derivatives of lamellarins that incorporate additional functionality in the form of alternative HBD, HBA, and ionizable groups at the various positions

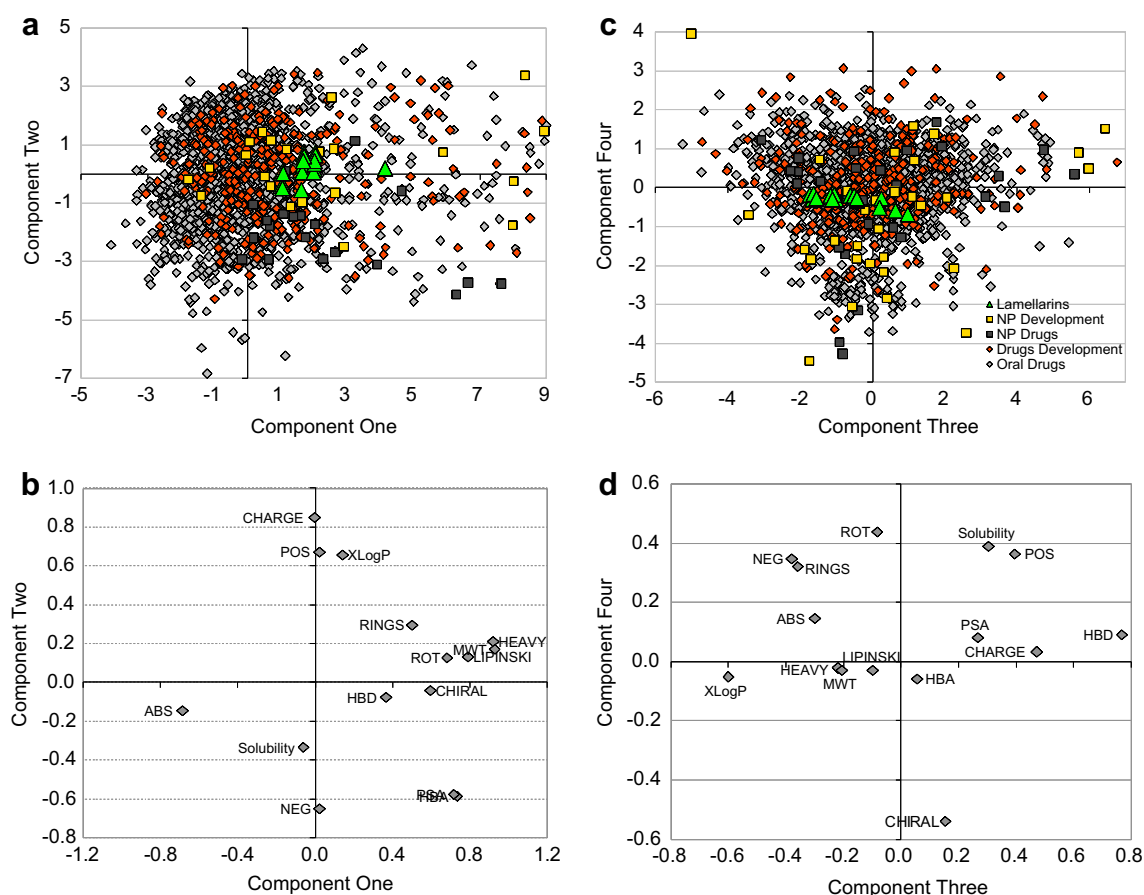


Fig. 1. PCA scores plot (top) and loadings plot (bottom) showing the relationship between the 3 natural product and 2 small molecule drug data sets using a range of computed molecular descriptors. Components 1 to 4 cumulatively described 49%, 63%, 73%, and 80% of the total variance, respectively. Lamellarin A is an outlier on component 1 due to its dramatically higher MWT and PSA, with lower ABS and Solubility scores. Note that 26% of NP drugs (12) and NP Development (9) compounds are excluded as they lie beyond 9 on component 1.

of substitution, as well as subtle changes to the lamellarin core. By virtually synthesizing and screening these molecules for both structural diversity and optimal physicochemical properties, we hope to efficiently explore the SAR of these compounds, while simultaneously making more developable molecules.

3. Conclusion

We have reported experimental and theoretical studies that help to increase our overall understanding of the physicochemical characteristics of lamellarins and how they compare to oral drugs, natural product drugs currently on the market, and new drugs in

development. We have put particular focus on lipophilicity, given it has widespread implications for multiple ADMET parameters, and because it is a difficult parameter to predict *in silico*. Thus, the experimental logP values of 25 lamellarins were determined using an industry standard HPLC method and correlated with the values calculated by different prediction methods. While most software assumes constant increments associated with related substituent changes, we show that this is not the case for these molecules, and that an equivalent substitution at different positions can have dramatically different effects. The discrepancies observed with theoretical methods emphasize the necessity of early experimental assessments to determine the lipophilicity characteristics of a given

Table 5
Mean and standard deviation of the molecular properties used in the profiling exercises.

ID	Oral drugs	NP drugs	Drugs in development	NP in development	Lamellarins
MWT	333.10 ± 121.09	568.20 ± 318.98	502.53 ± 485.41	711.87 ± 454.03	521.68 ± 27.02
OE-xlogP	2.48 ± 2.20	1.39 ± 3.51	2.40 ± 3.78	3.50 ± 3.07	3.40 ± 0.91
PSA	70.55 ± 45.22	176.07 ± 128.62	131.49 ± 209.37	178.88 ± 152.85	124.67 ± 12.56
CHARGE	0.26 ± 0.85	-0.30 ± 1.05	0.17 ± 1.26	0.34 ± 1.04	-
NEG	0.21 ± 0.41	0.48 ± 0.51	0.28 ± 0.45	0.22 ± 0.42	-
POS	0.48 ± 0.50	0.28 ± 0.46	0.46 ± 0.50	0.53 ± 0.51	-
HBA	2.77 ± 2.23	8.17 ± 5.00	4.9 ± 7.49	7.22 ± 5.96	1.06 ± 0.24
HBD	1.90 ± 1.68	4.57 ± 5.19	3.87 ± 8.51	5.09 ± 6.15	2.67 ± 1.14
Chiral centers	1.61 ± 2.73	7.39 ± 5.30	2.85 ± 5.65	7.44 ± 6.55	0.06 ± 0.24
ROT	5.48 ± 3.82	9.96 ± 7.28	11.03 ± 20.35	10.88 ± 12.18	4.88 ± 1.41
RINGS	1.84 ± 0.94	2.11 ± 1.14	2.44 ± 1.32	2.47 ± 1.29	2.00 ± 0.00
N	1791	46	2125	32	33

lead series. Having profiled a number of matched molecular pairs here, we have determined a set of more reliable logP increments (Table 4) which, if combined with logP increments determined for the core template or new templates, may be used to more reliably predict the lipophilicity of new lamellarin analogs. Our strategy moving forward is to use the corrected *in silico* logP estimates to help rationalize SAR, only benchmarking compounds that differ in terms of the template or introduce new functionality, saving material, operator time, and expense.

Lamellarins as a class lie towards the edge of drug-like chemical space. However, lamellarins do not have particularly extreme properties when compared to natural product treatments, either on the market or in development, which suggests they still represent a good starting point for a lead optimization campaign, given their diverse oncological activities. Considering their high MWT, moderate logP, along with low HBD and HBA counts, our strategy to move to more optimal area of chemical space involves the incorporation of additional polar functionality in the form of alternative HBD, HBA, and ionizable groups at the various positions of substitution, as well as larger changes to the lamellarin core to reduce their overall size.

In summary, the research work discussed herein is being used to more effectively direct our medicinal chemistry effort, with additional virtual studies being instigated to assess synthetic derivatives of lamellarins, to enable us to more efficiently explore the SAR of these compounds, while simultaneously making more developable, drug-like molecules.

4. Experimental protocol

4.1. Data sets

Natural sources of lamellarins are not sufficient to supply the quantities of compound required for comprehensive analytical or biological studies. Thus, all compounds which underwent experimental characterization in this study have been synthesized in our laboratory (Table 1). The details of the individual syntheses have been reported elsewhere [57].

The structures of oral marketed drugs [50] and compounds in development [51] were obtained from original quoted sources. The IDs of natural product drugs [4] and natural product compounds in development [3] were taken from the literature references they were reported in. The natural product structures were sourced from PubChem [58]. Compounds were excluded if they failed to calculate molecular descriptors. The full list of compounds used here can be found in the [Supplementary Material](#).

4.2. Experimental methods

Twenty-two naturally-occurring and three unnatural lamellarins, in groups 1 and 2 (Table 1), have been profiled in this study. Their logP values were experimentally determined using an industry standard reversed-phase HPLC method [59,60]. Briefly, the HPLC method entails analyzing each compound on an Agilent 1200 Series LC System (Agilent Technologies, Inc., Santa Clara, CA, USA) installed with a C18 column, using an isocratic elution (75% methanol/25% water) for up to 30 min.

The system was calibrated daily by determining the retention times (t_R) of 7 reference compounds with known logP values. Their retention factors (k) were then calculated, and the log k values were regressed against their corresponding literature logP values to generate a calibration curve. Subsequently, the retention factor of each lamellarin was determined using the same chromatographic conditions, and their logP value was then assessed from the

Table 6

Molecular descriptors computed in the study.

ID	Description	Ref.
HEAVY	No. of heavy atom count	[62]
CHIRAL	No. of chiral centers	[62]
HBA	No. of H-bond acceptors	[62]
HBD	No. of H-bond donors	[62]
MWT	Molecular weight	[62]
CHARGE	Net charge	[62]
NEG	No. of negative charges	[62]
POS	No. of positive charges	[62]
RINGS	No. of rings	[62]
ROT	No. of rotatable bonds	[62]
PSA	Polar surface area	[62]
LIPINSKI	No. of Lipinski failures	[33,62]
ABS	Absorption score	[34,62]
Solubility	Solubility score	[62]
OE-xlogP	logP prediction	[62]
MI-xlogP	logP prediction	[64]
FAF-xlogP	logP prediction	[65,66]
ACD LogP	logP prediction	[67]
ClogP	logP prediction	[68]
CSlogP ^a	logP prediction	[69]
AlogP	logP prediction	[70]

^a Crippen's fragmentation scheme used.

calibration curve constructed on the same day. Please refer to the [Supplementary Material](#) for further details.

4.3. Theoretical methods

Twenty-one commonly used molecular descriptors were computed for this study, consisting of 7 different logP predictions and 14 other molecular properties known to be important in defining drug-like property space (Table 6). These descriptors govern the key bulk property characteristics of molecules, and thus, are frequently used in compound profiling exercises [33,35,38,50].

The correlation between experimental and theoretical logP methods was investigated using linear regression in Microsoft Excel 2007 and SPSS 16.0 [61]. The relationship between lamellarins, oral drugs, natural product drugs, and compounds in development was assessed using PCA and OpenEye descriptors [62] only. The PCA model was also generated on oral drugs in SIMCA-P 10.0 [63], using standard settings (*i.e.*, mean centered and scaled descriptors, with the auto-fitting of components).

Acknowledgements

Financial support from the Thailand Research Fund (TRF; DBG5180015 to M.C., BRG5180013 to P.P.) is gratefully acknowledged. We also thank Dr. Prasat Kittakoop and Mr. Surasak Prachya (Laboratory of Natural Products, Chulabhorn Research Institute, Bangkok, Thailand) for their generous assistance with the reproducibility studies.

Appendix. Supplementary data

The supplementary data associated with this article can be found, in the online version, at [doi:10.1016/j.ejmech.2010.01.053](https://doi.org/10.1016/j.ejmech.2010.01.053).

References

- [1] J.W.-H. Li, J.C. Vederas, *Science* 325 (2009) 161–165.
- [2] M.S. Butler, *J. Nat. Prod.* 67 (2004) 2141–2153.
- [3] M.S. Butler, *Nat. Prod. Rep.* 25 (2008) 475–516.
- [4] A. Ganesan, *Curr. Opin. Chem. Biol.* 12 (2008) 306–317.
- [5] R.J. Andersen, D.J. Faulkner, C.-H. He, G.D. Van Duyne, J. Clardy, *J. Am. Chem. Soc.* 107 (1985) 5492–5495.

- [6] N. Lindquist, W. Fenical, G.D. Van Duyne, J. Clardy, *J. Org. Chem.* 53 (1988) 4570–4574.
- [7] A.R. Carroll, B.F. Bowden, J.C. Coll, *Aust. J. Chem.* 46 (1993) 489–501.
- [8] S. Urban, R.J. Capon, *Aust. J. Chem.* 49 (1996) 711–713.
- [9] M.V.R. Reddy, D.J. Faulkner, Y. Venkateswarlu, M.R. Rao, *Tetrahedron* 53 (1997) 3457–3466.
- [10] R.A. Davis, A.R. Carroll, G.K. Pierens, R.J. Quinn, *J. Nat. Prod.* 62 (1999) 419–424.
- [11] J. Ham, H. Kang, *Bull. Korean Chem. Soc.* 23 (2002) 163–166.
- [12] P. Krishnaiah, V.L.N. Reddy, G. Venkataramana, K. Ravinder, M. Srinivasulu, T.V. Raju, K. Ravikumar, D. Chandrasekar, S. Ramakrishna, Y. Venkateswarlu, *J. Nat. Prod.* 67 (2004) 1168–1171.
- [13] S.M. Reddy, M. Srinivasulu, N. Satyanarayana, A.K. Kondapi, Y. Venkateswarlu, *Tetrahedron* 61 (2005) 9242–9247.
- [14] S. Urban, M.S. Butler, R.J. Capon, *Aust. J. Chem.* 47 (1994) 1919–1924.
- [15] S. Urban, L. Hobbs, J.N.A. Hooper, R.J. Capon, *Aust. J. Chem.* 48 (1995) 1491–1494.
- [16] C. Bailly, *Curr. Med. Chem. Anti-Cancer Agents* 4 (2004) 363–378.
- [17] H. Fan, J. Peng, M.T. Hamann, J.-F. Hu, *Chem. Rev.* 108 (2008) 264–287.
- [18] A.R. Quesada, M.D. García Grávalos, J.L. Fernández Puentes, *Br. J. Cancer* 74 (1996) 677–682.
- [19] M.V.R. Reddy, M.R. Rao, D. Rhodes, M.S.T. Hansen, K. Rubins, F.D. Bushman, Y. Venkateswarlu, D.J. Faulkner, *J. Med. Chem.* 42 (1999) 1901–1907.
- [20] F. Ishibashi, S. Tanabe, T. Oda, M. Iwao, *J. Nat. Prod.* 65 (2002) 500–504.
- [21] C.P. Ridley, M.V.R. Reddy, G. Rocha, F.D. Bushman, D.J. Faulkner, *Bioorg. Med. Chem.* 10 (2002) 3285–3290.
- [22] M. Facompré, C. Tardy, C. Bal-Mahieu, P. Colson, C. Perez, I. Manzanares, C. Cuevas, C. Bailly, *Cancer Res.* 63 (2003) 7392–7399.
- [23] C. Tardy, M. Facompré, W. Laine, B. Baldeyrou, D. García-Grávalos, A. Francesch, C. Mateo, A. Pastor, J.A. Jiménez, I. Manzanares, C. Cuevas, C. Bailly, *Bioorg. Med. Chem.* 12 (2004) 1697–1712.
- [24] E. Marco, W. Laine, C. Tardy, A. Lansiaux, M. Iwao, F. Ishibashi, C. Bailly, *F. Gago, J. Med. Chem.* 48 (2005) 3796–3807.
- [25] M. Chittchang, P. Batsomboon, S. Ruchirawat, P. Ploypradith, *ChemMedChem* 4 (2009) 457–465.
- [26] D. Baunbæk, N. Trinkler, Y. Ferandin, O. Lozach, P. Ploypradith, S. Ruchirawat, F. Ishibashi, M. Iwao, L. Meijer, *Mar. Drugs* 6 (2008) 514–527.
- [27] J.L.F. Puentes, D. García Grávalos, A. Rodríguez Quesada, *World Patent WO/1997/001336* (1997).
- [28] J.L.F. Puentes, D. García Grávalos, A. Rodríguez Quesada, *U.S. Patent* 5,852,033 (1998).
- [29] J.L.F. Puentes, D. García Grávalos, A. Rodríguez Quesada, *U.S. Patent* 6,087,370 (2000).
- [30] A PharmaMar's report on <http://www.pharmamar.com/ElementoPrensa.aspx?prensa=247> (Presentations at AACR-NCI-EORTC International Conference demonstrate breadth and depth of PharmaMar's product pipeline, November 2003).
- [31] A PharmaMar's report on <http://www.pharmamar.com/ElementoPrensa.aspx?prensa=239> (PharmaMar presents preclinical data affirming the potential of its main compounds in sarcomas and leukaemias at the AACR Annual Meeting, April 2004).
- [32] A PharmaMar's report on <http://www.pharmamar.com/ElementoPrensa.aspx?prensa=145> (PharmaMar presents 13 posters at AACR highlighting clinical and preclinical development pipeline, April 2005).
- [33] C.A. Lipinski, F. Lombardo, B.W. Dominy, P.J. Feeney, *Adv. Drug Deliv. Rev.* 23 (1997) 3–25.
- [34] Y.C. Martin, *J. Med. Chem.* 48 (2005) 3164–3170.
- [35] M.P. Gleeson, *J. Med. Chem.* 51 (2008) 817–834.
- [36] T.I. Oprea, A.M. Davis, S.J. Teague, P.D. Leeson, *J. Chem. Inf. Comput. Sci.* 41 (2001) 1308–1315.
- [37] M.M. Hann, T.I. Oprea, *Curr. Opin. Chem. Biol.* 8 (2004) 255–263.
- [38] M.S. Lajiness, M. Vieth, J. Erickson, *Curr. Opin. Drug Discov. Dev.* 7 (2004) 470–477.
- [39] M.P. Gleeson, *J. Med. Chem.* 50 (2007) 101–112.
- [40] FILTER Manual version 2.0.1 on <http://www.eyesopen.com>.
- [41] Y.-J. Xu, H. Gao, *QSAR Comb. Sci.* 22 (2003) 422–429.
- [42] S. Weaver, M.P. Gleeson, *J. Mol. Graph. Model.* 26 (2008) 1315–1326.
- [43] F. Hollósy, J. Sepródi, L. Órfi, D. Erős, G. Kéri, M. Idei, *J. Chromatogr. B* 780 (2002) 355–363.
- [44] B. Hallgas, T. Patonay, A. Kiss-Szikszai, Z. Dobos, F. Hollósy, D. Erős, L. Órfi, G. Kéri, M. Idei, *J. Chromatogr. B* 801 (2004) 229–235.
- [45] B. Hallgas, Z. Dobos, E. Ósz, F. Hollósy, R.E. Schwab, E.Z. Szabó, D. Erős, M. Idei, G. Kéri, T. Lóránd, *J. Chromatogr. B* 819 (2005) 283–291.
- [46] B. Hallgas, Z. Dobos, A. Agócs, M. Idei, G. Kéri, T. Lóránd, G. Mészáros, *J. Chromatogr. B* 856 (2007) 148–155.
- [47] A.G. Leach, H.D. Jones, D.A. Cosgrove, P.W. Kenny, L. Ruston, P. MacFaul, J.M. Wood, N. Colclough, B. Law, *J. Med. Chem.* 49 (2006) 6672–6682.
- [48] M. Vrecl, M. Uršič, A. Pogačnik, L. Zupančič-Kralj, *J. Jan. Toxicol. Appl. Pharmacol.* 204 (2005) 170–174.
- [49] M.H. Abraham, P.P. Duce, D.V. Prior, D.G. Barratt, J.J. Morris, P.J. Taylor, *J. Chem. Soc. Perkin Trans. 2* (1989) 1355–1375.
- [50] J.R. Proudfoot, *Bioorg. Med. Chem. Lett.* 15 (2005) 1087–1090.
- [51] T.I. Oprea, T.K. Allu, D.C. Fara, R.F. Rad, L. Ostopovici, C.G. Bologna, *J. Comput. Aided Mol. Des.* 21 (2007) 113–119.
- [52] M.C. Wenlock, R.P. Austin, P. Barton, A.M. Davis, P.D. Leeson, *J. Med. Chem.* 46 (2003) 1250–1256.
- [53] T.J. Ritchie, C.N. Luscombe, S.J.F. Macdonald, *J. Chem. Inf. Model.* 49 (2009) 1025–1032.
- [54] R. O'Shea, H.E. Moser, *J. Med. Chem.* 51 (2008) 2871–2878.
- [55] D. Pla, A. Francesch, P. Calvo, C. Cuevas, R. Aligué, F. Albericio, M. Álvarez, *Bioconjug. Chem.* 20 (2009) 1100–1111.
- [56] D. Pla, M. Martí, J. Farrera-Sinfreu, D. Pulido, A. Francesch, P. Calvo, C. Cuevas, M. Royo, R. Aligué, F. Albericio, M. Álvarez, *Bioconjug. Chem.* 20 (2009) 1112–1121.
- [57] P. Ploypradith, T. Petchmanee, P. Sahakitpichan, N.D. Litvinas, S. Ruchirawat, *J. Org. Chem.* 71 (2006) 9440–9448.
- [58] PubChem on <http://pubchem.ncbi.nlm.nih.gov/>.
- [59] K. Valko, C. My Du, C. Bevan, D.P. Reynolds, M.H. Abraham, *Curr. Med. Chem.* 8 (2001) 1137–1146.
- [60] OECD Guidelines for Testing of Chemicals on http://www.oecd.org/document/40/0,3343,en_2649_34377_37051368_1_1_1_100.html.
- [61] SPSS; 16.0. SPSS Inc., Chicago, IL, USA, (2008).
- [62] FILTER; 2.0.1. OpenEye Scientific Software, Santa Fe, NM, USA, (2007) on <http://www.eyesopen.com>
- [63] SIMCA-P; 10.0. Umetrics AB, Umeå, Sweden, (2002) on <http://www.umetrics.com>.
- [64] Molinspiration Property Engine; 2009.01. Molinspiration Cheminformatics, Slovensky Grob, Slovak Republic, (2009) on <http://www.molinspiration.com>.
- [65] FAF-Drugs: Free ADME/tox Filtering. Ressource Parisienne en Bioinformatique Structurale (RPBS), Paris, France, (2006) on <http://bioserv.rpbs.univ-paris-diderot.fr/Help/FAFDrugs.html>.
- [66] M.A. Miteva, S. Violas, M. Montes, D. Gomez, P. Tuffery, B.O. Villoutreix, *Nucleic Acids Res.* 34 (2006) W738–744.
- [67] ACD/ChemSketch; 12.01. Advanced Chemistry Development, Inc., Toronto, ON, Canada, (2009) on <http://www.acdlabs.com>.
- [68] Bio-Loom; 1.5. BioByte Corporation, Claremont, CA, USA, (2005) on <http://www.biobyte.com>.
- [69] ChemBioDraw Ultra; 11.0.1. CambridgeSoft Corporation, Cambridge, MA, USA, (2007).
- [70] Accelrys® Discovery Studio®; 2.0. Accelrys Software Inc., San Diego, CA, USA, (2007).

DOI: 10.1002/cmdc.200800339

Cytotoxicities and Structure–Activity Relationships of Natural and Unnatural Lamellarins toward Cancer Cell Lines

Montakarn Chittchang,^[a, b] Paratchata Batsomboon,^[b] Somsak Ruchirawat,^[a, b] and Poonsakdi Ploypradith^{*[a, b]}

Twenty-two naturally occurring and three unnatural lamellarins were synthesized and evaluated for their cytotoxicities against cancer cells. Across eleven cancer cell lines derived from six different cancer types, the IC_{50} values of these compounds ranged from sub-nanomolar (0.08 nM) to micromolar (> 97.0 μ M). About one-fourth (6/25) and one-half (11/25) of these lamellarins are more potent than the positive control, etoposide, against at least six different cell lines and three different cell types, respectively. In

general, lamellarins D, X, ϵ , M, N, and dehydrolamellarin J are significantly more potent than the other lamellarins. The IC_{50} values were used to perform structure–activity relationship (SAR) studies by comparing the cytotoxic activities of several pairs of lamellarin structures that differ in selected substitution patterns. Our results not only reveal the importance of specific hydroxylation or methoxylation patterns for the first time, but also confirm prior findings and clarify some previous uncertainties.

Introduction

Lamellarins are a group of marine natural products initially isolated from mollusks and subsequently found in ascidians and sponges. Their discovery in 1985 by Faulkner and co-workers^[1] prompted research groups worldwide to screen their biological activities, conduct total or partial syntheses, and, more recently, investigate molecular mechanism(s) of their anticancer action. Interestingly, some lamellarins have been found to exhibit a wide array of promising biological activities, which include cytotoxicity, multi-drug resistance (MDR) reversal in some cancer cell lines, HIV-1 integrase inhibition, and immunomodulation.^[2,3]

Since 1985, over 35 of these polyaromatic pyrrole alkaloids have been isolated (Figure 1 and Table 1).^[1,4] Despite the lack

of other crucial information such as toxicity toward normal cell lines, chemical stability, and related pharmacological properties, considerable effort has been expended on the synthesis, biological evaluation, and the study of other biochemical properties on lamellarin D. This compound exhibits potent anticancer activity at nanomolar concentrations.^[5,6] Interactions between regions of lamellarin D and specific amino acid residues of the topoisomerase I–DNA ternary complex have been identified from molecular modeling studies.^[6] Additionally, the pro-apoptotic activity of lamellarin D has been correlated with its ability to promote DNA cleavage through stabilization of topoisomerase I–DNA covalent complexes and inhibition of the enzyme.^[7] Unlike lamellarin D and its structural analogues, the biological profiles—particularly the anticancer activities—of other lamellarins have been studied, but to a lesser extent.

Even though a majority of lamellarins (except lamellarins O–R) contain the same pentacyclic 2-pyrrolo(dihydro)isoquinoline lactone core and only differ in the substituents present on each ring (Figure 1 and Table 1), many exhibit rather diverse cytotoxic activities.^[8] Owing to their low natural abundance, total synthesis of the lamellarins is a pivotal alternative for pro-

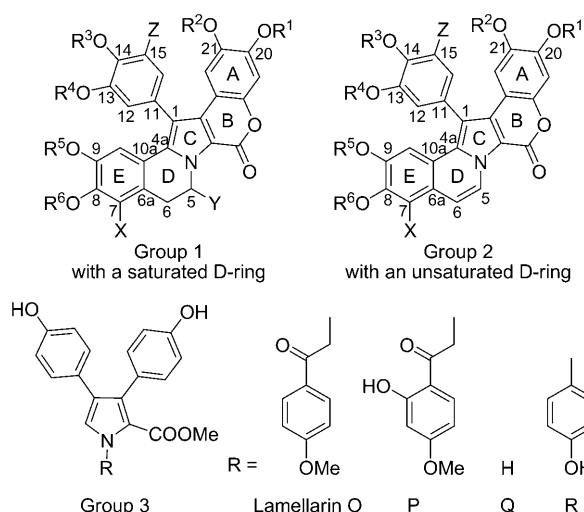


Figure 1. Structure of the lamellarins.

[a] Dr. M. Chittchang, Prof. Dr. S. Ruchirawat, Dr. P. Ploypradith
Laboratory of Medicinal Chemistry, Chulabhorn Research Institute
54 Moo 4, Vibhavadee-Rangsit Highway, Laksi, Bangkok 10210 (Thailand)
Fax: (+66) 2-574-2027
E-mail: poonsakdi@cri.or.th

[b] Dr. M. Chittchang, P. Batsomboon, Prof. Dr. S. Ruchirawat, Dr. P. Ploypradith
Chemical Biology Program, Chulabhorn Graduate Institute and
Center for Environmental Health, Toxicology and Management of
Chemicals
54 Moo 4, Vibhavadee-Rangsit Highway, Laksi, Bangkok 10210 (Thailand)

Supporting information for this article is available on the WWW under
<http://dx.doi.org/10.1002/cmdc.200800339>.

Table 1. Substituents around the lamellarin core.		Substituents								
Group 1	Group 2	R ¹	R ²	Z	R ³	R ⁴	R ⁵	R ⁶	X	Y
		Lamellarin A ^[a]	–	H	Me	H	H	Me	Me	Me
Lamellarin C	Lamellarin B	H	Me	H	H	Me	Me	Me	OMe	H
Lamellarin χ	Lamellarin D	H	Me	H	H	Me	Me	H	H	H
Lamellarin E	Lamellarin X	H	Me	H	Me	H	Me	Me	OH	H
Lamellarin F	Lamellarin ϵ	H	Me	H	Me	Me	Me	Me	OH	H
Lamellarin G	–	Me	H	H	Me	H	Me	H	H	H
–	Lamellarin H ^[a]	H	H	H	H	H	H	H	H	H
Lamellarin I	Lamellarin ζ	H	Me	H	Me	Me	Me	Me	OMe	H
Lamellarin J	Dehydrolam. J ^[b]	H	Me	H	Me	Me	Me	H	H	H
Lamellarin K	Lamellarin M	H	Me	H	H	Me	Me	Me	OH	H
Lamellarin L	Lamellarin N	H	Me	H	Me	H	Me	H	H	H
Lamellarin S ^[a]	–	H	H	H	H	H	Me	H	H	H
Lamellarin T	Lamellarin W	H	Me	H	Me	H	Me	Me	OMe	H
Lamellarin U	Lamellarin α	H	Me	H	Me	H	Me	Me	H	H
Lamellarin V ^[a]	–	H	Me	H	Me	H	Me	Me	OMe	OH
Lamellarin Y	Dehydrolam. Y ^[b]	H	Me	H	Me	H	H	Me	H	H
Lamellarin Z ^[a]	–	Me	H	H	H	H	Me	H	H	H
Lamellarin β ^[a]	–	H	H	H	Me	H	H	H	H	H
Lamellarin γ ^[a]	–	H	Me	OMe	–	Me	Me	Me	OH	H
–	Lamellarin ϕ ^[a]	H	Me	H	H	Me	H	Me	OMe	H
Dihydrolam. η ^[b,c]	Lamellarin η ^[c]	H	Me	H	Me	Me	Me	Me	H	H

[a] Synthesis in progress. [b] Unnatural lamellarins. [c] Not tested due to insolubility in DMSO.

viding sufficient quantities for further detailed biological evaluation. Because of their diverse biological activities, it is necessary to establish a comprehensive structure–activity relationship (SAR) for these compounds. Thus, a number of convergent and flexible synthetic routes have been designed and developed for the lamellarin framework.^[5,9]

Our research program on the total synthesis and medicinal aspects of lamellarins has focused on the design and execution of efficient synthetic routes.^[9f,j,m,o,s] Accordingly, natural and unnatural lamellarins with either a saturated or an unsaturated D-ring have been synthesized.^[9s] Herein, we report the evaluation of the cytotoxicities of these lamellarins against 11 cancer cell lines and disclose our observations on SARs that highlight the importance of the C5=C6 double bond in the D-ring and the substitution pattern on the periphery of the lamellarin core in relation to their cytotoxicity toward cancer cells.

Results and Discussion

Chemistry

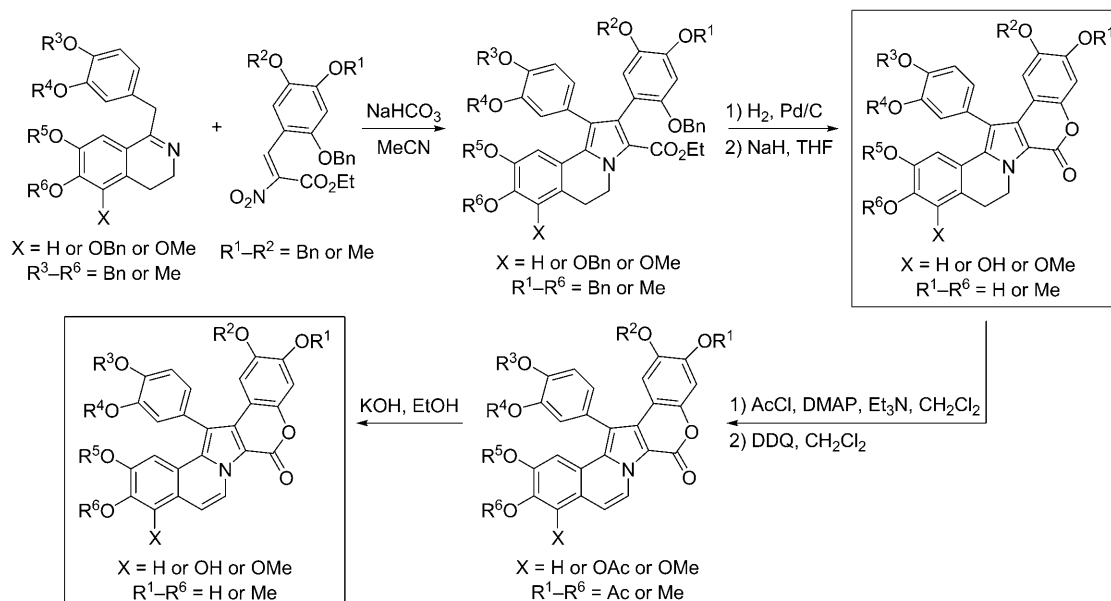
Lamellarins are classified into three structural groups, two of which possess either a “fused” saturated or unsaturated D-ring (groups 1 and 2, respectively; Figure 1). The third group, lamellarins O–R, on the other hand, contain an open structure lacking the B-, D-, and E-rings, and can be classified as 3,4-diaryl-2-carbomethoxypyrrole derivatives. Our modular synthetic strategies^[9s] have focused on the preparation of lamellarins with a saturated D-ring, which can then be converted directly into the corresponding lamellarins with an unsaturated D-ring via oxidation, as shown in Scheme 1. The key features of our synthetic strategies are: 1) the efficient Michael addition/ring clo-

sure (Mi-RC) condensation between the benzyldihydroisoquinoline and α -nitrocinnamate derivatives to form directly the 3,4-diaryl pyrrole core, 2) the sole use of benzyl and acetate as phenoxy protecting groups, 3) the stability of intermediates under the reaction conditions and to storage, and 4) minimal requirement of purification for each intermediate.

Cytotoxic activities

The cancer cell lines used in this study represent various types of cancer commonly found in a number of major tissues and organs. These include the hepatocellular carcinoma (HepG2 and S102) and cholangiocarcinoma (HuCCA-1) frequently found in Thailand. A multi-drug-resistant small-cell lung carcinoma (SCLC) cell line, H69AR, was also included in order to screen for potential candidates that may help circumvent the problem of multi-drug resistance. The use of human embryonic lung fibroblasts (MRC-5) serves to demonstrate the toxicity of selected lamellarins toward normal cells.

As shown in Table 2, a number of lamellarins exhibit potent anticancer activities, with IC₅₀ values in the nanomolar or low-micromolar range. While lamellarins D, K, and M are usually classified among the most cytotoxic molecules in the series,^[2] the results show that lamellarin N and dehydrolamellarin J are also promising candidates. These compounds are significantly more potent than the other lamellarins and the positive control, etoposide, in most cancer cell lines. Moreover, both of them exhibit relatively low toxicity toward MRC-5 cells, in contrast to the other compounds tested, especially lamellarins D, M, X, and ϵ , that have similar cytotoxic activities toward cancer cells.



Scheme 1. Synthetic route used for the preparation of natural and unnatural lamellarins with either a saturated or an unsaturated D-ring.

Table 2. Cytotoxic activities of lamellarins.^[a]

Compound	IC ₅₀ [μM]											
	Oral KB	Lung		Breast		Liver			Cervix	Blood cell		Fibroblast
		A549	H69AR	T47D	MDA-MB-231	HuCCA-1	HepG2	S102	HeLa	P388	HL-60	MRC-5
Lamellarin C	5.7	3.6	12.1	7.7	8.3	11.5	18.3	4.4	7.9	4.2	5.7	ND
Lamellarin B	4.4	5.4	6.4	0.2	4.4	5.3	0.8	5.9	4.8	6.1	6.2	68.1
Lamellarin χ	2.6	2.0	38.9	3.8	4.8	49.9	0.1	3.4	6.6	1.6	1.8	ND
Lamellarin D	0.04	0.06	0.4	0.00008	0.4	0.08	0.02	3.2	0.06	0.1	0.04	9.2
Lamellarin E	4.0	2.2	7.2	5.3	3.4	9.4	1.0	2.8	5.3	2.6	4.5	ND
Lamellarin X	0.08	0.3	0.3	0.006	0.08	0.04	0.2	1.6	0.09	0.3	0.2	10.1
Lamellarin F	4.2	4.4	10.1	4.6	3.7	8.8	0.5	2.7	6.4	3.1	3.6	ND
Lamellarin ε	0.3	0.3	2.3	0.006	0.3	0.07	0.1	2.1	0.3	0.3	0.1	25.8
Lamellarin G	3.0	4.0	7.4	8.6	15.0	49.9	1.5	9.6	4.2	1.6	7.5	ND
Lamellarin I	6.3	10.6	18.1	9.5	8.6	11.2	1.3	12.4	11.2	3.8	6.9	ND
Lamellarin ζ	4.7	10.6	23.3	0.09	4.7	6.3	0.3	7.9	8.3	7.2	12.3	> 89.7
Lamellarin J	> 97.0	1.1	> 97.0	13.0	7.4	> 97.0	0.4	19.4	> 97.0	0.8	0.9	ND
Dehydrolam. J	0.08	0.04	0.3	0.0001	0.4	0.006	0.01	2.1	0.08	0.08	0.04	> 97.4
Lamellarin K	0.9	4.2	4.3	0.09	0.4	3.4	1.0	4.4	2.8	3.4	3.8	ND
Lamellarin M	0.2	0.04	0.3	0.009	0.1	0.06	0.02	1.9	0.3	0.1	0.06	13.4
Lamellarin L	3.0	0.8	3.0	4.4	1.8	21.9	0.3	1.4	2.8	0.5	1.9	ND
Lamellarin N	0.06	0.04	0.06	0.0006	0.6	0.008	0.02	2.3	0.04	0.08	0.04	> 100.1
Lamellarin T	6.4	2.9	13.2	13.2	8.6	14.7	0.6	5.5	9.9	4.8	6.4	ND
Lamellarin W	5.3	5.2	4.4	4.2	5.2	4.2	0.9	5.8	5.0	5.6	6.7	28.5
Lamellarin U	3.9	0.9	8.7	10.3	4.5	44.6	0.6	3.0	5.0	1.8	4.5	ND
Lamellarin α	9.4	1.6	8.0	0.6	3.9	5.8	0.06	5.6	7.6	1.7	10.5	> 97.4
Lamellarin Y	5.0	0.9	14.8	7.2	8.0	37.9	0.6	4.3	29.9	1.0	5.0	ND
Dehydrolam. Y	0.8	1.3	7.6	0.08	0.6	1.4	0.4	6.2	1.6	0.9	3.4	31.0
Dihydrolam. η	NA	NA	NA	NA	NA	NA	NA	NA	NA	NA	NA	NA
Lamellarin η	NA	NA	NA	NA	NA	NA	NA	NA	NA	NA	NA	NA
Etoposide	0.5	1.1	45.9	0.08	0.2	6.8	0.2	1.5	0.4	0.4	2.3	> 85.0

[a] ND = not determined, as these group 1 lamellarins are generally less cytotoxic than their group 2 counterparts, and are therefore less likely to be toxic to normal cells. NA = not available due to insolubility of the compounds in DMSO. Cell lines used (in alphabetical order): A549, human non-small-cell lung carcinoma; H69AR, human multi-drug-resistant small-cell lung carcinoma; HeLa, human cervical adenocarcinoma; HepG2, human hepatocellular carcinoma; HL-60, human promyelocytic leukemia; HuCCA-1, human cholangiocarcinoma; KB, human oral epidermoid carcinoma; MDA-MB-231, human hormone-independent breast cancer 231; MRC-5, human fetal/embryonic lung fibroblast; P388, mouse lymphoid neoplasm; S102, human hepatocellular carcinoma; T47D, human hormone-dependent breast cancer.

Interestingly, lamellarin N and dehydrolamellarin J also demonstrate appreciable cytotoxic activity against the multi-drug-resistant H69AR cell line, relative to etoposide. It has been shown that some lamellarins effectively reverse multi-drug resistance by inhibiting P-glycoprotein.^[8] However, this might not be the case for H69AR cells, which, unlike most multi-drug-resistant cell lines, do not overexpress P-glycoprotein.^[10] In fact, the alternative resistance mechanisms in this cell line have been shown to involve decreased susceptibility to drug-induced DNA damage and reduced levels of topoisomerase II,^[11,12] as well as overexpression of multi-drug-resistance-associated protein (MRP).^[13,14]

Additionally, some lamellarins show selective cytotoxicities toward certain cancer cell lines, whereas some are broadly toxic against all cell lines under evaluation. The most prominent selectivity is observed with the human breast cancer T47D and MDA-MB-231 cells, which differ mainly in the presence and absence of estrogen receptors (ER), respectively. One plausible explanation is that these lamellarins may also act as anti-estrogens in inhibiting the proliferation of ER-positive T47D cells, whereas this mechanism may not be possible for ER-negative MDA-MB-231 cells. Nevertheless, the actual reasons for the selectivity remain to be investigated.

SAR studies

In an early attempt to correlate the structures of lamellarins with their cytotoxic activities, Quesada et al.^[8] observed that an increase in the number of methylations and/or methoxylations appears to cause a decrease in the antitumor activities of the 13 lamellarins tested in their studies. Most subsequent SAR studies have been directed at derivatives of lamellarin D by using their mechanism-based (i.e., topoisomerase I inhibition) activities in relation to their cytotoxicities against cancer cell lines. It has been demonstrated that the full pentacyclic structure of lamellarins is important for their biological activity. Simplification of the lamellarin D structure by opening the lactone ring results in a significant decrease in cytotoxicity toward certain human tumor cell lines.^[9] Another general observation made from these limited studies focusing on the lamellarin D series is that the planarity of the pharmacophore conferred by the C5=C6 double bond is also essential for cytotoxicity and topoisomerase I inhibition.^[6,15] Unfortunately, as reported by Quesada et al.,^[8] such a relationship does not hold for lamellarins K and M. These compounds contain the same substituents, but differ in the nature of the C5–C6 bond (see Table 1). However, they possess roughly the same cytotoxicity, and furthermore, lamellarin K triacetate is even more cytotoxic than lamellarin M triacetate.

Additionally, Ishibashi et al.^[5] have demonstrated that the hydroxy groups at the C8 and C20 positions of lamellarin D are important structural requirements for cytotoxic activity, whereas neither the hydroxy group at C14 nor the two methoxy groups at C13 and C21 are necessary. However, it was subsequently reported by Tardy et al.^[15] that all of the phenolic hydroxy groups at each of the C8, C14, and C20 positions of lamellarin D are important for maintaining the activity against

topoisomerase I and potent cytotoxic action. It was also found that these groups could be substituted with positively charged amino acid derivatives without loss of activity. Furthermore, it was pointed out in a review article that almost any modifications of the substitution pattern on lamellarin D decrease the cytotoxicity of the molecule.^[2]

The discrepancies of the previous findings observed with lamellarin D derivatives have prompted us to execute a more comprehensive SAR investigation of the lamellarins in groups 1 and 2, beyond the lamellarin D series, to clarify the importance of each substituent on the lamellarin skeleton. The number and diversity of the substitution patterns of the lamellarins investigated in this study allow us to compare the cytotoxic activities of several pairs of lamellarins, which differ only in substitution at the positions of interest.

The first structural element considered was the C5=C6 double bond in the D-ring. The importance of this functionality for the cytotoxic activities of these compounds was studied by comparing the IC₅₀ values of 11 pairs of lamellarins, each of which contains exactly the same substituents and differs only in the nature of the C5–C6 bond. As shown in Figure 2, the results unequivocally indicate that, in most cases, the presence of the C5=C6 double bond significantly decreases the IC₅₀

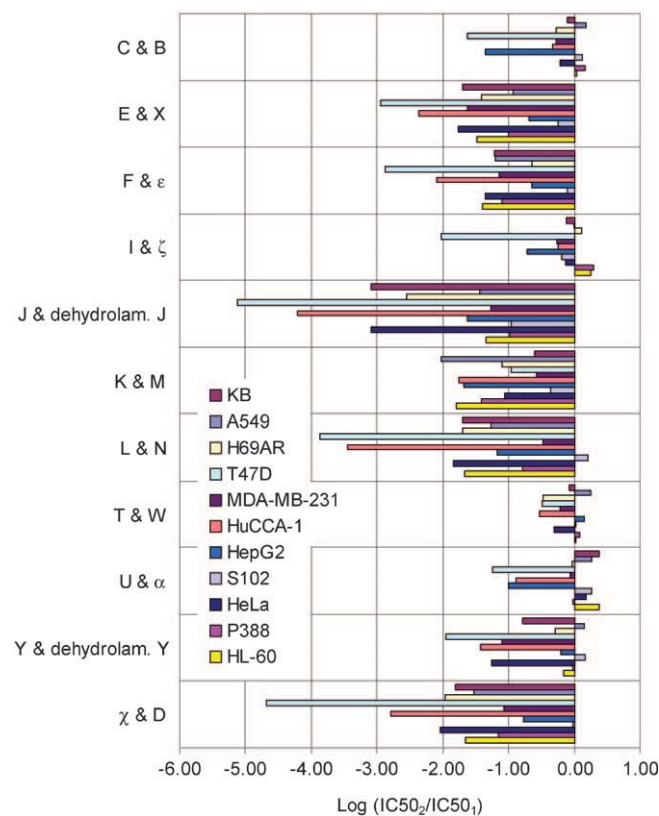


Figure 2. Contributions of the C5=C6 double bond in the D-ring to the cytotoxic activities of various lamellarins toward cell lines (indicated by color). The IC₅₀ values of two structures differing in one given position were compared, and the logarithm of the IC₅₀ ratio was subsequently determined with the IC₅₀ values of the compounds after and before the modification in the numerator and denominator, respectively. Positive log(IC₅₀ ratio) values indicate a loss of cytotoxic activity, whereas negative values show an increase in the activity upon the structural modification being considered.

values, that is, increases the cytotoxic activities of the lamellarins.

It has been pointed out previously that, in the case of lamellarin D, the planarity of the pentacyclic lamellarin core is essential for intercalation into DNA and topoisomerase I inhibition.^[6] On the other hand, replacement of the C5=C6 double bond in lamellarin D by a single bond in lamellarin 501, subsequently isolated from natural sources and named lamellarin χ , introduces a large kink into the core structure and abolishes the capacity of the molecule to insert between two consecutive base pairs in the DNA.

Among all the lamellarins investigated, the substituent at C7 may be a hydrogen atom, a hydroxy group, or a methoxy group. To our knowledge, the contribution of the substituent at this particular position to the cytotoxic activities of lamellarins has not been reported previously. As shown in Figure 3a, substitution of the hydrogen atom at C7 with a hydroxy group significantly increases the cytotoxicities of lamellarins with a C5=C6 double bond (compare lamellarin α and lamellarin X). On the other hand, methoxylation at this position may only slightly affect the cytotoxic activities of these compounds (Figure 3b). However, it is difficult to evaluate any trend conclusively in this case, as only two pairs of lamellarins were available for comparison.

Interestingly, the effect is significantly more pronounced if the C7 hydroxy group is replaced by a methoxy group. This clearly decreases the cytotoxic activities of the lamellarins, especially those containing a C5=C6 double bond (Figure 3c). These results indicate that the hydroxy group at this position is an important structural element that may also feature in an interaction with the putative biological target(s).

In the case of the substituent at C8 in the two pairs of the lamellarins examined in this study, the results clearly show that methylation of the hydroxy group at this position decreases cytotoxic activity (Figure 4). The effect is much more prominent if the C5=C6 single bond in lamellarin L and lamellarin U is replaced by a double bond in lamellarin N and lamellarin α , respectively. However, due to the rather limited number of lamellarins for direct comparison at this position, additional lamellarins that differ from the others exclusively at C8 are targets of our future investigations.

On the other hand, methylation of the hydroxy group at C9, C13, or C14 induces rather more subtle changes in cytotoxic activity (Supporting Information figures S1 and S2). Whereas the significance of the C9 hydroxy group has not been reported before, the relative lack of influence that substituents at C13 and C14 have toward cytotoxic activity agrees well with observations of the lamellarin D derivatives reported by Ishibashi et al.^[5] More importantly, switching the hydroxy and methoxy groups between these two positions does not significantly affect cytotoxicity in most cases (Supporting Information figure S3). Nevertheless, additional lamellarin derivatives with

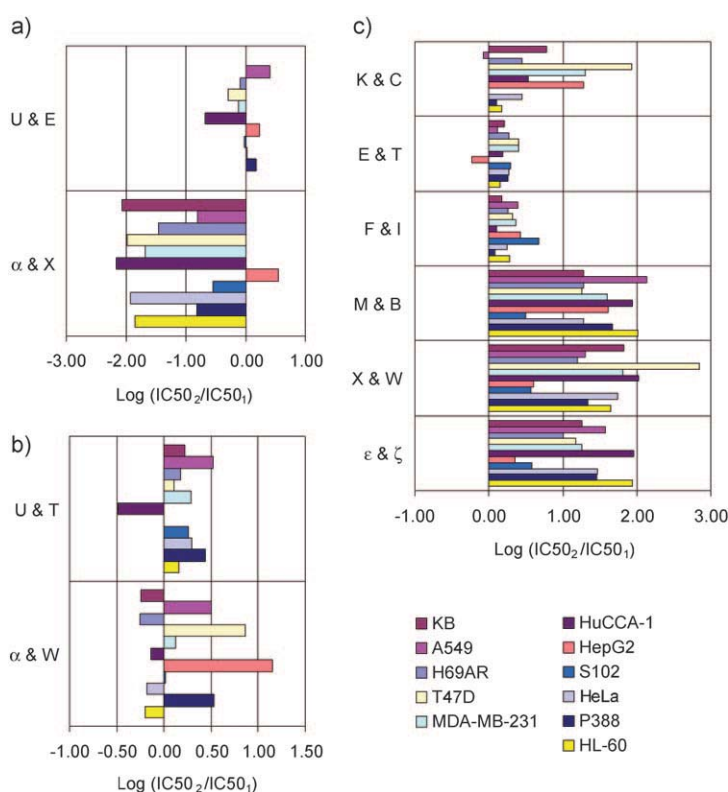


Figure 3. Contributions of the hydroxylation/methoxylation pattern at the C7 position of lamellarins to their cytotoxic activities: a) H vs. OH, b) H vs. OMe, c) OH vs. OMe. Increases or decreases in cytotoxicity were determined as described in Figure 2.

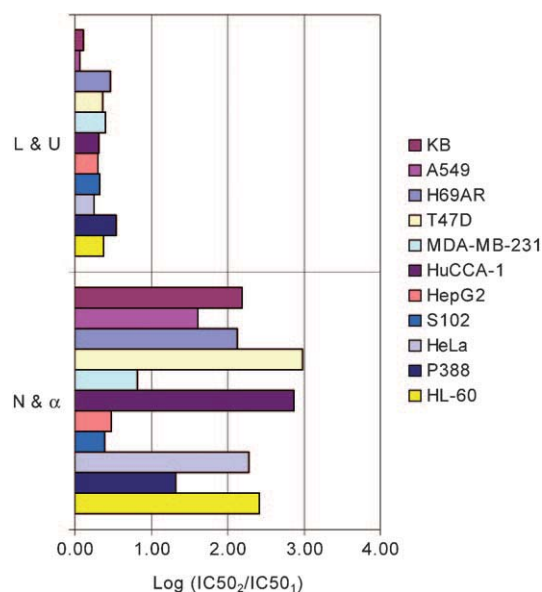


Figure 4. Contributions of the hydroxylation/methoxylation pattern (OH vs. Ome) at the C8 position of lamellarins to their cytotoxic activities. Changes in cytotoxicity were determined as described in Figure 2.

modified C13 and C14 substituents are currently being synthesized by our research group for further investigations.

Even though most naturally occurring lamellarins contain a hydroxy group at C20 and a methoxy group at C21, there is

one pair of lamellarins, lamellarin L and lamellarin G, in which these two substituents are reversed. As shown in Table 2, interchange of the C20 hydroxy and C21 methoxy groups of lamellarin L to provide lamellarin G results in a substantial decrease in cytotoxic activity against most of the cell lines tested in this study (Supporting Information figure S4). These results agree well with all previous findings, including the observation that the C20-sulfated form of lamellarins usually show little or no cytotoxicity, in contrast to the non-sulfated analogues with a free C20 hydroxy group. Instead, the presence of a sulfate group at this position appears to be a key structural element for HIV-1 integrase inhibition by lamellarins.^[9g]

According to all the results from our SAR studies, there appear to be four important structural elements that determine the cytotoxic activities of lamellarins toward cancer cells. These include the C5=C6 double bond as well as the C7, C8, and C20 hydroxy groups (Figure 5). Based on their cytotoxic activities, the lamellarins with an unsaturated D-ring may be subdivided into two categories (Table 3): those with lower cytotoxicities all contain only the C5=C6 double bond and a C20 hydroxy group, whereas the more potent compounds also contain a hydroxy group at either C7 or C8. Such a group may provide additional interactions with the target biological macromolecules. Notably, the other substituents that play a less

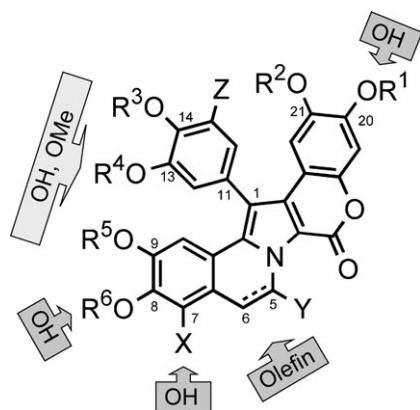


Figure 5. Important structural elements in the lamellarin skeleton.

important role are located toward the inner part of the lamellarin molecule.

Molecular modeling studies

The results from our preliminary molecular modeling studies using HyperChem 7.5 show that the C5=C6 double bond ensures planarity of the molecule and also affects the spatial array of the substituents around the periphery of the lamellarin skeleton, especially those on the E-ring (C7, C8, and C9). The group 1 lamellarins bearing a C5=C6 single bond are twisted, as most clearly observed if the molecules are viewed side-on from the E-ring (Figure 6a and 6c compared with Figure 6b and 6d, respectively), resulting in the spatial displacement of the substituents, most notably on the E-ring. As summarized in Table 4, the E-ring of group 1 lamellarins assumes a dihedral angle θ about C6a–C10a–C4a–C1 of much less than 180° ($164.7\text{--}166.7^\circ$), significantly different from the planarity otherwise present in the group 2 lamellarins ($\theta = 179.0\text{--}180.0^\circ$).

The orientation of the E-ring may be the factor that accounts for the more pronounced and more easily distinguished effects generally observed in the group 2 lamellarins as substituents are varied. These compounds with the unsaturated D-ring possess a more rigid framework and better alignments of the substituents around the pyrrole core than those in the group 1 lamellarins. Therefore, the C5=C6 double bond may exert its effect not only by making the molecule planar and thus suitable for intercalating the topoisomerase I–DNA complex, but also by spatially aligning the substituents, especially those on the E-ring, to their respective amino acid residues of the enzyme. It has been reported that the hydroxy groups at C8 and C20 are within hydrogen-bonding distance from Asn 722 and Glu 356 of the enzyme, respectively, whereas the ester carbonyl group interacts with the Arg 364 residue.^[6]

Conclusions

We have disclosed herein a comprehensive evaluation of the cytotoxic activities of the lamellarins against a number of

Group	Lamellarin	IC ₅₀ [μM] to MRC-5	Substituents								
			OR ¹ (C20)	OR ⁶ (C8)	X (C7)	OR ² (C21)	Z (C15)	OR ³ (C14)	OR ⁴ (C13)	OR ⁵ (C9)	Y (C5)
Less cytotoxic	Lamellarin B	68.1	OH	OMe	OMe	OMe	H	OH	OMe	OMe	H
	Lamellarin W	28.5	OH	OMe	OMe	OMe	H	OMe	OH	OMe	H
	Lamellarin ζ	> 89.7	OH	OMe	OMe	OMe	H	OMe	OMe	OMe	H
	Lamellarin α	> 97.4	OH	OMe	H	OMe	H	OMe	OH	OMe	H
	Dehydrolam. Y ^[b]	31.0	OH	OMe	H	OMe	H	OMe	OH	OH	H
Highly cytotoxic	Lamellarin D	9.2	OH	OH	H	OMe	H	OH	OMe	OMe	H
	Lamellarin N	> 100.1	OH	OH	H	OMe	H	OMe	OH	OMe	H
	Dehydrolam. J ^[b]	> 97.4	OH	OH	H	OMe	H	OMe	OMe	OMe	H
	Lamellarin M	13.4	OH	OMe	OH	OMe	H	OH	OMe	OMe	H
	Lamellarin X	10.1	OH	OMe	OH	OMe	H	OMe	OH	OMe	H
	Lamellarin ϵ	25.8	OH	OMe	OH	OMe	H	OMe	OMe	OMe	H

[a] See Table 2. [b] Unnatural lamellarins.

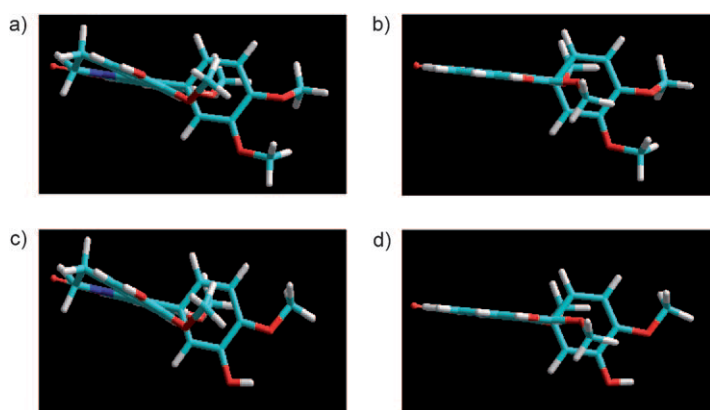


Figure 6. Energy-minimized structures of selected lamellarins calculated by using the AM1 method in HyperChem 7.5: a) lamellarin J (with a dihedral angle θ about C6a–C10a–C4a–C1 of 164.7°), b) dehydrolamellarin J ($\theta = 179.9^\circ$), c) lamellarin L ($\theta = 164.8^\circ$), d) lamellarin N ($\theta = 179.8^\circ$).

Lamellarin	Dihedral angle θ [°]	
	6a–10a–4a–1	4a–1–11–12
Lamellarin C	166.6	88.3
Lamellarin B	180.0	91.8
Lamellarin χ	165.1	89.4
Lamellarin D	180.0	91.6
Lamellarin E	164.9	89.5
Lamellarin X	179.0	90.4
Lamellarin F	164.9	89.3
Lamellarin ϵ	179.8	91.8
Lamellarin I	166.7	88.6
Lamellarin ζ	179.9	97.4
Lamellarin J	164.7	90.2
Dehydrolam. J	179.9	92.2
Lamellarin K	165.2	88.8
Lamellarin M	179.8	92.3
Lamellarin L	164.8	89.7
Lamellarin N	179.8	90.6
Lamellarin T	166.4	87.8
Lamellarin W	179.9	91.8
Lamellarin U	164.8	89.8
Lamellarin α	179.9	91.0
Lamellarin Y	165.5	86.9
Dehydrolam. Y	179.9	89.1
Dihydrolam. η	165.2	90.0
Lamellarin η	179.9	93.4

cancer cell lines. This study reveals that some of these compounds may be potential candidates for anticancer drug development. In addition, the results of the SAR studies have helped delineate the important structural elements in the lamellarin skeleton that contribute to cytotoxicity. These data will be employed for the structure optimization of these compounds in order to improve their efficacy, safety, as well as their physicochemical and pharmacokinetic properties.

The contributions from the C5=C6 double bond as well as the C8 and C20 hydroxy groups toward the overall anticancer activity are in good agreement with previously reported data. Importantly, this study reveals for the first time a significant contribution from the C7 substituent. Previous SAR studies

have focused on lamellarin D and its derivatives that only possess a hydrogen atom at C7. It is noted that because the point-to-point comparisons of substituents at C13 and C14 give unclear results, possibly due to their flexibility, the importance of these positions toward anticancer activity remains to be evaluated.

Information from our current and planned SAR studies is critical for streamlining structural requirements for good anticancer activity. Further structural modifications that increase aqueous solubility or lower toxicity toward normal cells can then be made at those positions known not to have a marked effect on the anticancer activity.

Experimental Section

Syntheses of lamellarins

Two series of natural and unnatural lamellarins, containing either a saturated or an unsaturated D-ring, were previously synthesized and fully characterized using our established methodologies.^[9s] All compounds were purified by crystallization from appropriate solvent systems, and the purified lamellarins were stored at 4 °C without solvent until use.

Spectroscopic data (¹H NMR, ¹³C NMR, and HRMS-TOF) were used to confirm the identity of the compounds by comparing them with previously reported data. For unnatural lamellarins, their spectroscopic data were correlated with those of the natural lamellarins for structure elucidation. The purity of compounds was estimated based on their melting point ranges, the cleanliness of both ¹H NMR and ¹³C NMR spectra, as well as their HPLC traces. Only trace amounts of impurities, if any, could be detected by HPLC analyses (Supporting Information table S1).

Cell culture

Four commercially available cancer cell lines (A549, H69AR, HepG2, and T47D) were obtained from the American Type Culture Collection (ATCC, Manassas, VA, USA). Additionally, KB and P388 cell lines were obtained from the University of Illinois at Chicago (Chicago, IL, USA), whereas HeLa, HL-60, and MDA-MB-231 cell lines were obtained from the University of Texas M. D. Anderson Cancer Center (Houston, TX, USA). Human cholangiocarcinoma (HuCCA-1) and human hepatocellular carcinoma (S102) cells were obtained from Thai patients as previously reported.^[16,17] The human lung fibroblast (MRC-5) cells were generously provided by the Armed Force Research Institute of Medical Sciences (AFRIMS, Bangkok, Thailand).

All cell lines were maintained using standard procedures in the appropriate culture media supplemented with the nutrients essential for each cell line (Supporting Information table S2). All culture media and fetal bovine serum (FBS) were obtained from HyClone Laboratories (Logan, UT, USA), whereas L-glutamine, dimethyl sulfoxide (DMSO), glucose, sodium pyruvate, non-essential amino acids, bovine insulin, crystal violet, 2,3-bis[2-methoxy-4-nitro-5-sulphophenyl]-2H-tetrazolium-5-carboxyanilide (XTT) sodium, phenazine methosulfate (PMS), and etoposide were obtained from Sigma (St. Louis, MO, USA). All materials were used as received.

Cytotoxicity assays

All lamellarins were solubilized in DMSO and tested for their cytotoxic activities against a panel of 11 cancerous and one normal (MRC-5) cell lines. Briefly, the cells suspended in the corresponding culture medium (100 μL for adherent cells and 75 μL for suspended cells, i.e., P388 and HL-60 cells) were inoculated in 96-well microtiter plates (Corning Inc., NY, USA) at a density of 10 000–20 000 cells per well, and incubated at 37 °C in a humidified atmosphere with 95% air and 5% CO_2 . After 24 h, an equal volume of additional medium containing either the serial dilutions of the test compounds, positive control (etoposide), or negative control (DMSO) was added to the desired final concentrations, and the microtiter plates were further incubated for an additional 48 h.

The number of surviving cells in each well was determined using either crystal violet staining (for adherent cells) or XTT assay (for suspended cells), as described below, in order to determine the IC_{50} , which is defined as the concentration that inhibits cell growth by 50% (relative to negative control) after 48 h of continuous exposure to each test compound. Within each experiment, determinations were done in triplicate, and each compound was tested in at least two separate experiments. Any experiments with a variation greater than 10% were excluded from the analysis. The results are expressed as the mean IC_{50} value; standard deviations are omitted for visual clarity.

For the crystal violet staining, supernatants were discarded, and the cells were washed twice with 10 mM phosphate-buffered saline (PBS; 100 μL well⁻¹), fixed with 95% ethanol (100 μL well⁻¹) for at least 5 min, and then stained with a solution of crystal violet (0.5%) in 25% methanol (50 μL well⁻¹) for 10 min. Afterward, the cells were air dried and subsequently lysed with a solution of HCl (0.1 N) in absolute methanol (100 μL well⁻¹). The absorbance at 540 nm was measured using a Multiskan Ascent microtiter plate reader (Labsystems, Helsinki, Finland). The percentage of surviving cells was then calculated for each concentration of the test compounds by comparing the absorbance of each sample well to the average absorbance of the negative control wells.

For the XTT assay, 75 μL of the mixture prepared from 1 mg mL⁻¹ XTT sodium (5 mL) and 0.383 mg mL⁻¹ PMS (100 μL) was added to each well, and the microtiter plates were further incubated for 4 h. The absorbance of the orange formazan compounds formed was measured at both 492 and 690 nm (reference absorbance) using a SPECTRA max PLUS 384 microplate reader (Molecular Devices, Sunnyvale, CA, USA). The absolute absorbance ($\Delta A = A_{492} - A_{690}$) was then calculated for each well, and the percentage of surviving cells compared with control was determined by comparing ΔA_{sample} with $\Delta A_{\text{control}}$.

SAR studies

The mean IC_{50} values obtained from the cytotoxicity assays were used to perform SAR studies in a systematic manner. To determine the importance of a particular structural component for the cytotoxic activity of lamellarins, the IC_{50} values of the two structures differing only in that particular position were compared, and the logarithm of the IC_{50} ratio was subsequently determined with the IC_{50} values of the compounds after and before the modification in the numerator and denominator, respectively. Positive log (IC_{50} ratio) values indicate a loss of cytotoxic activity, whereas negative values show an increase in the activity upon the structural modification being considered. To account for experimental variation, the contribution from the position of interest to the cytotoxic

activity was deemed significant only when $|\log(\text{IC}_{50} \text{ ratio})| > 1$, meaning that the IC_{50} value either increased or decreased by at least 10-fold upon modification at that particular position.

Acknowledgements

Financial support from the Thailand Research Fund (TRF; DBG5180015 to M.C., BRG5180013 to P.P.) is gratefully acknowledged. The authors are thankful to Dr. Sumalee Tangpradabkul (Department of Biochemistry, Faculty of Science, Mahidol University, Bangkok, Thailand) and Dr. Stitaya Sirisinha's research group (Department of Microbiology, Faculty of Science, Mahidol University, Bangkok, Thailand) for providing the S102 and HuCCA-1 cells, respectively. Special thanks go to Ms. Pakamas Intachote (Laboratory of Immunology, Chulabhorn Research Institute), Ms. Khajeelak Chiablaem (Laboratory of Biochemistry, Chulabhorn Research Institute), and Ms. Busakorn Saimanee (Integrated Research Unit, Chulabhorn Research Institute) for conducting the cytotoxicity assays. The authors are also grateful to Dr. Prasat Kittakooop and Mr. Surasak Prachya (Laboratory of Natural Products, Chulabhorn Research Institute) for their kind assistance with HPLC analyses.

Keywords: antitumor agents • lamellarins • marine alkaloids • nitrogen heterocycles • structure–activity relationships

- [1] R. J. Andersen, D. J. Faulkner, C.-H. He, G. D. Van Duyne, J. Clardy, *J. Am. Chem. Soc.* **1985**, *107*, 5492–5495.
- [2] C. Bailly, *Curr. Med. Chem. Anti-Cancer Agents* **2004**, *4*, 363–378.
- [3] H. Fan, J. Peng, M. T. Hamann, J.-F. Hu, *Chem. Rev.* **2008**, *108*, 264–287.
- [4] a) N. Lindquist, W. Fenical, G. D. Van Duyne, J. Clardy, *J. Org. Chem.* **1988**, *53*, 4570–4574; b) A. R. Carroll, B. F. Bowden, J. C. Coll, *Aust. J. Chem.* **1993**, *46*, 489–501; c) S. Urban, M. S. Butler, R. J. Capon, *Aust. J. Chem.* **1994**, *47*, 1919–1924; d) S. Urban, L. Hobbs, J. N. A. Hooper, R. J. Capon, *Aust. J. Chem.* **1995**, *48*, 1491–1494; e) S. Urban, R. J. Capon, *Aust. J. Chem.* **1996**, *49*, 711–713; f) M. V. R. Reddy, D. J. Faulkner, Y. Venkateswarlu, M. R. Rao, *Tetrahedron* **1997**, *53*, 3457–3466; g) R. A. Davis, A. R. Carroll, G. K. Pierens, R. J. Quinn, *J. Nat. Prod.* **1999**, *62*, 419–424; h) J. Ham, H. Kang, *Bull. Korean Chem. Soc.* **2002**, *23*, 163–166; i) P. Krishnaiah, V. L. N. Reddy, G. Venkataramana, K. Ravinder, M. Srinivasulu, T. V. Raju, K. Ravikumar, D. Chandrasekar, S. Ramakrishna, Y. Venkateswarlu, *J. Nat. Prod.* **2004**, *67*, 1168–1171; j) S. M. Reddy, M. Srinivasulu, N. Satyanarayana, A. K. Kondapi, Y. Venkateswarlu, *Tetrahedron* **2005**, *61*, 9242–9247.
- [5] F. Ishibashi, S. Tanabe, T. Oda, M. Iwao, *J. Nat. Prod.* **2002**, *65*, 500–504.
- [6] M. Facompré, C. Tardy, C. Bal-Mahieu, P. Colson, C. Perez, I. Manzanares, C. Cuevas, C. Bailly, *Cancer Res.* **2003**, *63*, 7392–7399.
- [7] M. Vanhuyse, J. Kluzza, C. Tardy, G. Otero, C. Cuevas, C. Bailly, A. Lansiaux, *Cancer Lett.* **2005**, *221*, 165–175.
- [8] A. R. Quesada, M. D. García Grávalos, J. L. Fernández Puentes, *Br. J. Cancer* **1996**, *74*, 677–682.
- [9] a) M. Banwell, B. Flynn, D. Hockless, *Chem. Commun.* **1997**, 2259–2260; b) A. Heim, A. Terpin, W. Steglich, *Angew. Chem.* **1997**, *109*, 158–159; *Angew. Chem. Int. Ed. Engl.* **1997**, *36*, 155–156; c) F. Ishibashi, Y. Miyazaki, M. Iwao, *Tetrahedron* **1997**, *53*, 5951–5962; d) D. L. Boger, C. W. Boyce, M. A. Labroli, C. A. Sehon, Q. Jin, *J. Am. Chem. Soc.* **1999**, *121*, 54–62; e) C. Peschko, C. Winkhofer, W. Steglich, *Chem. Eur. J.* **2000**, *6*, 1147–1152; f) S. Ruchirawat, T. Mutarapat, *Tetrahedron Lett.* **2001**, *42*, 1205–1208; g) C. P. Ridley, M. V. R. Reddy, G. Rocha, F. D. Bushman, D. J. Faulkner, *Bioorg. Med. Chem.* **2002**, *10*, 3285–3290; h) P. Cironi, I. Manzanares, F. Albericio, M. Álvarez, *Org. Lett.* **2003**, *5*, 2959–2962; i) M. Iwao, T. Takeuchi, N. Fujikawa, T. Fukuda, F. Ishibashi, *Tetrahedron Lett.* **2003**, *44*, 4443–4446; j) P. Ploypradith, W. Jinaglueng, C. Pavaró, S. Ruchirawat, *Tetrahedron Lett.* **2003**, *44*, 1363–1366; k) S. T. Handy, Y. Zhang, H. Breg-

- man, *J. Org. Chem.* **2004**, *69*, 2362–2366; l) M. Marfil, F. Albericio, M. Álvarez, *Tetrahedron* **2004**, *60*, 8659–8668; m) P. Ploypradith, C. Mahidol, P. Sahakitpichan, S. Wongbundit, S. Ruchirawat, *Angew. Chem.* **2004**, *116*, 884–886; *Angew. Chem. Int. Ed.* **2004**, *43*, 866–868; n) D. Pla, A. Marchal, C. A. Olsen, F. Albericio, M. Álvarez, *J. Org. Chem.* **2005**, *70*, 8231–8234; o) P. Ploypradith, R. K. Kagan, S. Ruchirawat, *J. Org. Chem.* **2005**, *70*, 5119–5125; p) Y.-C. You, G. Yang, A.-L. Wang, D.-P. Li, *Curr. Appl. Phys.* **2005**, *5*, 535–537; q) N. Fujikawa, T. Ohta, T. Yamaguchi, T. Fukuda, F. Ishibashi, M. Iwao, *Tetrahedron* **2006**, *62*, 594–604; r) D. Pla, A. Marchal, C. A. Olsen, A. Francesch, C. Cuevas, F. Albericio, M. Álvarez, *J. Med. Chem.* **2006**, *49*, 3257–3268; s) P. Ploypradith, T. Petchmanee, P. Sahakitpichan, N. D. Litvinas, S. Ruchirawat, *J. Org. Chem.* **2006**, *71*, 9440–9448; t) T. Yamaguchi, T. Fukuda, F. Ishibashi, M. Iwao, *Tetrahedron Lett.* **2006**, *47*, 3755–3757; u) J. C. Liermann, T. Opatz, *J. Org. Chem.* **2008**, *73*, 4526–4531.
- [10] S. E. L. Mirski, J. H. Gerlach, S. P. C. Cole, *Cancer Res.* **1987**, *47*, 2594–2598.
- [11] S. P. C. Cole, E. R. Chanda, F. P. Dicke, J. H. Gerlach, S. E. L. Mirski, *Cancer Res.* **1991**, *51*, 3345–3352.
- [12] C. D. Evans, S. E. L. Mirski, M. K. Danks, S. P. C. Cole, *Cancer Chemother. Pharmacol.* **1994**, *34*, 242–248.
- [13] S. P. C. Cole, G. Bhardwaj, J. H. Gerlach, J. E. Mackie, C. E. Grant, K. C. Almquist, A. J. Stewart, E. U. Kurz, A. M. V. Duncan, R. G. Deeley, *Science* **1992**, *258*, 1650–1654.
- [14] D. R. Hipfner, S. D. Gauldie, R. G. Deeley, S. P. C. Cole, *Cancer Res.* **1994**, *54*, 5788–5792.
- [15] C. Tardy, M. Facompré, W. Laine, B. Baldeyrou, D. García-Gravalos, A. Francesch, C. Mateo, A. Pastor, J. A. Jiménez, I. Manzanares, C. Cuevas, C. Bailly, *Bioorg. Med. Chem.* **2004**, *12*, 1697–1712.
- [16] S. Sirisinha, T. Tengchaisri, S. Boonpucknavig, N. Prempracha, S. Ratana-rapee, A. Pausawasdi, *Asian Pac. J. Allergy Immunol.* **1991**, *9*, 153–157.
- [17] K. Laohathai, N. Bhamarapavati, *Am. J. Pathol.* **1985**, *118*, 203–208.

Received: October 14, 2008

Revised: November 14, 2008

Published online on January 16, 2009

Article

Anticancer Alkaloid Lamellarins Inhibit Protein Kinases

Dianne Baunbæk ¹, Nolwenn Trinkler ¹, Yoan Ferandin ¹, Olivier Lozach ¹, Poonsakdi Ploypradith ², Somsak Rucirawat ², Fumito Ishibashi, Masatomo Iwao ⁴ and Laurent Meijer ^{1,*}

¹ C.N.R.S., Cell Cycle Group, Station Biologique, B.P. 74, 29682 Roscoff Cedex, Bretagne, France

² Laboratory of Medicinal Chemistry, Chulaborhn Research Institute, Vipavadee-Rangsit Highway, Bangkok 10210, Thailand

³ Division of Marine Life Science and Biochemistry, Faculty of Fisheries, Nagasaki University, 1-14 Bunkyo-machi, Nagasaki 852-8521, Japan

⁴ Department of Applied Chemistry, Faculty of Engineering, Nagasaki University, 1-14 Bunkyo-machi, Nagasaki 852-8521, Japan

* Author to whom correspondence should be addressed; E-mail: meijer@sb-roscoff.fr

Received: 2 August 2008; in revised form: 18 September 2008 / Accepted: 26 September 2008 / Published: 7 October

Abstract: Lamellarins, a family of hexacyclic pyrrole alkaloids originally isolated from marine invertebrates, display promising anti-tumor activity. They induce apoptotic cell death through multi-target mechanisms, including inhibition of topoisomerase I, interaction with DNA and direct effects on mitochondria. We here report that lamellarins inhibit several protein kinases relevant to cancer such as cyclin-dependent kinases, dual-specificity tyrosine phosphorylation activated kinase 1A, casein kinase 1, glycogen synthase kinase-3 and PIM-1. A good correlation is observed between the effects of lamellarins on protein kinases and their action on cell death, suggesting that inhibition of specific kinases may contribute to the cytotoxicity of lamellarins. Structure/activity relationship suggests several paths for the optimization of lamellarins as kinase inhibitors.

Keywords: lamellarin, kinase inhibitor, cyclin-dependent kinases, CK1, DYRK-1A, GSK-3

Abbreviations: CDK, cyclin-dependent kinase; CK1, casein kinase-1; DYRK1A, dual-specificity tyrosine-phosphorylated and regulated kinase 1A; FCS, fetal calf serum; GSK-3, glycogen synthase kinase-3; GST, Glutathione-S-transferase; MBP, myelin basic

protein; **MTS**, 3- (4,5-dimethylthiazol-2-yl)-5- (3-carboxymethoxyphenyl)-2- (4-sulfophenyl)-2H-tetrazolium; **PARP**, poly (ADP-ribose) polymerase.

1. Introduction

Marine organisms constitute an original and relatively untapped source of new enzymes and novel drugs of great biotechnological and pharmaceutical applications potential [reviewed in 1-2]. Cephalosporins, ara-C and ara-A represent the first molecules of marine origin which have reached the market. Quite a few molecules derived from marine organisms are now being investigated in clinical tests, essentially against cancer, inflammation, chronic pain and neurodegenerative diseases. In the cancer field, ecteinascidin 743 (yondelis), dehydrodidemnin B (aplidine), bryostatin-1, dolastatin and analogs, ziconotide (Prialt), discodermolide are some of the most advanced compounds. Other molecules, rather than being investigated as potential clinical drugs, have been developed as important pharmacological tools for cell biology, such as okadaic acid, kainic acid, latrunculin, tetrodotoxin, saxitoxin.

Among the promising anti-cancer drug candidates derived from marine invertebrates is the family of lamellarins [reviewed in 3-5]. These hexacyclic pyrrole alkaloids were first isolated in 1985 from a prosobranch mollusk of the genus *Lamellaria* [6]. They were later extracted from and identified in various species of ascidians [7-14] and sponges [15-16] collected from very diverse areas. Over 38 lamellarins (A-Z and α - γ) have been described [reviewed in 4, 5]. Following the discovery of the potent anti-proliferative and pro-apoptotic activities of lamellarins [17-24], their biological activities have been extensively studied. Lamellarins are potent inhibitors of topoisomerase I [19-21], they interact with DNA [19] and they target mitochondria directly and induce the release of cytochrome C and apoptosis-inducing factor (AIF) [23, 24]. They also function as multi-drug resistance reversal drugs [17, 22]. Furthermore, Lamellarin α 20-sulfate inhibits HIV-1 integrase [14, 26, 27].

In the course of screening for pharmacological inhibitors of disease-relevant protein kinases such as cyclin-dependent kinases (CDKs) [28, 29], glycogen synthase kinase-3 (GSK-3) [30], PIM1 [31], “dual-specificity, tyrosine phosphorylation regulated kinase 1A” (DYRK1A) [32-34], casein kinase 1 (CK1) [35], we discovered that several lamellarins inhibit the catalytic activity of some of these kinases. We here report on the kinase inhibitory activity of 22 lamellarins [18, 36, 37] on 6 protein kinases. These lamellarins were also tested in parallel for their effects on the survival of human neuroblastoma SH-SY5Y cells and the expression of a selection of key proteins. The contribution of kinase inhibition to the anti-tumor properties of lamellarins is discussed.

CDK1/cyclin B is essential for G1/S and G2/M phase transition of the cell cycle. Inhibition of CDK1/cyclin B leads to cell cycle arrest eventually leading ultimately to cell death. Deregulation of CDK5/p25 has been associated with neurodegenerative diseases including Alzheimer’s disease, therefore it was included in the panel of kinases tested. In addition to inactivating glycogen synthase, GSK-3 α / β is also implicated in control of the cellular response to DNA damage and is directly involved in Alzheimer’s disease. PIM-1 is up-regulated in prostate cancers. DYRK1A, suspected to play a role in Down’s syndrome and Alzheimer’s disease, is thought to participate in central nervous

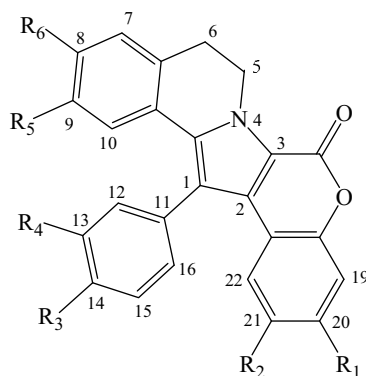
system development, in growth control, and development. Likewise, CK1 is implicated in regulation of various physiological processes, and in diseases such as cancers and Alzheimer's disease.

2. Results and Discussion

2.1. Lamellarins inhibit protein kinases

While screening marine natural products for new chemical inhibitors of protein kinases, we found lamellarin D to display significant activity. We thus initially assembled a small collection of natural and synthetic lamellarin analogs (Table 1).

Table 1. Structure of the lamellarins used in this study. A single (—) or a double (==) bond is present between C5 and C6, depending on the molecule. Me, methyl; i-Pr, isopropyl. **22**: -OH at position 7.



#	Lamellarin	R1	R2	R3	R4	R5	R6	5-6
1	lamellarin D	OH	OMe	OH	OMe	OMe	OH	==
2	lamellarin α	OH	OMe	OH	OMe	OMe	OMe	==
3	di-H-lamellarin D	OH	OMe	OH	OMe	OMe	OH	—
4	lamellarin H	OH	OH	OH	OH	OH	OH	==
5	di-H-lamellarin H	OH	OH	OH	OH	OH	OH	—
6	lamellarin N	OH	OMe	OMe	OH	OMe	OH	==
7	lamellarin L	OH	OMe	OMe	OH	OMe	OH	—
8	lamellarin G tri-OMe	OMe	OMe	OMe	OMe	OMe	OMe	—
9	lamellarin 3	OH	H	OH	OMe	OMe	OH	==
10	lamellarin 4	H	OMe	OH	OMe	OMe	OH	==
11	lamellarin 5	OH	OMe	OMe	OMe	OMe	OMe	==
12	lamellarin 6	OH	OMe	OH	H	OMe	OH	==
13	lamellarin 7	OH	OMe	H	OMe	OMe	OH	==
14	lamellarin 8	H	H	OH	OMe	OMe	OH	==
15	lamellarin 9	H	H	OH	OH	OH	OH	==

Table 1. Cont.

16	lamellarin 11	H	H	OMe	OMe	OMe	OMe	==
17	lamellarin 12	∩-CH ₂ -O		OMe	OMe	OMe	OMe	==
18	lamellarin 33	O <i>i</i> -Pr	OMe	O <i>i</i> -Pr	OMe	OMe	O <i>i</i> -Pr	==
19	lamellarin 31	O <i>i</i> -Pr	OMe	O <i>i</i> -Pr	OMe	OMe	O <i>i</i> -Pr	—
20	lamellarin 34	O <i>i</i> -Pr	OMe	OMe	O <i>i</i> -Pr	OMe	O <i>i</i> -Pr	==
21	lamellarin 32	O <i>i</i> -Pr	OMe	OMe	O <i>i</i> -Pr	OMe	O <i>i</i> -Pr	—
22	lamellarin K	OH	OMe	OH	OMe	OMe	OMe	—

All compounds were run on our kinase assay panel comprising CDK1/cyclin B, CDK5/p25, GSK-3 α/β , PIM-1, DYRK1A, CK1. Results are presented in Table 2. They show that some lamellarins are potent inhibitors of various protein kinases. The limited number of lamellarin analogs precludes a solid structure/activity relationship study. Nevertheless, striking differences in kinase inhibitory activity are observed following minor changes at the lamellarin chemical structure. For example,

- removal of the hydroxyl at R1 modestly modifies the activity (except GSK-3, DYRK1A and CK1), compare lamellarin D (**1**) and lamellarin 4 (**10**).
- removal of the hydroxyl at R2 results in minor changes in activity (except DYRK1A and CK1), compare lamellarin D (**1**) and lamellarin 3 (**9**).
- removal of the hydroxyl at R3 results in major reduction in activity, compare lamellarin D (**1**) and lamellarin 7 (**13**).
- removal of the hydroxyl at R4 results in enhanced inhibitory activity, compare lamellarin D (**1**) and lamellarin 6 (**12**).
- O-methylation at R6 results in massive loss of inhibitory activity, compare lamellarin D (**1**) and lamellarin α (**2**).
- replacing the hydroxyl groups of lamellarin D (**1**) at R₁, R₃, and R₆ by O-isopropyl completely abolishes inhibitory activity, see lamellarin 31 (**18**) and 33 (**19**). This is also the case when substituting hydroxyl to isopropyl at positions R₁, R₄, and R₆ of lamellarin N (**6**), lamellarin 32 (**21**) and 34 (**20**).
- transposition of the substitutions at R₃ and R₄ of lamellarin D (**1**), resulting in lamellarin N (**6**), lead to 10-fold enhanced kinase inhibitory activity.
- Reduction in activity due to saturation of D-ring double bond (C5=C6) has previously been reported to be due to loss of planarity and therefore steric hindrance in ATP pocket of targets [19]. Kinase inhibitory activities of lamellarins are generally reduced when the D-ring double bond is saturated, compare lamellarins D (**1**) with di-H-lamellarin (**3**), and lamellarins N (**6**) with lamellarin L (**7**).

Altogether these results suggest complex but specific interactions between lamellarins' substituents and their kinase targets. Co-crystal structure would be most helpful to understand these interactions and optimize lamellarins as kinase inhibitors.

Table 2. Biological activity of lamellarins. Each lamellarin was tested on 6 protein kinases. Enzyme activities were assayed as described in the Experimental section. Results are reported as IC₅₀ values (expressed in μM) estimated from the dose-response curves. -, no inhibitory activity was detected (highest concentration tested is indicated in parentheses). Lamellarins were also tested for their effect on the survival of human neuroblastoma SH-SY5Y cells, using the MTS assay (IC₅₀ values expressed in μM). The effect of some lamellarins on HeLa cells [18] is provided for comparison. Nt, not tested.

#	Lamellarin	CDK1/ cyclin B	CDK5 / p25	GSK -3α/β	PIM 1	DYRK1A	CK1	SH- SY5Y	HeLa [18]
1	lamellarin D	0.50	0.55	0.3	0.10	0.45	13.0	0.019	0.011
2	lamellarin α	8.0	> 10	1.4	0.59	5.0	7.9	-(10)	
3	di-H-lamellarin D	1.85	0.11	0.9	0.20	0.50	5.9	0.41	nt
4	lamellarin H	-(10)	-(10)	9.5	-(10)	-(10)	5.3	0.45	> 100
5	di-H-lamellarin H	-(10)	-(10)	0.67	-(10)	-(10)	5.2	2.55	nt
6	lamellarin N	0.070	0.025	0.005	0.055	0.035	-(10)	0.025	nt
7	lamellarin L	0.38	0.1	0.041	0.25	0.14	-(10)	0.7	nt
8	lamellarin G tri- OMe	-(10)	-(10)	-(10)	-(10)	> 10	-(10)	-(100)	nt
9	lamellarin 3	0.53	0.60	0.58	0.15	0.06	0.41	0.056	0.04
10	lamellarin 4	2.0	0.6	0.05	0.05	0.08	1.3	0.79	0.85
11	lamellarin 5	-(10)	-(10)	-(10)	2.0	-(10)	-(10)	8.0	2.5
12	lamellarin 6	0.10	0.03	0.13	0.33	0.09	0.8	0.11	0.04
13	lamellarin 7	4.3	2.1	2.1	-(10)	-(10)	-(10)	0.14	0.07
14	lamellarin 8	5	0.9	2.2	0.7	1.0	-(10)	2.65	4.0
15	lamellarin 9	-(10)	-(10)	-(10)	-(10)	-(10)	-(10)	-(10)	1.1
16	lamellarin 11	-(10)	-(10)	-(10)	-(10)	-(10)	-(10)	-(10)	5.7
17	lamellarin 12	-(10)	-(10)	-(10)	-(10)	-(10)	-(10)	-(10)	> 100
18	lamellarin 33	-(10)	-(10)	-(10)	-(10)	-(10)	-(10)	-(100)	nt
19	lamellarin 31	-(10)	-(10)	-(10)	-(10)	-(10)	-(10)	-(100)	nt
20	lamellarin 34	-(10)	-(10)	-(10)	-(10)	-(10)	-(10)	-(100)	nt
21	lamellarin 32	-(10)	-(10)	-(10)	-(10)	-(10)	-(10)	-(100)	nt
22	lamellarin K	-(10)	-(10)	-(10)	0.6	-(10)	6.0	-(30)	nt

2.2. Selectivity of lamellarins

Although most active compounds were active on all six kinases, a few lamellarins displayed apparent selectivity towards some kinases, suggesting that some degree of selectivity might be gained following the synthesis of more analogs. We next tested the selectivity of lamellarin N on the Cerep kinase selectivity panel (Table 3). Results show that lamellarin N does not inhibit all, but displays some selectivity for a few kinases, some of which are major cancer targets (VEGFR1/2, Flt-3, PDGFR, Lck, Lyn). Inhibition of protein kinases by the tested compounds observed could also possibly be due to non-specific interactions, raising the need for more analogues having a higher specificity for a

limited amount of kinases. Hopefully more selective lamellarin analogues can be designed when their interaction mode will be better understood.

Table 3. Kinase inhibition selectivity of lamellarin N evaluated on the CEREP Kinase Selectivity Panel (44 kinases). Preparation and assay of kinases are described [44] (www.cerep.com). Enzymes were assayed in the presence of 10 μ M lamellarin N, and kinase activities expressed as % of control kinase activity, *i.e.* in the absence of inhibitor. ≥ 80 % inhibition at 10 μ M is underlined in grey.

Protein Kinase	Activity (% of control)	SEM (%)
Abl kinase (h)	61.4	0.8
Akt1/PKB α (h)	104.6	2.6
AMPK α	42.4	0.9
BMX kinase (h) (Etk)	60.8	5.4
Brk (h)	72.8	4.7
CaMK2 α (h)	38.2	2.2
CaMK4 (h)	89.9	3.1
CDC2/CDK1 (h) (cycB)	20.4	0.6
CDK2 (h) (cycE)	57.1	0.3
CHK1 (h)	93.3	1.9
CHK2 (h)	47.6	0.6
c-Met kinase (h)	92.1	1.6
CSK (h)	47.4	2.5
EphB4 kinase (h)	89.7	0.9
ERK1 (h)	94.1	0.1
ERK2 (h) (P42mapk)	79.9	1.4
FGFR2 kinase (h)	19.8	0.6
FGFR4 kinase (h)	62.5	0.3
FLT-1 kinase (h) (VEGFR1)	4.0	0.2
FLT-3 kinase (h)	0.4	0.4
Fyn kinase (h)	20.1	1.2
IGF1R kinase (h)	87.2	1.6
IRK (h) (InsR)	46.7	1.6
JNK 2 (h)	15.7	1.8
KDR kinase (h) (VEGFR2)	7.4	1.1
Lck kinase (h)	7.1	0.7
Lyn kinase (h)	7.2	0.5
MAPKAPK2 (h)	96.6	2.1
MEK1/MAP2K1 (h)	81.5	1.0
p38 α kinase (h)	97.4	1.4
p38 δ kinase (h)	96.0	0.9
p38 γ kinase (h)	79.6	0.6

Table 3. Cont.

PDGFR β kinase (h)	1.8	0.4
PDK1 (h)	89.8	0.6
PKA (h)	80.0	4.6
PKC α (h)	91.7	7.6
PKC β 1 (h)	102.0	1.8
PKC γ (h)	94.1	1.9
Ret kinase (h)	1.8	0.4
ROCK2 (h)	103.3	0.9
RSK2 (h)	44.5	0.5
Src kinase (h)	56.2	0.4
Syk (h)	97.1	0.7
TRKA (h)	0.8	0.3

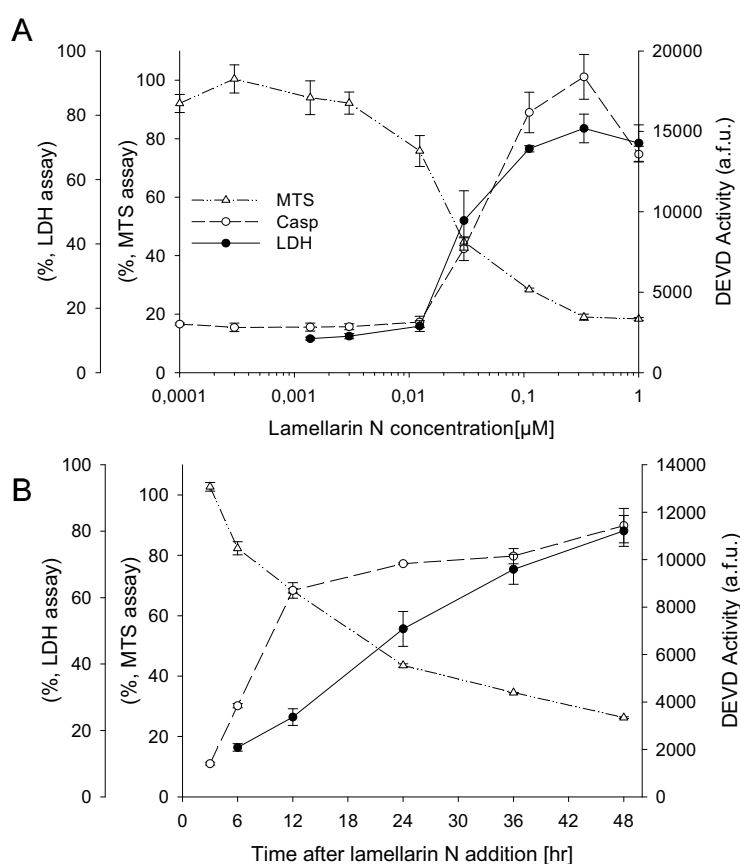
2.3. Cell death induction by lamellarins

We next tested the effects of each lamellarin, at an initial 10 μ M concentration, on the survival of the neuroblastoma SH-SY5Y cell line after 48 h exposure (Table 2). Cell survival was estimated by the MTS reduction assay. Several compounds showed clear effects on the SH-SY5Y cell survival rate. A complete dose-response curve was performed for these active compounds after 24 h and 48 h exposure and the IC₅₀ values were calculated (Table 2). The most active compounds were lamellarin D (**1**) (IC₅₀: 0.019 μ M), lamellarin N (**6**) (IC₅₀: 0.025 μ M), lamellarin 3 (**9**) (IC₅₀: 0.056 μ M), and lamellarin 6 (**12**) (IC₅₀: 0.11 μ M). These lamellarins share a hydroxyl group at R1 and R6, an O-methyl group at R5, and a double bond between C5 and C6. As observed with the kinase inhibitory activity, a saturated C5-C6 bond instead of a double bond leads to an decrease in activity (compare compounds **1** and **3**, **4** and **5**, **6** and **7**). Lamellarins which were totally inactive on kinases were devoid of effects on cell death. Altogether these first results suggest that kinase inhibition may contribute to the effects of lamellarins on cell proliferation and cell death.

SH-SY5Y cells were next incubated with a range of lamellarin N concentrations or at 1 μ M over 48 hrs. Cell survival was monitored by the MTS reduction assay, cell death was assessed by the LDH release assay and caspase activation was measured using DEVD as a substrate (Figure 1). Kinetics and dose-response curves show that cells start dying rapidly after lamellarin N (half-life: 20 hours) at doses as low as 0.05 μ M.

Expression of p53, p21^{CIP1} & Mcl-1 and PARP cleavage were next evaluated by Western blotting (Figure 2). Induction of PARP cleavage and p53 and p21 expression already takes place after 6 hour treatment with lamellarin N (Figure 2) and at concentration as low as 0.1 μ M (data not shown). Interestingly, in contrast to the effects observed with roscovitine and other CDK inhibitors [42], the survival factor Mcl-1 is not down-regulated (Figure 2). Thus lamellarin N is able to trigger cell death in the presence of a constant level of the survival factor Mcl-1. As Mcl-1 confers resistance to the BCL-2 selective antagonist ABT-737 and to the proteasome inhibitor bortezomib [43], lamellarins might favorably combine with these treatments.

Figure 1. Dose- and time- dependent induction of cell death by lamellarin N. (A) Neuroblastoma SH-SY5Y cells were treated with lamellarin N at various concentrations. Cell death was measured by LDH release, cell survival was assessed by the MTS reduction assay, and caspase 3 activity was monitored as DEVDase activity. MTS and LDH assay were carried out 48 hours after treatment with lamellarin N. The caspase assay was carried out 24 hours after treatment. (B) Kinetics of cell survival, cell death and caspases activation following exposure of SH-SY5Y cells to 1 μ M lamellarin N. Average of 3 independent experiments performed in triplicate. The standard deviation (\pm SD) is indicated by error bars.

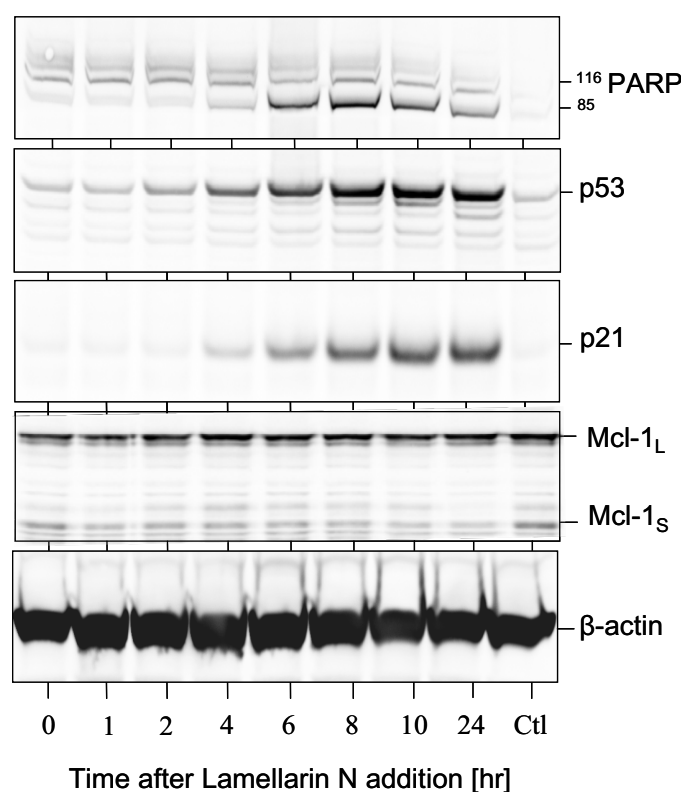


3. Conclusions

In conclusion, we have identified new molecular targets of lamellarins. Combined with the well-supported effects of lamellarins on topoisomerase 1, kinase inhibition may underlie the promising anti-tumor properties of lamellarins. This work is now currently being extended in several directions: (i) synthesis and biological evaluation of new analogs, to allow the identification of more potent and more selective lamellarins as kinase inhibitors; (ii) optimization on the most cancer-relevant kinases; (iii) identification of the molecular mechanism of action of lamellarins on kinases (enzymological analysis, co-crystal structures); (iv) investigation of the contribution of kinase inhibition to the promising anti-tumoral effects of lamellarins (and the synergy with previously identified mechanisms of action); (v) conversely, identification of lamellarin analogues devoid of kinase inhibitory properties but still able to interact with topoisomerase 2, possibly leading to compounds with less toxic side effects.

Identification of the key kinase targets of biologically active lamellarins or, in contrast, elimination of the kinase inhibition properties of lamellarins should be used to optimize this family of compounds towards selective and potent anti-tumor agents.

Figure 2. Lamellarin N triggers PARP cleavage, p53 & p21^{CIP1} upregulation, but not Mcl-1 down-regulation. SH-SY5Y cells treated at time 0 with 1 μ M lamellarin N. Cells were harvested at different time-points and protein extracted for SDS-PAGE followed by Western blot analysis using antibodies directed against PARP, p53, p21^{CIP1}, or Mcl-1, as described in the materials and methods section. β -actin was used as loading control. “Ctrl” denoted untreated sample after 10 hours.



5. Experimental Procedures

5.1. Chemistry

Compounds **2**, **4**, **5** (lamellarin N), **6**, **7** and **17-20** were synthesized employing Hinsberg-type pyrrole formation and Suzuki-Miyaura cross-couplings as the key reactions as previously described [37]. Compounds **1**, **3** and **8-16** were synthesized by the previous methods in which the pyrrole core was constructed by N-ylide mediated intramolecular condensation [18, 36].

5.2. Kinase preparation and assays

Kinase activities were assayed in buffer A (10 mM MgCl₂, 1 mM EGTA, 1 mM DTT, 25 mM Tris-HCl pH 7.5, 50 μ g heparin/ml) or C (60 mM β -glycerophosphate, 15 mM *p*-nitrophenyl phosphate, 25

mM MOPS (pH 7.2), 5 mM EGTA, 15 mM MgCl₂, 1 mM dithiothreitol, 1 mM sodium vanadate, 1 mM phenylphosphate, 0.1 % Nonidet P-40), at 30°C, at a final ATP concentration of 15 μM. Blank values were subtracted and activities calculated as pmoles of phosphate incorporated during a 30 min. incubation. The activities were expressed in % of the maximal activity, *i.e.* in the absence of inhibitors. Controls were performed with appropriate dilutions of dimethylsulfoxide. Unless otherwise stated, the P81 phosphocellulose assay was used.

CDK1/cyclin B was extracted in homogenization buffer (60 mM β-glycerophosphate, 15 mM p-nitrophenylphosphate, 25 mM Mops (pH 7.2), 15 mM EGTA, 15 mM MgCl₂, 1 mM DTT, 1 mM sodium vanadate, 1 mM NaF, 1 mM phenylphosphate, 10 μg leupeptin/ml, 10 μg aprotinin/ml, 10 μg soybean trypsin inhibitor/ml and 100 μM benzamidine) from M phase starfish (*Marthasterias glacialis*) oocytes and purified by affinity chromatography on p9^{CKShs1}-sepharose beads, from which it was eluted by free p9^{CKShs1} as previously described [38]. The kinase activity was assayed in buffer C, with 1 mg histone H1 /ml, in the presence of 15 μM [γ-³³P] ATP (3,000 Ci/mmol; 1 mCi/ml) in a final volume of 30 μl. After 30 min. incubation at 30°C, 25 μl aliquots of supernatant were spotted onto 2.5 x 3 cm pieces of Whatman P81 phosphocellulose paper, and, 20 sec. later, the filters were washed five times (for at least 5 min. each time) in a solution of 10 ml phosphoric acid/liter of water. The wet filters were counted in the presence of 1 ml ACS (Amersham) scintillation fluid.

CDK5/p25 was reconstituted by mixing equal amounts of recombinant human CDK5 and p25 expressed in *E. coli* as GST (Glutathione-S-transferase) fusion proteins and purified by affinity chromatography on glutathione-agarose (vectors kindly provided by Dr. L.H. Tsai) (p25 is a truncated version of p35, the 35 kDa CDK5 activator). Its activity was assayed with histone H1 in buffer C as described for CDK1/cyclin B.

GSK-3α/β was purified from porcine brain by affinity chromatography on immobilized axin [39]. It was assayed, following a 1/100 dilution in 1 mg BSA/ml 10 mM DTT, with 5 μl 4 μM GS-1, a GSK-3 selective substrate, (YRRAAVPPSPSLSRHSSPHQSpEDEEE, obtained from Millegen (31682 Labège, France), in buffer A, in the presence of 15 μM [γ-³³P] ATP in a final volume of 30 μl. After 30 min. incubation at 30°C, 25 μl aliquots of supernatant were processed as described above.

PIMI was expressed as a GST-fusion protein in *E. coli* and purified by affinity chromatography on glutathione-agarose. Its kinase activity was assayed for 30 min. with histone H1 in buffer C as described for CDK1/cyclin B.

DYRK1A was expressed as a GST fusion protein in *E. coli* (vector kindly provided by Dr. W. Becker, Institute for Pharmacology and Toxicology, Aachen, Germany) and affinity purified on glutathione-agarose. Its kinase activity was assayed in buffer C, with 0.16 mg myelin basic protein (MBP)/ml, in the presence of 15 μM [γ-³³P] ATP in a final volume of 30 μl. After 30 min incubation at 30°C, 25 μl aliquots of supernatant were treated as described above.

CK1 was purified from porcine brain by affinity chromatography on immobilized axin fragment [40]. The mixture of native CK1 isoforms (essentially CK1 δ and CK1 ϵ) was assayed in three-fold diluted buffer C, using 25 μ M CKS peptide, a CK1 selective substrate (RRKHAAIGpSAYSITA, synthesized by Millegen (Labège, France)). Assays were performed for 30 min. at 30°C, as described for GSK-3.

5.3. Cell viability and cell death

SH-SY5Y human neuroblastoma cells were grown in DMEM supplemented with 2mM L-glutamine (Invitrogen, Cergy Pontoise, France), plus antibiotics (penicillin-streptomycin) and a 10% volume of fetal calf serum (FCS) (Invitrogen). Cell viability was determined by means of the MTS (3- (4,5-dimethylthiazol-2-yl)-5- (3-carboxymethoxyphenyl)-2- (4-sulfophenyl)-2H -tetrazolium) reduction method as previously described [41]. Cell death was (also) assayed by LDH release. Lactate dehydrogenase is a stable cytosolic enzyme that is released upon cell lysis [40]. SH-SY5Y cells were also subjected to caspase activity assays. These are based on cleavage of a synthetic caspase substrate DEVD (MP Biomedicals, 199423), a substrate of active caspase 3/6/7. The assay was carried out according to manufacturer's instructions [41].

5.4. Protein extraction, SDS-PAGE and Western Blotting

At given time points and lamellarin doses, SH-SY5Y cells were harvested in phosphate buffered saline (PBS) with commercially available protease inhibitors (Roche, 11836145001). Cells were homogenized by sonication in homogenization buffer supplemented with 0.1% NP-40 and protease inhibitors. The homogenization buffer consist of: 25mM MOPS, 15mM EGTA, 15mM MgCl₂, 1mM sodium orthovanadate, 1mM sodium fluoride, 60mM β -glycerophosphate, 2mM DTT, 15mM p-nitrophenylphosphate, and 1mM phenyl phosphate-di-sodium salt (all reagents supplied by Sigma). Sonication retrieved proteins. Cellular proteins were subjected to electrophoresis in SDS 10% polyacrylamide gels and transferred to a PVDF membrane (Invitrogen). Membranes were incubated with primary antibodies directed against p53 (Santa Cruz Biotech, sc-263) (1:1000), p21^{CIP1} (Calbiochem, OP64) (1:1000) or poly (ADP-ribose) polymerase (PARP) (Santa Cruz Biotech, sc-7150) (1:500). Appropriate secondary antibodies conjugated to horseradish peroxidase (Biorad) were added to visualize the proteins using the ECL detection system.

4. Acknowledgements

This research was supported a grant from the EEC (FP6-2002-Life Sciences & Health, PRO-KINASE Research Project) (LM), and a "Cancéropole Grand-Ouest" grant (LM). DB was supported by the FP6- Marie Curie Action -ESTeam MEST-CT-2005-020737 program.

References and Notes

1. Bourguet-Kondracki, M.L.; Kornprobst, J.M. Marine pharmacology: potentialities in the treatment of infectious diseases, osteoporosis and Alzheimer's disease. *Adv. Biochem. Eng. Biotechnol.* **2005**, *97*, 105-131.
2. Simmons, T.L.; Andrianasolo, E.; McPhail, K.; Flatt, P.; Gerwick, W.H. Marine natural products as anticancer drugs. *Mol. Cancer Ther.* **2005**, *4*, 333-342.
3. Cironi, P.; Albericio, F.; Alvarez, M. Lamellarins: isolation, activity and synthesis, *Progr. Heterocycl. Chem.* **2004**, *16*, 1-26.
4. Bailly, C. Lamellarins, from A to Z: a family of anticancer marine pyrrole alkaloids. *Curr. Med. Chem. Anti-Cancer Agents* **2004**, *4*, 363-378.
5. Fan, R.H.; Peng, J.; Hamann, M.T.; Hu, J.F. Lamellarins and related pyrrole-derived alkaloids from marine organisms. *Chem. Rev.* **2008**, *108*, 264-287.
6. Andersen, R.J.; Faulkner, D.J.; He, C.H.; Van Duyne, G.D.; Clardy, J. Metabolites of the marine prosobranch mollusk *Lamellaria* sp. *J. Am. Chem. Soc.* **1985**, *107*, 5492-5495.
7. Lindquist, N.; Fenical, W.; Van Duyne, G.D.; Clardy, J. New alkaloids of the lamellarin class from the marine ascidian *Didemnum chartaceum* (Sluiter, 1909). *J. Org. Chem.* **1988**, *53*, 4570-4574.
8. Carroll, A.R.; Bowden, B.F.; Coll, J.C. Studies of Australian ascidians. I. Six new lamellarin-class alkaloids from a colonial ascidian, *Didemnum* sp. *Austr. J. Chem.* **1993**, *46*, 489-501.
9. Urban, S.; Capon, R.J. Lamellarin S: A New Aromatic Metabolite from an Australian Tunicate *Didemnum* sp. *Aust. J. Chem.* **1996**, *49*, 711-713.
10. Reddy, M.V.R.; Faulkner, D.J.; Venkateswarlu, Y.; Rao, M.R. New lamellarin alkaloids from an unidentified ascidian from the Arabian Sea. *Tetrahedron* **1997**, *53*, 3457-3466.
11. Davis, R.A.; Carroll, A.R.; Pierens, G.K.; Quinn, R.J. New lamellarin alkaloids from the Australian ascidian, *Didemnum chartaceum*. *J. Nat. Prod.* **1999**, *62*, 419-424.
12. Ham, J.; Kang, H. A novel cytotoxic alkaloid of lamellarin class from a marine ascidian *Didemnum* sp. *Bull. Korean Chem. Soc.* **2002**, *23*, 163-166.
13. Reddy, S.M.; Srinivasulu, M.; Satyanarayana, N.; Kondapi, A.K.; Venkateswarlu, Y. New potent cytotoxic lamellarin alkaloids from Indian ascidian *Didemnum obscurum*. *Tetrahedron* **2005**, *61*, 9242-9247.
14. Reddy, M.V.; Rao, M.R.; Rhodes, D.; Hansen, M.S.; Rubins, K.; Bushman, F.D.; Venkateswarlu, Y.; Faulkner, D.J. Lamellarin alpha 20-sulfate, an inhibitor of HIV-1 integrase active against HIV-1 virus in cell culture. *J. Med. Chem.* **1999**, *42*, 1901-1907.
15. Urban, S.; Butler, M.S.; Capon, R.J. Lamellarins O and P: New Aromatic Metabolites from the Australian Marine Sponge *Dendrilla cactos*. *Aust. J. Chem.* **1994**, *47*, 1919-1924.
16. Urban, S.; Hobbs, L.; Hooper, J.N.A.; Capon, R.J. Lamellarins Q and R: New Aromatic Metabolites from an Australian Marine Sponge *Dendrilla cactos*. *Aust. J. Chem.* **1995**, *48*, 1491-1494.
17. Quesada, A.R.; Garcia Gravalos, M.D.; J.L. Fernandez Puentes Polyaromatic alkaloids from marine invertebrates as cytotoxic compounds and inhibitors of multidrug resistance caused by P-glycoprotein, *Br. J. Cancer*, **1996**, *74*, 677-682.

18. F. Ishibashi, S. Tanabe, T. Oda, M. Iwao, Synthesis and structure-activity relationship study of lamellarin derivatives, *J. Nat. Prod.*, **2002**, *65*, 500-504.
19. M. Facompre, C. Tardy, C. Bal-Mahieu, P. Colson, C. Perez, I. Manzanares, C. Cuevas, C. Bailly, Lamellarin D: a novel potent inhibitor of topoisomerase I, *Cancer Res.*, **2003**, *63*, 7392-7399.
20. C. Tardy, M. Facompre, W. Laine, B. Baldeyrou, D. Garcia-Gravalos, A. Francesch, C. Mateo, A. Pastor, J.A. Jimenez, I. Manzanares, C. Cuevas, C. Bailly, Topoisomerase I-mediated DNA cleavage as a guide to the development of antitumor agents derived from the marine alkaloid lamellarin D: trimethylester derivatives incorporating amino acid residues, *Bioorg. Med. Chem.*, **2004**, *12*, 1697-1712.
21. E. Marco, W. Laine, C. Tardy, A. Lansiaux, M. Iwao, F. Ishibashi, C. Bailly, F. Gago, Molecular determinants of topoisomerase I poisoning by lamellarins: comparison with camptothecin and structure-activity relationships, *J. Med. Chem.*, **2005**, *48*, 3796-3807.
22. M. Vanhuysse, J. Kluza, C. Tardy, G. Otero, C. Cuevas, C. Bailly, A. Lansiaux, Lamellarin D: a novel pro-apoptotic agent from marine origin insensitive to P-glycoprotein-mediated drug efflux, *Cancer Lett.*, **2005**, *22*, 165-175.
23. J. Kluza, M.A. Gallego, A. Loyens, J.C. Beauvillain, J.M. Sousa-Faro, C. Cuevas, P. Marchetti, C. Bailly, Cancer cell mitochondria are direct proapoptotic targets for the marine antitumor drug lamellarin D, *Cancer Res.*, **2006**, *66*, 3177-3187.
24. M.A. Gallego, C. Ballot, J. Kluza, N. Hajji, A. Martoriati, L. Castéra, C. Cuevas, P. Formstecher, B. Joseph, G. Kroemer, C. Bailly, P. Marchetti, Overcoming chemoresistance of non-small cell lung carcinoma through restoration of an AIF-dependent apoptotic pathway, *Oncogene*, **2008**, *27*, 1981-1992.
25. M.G. Banwell, E. Hamel, D.C. Hockless, P. Verdier-Pinard, A.C. Willis, D.J. Wong, 4,5-Diaryl-1H-pyrrole-2-carboxylates as combretastatin A-4/lamellarin T hybrids: Synthesis and evaluation as anti-mitotic and cytotoxic agents, *Bioorg. Med. Chem.*, **2006**, *14*, 4627-4638.
26. C.P. Ridley, M.V. Reddy, G. Rocha, F.D. Bushman, D.J. Faulkner, Total synthesis and evaluation of lamellarin alpha 20-Sulfate analogues, *Bioorg. Med. Chem.*, **2002**, *10*, 3285-3290.
27. T. Yamaguchi, T. Fukuda, F. Ishibashi, M. Iwao, The first total synthesis of lamellarin α 20-sulfate, a selective inhibitor of HIV-1 integrase. *Tetrahedron*, in press.
28. Malumbres, M., and Barbacid, M. Mammalian cyclin-dependent kinases, *Trends Biochem. Sci.*, **2005**, *30*, 630-641.
29. M. Knockaert, P. Greengard, L. Meijer, Pharmacological inhibitors of cyclin-dependent kinases, *Trends Pharmacol. Sci.*, **2002**, *23*, 417-425.
30. L. Meijer, M. Flajolet, P. Greengard, Pharmacological inhibitors of glycogen synthase kinase-3, *Trends Pharmacol. Sci.*, **2004**, *25*, 471-480.
31. M. Bachmann, T. Moroy, The serine/threonine kinase Pim-1, *Int. J. Biochem. Cell Biol.*, **2005**, *37*, 726-730.
32. J. Galceran, K. de Graaf, F.J. Tejedor, W. Becker, The MNB/DYRK1A protein kinase: genetic and biochemical properties, *J. Neural. Transm. Suppl.*, **2003**, *67*, 139-148.
33. B. Hammerle, C. Elizalde, J. Galceran, W. Becker, F.J. Tejedor, The MNB/DYRK1A protein kinase: neurobiological functions and Down syndrome implications, *J. Neural Transm. Suppl.*, **2003**, *67*, 129-137.

34. Ferrer, M. Barrachina, B. Puig, M. Martinez de Lagran, E. Marti, J. Avila, M. Dierssen, Constitutive Dyrk1A is abnormally expressed in Alzheimer disease, Down syndrome, Pick disease, and related transgenic models, *Neurobiol. Dis.*, **2005**, *20*, 392-400.
35. U. Knippschild, S. Wolff, G. Giamas, C. Brockschmidt, M. Wittau, P.U. Wurl, T. Eismann, M. Stoter, The role of the casein kinase 1 (CK1) family in different signaling pathways linked to cancer development, *Onkologie*, **2005**, *28*, 508-514.
36. F. Ishibashi, Y. Miyazaki, M. Iwao, Total syntheses of lamellarin D and H. The first synthesis of lamellarin-class marine alkaloids, *Tetrahedron*, **1997**, *53*, 5951-5962.
37. N. Fujikawa, T. Ohta, T. Yamaguchi, T. Fukuda, F. Ishibashi, M. Iwao, Total synthesis of lamellarin D, L, and N. *Tetrahedron*, **2006**, *62*, 594-604.
38. L. Meijer, A. Borgne, O. Mulner, J.P.J. Chong, J.J. Blow, N. Inagaki, M. Inagaki, J.G. Delcros, J.P. Moulinoux, Biochemical and cellular effects of roscovitine, a potent and selective inhibitor of the cyclin-dependent kinases cdc2, cdk2 and cdk5, *Eur. J. Biochem.*, **1997**, *24*, 527-536.
39. Primot, B. Baratte, M. Gompel, A. Borgne, S. Liabeuf, J.L. Romette, F. Costantini, L. Meijer, Purification of GSK-3 by affinity chromatography on immobilised axin, *Protein Expr. & Purif.*, **2000**, *20*, 394-404.
40. J. Reinhardt, Y. Ferandin, L. Meijer, Purification CK1 by affinity chromatography on immobilised axin, *Protein Expr. & Purif.*, **2007**, *54*, 101-109.
41. J. Ribas, J. Boix, Cell differentiation, caspase inhibition, and macromolecular synthesis blockage, but not BCL-2 or BCL-XL proteins, protect SH-SY5Y cells from apoptosis triggered by two CDK inhibitory drugs, *Exp. Cell Res.*, **2004**, *295*, 9-24.
42. Bettayeb, K., Oumata, N., Echalié, A., Ferandin, Y., Endicott, J., Galons, H. and Meijer, L., 2008. CR8, a potent and selective, roscovitine-derived inhibitor of cyclin-dependent kinases. *Oncogene*, in press.
43. M. Nguyen, R.C. Marcellus, A. Roulston, M. Watson, L. Serfass, S.R. Murthy Madiraju, D. Goulet, J. Viallet, L. Bélec, X. Billot, S. Acoca, E. Purisima, A. Wiegman, L. Cluse, R.W. Johnstone, P. Beauparlant, G.C. Shore, Small molecule obatoclax (GX15-070) antagonizes MCL-1 and overcomes MCL-1-mediated resistance to apoptosis, *Proc. Natl. Acad. Sci. U.S.A.*, **2007**, *104*, 19512-19517.
44. S. Bach, M. Knockaert, O. Lozach, J. Reinhardt, B. Baratte, S. Schmitt, S.P. Coburn, L. Tang, T. Jiang, D.C. Liang, H. Galons, J.F. Dierick, F. Totzke, C. Schächtele, A.S. Lerman, A. Carnero, Y. Wan, N. Gray, L. Meijer, Roscovitine targets: protein kinases and pyridoxal kinase, *J. Biol. Chem.*, **2005**, *280*, 31208-31219.

Provided for non-commercial research and education use.
Not for reproduction, distribution or commercial use.



This article appeared in a journal published by Elsevier. The attached copy is furnished to the author for internal non-commercial research and education use, including for instruction at the authors institution and sharing with colleagues.

Other uses, including reproduction and distribution, or selling or licensing copies, or posting to personal, institutional or third party websites are prohibited.

In most cases authors are permitted to post their version of the article (e.g. in Word or Tex form) to their personal website or institutional repository. Authors requiring further information regarding Elsevier's archiving and manuscript policies are encouraged to visit:

<http://www.elsevier.com/copyright>



Contents lists available at ScienceDirect

Tetrahedron

journal homepage: www.elsevier.com/locate/tet



Factors affecting orthogonality in the deprotection of 2,4-di-protected aromatic ethers employing solid-supported acids

Kassrin Tangdenpaisal^a, Supanee Sualek^a, Somsak Ruchirawat^{a,b,c}, Poonsakdi Ploypradith^{a,b,*}

^aLaboratory of Medicinal Chemistry, Chulabhorn Research Institute, Vipavadee-Rangsit Highway, Bangkok 10210, Thailand

^bProgram in Chemical Biology, Chulabhorn Graduate Institute and the Center of Excellence on Environmental Health, Toxicology and Management of Chemicals, Vipavadee-Rangsit Highway, Bangkok 10210, Thailand

^cProgram on Research and Development of Synthetic Drugs, Institute of Science and Technology for Research and Development, Mahidol University, Salaya Campus, Nakhon Pathom, Thailand

ARTICLE INFO

Article history:

Received 6 January 2009

Received in revised form 12 March 2009

Accepted 26 March 2009

Available online 1 April 2009

ABSTRACT

Selective deprotection of aromatic ethers bearing two protecting groups on the same aromatic ring by solid-supported acids (Amberlyst-15 and PTS-Si) was systematically investigated. *ortho*-Directing protonation by the carbonyl group as well as carbocation stability and quenching are the important determining factors for the orthogonal deprotection process. Stabilized carbocations (e.g., those from the MOM and PMB groups) could be removed with high selectivity.

© 2009 Elsevier Ltd. All rights reserved.

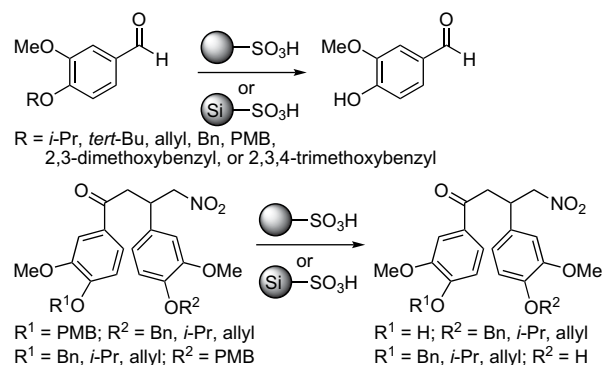
1. Introduction

Syntheses of complex natural products containing various functional groups inevitably involve the use of protecting groups. However, devising an appropriate strategy for protecting group manipulation is frequently challenging because the methods of introducing and removing such protecting groups must be compatible with other functional groups present in the molecules.^{1,2} In addition, selective methods for removing a protecting group in the presence of other functional groups as well as other protecting groups are frequently required.^{3–16} Thus, developing a general but selective method of deprotection can significantly reduce the number of steps in the protection/deprotection and render the overall syntheses less cumbersome and lengthy while more efficient and elegant.

Solid-supported reagents have been extensively used in organic synthesis and have drawn much attention from many research groups including ours because they are attractive alternatives to perform reactions more efficiently.^{17–22} Immobilizing reagents on solid supports simplifies the experimental procedures by eliminating the necessity of aqueous workup. In addition, the use of solid-supported reagents provided better chemical selectivity for some transformations when compared with the solution-phase counterpart.^{17,20} More importantly, conventional means such as TLC could be used to monitor the reaction progress.

Recently, our program has been involved with the use of solid-supported reagents in the synthesis of lamellarins and in the

deprotection of aromatic ethers.^{20–22} Our preliminary results of the deprotection of aromatic ethers employing solid-supported acids showed that the *p*-TsOH immobilized on either silica (PTS-Si) or polystyrene (PS)-divinyl benzene (DVB) polymer (Amberlyst-15) effectively cleaved various phenolic *O*-protecting groups (Scheme 1).²² When two protecting groups were present simultaneously in the same molecule but on different aromatic rings, the group, which generated a more stabilized carbocation such as the *p*-methoxybenzyl (PMB) was removed orthogonally over the other (*i*-Pr, Bn, or allyl). Thus, carbocations were presumably the intermediates generated during the acid-mediated cleavage of these protecting groups. Carbocation stability is anticipated to play a critical role for the orthogonality. Herein, we wish to report our systematic investigation in the selective deprotection of aromatic



Scheme 1. Preliminary deprotection of aromatic ethers employing Amberlyst-15 and PTS-Si.

* Corresponding author. Tel.: +662 574 0622; fax: +662 574 2027.

E-mail address: poonsakdi@cri.or.th (P. Ploypradith).

ethers, which bear two protecting groups on the same aromatic rings, employing PTS-Si and Amberlyst-15 to determine the effects of *ortho*-directing protonation by the carbonyl group as well as the carbocation stability and quenching.

2. Results and discussion

The presence of two protecting groups on the same aromatic rings is arguably one of the most challenging systems to optimize for the orthogonal removal due to the susceptible nature of poly-oxygenation on the aromatic ring towards the undesired Friedel–Crafts (FC)-type side reactions between the mono-deprotected product and the carbocations. We anticipated that the *ortho*-directing protonation by the carbonyl group may play an important role in the selective deprotection by directing the protonation to occur more readily on the oxygen of the protecting group *ortho* to a carbonyl-containing substituent (e.g., ester, aldehyde, or ketone). On the other hand, because the reaction mechanism implicated the intermediacy of carbocations during the deprotection, the carbocation stability and quenching was also an important consideration.

In addition to the *i*-Pr, Bn and PMB protecting groups, the methoxymethyl (MOM) group was also employed in this study. Among these four groups, the MOM group is the most easily cleaved because the resulting carbocation is stabilized by the nearby methoxy group. The benzyl-type carbocations from the Bn and PMB groups are resonance stabilized. However, the *i*-Pr cation is a localized secondary carbocation. Thus, on the basis of carbocation stability alone, the order of the C–O cleavage would follow MOM>PMB>Bn>*i*-Pr.

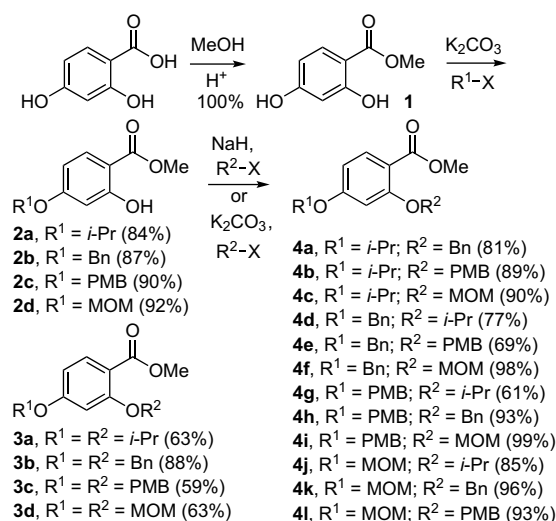
From the proposed mechanism of carbocation quenching, the *i*-Pr cation would form propene by losing a proton on the adjacent carbon. In contrast, due to the lack of such proton, the corresponding carbocations from the Bn, PMB and MOM groups are possibly quenched by nucleophile(s) such as toluene, which was used as solvent for these deprotection reactions, via the FC-type reactions. Thus, from this regard, it appears that the *i*-Pr cation may be quenched more effectively than others due to the thermodynamically favourable generation of propene.

The MOM as well as the *i*-Pr, Bn and PMB ethers of vanillin was used as models to establish the optimal reaction conditions for their removal without the contribution from the *ortho*-directing protonation by the carbonyl group. The optimal conditions for the *i*-Pr, Bn and PMB ethers of vanillin have been reported.^{21,22} After some experimentation, the optimal conditions for the MOM ether of vanillin were found for Amberlyst-15 (40 °C for 72 h) and PTS-Si (40 °C for 5 h), which provided vanillin in 93% and 97% yields, respectively.²³

To determine the effects of *ortho*-directing protonation by the carbonyl group as well as carbocation stability and quenching on the orthogonal deprotection of different protecting groups on the same aromatic ring, a number of similarly as well as differently di-protected 2,4-dihydroxy methylbenzoates were prepared (Scheme 2).

First, 2,4-dihydroxybenzoic acid was converted to its methyl ester **1** in quantitative yield. The *ortho*-hydroxy group of **1** was less acidic due to the intramolecular H-bonding with the carbonyl group, making it possible to selectively protect the more acidic *para*-hydroxy group first using weaker bases or lower temperatures. Under such reaction conditions, the mono-protected 2-hydroxy-4-alkoxybenzoates **2a–d** were obtained in good to excellent yields (84–92%). The similarly di-protected products **3a–d** were obtained as by-products from this selective protection of the *para*-hydroxy group or directly as the products of the dialkylation of **1**. The *ortho*-hydroxy group could be protected subsequently using stronger bases such as NaH or at higher temperatures. The overall two-step sequential protection process furnished the desired differently di-protected compounds **4a–l** in good to excellent yields (61–99%).

When the bis-protected benzoates **3a–d** were employed, all protecting groups at the position *ortho* to the ester carbonyl group



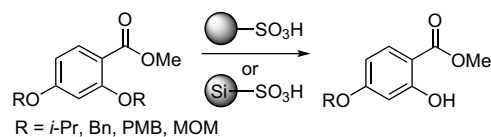
Scheme 2. Di-protected 2,4-dihydroxy benzoates (**3a–l**).

were orthogonally removed in moderate to good yields (Table 1; 30%–98%). When the two protecting groups were identical, the *ortho*-directing protonation by the carbonyl group normally directed the selectivity of the deprotection. However, the PMB group exhibited only moderate selectivity (entries 5 and 6). The *para*-PMB could undergo competitive deprotection with the *ortho*-PMB.²⁴

The benzyl carbocation could be effectively scavenged by MeOH, giving the mono-deprotected product in 89%–98% yields. However, the PMB cation was apparently too stabilized for effective quenching by MeOH. Methanol also competed for protons and thus slowed down the overall rate of deprotection reactions. For **3c** and **d**, adding MeOH to the reactions gave poorer yields of the desired products.²⁵

After establishing that *ortho*-directing protonation by the carbonyl group could direct the orthogonal deprotection of the similarly di-protected benzoates **3a–d**, all other differently di-protected benzoates **4a–l** were studied and the results were summarized in Table 2. In general, contribution from the *ortho*-directing protonation by the carbonyl group was more pronounced than those from carbocation stability and quenching. Protecting groups at the *ortho* position were removed preferentially over the others at the *para* position.

Table 1
Selective *ortho*-deprotection of similarly di-protected **3a–d**^a



Entry	Comp	R	Acid ^b	Prod	Temp ^c (°C)	Time ^d (h)	Yield (%)
1	3a	<i>i</i> -Pr	A	2a	80	4.0	81
2	3a	<i>i</i> -Pr	B	2a	80	2.0	86
3 ^e	3b	Bn	A	2b	80	4.0	89
4 ^e	3b	Bn	B	2b	80	4.5	98
5 ^f	3c	PMB	A	2c	rt	24	30
6 ^g	3c	PMB	B	2c	65	0.5	68
7 ^h	3d	MOM	A	2d	rt	1.0	60
8 ⁱ	3d	MOM	B	2d	0	0.5	86

^a The reactions were performed in toluene.

^b A=Amberlyst-15; B=PTS-Si.

^c Lowest temperatures for the best yields of the products.

^d Shortest reaction times for the best yields of the products.

^e MeOH (4–10 equiv) was added.

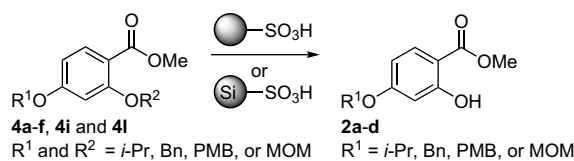
^f Yield: 14% of **1** and 28% of **3c**.

^g Yield: 16% of **1** and 5% of **3c**.

^h Yield: 13% of **1** and 5% of **3d**.

ⁱ Yield: 4% of **1**.

Table 2
Orthogonal *ortho*-deprotection of differently di-protected benzoates **4a–f**, **4i** and **4l**^a



Entry	Compound	R ¹	R ²	Deprotected group	Product	MeOH ^b (equiv)	Temp ^c (°C)	Time ^d (h)	Yield ^e (%)
1	4a	<i>i</i> -Pr	Bn	Bn	2a	10	80	4.5, 4.0	81, 99
2	4b	<i>i</i> -Pr	PMB	PMB	2a	10	65	0.5, 2.0	89, 87
3 ^f	4c	<i>i</i> -Pr	MOM	MOM	2a	none	rt	0.83, 0.5	90, 95
4	4d	Bn	<i>i</i> -Pr	<i>i</i> -Pr	2b	none	80, 90	5.0, 1.0	83, 60
5	4e	Bn	PMB	PMB	2b	10	65	1.5, 1.5	82, 85
6	4f	Bn	MOM	MOM	2b	none	rt	1.5, 0.42	99, 99
7	4i	PMB	MOM	MOM	2c	none	0, rt	2, 0.67	99, 99
8 ^g	4l	MOM	PMB	PMB	2d	2.5	40	3.0, 0.25	50, 65

^a The reactions were performed in toluene, with 0.6 equiv of the acid.

^b The amount of MeOH could not exceed 40 equiv (ca. 10% MeOH in toluene v/v). Greater amount of MeOH competed with the benzoates for protonation and the deprotection reactions would not proceed.

^c Lowest temperatures required for the complete consumption of starting materials. The first numbers are the temperature for the reactions employing Amberlyst-15 while the second numbers for those employing PTS-Si. Single numbers in the temperature column mean identical temperatures for both acids.

^d Shortest amount of times required for the complete consumption of starting materials. The first numbers are time for the reactions employing Amberlyst-15 while the second numbers for those employing PTS-Si.

^e Isolated and optimized yields. The first numbers are the yields from reactions employing Amberlyst-15 while the second are those employing PTS-Si.

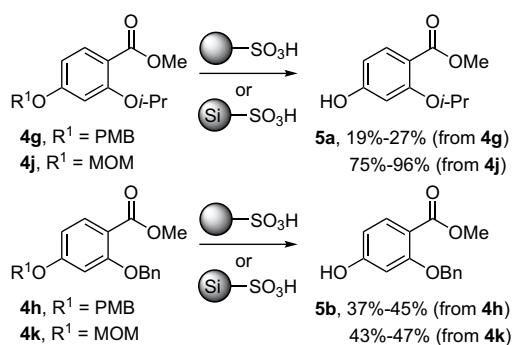
^f By-products from *p*-QM were obtained in 10% from **4c** (Amberlyst-15).

^g Other by-products were inseparable mixtures of the corresponding *o*- and *p*-PMBylated FC-type aromatic compounds.

The deprotection reactions of compounds **4a–f**, with the *i*-Pr and Bn groups at the *para* position, occurred exclusively on the protecting groups at the *ortho* position. In fact, both *ortho*-directing protonation by the carbonyl group as well as carbocation stability and quenching would predict the observed selectivity in compounds **4a–c** and **4e,f** because the protecting groups at the *ortho* position gave more stabilized carbocations following their acid-mediated cleavage. In addition, the *ortho*-directing protonation by the carbonyl group was even more important than the carbocation stability and quenching as the *ortho* *i*-Pr group was removed preferentially over the *para* Bn group in compound **4d**.

Deprotection studies of the benzoates **4i** and **l** also supported the importance of the *ortho*-directing protonation by the carbonyl group. If considering the carbocation stability and nucleophilic quenching of the carbocations from the MOM and PMB groups alone, selective removal could be difficult due to the rather similar stability of the two carbocations generated from the cleavage of these groups. However, the results were unequivocal (entries 7 and 8). Selectivity for the deprotection between these two groups did not depend on the type of the protecting group but on the position. The group on the *ortho* position was removed preferentially.

The importance of the combined carbocation stability and the nucleophilic quenching could compete with the *ortho*-directing protonation by the carbonyl group (Scheme 3). For example, the

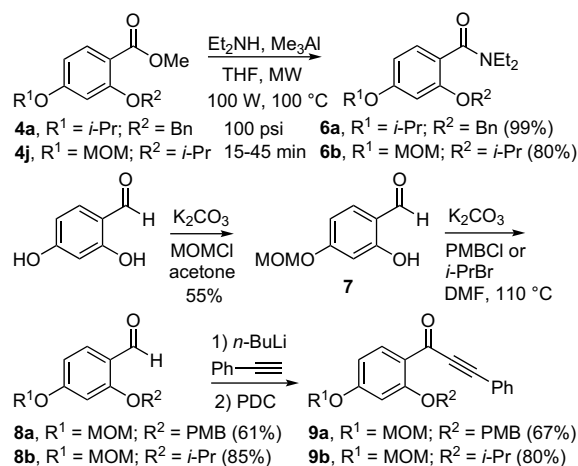


Scheme 3. Orthogonal *para*-deprotection of differently di-protected benzoates **4g,h** and **4j,k**.

PMB and MOM groups at the position *para* to the ester carbonyl group in compounds **4g,h** and **4j,k** could be removed over the *ortho* *i*-Pr as well as Bn groups to provide the corresponding products **5a** and **b**.

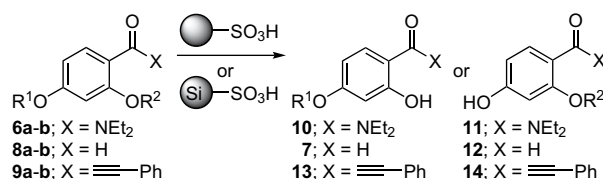
Thus, when a stabilized carbocation with efficient quenching could be generated from a protecting group, the contribution from carbocation stability and quenching became significant. In most cases, the low yields of the reactions were the results of the FC-type C-alkylation side reactions between the desired mono-protected product and the carbocations generated. It can be implied that, in these cases, the rates of deprotecting the *para*-protecting groups, which generated more stable carbocations, were slower than the FC-type reactions. Thus, when the reactions proceeded until complete consumption of the starting materials, the FC-type reactions already occurred to large extent.²⁶ It is noteworthy that the di-deprotected by-products were not observed.

To demonstrate the scope and compatibility with other functional groups of the method, the following 2,4-di-protected compounds were prepared (Scheme 4). The methylbenzoates **4a** and **j** were converted directly to the corresponding *N,N*-diethyl benzamides **6a** and **b**. 2,4-Dihydroxybenzaldehyde was converted to the



Scheme 4. Synthesis of **6a,b**, **8a,b** and **9a,b**.

Table 3

Orthogonal deprotection of **6a,b**, **8a,b** and **9a,b**^a

Entry	Compound	R ¹	R ²	Deprotected group	Product	Acid ^b	MeOH (equiv)	Temp ^c (°C)	Time ^d (h)	Yield ^e (%)
1 ^f	6a	<i>i</i> -Pr	Bn	Bn	10	B	25	80	50	40 (45)
2	6b	MOM	<i>i</i> -Pr	MOM	11	A	12	40	5.5	92
3 ^g	8a	MOM	PMB	PMB	7	A,B	—	—	—	0
4	8b	MOM	<i>i</i> -Pr	MOM	12	A	10	40	54	74
5	9a	MOM	PMB	PMB	13	A	2.5	40	0.25	67
6	9b	MOM	<i>i</i> -Pr	MOM	14	B	1.0	50	72	54 (60)

^a The reactions were performed in toluene, with 0.6 equiv of the acid.^b A=Amberlyst-15; B=PTS-Si.^c Lowest temperatures required for the complete consumption of starting materials.^d Shortest amount of times required for the complete consumption of starting materials.^e Isolated and optimized yields. The numbers in parentheses are those based on reacted starting materials.^f Other by-products included the benzylated mono-deprotected FC-type products (ca. 7% yield), benzylated di-deprotected FC-type products (ca. 21% yield) and the di-deprotected product (ca. 18% yield).^g The starting material was completely consumed but the reaction gave a complex mixture of PMBylated mono-deprotected products and PMBylated di-deprotected products without isolable amount of the desired product **7**.

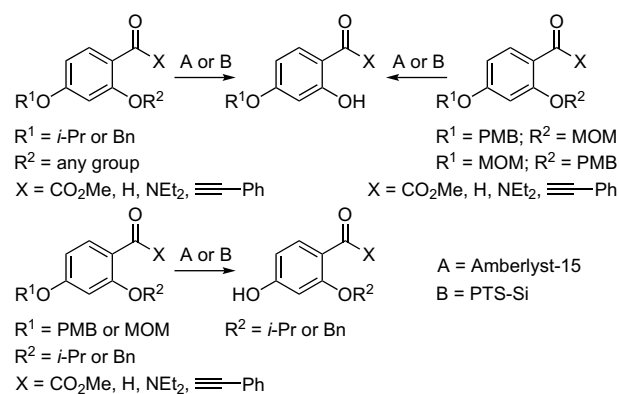
MOM ether **7**, which was subsequently protected to furnish the 2,4-di-protected benzaldehydes **8a,b**. The corresponding aryl phenylpropynones **9a,b** were synthesized from **8a,b** via phenyl acetylide addition followed by PDC oxidation.

The protecting groups (R¹ and R²) were selected based on the good selectivity and yields of the product upon orthogonal removal shown in Table 2 and Scheme 3. As summarized in Table 3, the results were generally in accordance with those obtained from the benzoates (Table 2). It is interesting to note that the deprotection conditions are compatible with the benzamide, benzaldehyde and aryl phenylpropynone moieties. Thus, it is possible to remove the Bn and PMB groups in compounds **6a**, **8a**²⁷ and **9a**. These results supported the *ortho*-directing protonation for the selective deprotection of R². On the other hand, the MOM group at R¹ was consistently and selectively removed over the *i*-Pr group at R² (entries 2, 4 and 6), indicating the importance of the selective cleavage of the protecting group leading to the more stable carbocation.

The use of solid-supported acids (Amberlyst-15 or PTS-Si) for cleaving these aromatic ethers offers several advantages over the use of a conventional acid such as *p*-TsOH under similar reaction conditions. Due to the greater surface area of these solid-supported acids,²⁸ the reactions proceeded faster. While the deprotection of compound **4a** with Amberlyst-15 or PTS-Si took 4–4.5 h, a similar reaction using *p*-TsOH required 10 h. Yields of the products from the reactions using solid-supported acids are comparable to those using conventional acids.²⁹ For example, deprotection of compounds **4a** and **d** using *p*-TsOH gave **2a** and **b** in 70% and 75% yields, respectively. In addition, the reactions required virtually no aqueous workup and only simple filtration to remove the solid-supported materials was necessary.

3. Conclusion

In summary, a number of optimized reaction conditions³⁰ were found for orthogonal deprotection of compounds containing two different phenol-protecting groups on the same aromatic ring. In general, the *ortho*-directing protonation by the carbonyl group plays an important role as the group *ortho* to the carbonyl group is removed with high selectivity over the other at the *para* position. This is the case when *i*-Pr or Bn group is present at the 4-position. However, such preference could be partially or entirely reversed in



Scheme 5. Schematic summary of selective deprotections.

case of the MOM or PMB group at the 4-position which could generate stabilized carbocations. Thus, in some of those cases, carbocation stability became a significant competing determinant. In addition, the deprotection conditions showed good compatibility with the benzamide, benzaldehyde and aryl phenyl propynone moieties.

A schematic summary of the selective deprotections is shown in Scheme 5. When the 4-position contains *i*-Pr or Bn, *ortho*-directing protonation by the carbonyl group governs the selective removal of any protecting group at the 2-position. For PMB and MOM groups at the 4-position, selective deprotection depends largely on the nature of the protecting group at the 2-position. If the 2-position contains *i*-Pr or Bn, the PMB or MOM group can be selectively removed. However, when the 2-position is PMB or MOM, the *ortho*-directing protonation directs the selective removal of the group at the 2-position.

4. Experimental

4.1. General experimental methods

Unless otherwise noted: reactions were run in oven-dried round-bottomed flasks. Tetrahydrofuran (THF) was distilled from sodium benzophenone ketyl while dichloromethane (DCM) from

calcium hydride prior to use. All other compounds were used as received from the suppliers. PTS-Si (*p*-TsOH immobilized on silica) used in these experiments was purchased from Silicycle with the surface area of 500 m²/g as indicated by the supplier. Other commercially available PTS-Si from other suppliers were not evaluated and thus other PTS-Si may or may not yield the results similar to those reported in this study. The crude reaction mixtures were concentrated under reduced pressure by removing organic solvents on rotary evaporator. Column chromatography was performed using silica gel 60 (particle size 0.06–0.2 mm; 70–230 mesh ASTM). Analytical thin-layer chromatography (TLC) was performed with silica gel 60 F₂₅₄ aluminium sheets. Chemical shifts for ¹H nuclear magnetic resonance (NMR) spectra were reported in parts per million (ppm, δ) downfield from tetramethylsilane. Splitting patterns are described as singlet (s), doublet (d), triplet (t), quartet (q), multiplet (m), broad (br) and doublet of doublet (dd). Resonances for infrared (IR) spectra were reported in wavenumbers (cm⁻¹). Low resolution (LRMS) mass spectra were obtained either using electron ionization (EI) or time-of-flight (TOF) while high resolution (HRMS) mass spectra were obtained using time-of-flight (TOF). Melting points were uncorrected.

4.1.1. 3-Methoxy-4-methoxymethoxybenzaldehyde

To a stirred suspension of vanillin (1.52 g, 10 mmol) in acetone (15 mL) was added anhydrous K₂CO₃ (2.07 g, 15 mmol) at rt and the reaction mixture was stirred at rt for 5 min. Chloromethyl methyl ether (1.14 mL, 15 mmol) was added dropwise into the reaction flask and the mixture was stirred at 10–15 °C for 1.5 h. Water (20 mL) and EtOAc (20 mL) were added and two phases were separated. The aqueous phase was extracted with EtOAc (2 × 20 mL). The combined organic layers were washed with brine (25 mL), dried over Na₂SO₄, filtered and concentrated under reduced pressure to give the crude product, which was purified by column chromatography on silica (30% EtOAc/hexanes) to give the product as a white solid (1.87 g, 9.54 mmol, 95%). Mp (MeOH) 44–45 °C. IR (neat): ν_{\max} 2940, 2831, 1682, 1587, 1507, 1261 cm⁻¹. ¹H NMR (200 MHz, CDCl₃): δ 3.53 (s, 3H), 3.96 (s, 3H), 5.34 (s, 2H), 7.23–7.33 (m, 1H), 7.39–7.49 (m, 2H), 9.88 (s, 1H). ¹³C NMR (50 MHz, CDCl₃): δ 56.0, 56.5, 94.9, 109.3, 114.5, 126.4, 131.0, 150.0, 151.9, 191.0. LRMS (EI) *m/z* (rel intensity) 197 (M+H⁺, 21), 196 (M⁺, 68), 166 (100), 165 (27), 77 (17), 45 (37). TOF-HRMS calcd for C₁₀H₁₃O₄ (M+H⁺) 197.0808, found 197.0805.

4.1.2. Methyl 2,4-dihydroxybenzoate (**1**)

To a stirred solution of 2,4-dihydroxybenzoic acid (12.0 g, 77.9 mmol) in MeOH (60 mL) was added concd H₂SO₄ (5 mL) and the mixture was refluxed for 20 h. After cooling to rt, MeOH was removed under reduced pressure and the residue was poured into ice water (200 mL). The precipitates were collected and washed with water. The solid was recrystallized (MeOH/hexanes) to give the product (13.0 g, 77.3 mmol, 99%) as a white solid. Mp (EtOAc/hexanes) 112–114 °C (lit.³¹ 118–121 °C; lit.³² 116–117 °C). ¹H NMR (200 MHz, CDCl₃): δ 3.90 (s, 3H), 6.33–6.39 (m, 2H), 7.68–7.73 (m, 1H). ¹³C NMR (50 MHz, CDCl₃): δ 51.9, 102.8, 105.1, 108.1, 131.7, 163.1, 163.3, 170.5. LRMS (EI) *m/z* (rel intensity) 169 (M+H⁺, 20), 168 (M⁺, 67), 137 (53), 136 (100), 108 (67), 80 (13), 52 (19). These spectroscopic data are identical to those reported previously.^{33–36}

4.2. Preparation of mono-protected benzoates (2a–d)

4.2.1. Methyl 2-hydroxy-4-isopropoxybenzoate (**2a**)

A mixture of **1** (4.00 g, 23.8 mmol), isopropyl bromide (3.42 mL, 36 mmol), anhydrous K₂CO₃ (5.00 g, 36 mmol) in DMF (30 mL) was stirred at 70 °C for 4 h. After being cooled to rt, water (30 mL) and EtOAc (30 mL) were added. The two phases were separated and the aqueous phase was extracted with EtOAc (2 × 20 mL). The combined

organic layers were washed with water (4 × 20 mL), brine (30 mL), dried over Na₂SO₄, filtered and concentrated under reduced pressure to give crude product, which was purified by column chromatography on silica (30% EtOAc/hexanes) to give the desired product as a white solid (4.10 g, 19.5 mmol, 81%). Mp (EtOAc/hexanes) 46–48 °C (no previous literature values given). ¹H NMR (200 MHz, CDCl₃): δ 1.35 (d, *J*=5.8 Hz, 6H), 3.90 (s, 3H), 4.58 (sept, *J*=5.8 Hz, 1H), 6.37 (d, *J*=1.8 Hz, 1H), 6.42 (s, 1H), 7.71 (dd, *J*=9.6, 1.8 Hz, 1H), 10.9 (s, 1H). ¹³C NMR (50 MHz, CDCl₃): δ 21.8, 51.9, 70.1, 101.8, 104.9, 108.6, 131.2, 163.2, 164.0, 170.4. LRMS (EI) *m/z* (rel intensity) 211 (M+H⁺, 34), 210 (M⁺, 100), 168 (4), 136 (12). These spectroscopic data were identical to those reported previously.³⁷

4.2.2. Methyl 4-benzyloxy-2-hydroxybenzoate (**2b**)

A mixture of **1** (2.78 g, 16.5 mmol) and anhydrous K₂CO₃ (3.11 g, 22.5 mmol) in acetone (15 mL) was stirred at rt for 5 min. Benzyl bromide (1.96 mL, 16.5 mmol) was added dropwise into the reaction flask and the mixture was stirred at 10–15 °C for 3 h. Water (20 mL) and EtOAc (20 mL) were added and two phases were separated. The aqueous phase was extracted with EtOAc (2 × 20 mL). The combined organic layers were washed with brine (25 mL), dried over Na₂SO₄, filtered and concentrated under reduced pressure to give the crude product, which was purified by column chromatography on silica (30% EtOAc/hexanes) to give the product as a white solid (3.20 g, 14.0 mmol, 85%). Mp (MeOH) 103–105 °C. IR (neat): ν_{\max} 3100 (br), 3064, 3034, 2956, 1661, 1619, 1441, 1347, 1254, 1215 cm⁻¹. ¹H NMR (200 MHz, CDCl₃): δ 3.90 (s, 3H), 5.07 (s, 2H), 6.48–6.53 (m, 2H), 7.37–7.40 (m, 5H), 7.74 (d, *J*=9.4 Hz, 1H), 11.0 (s, 1H). The material is commercially available.^{38,39}

4.2.3. Methyl 2-hydroxy-4-(4-methoxy)benzyloxybenzoate (**2c**)

A mixture of **1** (0.21 g, 1.20 mmol) and anhydrous K₂CO₃ (0.25 g, 1.80 mmol) in DMF (10 mL) was stirred at rt for 5 min. *para*-Methoxybenzyl chloride (0.28 g, 1.80 mmol) was added dropwise into the reaction flask and the mixture was stirred at 10–15 °C for 3 h. Water (10 mL) and EtOAc (10 mL) were added and the two phases were separated. The aqueous phase was extracted with EtOAc (2 × 10 mL). The combined organic layers were washed with brine (15 mL), dried over Na₂SO₄, filtered and concentrated under reduced pressure to give the crude product, which was purified by column chromatography on silica (30% EtOAc/hexanes) to give the product as a white solid (0.31 g, 1.08 mmol, 90%). Mp (EtOAc/hexanes) 89–90 °C. IR (neat): ν_{\max} 3081, 1662, 1613, 1348, 1251 cm⁻¹. ¹H NMR (200 MHz, CDCl₃): δ 3.81 (s, 3H), 3.91 (s, 3H), 4.99 (s, 2H), 6.43–6.60 (m, 2H), 6.92 (d, *J*=8.8 Hz, 2H), 7.35 (d, *J*=8.8 Hz, 2H), 7.74 (d, *J*=8.0 Hz, 1H), 11.0 (s, 1H). ¹³C NMR (50 MHz, CDCl₃): δ 52.0, 55.3, 69.9, 101.5, 105.5, 108.1, 114.0, 128.0, 129.3, 131.2, 159.6, 163.6, 164.7, 170.4. LRMS (EI) *m/z* (rel intensity) 288 (M⁺, 5), 121 (100). TOF-HRMS calcd for C₁₆H₁₇O₅ (M+H⁺) 289.1071, found 289.1070.

4.2.4. Methyl 2-hydroxy-4-methoxymethoxybenzoate (**2d**)

A mixture of **1** (3.00 g, 16.2 mmol) and anhydrous K₂CO₃ (3.36 g, 24.4 mmol) in acetone (40 mL) was stirred at rt for 5 min. Chloromethyl methyl ether (1.85 mL, 24.4 mmol) was added dropwise at 0 °C into the reaction flask. The reaction was heated to 60 °C for 2.5 h. After being cooled to rt, water (20 mL) and EtOAc (20 mL) were added and the two phases were separated. The aqueous phase was extracted with EtOAc (2 × 20 mL). The combined organic layers were washed with brine (20 mL), dried over Na₂SO₄, filtered and concentrated under reduced pressure to give the crude product, which was purified by column chromatography on silica (30% EtOAc/hexanes) to furnish the product as a white solid (3.13 g, 14.9 mmol, 92%). Mp (EtOAc/hexanes) 35–36 °C. IR (neat): ν_{\max} 3145, 2956, 1668, 1621, 1582, 1501, 1440, 1345, 1220, 1074 cm⁻¹. ¹H NMR (200 MHz, CDCl₃): δ 3.45 (s, 3H), 3.88 (s, 3H), 5.16 (s, 2H), 6.50 (dd, *J*=8.8, 2.2 Hz, 1H), 6.59 (d, *J*=2.2 Hz, 1H), 7.71 (d, *J*=8.8 Hz, 1H),

10.9 (s, 1H). ^{13}C NMR (50 MHz, CDCl_3): δ 51.9, 56.1, 93.9, 103.4, 106.4, 108.2, 131.2, 163.0, 163.4, 172.2. LRMS (EI) m/z (rel intensity) 212 (M^+ , 50), 182 (49), 150 (96), 122 (42), 45 (100). TOF-HRMS calcd for $\text{C}_{10}\text{H}_{13}\text{O}_5$ ($\text{M}+\text{H}^+$) 213.0757, found 213.0754.

4.3. General procedure for the preparation of similarly di-protected benzoates (3a–d)

A mixture of **1** (1.0 equiv) and anhydrous K_2CO_3 (3.0 equiv) in DMF (2 mL/mmol of **1**) was stirred at rt for 5 min. Alkyl or aryl-methylene (benzyl-type) halide (3.0 equiv) was added dropwise and the reaction mixture was heated to 100 °C for 4.5 h. After being cooled to rt, water and EtOAc were added. The aqueous phase was extracted with EtOAc. The combined organic layers were washed with brine, dried over Na_2SO_4 , filtered and concentrated under reduced pressure to give the crude product, which was further purified by column chromatography on silica (20% EtOAc/hexanes) to furnish the products **3a–d**.

4.3.1. Methyl 2,4-diisopropoxybenzoate (3a)

IR (neat): ν_{max} 2982, 1760, 1697, 1241, 1200 cm^{-1} . ^1H NMR (200 MHz, CDCl_3): δ 1.21 (t, $J=7.2$ Hz, 3H), 1.32 (t, $J=7.0$ Hz, 3H), 2.52 (s, 3H), 3.35 (s, 3H), 4.14 (q, $J=7.2$ Hz, 2H), 4.25 (q, $J=7.0$ Hz, 2H), 6.54 (s, 1H), 7.22–7.45 (m, 4H). ^{13}C NMR (50 MHz, CDCl_3): δ 11.5, 14.0, 14.5, 31.5, 59.1, 64.7, 110.5, 111.8, 122.1, 126.0, 126.1, 127.5, 129.4, 132.2, 136.9, 149.5, 153.0, 165.5. LRMS (EI) m/z (rel intensity) 332 ($\text{M}+\text{H}^+$, 16), 331 (M^+ , 100), 259 (25), 230 (43), 185 (31). TOF-HRMS calcd for $\text{C}_{18}\text{H}_{22}\text{NO}_5$ ($\text{M}+\text{H}^+$) 332.1492, found 332.1489. These spectroscopic data are identical to those reported previously.²²

4.3.2. Methyl 2,4-dibenzoyloxybenzoate (3b)

Mp (MeOH) 68–70 °C. IR (neat): ν_{max} 3032, 1721, 1606, 1253, 1143 cm^{-1} . ^1H NMR (200 MHz, CDCl_3): δ 3.87 (s, 3H), 5.07 (s, 2H), 5.14 (s, 2H), 6.52–6.66 (m, 2H), 7.22–7.58 (m, 10H), 7.89 (d, $J=8.8$ Hz, 1H). ^{13}C NMR (50 MHz, CDCl_3): δ 51.7, 70.2, 70.6, 101.5, 106.1, 113.3, 126.5, 127.5, 127.8, 128.2, 128.5, 128.7, 133.9, 136.2, 136.7, 160.2, 163.2, 166.2. LRMS (EI) m/z (rel intensity) 348 (M^+ , 14), 316 (65), 181 (35), 91 (100). TOF-HRMS calcd for $\text{C}_{22}\text{H}_{21}\text{O}_4$ ($\text{M}+\text{H}^+$) 349.1434, found 349.1403.

4.3.3. Methyl 2,4-di-(4-methoxy)benzoyloxybenzoate (3c)

Mp (MeOH) 67–68 °C. IR (neat): ν_{max} 2950, 1720, 1606, 1516, 1242, 1172, 1029 cm^{-1} . ^1H NMR (200 MHz, CDCl_3): δ 3.81 (s, 6H), 3.85 (s, 3H), 4.98 (s, 2H), 5.06 (s, 2H), 6.57 (d, $J=6.6$ Hz, 1H), 6.34 (s, 1H), 6.91 (d, $J=8.6$ Hz, 4H), 7.33 (d, $J=8.6$ Hz, 2H), 7.41 (d, $J=8.6$ Hz, 2H), 7.88 (d, $J=8.6$ Hz, 1H). ^{13}C NMR (50 MHz, CDCl_3): δ 51.6, 55.3, 70.0, 70.5, 101.6, 106.1, 113.2, 113.9, 114.1, 128.2, 128.4, 128.7, 129.3, 133.8, 159.3, 160.3, 163.2, 166.2. TOF-LRMS m/z (rel intensity) 431 ($\text{M}+\text{Na}^+$, 100). TOF-HRMS calcd for $\text{C}_{24}\text{H}_{24}\text{NaO}_6$ ($\text{M}+\text{Na}^+$) 431.1465, found 431.1465.

4.3.4. Methyl 2,4-dimethoxymethoxybenzoate (3d)

IR (neat): ν_{max} 2952, 1723, 1606, 1249, 1135 cm^{-1} . ^1H NMR (200 MHz, CDCl_3): δ 3.42 (s, 3H), 3.48 (s, 3H), 3.81 (s, 3H), 5.15 (s, 2H), 5.20 (s, 2H), 6.66 (dd, $J=8.8, 2.2$ Hz, 1H), 6.68 (d, $J=2.2$ Hz, 1H), 7.77 (d, $J=8.8$ Hz, 1H). ^{13}C NMR (50 MHz, CDCl_3): δ 51.2, 55.7, 55.9, 93.7, 94.7, 104.0, 108.2, 113.9, 132.8, 158.3, 161.0, 165.4. LRMS (EI) m/z (rel intensity) 256 (M^+ , 55), 225 (100). TOF-HRMS calcd for $\text{C}_{12}\text{H}_{17}\text{O}_6$ ($\text{M}+\text{H}^+$) 257.1020, found 257.1027.

4.4. General procedure for the preparation of differently di-protected benzoates (4a–l)

A mixture of mono-protected benzoates **2a–d** (1.0 equiv), base (K_2CO_3 or NaH; 1.5 equiv) in DMF (2.5 mL/mmol) was stirred at appropriate temperature (see Table 4 below) before the addition of the alkyl or arylmethylene (benzyl-type) halides (1.5 equiv). The

Table 4

Reaction conditions for the preparation of **4a–l**

Comp	Base	Temp ^a (°C)	Temp ^b (°C)	Time (h)	Prod	Yield (%)
2a	K_2CO_3	rt	110	4.5	4a	81
2a	K_2CO_3	rt	110	3.0	4b	89
2a	NaH	0	rt	1.5	4c	90
2b	K_2CO_3	rt	110	3.3	4d	77
2b	K_2CO_3	rt	110	3.0	4e	69
2b	NaH	0	rt	1.5	4f	98
2c	K_2CO_3	rt	110	2.0	4g	61
2c	K_2CO_3	rt	110	0.5	4h	93
2c	NaH	0	rt	1.0	4i	99
2d	K_2CO_3	rt	110	18	4j	85
2d	K_2CO_3	rt	110	0.5	4k	96
2d	K_2CO_3	rt	110	5.0	4l	93

^a Temperature at which the base was added.

^b Temperature of the reaction mixture.

resulting mixture was stirred at temperature and for the duration as indicated in Table 4. Water and EtOAc were added. The aqueous phase was extracted with EtOAc. The combined organic layers were washed with brine, dried over Na_2SO_4 , filtered and concentrated under reduced pressure to give the crude product, which was further purified by column chromatography on silica (25% EtOAc/hexanes) to furnish the desired products **4a–l**.

4.4.1. Methyl 2-benzoyloxy-4-isopropoxybenzoate (4a)

Mp (MeOH) 73.9–75.3 °C (no previous literature values given). IR (neat): ν_{max} 2978, 2924, 1722, 1604, 1572, 1502, 1437, 1249, 1184, 1132, 1085 cm^{-1} . ^1H NMR (200 MHz, CDCl_3): δ 1.33 (d, $J=5.8$ Hz, 6H), 3.88 (s, 3H), 4.58 (sept, $J=5.8$ Hz, 1H), 5.16 (s, 2H), 6.45–6.49 (m, 2H), 7.28–7.42 (m, 3H), 7.49–7.52 (m, 2H), 7.85 (d, $J=9.6$ Hz, 1H). ^{13}C NMR (50 MHz, CDCl_3): δ 21.8, 51.5, 70.1, 70.5, 102.1, 106.6, 126.7, 127.6, 128.4, 133.7, 136.7, 160.3, 162.5, 166.1. LRMS (EI) m/z (rel intensity) 301 ($\text{M}+\text{H}^+$, 5), 300 (M^+ , 17), 268 (45), 226 (29), 168 (10), 136 (23), 92 (18), 91 (100), 81 (7), 41 (41). TOF-HRMS calcd for $\text{C}_{18}\text{H}_{21}\text{O}_4$ ($\text{M}+\text{H}^+$) 301.1434, found 301.1435. These spectroscopic data are identical to those reported previously.²²

4.4.2. Methyl 4-isopropoxy-2-(4-methoxy)benzoyloxybenzoate (4b)

IR (neat): ν_{max} 2978, 1721, 1604, 1572, 1514, 1439, 1244, 1174 cm^{-1} . ^1H NMR (200 MHz, CDCl_3): δ 1.33 (d, $J=6.0$ Hz, 6H), 3.81 (s, 3H), 3.85 (s, 3H), 4.57 (sept, $J=6.0$ Hz, 1H), 5.08 (s, 2H), 6.48 (d, $J=8.4$ Hz, 1H), 6.50 (s, 1H), 6.92 (d, $J=8.4$ Hz, 2H), 7.43 (d, $J=8.4$ Hz, 2H), 7.85 (d, $J=8.4$ Hz, 1H). ^{13}C NMR (50 MHz, CDCl_3): δ 21.9, 51.6, 55.3, 70.1, 70.5, 102.3, 106.7, 112.6, 113.9, 128.4, 128.8, 133.7, 159.3, 160.4, 162.5, 166.2. LRMS (EI) m/z (rel intensity) 330 (M^+ , 8), 241 (17), 121 (100). TOF-HRMS calcd for $\text{C}_{19}\text{H}_{23}\text{O}_5$ ($\text{M}+\text{H}^+$) 331.1540, found 331.1541.

4.4.3. Methyl 4-isopropoxy-2-methoxymethoxybenzoate (4c)

IR (neat): ν_{max} 2979, 1723, 1605, 1573, 1498, 1434, 1250 cm^{-1} . ^1H NMR (400 MHz, CDCl_3): δ 1.34 (d, $J=6.0$ Hz, 6H), 3.52 (s, 3H), 3.85 (s, 3H), 4.59 (sept, $J=6.0$ Hz, 1H), 5.23 (s, 2H), 6.53 (dd, $J=8.8, 2.4$ Hz, 1H), 6.70 (d, $J=2.4$ Hz, 1H), 7.81 (d, $J=8.4$ Hz, 1H). ^{13}C NMR (100 MHz, CDCl_3): δ 21.9, 51.6, 56.3, 70.1, 95.2, 104.1, 108.0, 112.9, 133.4, 159.0, 162.3, 166.0. LRMS (EI) m/z (rel intensity) 255 ($\text{M}+\text{H}^+$, 82), 254 (M^+ , 100), 223 (94), 207 (45), 181 (30), 151 (38). TOF-HRMS calcd for $\text{C}_{13}\text{H}_{19}\text{O}_5$ ($\text{M}+\text{H}^+$) 255.1227, found 255.1219.

4.4.4. Methyl 4-benzoyloxy-2-isopropoxybenzoate (4d)

IR (neat): ν_{max} 2978, 1724, 1604, 1572, 1242, 1188 cm^{-1} . ^1H NMR (200 MHz, CDCl_3): δ 1.35 (d, $J=6.0$ Hz, 6H), 3.84 (s, 3H), 4.52 (sept, $J=6.0$ Hz, 1H), 5.08 (s, 2H), 6.48–6.63 (m, 2H), 7.28–7.49 (m, 5H), 7.82 (d, $J=9.4$ Hz, 1H). ^{13}C NMR (50 MHz, CDCl_3): δ 22.0, 51.5, 70.2, 71.9, 103.0, 106.0, 114.2, 127.5, 128.2, 128.7, 133.7, 136.3, 159.8, 163.0, 166.3. LRMS (EI) m/z (rel intensity) 300 (M^+ , 22), 226 (12), 91 (100). TOF-HRMS calcd for $\text{C}_{18}\text{H}_{21}\text{O}_4$ ($\text{M}+\text{H}^+$) 301.1434, found 301.1426.

4.4.5. Methyl 4-benzyloxy-2-(4-methoxy)benzyloxybenzoate (**4e**)

Mp (MeOH) 71–73 °C. IR (neat): ν_{\max} 2949, 1721, 1606, 1514, 1244, 1174, 1027 cm^{-1} . ^1H NMR (200 MHz, CDCl_3): δ 3.82 (s, 3H), 3.87 (s, 3H), 5.07 (s, 4H), 6.57–6.63 (m, 2H), 6.93 (d, $J=8.8$ Hz, 2H), 7.37–7.45 (m, 6H), 7.88 (d, $J=8.8$ Hz, 2H). ^{13}C NMR (50 MHz, CDCl_3): δ 51.6, 55.2, 70.1, 70.3, 101.4, 105.9, 113.0, 113.9, 127.5, 128.2, 128.4, 128.5, 128.7, 133.8, 136.1, 159.1, 160.2, 163.1, 166.1. LRMS (EI) m/z (rel intensity) 378 (M^+ , 11), 287 (15), 121 (100), 91 (28). TOF-HRMS calcd for $\text{C}_{23}\text{H}_{23}\text{O}_5$ ($\text{M}+\text{H}^+$) 379.1540, found 379.1542.

4.4.6. Methyl 4-benzyloxy-2-methoxymethoxybenzoate (**4f**)

Mp (MeOH) 61–62 °C. IR (neat): ν_{\max} 2951, 1724, 1607, 1255, 1142 cm^{-1} . ^1H NMR (200 MHz, CDCl_3): δ 3.52 (s, 3H), 3.86 (s, 3H), 5.09 (s, 2H), 5.24 (s, 2H), 6.64 (dd, $J=8.8, 2.2$ Hz, 1H), 6.83 (d, $J=2.2$ Hz, 1H), 7.38–7.48 (m, 5H), 7.83 (d, $J=8.8$ Hz, 1H). ^{13}C NMR (50 MHz, CDCl_3): δ 51.7, 56.3, 70.9, 95.1, 103.4, 107.5, 113.4, 127.5, 128.2, 128.6, 133.4, 136.1, 158.9, 162.9, 165.9. LRMS (EI) m/z (rel intensity) 302 (M^+ , 9), 238 (27), 91 (100). TOF-HRMS calcd for $\text{C}_{17}\text{H}_{19}\text{O}_5$ ($\text{M}+\text{H}^+$) 303.1227, found 303.1222.

4.4.7. Methyl 2-isopropoxy-4-(4-methoxy)benzyloxybenzoate (**4g**)

IR (neat): ν_{\max} 2978, 1724, 1604, 1514, 1243, 1109 cm^{-1} . ^1H NMR (200 MHz, CDCl_3): δ 1.36 (d, $J=6.0$ Hz, 6H), 3.81 (s, 3H), 3.84 (s, 3H), 4.52 (sept, $J=6.0$ Hz, 1H), 4.99 (s, 2H), 6.44–6.62 (m, 2H), 6.92 (d, $J=8.8$ Hz, 2H), 7.35 (d, $J=8.8$ Hz, 2H), 7.82 (d, $J=9.6$ Hz, 1H). ^{13}C NMR (50 MHz, CDCl_3): δ 21.9, 51.5, 55.2, 69.9, 71.7, 102.7, 105.7, 113.7, 114.0, 128.1, 129.3, 133.6, 159.5, 159.7, 163.0, 166.3. LRMS (EI) m/z (rel intensity) 330 (M^+ , 2), 121 (100). TOF-HRMS calcd for $\text{C}_{19}\text{H}_{23}\text{O}_5$ ($\text{M}+\text{H}^+$) 331.1540, found 331.1536.

4.4.8. Methyl 2-benzyloxy-4-(4-methoxy)benzyloxybenzoate (**4h**)

Mp (MeOH) 66–67 °C. IR (neat): ν_{\max} 2949, 1720, 1605, 1514, 1245, 1172 cm^{-1} . ^1H NMR (200 MHz, CDCl_3): δ 3.82 (s, 3H), 3.87 (s, 3H), 4.99 (s, 2H), 5.14 (s, 2H), 6.53–6.65 (m, 2H), 6.92 (d, $J=8.0$ Hz, 2H), 7.28–7.57 (m, 7H), 7.89 (d, $J=9.4$ Hz, 1H). ^{13}C NMR (50 MHz, CDCl_3): δ 51.6, 55.3, 70.0, 70.6, 101.5, 106.1, 113.1, 114.1, 126.8, 127.7, 128.2, 128.5, 129.3, 133.9, 136.7, 159.7, 160.2, 163.3, 166.2. LRMS (EI) m/z (rel intensity) 378 (M^+ , 3), 211 (16), 121 (100), 91 (20). TOF-HRMS calcd for $\text{C}_{23}\text{H}_{23}\text{O}_5$ ($\text{M}+\text{H}^+$) 379.1540, found 379.1546.

4.4.9. Methyl 2-methoxymethoxy-4-(4-methoxy)benzyloxybenzoate (**4i**)

Mp (MeOH) 50–52 °C. IR (neat): ν_{\max} 2925, 1722, 1606, 1515, 1245, 1094 cm^{-1} . ^1H NMR (200 MHz, CDCl_3): δ 3.51 (s, 3H), 3.80 (s, 3H), 3.85 (s, 3H), 4.99 (s, 2H), 5.23 (s, 2H), 6.62 (dd, $J=8.8, 2.2$ Hz, 1H), 6.81 (d, $J=2.2$ Hz, 1H), 6.91 (d, $J=8.8$ Hz, 2H), 7.35 (d, $J=8.8$ Hz, 2H), 7.83 (d, $J=8.8$ Hz, 1H). ^{13}C NMR (50 MHz, CDCl_3): δ 51.6, 55.2, 56.3, 69.9, 95.0, 103.3, 107.4, 113.3, 113.9, 128.0, 129.3, 133.3, 158.8, 159.5, 163.0, 165.9. LRMS (EI) m/z (rel intensity) 332 (M^+ , 0.4), 121 (100). TOF-HRMS calcd for $\text{C}_{18}\text{H}_{21}\text{O}_6$ ($\text{M}+\text{H}^+$) 333.1333, found 333.1334.

4.4.10. Methyl 2-isopropoxy-4-methoxymethoxybenzoate (**4j**)

IR (neat): ν_{\max} 2977, 1727, 1605, 1576, 1499, 1436, 1245 cm^{-1} . ^1H NMR (200 MHz, CDCl_3): δ 1.38 (d, $J=6.2$ Hz, 6H), 3.48 (s, 3H), 3.84 (s, 3H), 4.55 (sept, $J=6.2$ Hz, 1H), 5.19 (s, 2H), 6.57–6.66 (m, 2H), 7.74–7.83 (m, 1H). ^{13}C NMR (50 MHz, CDCl_3): δ 22.0, 51.5, 56.2, 71.9, 94.2, 103.8, 107.5, 115.0, 133.4, 159.7, 161.5, 166.3. LRMS (EI) m/z (rel intensity) 255 ($\text{M}+\text{H}^+$, 52), 254 (M^+ , 100), 223 (24). TOF-HRMS calcd for $\text{C}_{13}\text{H}_{19}\text{O}_5$ ($\text{M}+\text{H}^+$) 255.1227, found 255.1223.

4.4.11. Methyl 2-benzyloxy-4-methoxymethoxybenzoate (**4k**)

IR (neat): ν_{\max} 2951, 1722, 1605, 1436, 1247, 1139 cm^{-1} . ^1H NMR (200 MHz, CDCl_3): δ 3.46 (s, 3H), 3.87 (s, 3H), 5.16 (s, 2H), 5.17 (s, 2H), 6.66 (dd, $J=10.2, 2.2$ Hz, 1H), 6.69 (d, $J=2.2$ Hz, 1H), 7.20–7.58 (m, 5H), 7.86 (d, $J=10.2$ Hz, 1H). ^{13}C NMR (50 MHz, CDCl_3): δ 51.7,

56.2, 70.4, 94.1, 102.0, 107.5, 113.6, 126.8, 127.7, 128.4, 133.7, 136.5, 160.0, 161.6, 166.1. LRMS (EI) m/z (rel intensity) 302 (M^+ , 15), 270 (54), 238 (32), 91 (100), 65 (13). TOF-HRMS calcd for $\text{C}_{17}\text{H}_{19}\text{O}_5$ ($\text{M}+\text{H}^+$) 303.1227, found 303.1228.

4.4.12. Methyl 2-(4-methoxy)benzyloxy-4-methoxymethoxybenzoate (**4l**)

IR (neat): ν_{\max} 2951, 1722, 1606, 1577, 1514, 1244 cm^{-1} . ^1H NMR (200 MHz, CDCl_3): δ 3.47 (s, 3H), 3.81 (s, 3H), 3.86 (s, 3H), 5.10 (s, 2H), 5.18 (s, 2H), 6.60–6.73 (m, 2H), 6.92 (d, $J=8.8$ Hz, 2H), 7.43 (d, $J=8.8$ Hz, 2H), 7.84 (d, $J=8.8$ Hz, 1H). ^{13}C NMR (50 MHz, CDCl_3): δ 51.7, 55.3, 56.2, 70.5, 94.3, 102.4, 107.7, 114.0, 128.6, 128.7, 133.6, 159.3, 160.2, 161.7, 166.2. LRMS (EI) m/z (rel intensity) 332 (M^+ , 2), 122 (9), 121 (100), 91 (5), 77 (4). TOF-HRMS calcd for $\text{C}_{18}\text{H}_{21}\text{O}_6$ ($\text{M}+\text{H}^+$) 333.1333, found 333.1333.

4.5. General procedure for the deprotection

To a stirred solution of **3a–d** or **4a–l** (1.0 equiv) in toluene (20 mL/mmol of **3a–d** or **4a–l**) was added the solid-supported acid (either Amberlyst-15 (loading: 4.81 mmol/g) or PTS-Si (loading: 0.81 mmol/g); 0.6 equiv). The reaction mixture was kept at temperature and for the duration as indicated in Table 2. The reaction mixture was filtered and the solid-supported material was washed extensively with EtOAc. The filtrate was then concentrated under reduced pressure. The product was obtained by following column chromatography on silica (20% EtOAc/hexanes).

4.5.1. Methyl 4-hydroxy-2-isopropoxybenzoate (**5a**)

Mp (MeOH) 113–115 °C. IR (neat): ν_{\max} 3323 (br), 2980, 1698, 1604, 1577, 1454, 1435, 1252, 1135 cm^{-1} . ^1H NMR (200 MHz, CDCl_3): δ 1.29 (d, $J=6.0$ Hz, 6H), 3.83 (s, 3H), 4.42 (sept, $J=6.0$ Hz, 1H), 6.41–6.45 (m, 2H), 7.58 (apparent br s, 1H), 7.73 (d, $J=8.8$ Hz, 1H). ^{13}C NMR (50 MHz, CDCl_3): δ 21.8, 51.8, 71.6, 102.3, 107.7, 112.0, 133.9, 160.2, 161.7, 167.3. LRMS (EI) m/z (rel intensity) 211 ($\text{M}+\text{H}^+$, 11), 210 (M^+ , 99), 168 (83), 137 (50), 136 (100), 108 (43). TOF-HRMS calcd for $\text{C}_{11}\text{H}_{15}\text{O}_4$ ($\text{M}+\text{H}^+$) 211.0965, found 211.0961.

4.5.2. Methyl 2-benzyloxy-4-hydroxybenzoate (**5b**)

Mp (MeOH) 138–140 °C. IR (neat): ν_{\max} 3311 (br), 1689, 1579, 1243, 1088 cm^{-1} . ^1H NMR (200 MHz, CDCl_3): δ 3.86 (s, 3H), 5.09 (s, 2H), 6.43 (d, $J=8.8$ Hz, 1H), 6.46 (s, 1H), 7.22–7.54 (m, 5H), 7.78 (d, $J=8.8$ Hz, 1H). ^{13}C NMR (50 MHz, CDCl_3): δ 51.7, 70.2, 101.1, 107.7, 111.2, 126.7, 127.7, 128.4, 134.0, 136.5, 160.6, 162.0, 166.8. LRMS (EI) m/z (rel intensity) 258 (M^+ , 7), 226 (31), 91 (100). TOF-HRMS calcd for $\text{C}_{15}\text{H}_{15}\text{O}_4$ ($\text{M}+\text{H}^+$) 259.0965, found 259.0958.

4.6. Preparation of the benzamides **6a** and **b**

4.6.1. 2-Benzyloxy-*N,N*-diethyl-4-isopropoxybenzamide (**6a**)

A 10 mL microwave vessel was charged with the methyl benzoate **4a** (0.60 g, 2.0 mmol), *N,N*-diethylamine (1.45 mL, 14.0 mmol), Me_3Al (2.0 M in toluene, 1.5 mL, 3.0 mmol) and THF (2 mL) at rt. The vessel was sealed and heated in the microwave reactor at 100 °C and 100 psi with the power set at 100 W for 45 min. At that time, the reaction was quenched with 2 N HCl and the mixture was extracted with EtOAc (3 \times 10 mL). The combined organic layers were washed with brine, dried over Na_2SO_4 , filtered and concentrated under reduced pressure to give the crude product. Further purification of the crude by column chromatography on silica (30% EtOAc/hexanes) furnished the desired product as a colourless oil (0.68 g, 2.0 mmol, 99%). IR (neat): ν_{\max} 2975, 1630, 1429, 1276, 1175 cm^{-1} . ^1H NMR (400 MHz, CDCl_3): δ 0.99 (t, $J=7.1$ Hz, 3H), 1.15 (t, $J=7.1$ Hz, 3H), 1.33 (d, $J=6.0$ Hz, 6H), 3.10–3.40 (br m, 3H), 3.79 (br s, 1H), 4.54 (sept, $J=6.0$ Hz, 1H), 5.05 (s, 2H), 6.49–6.53 (m, 2H), 7.13–7.17 (m, 1H), 7.29–7.41 (m, 5H). ^{13}C NMR (100 MHz, CDCl_3):

δ 12.7, 14.0, 22.0, 38.7, 42.7, 70.0, 70.2, 101.6, 107.1, 120.0, 127.0, 127.8, 128.4, 136.7, 155.5, 159.4, 168.7. LRMS (EI) m/z (rel intensity) 342 ($M+H^+$, 25), 341 (M^+ , 24), 269 (62), 227 (57), 179 (29), 91 (100). TOF-HRMS calcd for $C_{21}H_{28}NO_3$ ($M+H^+$) 342.2064, found 342.2058.

4.6.2. *N,N*-Diethyl-2-isopropoxy-4-methoxymethoxybenzamide (**6b**)

A 10 mL microwave vessel was charged with the methyl benzoate **4j** (0.21 g, 0.84 mmol), *N,N*-diethylamine (0.61 mL, 5.85 mmol), Me_3Al (2.0 M in toluene, 0.63 mL, 1.26 mmol) and THF (0.85 mL) at rt. The vessel was sealed and heated in the microwave reactor at 100 °C and 100 psi with the power set at 100 W for 15 min. At that time, the reaction was quenched with 2 N HCl and the mixture was extracted with EtOAc (3×5 mL). The combined organic layers were washed with brine, dried over Na_2SO_4 , filtered and concentrated under reduced pressure to give the crude product. Further purification of the crude by column chromatography on silica (30% EtOAc/hexanes) furnished the desired product as a colourless oil (0.20 g, 0.68 mmol, 80%). IR (neat): ν_{max} 2975, 1629, 1431, 1274, 1154 cm^{-1} . 1H NMR (400 MHz, $CDCl_3$): δ 1.03 (t, $J=7.1$ Hz, 3H), 1.22 (t, $J=7.1$ Hz, 3H), 1.30 (d, $J=6.0$ Hz, 6H), 3.06–3.33 (br m, 3H), 3.48 (s, 3H), 3.76–3.92 (br m, 1H), 4.50 (sept, $J=6.1$ Hz, 1H), 5.16 (s, 2H), 6.57 (d, $J=2.2$ Hz, 1H), 6.63 (dd, $J=8.3, 2.2$ Hz, 1H), 7.12 (d, $J=8.3$ Hz, 1H). ^{13}C NMR (100 MHz, $CDCl_3$): δ 12.9, 14.0, 22.0, 38.5, 42.5, 56.0, 70.7, 94.5, 102.5, 107.8, 122.1, 128.4, 154.6, 158.6, 168.7. LRMS (EI) m/z (rel intensity) 296 ($M+H^+$, 46), 295 (M^+ , 56), 294 ($M-H^+$, 100), 252 (85), 223 (68), 181 (35), 151 (39). TOF-HRMS calcd for $C_{16}H_{26}NO_4$ ($M+H^+$) 296.1856, found 296.1849.

4.7. Preparation of the aryl phenylpropynones **9a** and **b**

4.7.1. 2-Hydroxy-4-methoxymethoxybenzaldehyde (**7**)

Using a procedure similar to that for the preparation of compound **2d**, compound **7** was prepared from 2,4-dihydroxybenzaldehyde (2.79 g, 20 mmol). Compound **7** (2.00 g, 11 mmol, 55%) was obtained as a white solid. Mp (EtOAc/hexanes) 53–54 °C. IR (neat): ν_{max} 2831, 1626, 1500, 1221, 1153 cm^{-1} . 1H NMR (400 MHz, $CDCl_3$): δ 3.49 (s, 3H), 5.23 (s, 2H), 6.61 (d, $J=2.2$ Hz, 1H), 6.65 (dd, $J=8.6, 2.2$ Hz, 1H), 7.46 (d, $J=8.6$ Hz, 1H), 9.74 (s, 1H), 11.4 (s, 1H). ^{13}C NMR (100 MHz, $CDCl_3$): δ 56.4, 94.0, 103.4, 109.0, 115.9, 135.4, 164.1, 164.3, 194.6. LRMS (EI) m/z (rel intensity) 183 ($M+H^+$, 100), 182 (M^+ , 69), 167 (33). TOF-HRMS calcd for $C_9H_{11}O_4$ ($M+H^+$) 183.0652, found 183.0640.

4.7.2. 2-(4-Methoxy)benzyloxy-4-methoxymethoxybenzaldehyde (**8a**)

Using the procedure similar to that for the preparation of compound **4l**, compound **8a** was prepared from compound **7** (0.91 g, 5.00 mmol). Compound **8a** (0.92 g, 3.05 mmol, 61%) was obtained as a yellow oil. IR (neat): ν_{max} 2935, 1676, 1597, 1514, 1247 cm^{-1} . 1H NMR (200 MHz, $CDCl_3$): δ 3.48 (s, 3H), 3.81 (s, 3H), 5.07 (s, 2H), 5.21 (s, 2H), 6.68 (dd, $J=8.6, 2.2$ Hz, 1H), 6.70 (s, 1H), 6.92 (d, $J=8.7$ Hz, 2H), 7.36 (d, $J=8.7$ Hz, 2H), 7.80 (d, $J=8.6$ Hz, 1H), 10.4 (s, 1H). ^{13}C NMR (50 MHz, $CDCl_3$): δ 55.2, 56.3, 70.2, 94.1, 100.6, 108.4, 114.0, 119.8, 127.8, 129.1, 130.1, 159.6, 162.7, 163.6, 188.4. LRMS (EI) m/z (rel intensity) 302 (M^+ , 5), 121 (100). TOF-HRMS calcd for $C_{17}H_{19}O_5$ ($M+H^+$) 303.1227, found 303.1230.

4.7.3. 2-Isopropoxy-4-methoxymethoxybenzaldehyde (**8b**)

Using the procedure similar to that for the preparation of compound **4j**, compound **8b** was prepared from compound **7** (0.22 g, 1.20 mmol). Compound **8b** (0.23 g, 1.02 mmol, 85%) was obtained as a yellow oil. IR (neat): ν_{max} 2978, 1678, 1597, 1256 cm^{-1} . 1H NMR (400 MHz, $CDCl_3$): δ 1.40 (d, $J=6.1$ Hz, 6H), 3.49 (s, 3H), 4.64 (sept, $J=6.1$ Hz, 1H), 5.22 (s, 2H), 6.60 (d, $J=2.1$ Hz, 1H), 6.65 (ddd,

$J=8.7, 2.1, 0.7$ Hz, 1H), 7.79 (d, $J=8.7$ Hz, 1H), 10.3 (d, $J=0.7$ Hz, 1H). ^{13}C NMR (100 MHz, $CDCl_3$): δ 21.9, 56.3, 71.1, 94.1, 101.4, 108.1, 120.4, 130.0, 162.2, 163.6, 188.8. LRMS (EI) m/z (rel intensity) 225 ($M+H^+$, 100), 224 (M^+ , 47), 209 (35). TOF-HRMS calcd for $C_{12}H_{17}O_4$ ($M+H^+$) 225.1121, found 225.1112.

4.7.4. 1-(2-(4-Methoxy)benzyloxy-4-(methoxymethoxy)phenyl)-3-phenylprop-2-yn-1-one (**9a**)

To a stirred solution of phenyl acetylene (0.23 mL, 2.1 mmol) in anhydrous THF (19 mL) was added *n*-BuLi (3.47 M in hexanes, 0.62 mL, 2.15 mmol) at -78 °C and the resulting mixture was stirred at that temperature for 40 min. At that time, a solution of **8a** (0.60 g, 2.00 mmol) in THF (13 mL) was added via syringe. The reaction mixture was stirred at -78 °C for 15 min, slowly warmed up to rt at which the reaction was stirred for 16 h. The reaction was quenched by adding saturated solution of NH_4Cl . Water (20 mL) and EtOAc (20 mL) were added and the two phases were separated. The aqueous phase was extracted with EtOAc (2×15 mL). The combined organic layers were washed with brine (25 mL), dried over Na_2SO_4 , filtered and concentrated under reduced pressure to give the crude product (0.76 g), which was used in the next step without further purification.

To a stirred suspension of pyridinium dichromate (PDC; 1.06 g, 2.82 mmol) in DCM (10 mL) at 0 °C was added the crude solution (0.76 g) in DCM (8 mL) via pipette over 5 min. The reaction mixture was stirred at 0 °C and then warmed up to rt at which it was allowed to stir for 16 h. The mixture was filtered through a plug of Celite® and the resulting filtrate was concentrated under reduced pressure to give the crude mixture, which was further purified by column chromatography on silica (20% EtOAc/hexanes) to furnish the desired product as a yellow solid (0.54 g, 1.34 mmol, 67% over two steps). Mp (EtOAc/hexanes) 93–94 °C. IR (neat): ν_{max} 2934, 2197, 1610, 1587, 1514, 1248 cm^{-1} . 1H NMR (200 MHz, $CDCl_3$): δ 3.49 (s, 3H), 3.76 (s, 3H), 5.14 (s, 2H), 5.23 (s, 2H), 6.70 (dd, $J=9.7, 2.2$ Hz, 1H), 6.73 (s, 1H), 6.81 (d, $J=8.8$ Hz, 2H), 7.22–7.40 (m, 5H), 7.43 (d, $J=8.8$ Hz, 2H), 8.07 (d, $J=9.7$ Hz, 1H). ^{13}C NMR (50 MHz, $CDCl_3$): δ 55.1, 56.3, 70.5, 89.6, 91.3, 94.1, 101.3, 107.8, 113.9, 120.8, 121.2, 127.9, 128.2, 129.1, 129.9, 132.7, 134.2, 159.3, 160.8, 162.9, 175.1. LRMS (EI) m/z (rel intensity) 403 ($M+H^+$, 27), 402 (M^+ , 77), 357 (34), 181 (45), 121 (100). TOF-HRMS calcd for $C_{25}H_{23}O_5$ ($M+H^+$) 403.1540, found 403.1546.

4.7.5. 1-(2-Isopropoxy-4-(methoxymethoxy)phenyl)-3-phenylprop-2-yn-1-one (**9b**)

To a stirred solution of phenyl acetylene (0.26 mL, 2.4 mmol) in anhydrous THF (20 mL) was added *n*-BuLi (3.47 M in hexanes, 0.63 mL, 2.20 mmol) at -78 °C and the resulting mixture was stirred at that temperature for 40 min. At that time, a solution of **8b** (0.45 g, 2.00 mmol) in THF (13 mL) was added via syringe. The reaction mixture was stirred at -78 °C for 15 min, slowly warmed up to rt at which the reaction was stirred for 16 h. The reaction was quenched by adding saturated solution of NH_4Cl . Water (20 mL) and EtOAc (20 mL) were added and the two phases were separated. The aqueous phase was extracted with EtOAc (2×15 mL). The combined organic layers were washed with brine (25 mL), dried over Na_2SO_4 , filtered and concentrated under reduced pressure to give the crude product (0.76 g), which was used in the next step without further purification.

To a stirred suspension of pyridinium dichromate (PDC; 1.13 g, 3.00 mmol) in DCM (12 mL) at 0 °C was added the crude solution (0.65 g) in DCM (8 mL) via pipette over 5 min. The reaction mixture was stirred at 0 °C and then warmed up to rt at which it was allowed to stir for 16 h. The mixture was filtered through a plug of Celite® and the resulting filtrate was concentrated under reduced pressure to give the crude mixture, which was further purified by column chromatography on silica (20% EtOAc/hexanes) to furnish

the desired product as a yellow solid (0.52 g, 1.60 mmol, 80% over two steps). Mp (EtOAc/hexanes) 68–69 °C. IR (neat): ν_{\max} 2978, 2197, 1613, 1587, 1489, 1268 cm^{-1} . ^1H NMR (400 MHz, CDCl_3): δ 1.40 (d, $J=6.1$ Hz, 6H), 3.50 (s, 3H), 4.66 (sept, $J=6.1$ Hz, 1H), 5.23 (s, 2H), 6.44 (d, $J=2.2$ Hz, 1H), 6.74 (dd, $J=8.7, 2.2$ Hz, 1H), 7.35–7.46 (m, 3H), 7.59–7.62 (m, 2H), 7.99 (d, $J=8.7$ Hz, 1H). ^{13}C NMR (100 MHz, CDCl_3): δ 21.9, 56.3, 71.4, 89.9, 90.9, 94.1, 102.2, 107.6, 121.2, 122.1, 128.5, 129.9, 132.5, 133.9, 160.2, 162.8, 175.5. LRMS (EI) m/z (rel intensity) 325 ($\text{M}+\text{H}^+$, 100), 309 (55), 281 (35), 251 (40). TOF-HRMS calcd for $\text{C}_{20}\text{H}_{21}\text{O}_4$ ($\text{M}+\text{H}^+$) 325.1434, found 325.1431.

4.8. Deprotection of 6a,b, 8a,b and 9a,b

Using the procedure similar to the general procedure for the deprotection (4.4) mentioned above, compounds **6a,b**, **8a,b** and **9a,b** were subjected to selective deprotection conditions as indicated in Table 3.

4.8.1. *N,N*-Diethyl-2-hydroxy-4-isopropoxybenzamide (**10**)

IR (neat): ν_{\max} 3145 (br), 2976, 1613, 1580, 1428, 1111 cm^{-1} . ^1H NMR (400 MHz, CDCl_3): δ 1.21 (t, $J=7.1$ Hz, 6H), 1.27 (d, $J=6.1$ Hz, 6H), 3.34 (q, $J=7.1$ Hz, 4H), 4.49 (sept, $J=6.1$ Hz, 1H), 6.28 (dd, $J=8.8, 2.5$ Hz, 1H), 6.42 (d, $J=2.5$ Hz, 1H), 7.21 (d, $J=8.8$ Hz, 1H), 10.6 (s, 1H). ^{13}C NMR (100 MHz, CDCl_3): δ 13.4, 21.9, 42.2, 69.9, 103.2, 106.9, 109.6, 128.7, 161.3, 161.7, 171.9. LRMS (EI) m/z (rel intensity) 503 ($2\text{M}+\text{H}^+$, 85), 502 (2M^+ , 100), 252 ($\text{M}+\text{H}^+$, 99), 137 (19), 72 (20). TOF-HRMS calcd for $\text{C}_{14}\text{H}_{22}\text{NO}_3$ ($\text{M}+\text{H}^+$) 252.1594, found 252.1586.

4.8.2. *N,N*-Diethyl-4-hydroxy-2-isopropoxybenzamide (**11**)

IR (neat): ν_{\max} 3173 (br), 2976, 1582, 1434, 1290 cm^{-1} . ^1H NMR (200 MHz, CDCl_3): δ 1.00 (t, $J=7.1$ Hz, 3H), 1.08–1.29 (m, 9H), 2.97–3.40 (m, 3H), 3.66–4.00 (m, 1H), 4.21 (sept, $J=6.0$ Hz, 1H), 6.20 (dd, $J=8.1, 2.2$ Hz, 1H), 6.26 (d, $J=2.2$ Hz, 1H), 6.87 (d, $J=8.1$ Hz, 1H), 9.22 (br s, 1H). ^{13}C NMR (50 MHz, CDCl_3): δ 12.6, 13.9, 22.0, 39.1, 43.0, 70.3, 101.5, 107.9, 118.2, 128.1, 154.6, 159.3, 170.6. LRMS (EI) m/z (rel intensity) 252 ($\text{M}+\text{H}^+$, 59), 250 ($\text{M}-\text{H}^+$, 63), 208 (71), 137 (100). TOF-HRMS calcd for $\text{C}_{14}\text{H}_{22}\text{NO}_3$ ($\text{M}+\text{H}^+$) 252.1594, found 252.1595.

4.8.3. 4-Hydroxy-2-isopropoxybenzaldehyde (**12**)

IR (neat): ν_{\max} 3149 (br), 2978, 1658, 1572, 1460, 1264 cm^{-1} . ^1H NMR (400 MHz, CDCl_3): δ 1.39 (d, $J=6.1$ Hz, 6H), 1.91 (br s, 1H), 4.62 (sept, $J=6.1$ Hz, 1H), 6.47 (d, $J=2.0$ Hz, 1H), 6.48–6.52 (m, 1H), 7.76 (d, $J=8.5$ Hz, 1H), 10.3 (d, $J=0.4$ Hz, 1H). ^{13}C NMR (100 MHz, CDCl_3): δ 21.9, 71.1, 100.5, 108.6, 118.9, 130.7, 163.2, 164.1, 189.6. LRMS (EI) m/z (rel intensity) 181 ($\text{M}+\text{H}^+$, 100), 180 (M^+ , 20), 138 (31). TOF-HRMS calcd for $\text{C}_{10}\text{H}_{13}\text{O}_3$ ($\text{M}+\text{H}^+$) 181.0859, found 181.0846.

4.8.4. 1-(2-Hydroxy-4-methoxymethoxyphenyl)-3-phenylpropynone (**13**)

Mp (EtOAc/hexanes) 73–74 °C. IR (neat): ν_{\max} 2933, 2201, 1618, 1578, 1490, 1348 cm^{-1} . ^1H NMR (400 MHz, CDCl_3): δ 3.49 (s, 3H), 5.24 (s, 2H), 6.62 (d, $J=2.3$ Hz, 1H), 6.64 (dd, $J=8.7, 2.3$ Hz, 1H), 7.40–7.51 (m, 3H), 7.66–7.70 (m, 2H), 8.03 (d, $J=8.7$ Hz, 1H), 12.1 (s, 1H). ^{13}C NMR (100 MHz, CDCl_3): δ 56.4, 93.6, 94.0, 95.2, 103.4, 109.0, 116.0, 119.9, 128.7, 130.9, 133.0, 134.8, 164.4, 165.2, 180.5. LRMS (EI) m/z (rel intensity) 282 (M^+ , 92), 281 (100), 251 (35), 209 (46). TOF-HRMS calcd for $\text{C}_{17}\text{H}_{15}\text{O}_4$ ($\text{M}+\text{H}^+$) 283.0965, found 283.0971.

4.8.5. 1-(4-Hydroxy-2-isopropoxyphenyl)-3-phenylpropynone (**14**)

Mp (EtOAc/hexanes) 107–108 °C. IR (neat): ν_{\max} 3226 (br), 2979, 2196, 1603, 1552, 1292 cm^{-1} . ^1H NMR (400 MHz, CDCl_3): δ 1.35 (d, $J=6.1$ Hz, 6H), 4.60 (sept, $J=6.1$ Hz, 1H), 6.54 (s, 1H), 6.59 (dd, $J=8.7, 1.5$ Hz, 1H), 7.33–7.44 (m, 3H), 7.53–7.57 (m, 2H), 8.01 (d, $J=8.7$ Hz, 1H), 8.37 (br s, 1H). ^{13}C NMR (100 MHz, CDCl_3): δ 21.8, 71.4, 89.6, 92.6, 101.3, 108.5, 119.8, 120.8, 128.5, 130.2, 132.6, 135.2, 161.4, 164.0, 176.3. LRMS (EI) m/z (rel intensity) 281 ($\text{M}+\text{H}^+$, 16), 265 (21), 237

(100), 210 (33). TOF-HRMS calcd for $\text{C}_{18}\text{H}_{17}\text{O}_3$ ($\text{M}+\text{H}^+$) 281.1172, found 281.1170.

Acknowledgements

Financial support from the Thailand Research Fund (TRF) for P.P. (BRG5180013) and S.R. and from the Center of Excellence on Environmental Health, Toxicology and Management of Chemicals (ETM) is gratefully acknowledged. Supattra Karnkla, Jarusporn Inkaporn and Anan Kanitanupan are acknowledged for their technical assistance.

Supplementary data

Supplementary data associated with this article can be found in the online version, at doi:10.1016/j.tet.2009.03.089.

References and notes

- Greene, T. W.; Wuts, P. G. M. *Protective Groups in Organic Synthesis*, 3rd ed.; John Wiley & Sons: New York, NY, 1999.
- Kocienski, P. J. *Protecting Groups*, 3rd ed.; Georg Thieme: Stuttgart, 2003.
- Cappa, A.; Marcantoni, E.; Torregiani, E. *J. Org. Chem.* **1999**, *64*, 5696–5699.
- Papageorgiou, E. A.; Gaunt, M. J.; Yu, J.-Q.; Spencer, J. B. *Org. Lett.* **2000**, *2*, 1049–1051.
- Marković, D.; Vogel, P. *Org. Lett.* **2004**, *6*, 2693–2696.
- Aristegui, S. R.; El-Murr, M. E.; Golding, B. T.; Griffin, R. J.; Hardcastle, I. R. *Org. Lett.* **2006**, *8*, 5927–5929.
- Bartoli, G.; Bosco, M.; Carlone, A.; Dalpozzo, R.; Locatelli, M.; Melchiorre, P.; Sambri, L. *J. Org. Chem.* **2006**, *71*, 9580–9588.
- Ganguly, N. C.; Dutta, S.; Datta, M. *Tetrahedron Lett.* **2006**, *47*, 5807–5810.
- Srinivasu Pothukanuri, S.; Winssinger, N. *Org. Lett.* **2007**, *9*, 2223–2225.
- Cieślak, J.; Kauffman, J. S.; Kolodziejski, M. J.; Lloyd, J. R.; Beaucage, S. L. *Org. Lett.* **2007**, *9*, 671–674.
- Umali, A. P.; Crampton, H. L.; Simanek, E. E. *J. Org. Chem.* **2007**, *72*, 9866–9874.
- Tsukamoto, H.; Suzuki, T.; Sato, M.; Kondo, Y. *Tetrahedron Lett.* **2007**, *48*, 8438–8441.
- Murali, C.; Shashidhar, M. S.; Gopinath, C. S. *Tetrahedron* **2007**, *63*, 4149–4155.
- Quai, M.; Repetto, C.; Barbaglia, W.; Cereda, E. *Tetrahedron Lett.* **2007**, *48*, 1241–1245.
- Nishimura, T.; Yamada, K.; Takebe, T.; Yokoshima, S.; Fukuyama, T. *Org. Lett.* **2008**, *10*, 2601–2604.
- Xu, Y.; Tang, S.; Han, J.; She, X.; Pan, X. *Tetrahedron Lett.* **2008**, *49*, 3634–3637.
- Ley, S. V.; Baxendale, I. R.; Bream, R. N.; Jackson, P. S.; Leach, A. G.; Longbottom, D. A.; Nesi, M.; Scott, J. S.; Storer, R. I.; Taylor, S. J. *J. Chem. Soc., Perkin Trans. 1* **2000**, 3815–4195.
- Karimi, B.; Zareyee, D. *Tetrahedron Lett.* **2005**, *46*, 4661–4665.
- Das, B.; Reddy, K. R.; Thirupathi, P. *Tetrahedron Lett.* **2006**, *47*, 5855–5857.
- Ploypradith, P.; Kagan, R. K.; Ruchirawat, S. *J. Org. Chem.* **2005**, *70*, 5119–5125.
- Petchmanee, T.; Ploypradith, P.; Ruchirawat, S. *J. Org. Chem.* **2006**, *71*, 2892–2895.
- Ploypradith, P.; Cheryklin, P.; Niyomtham, N.; Bertoni, D. R.; Ruchirawat, S. *Org. Lett.* **2007**, *9*, 2637–2640.
- For other conditions to remove the aromatic MOM ethers, see: Miyake, H.; Tsumura, T.; Sasaki, M. *Tetrahedron Lett.* **2004**, *45*, 7213–7215.
- Poor to moderate yields of the desired products (30% for Amberlyst-15 and 68% for PTS-Si) resulted from the PMBylated C-alkylation side reactions, which gave the corresponding FC-type by-products for the remaining mass accounts.
- For **3c**, 52% and 35% yields of **2c** were obtained using PTS-Si with MeOH (10 and 25 equiv, respectively). For **3d**, 35% and 69% yields of **2d** were obtained using Amberlyst-15 and PTS-Si in the presence of MeOH (10 equiv), respectively.
- Anisole was employed as a cation scavenger for the PMB cation but resulted in even more complicated reaction mixtures without any remarkable difference for the decrease of the by-products from the FC-type C-alkylation.
- Despite 0% yield of the desired mono-PMB-deprotected product **10** (see Table 3), the product mixture obtained from the reaction contained the mono-deprotected product, which was further alkylated via the FC-type process. It seems that the rates of the subsequent FC-type reactions of both mono- and di-deprotected are faster than the initial deprotection reaction.
- As listed by the suppliers, the surface areas of Amberlyst-15 and PTS-Si are 45 and 500 m^2/g , respectively.
- For comparison of yields in other systems, see Refs. 21 and 22.
- The reaction conditions were optimized for the lowest temperature and shortest time required for complete consumption of starting materials with minimal amount of the di-deprotected, the C-alkylated FC-type and/or other (e.g., *p*-QM) by-products.
- Syracuse Research Corporation of Syracuse, New York.
- Beger, J. *J. Prakt. Chem. (Leipzig)* **1983**, *V325*, P708–P718.
- Guo, W.; Li, J.; Fan, N.; Wu, W.; Zhou, P.; Xia, C. *Synth. Commun.* **2005**, *35*, 145–152.

34. Legrand, S.; Nordlander, G.; Nordenhem, H.; Borg-Karlson, A.-K.; Unelius, C. R. *Z. Naturforsch.* **2004**, *59b*, 829–835.
35. Bokotey, S.; Kovari-Radkai, M.; Podanyi, B.; Ritz, I.; Hanusz, M.; Batori, S. *Synth. Commun.* **2002**, *32*, 2325–2343.
36. Tatsuta, K.; Tanaka, Y.; Kojima, M.; Ikegami, H. *Chem. Lett.* **2002**, 14–15.
37. Varga, M.; Batori, S.; Kovari-Radkai, M.; Prohaszka-Nemet, I.; Vitanyi-Morvai, M.; Bocskey, Z.; Bokotey, S.; Simon, K.; Hermecz, I. *Eur. J. Org. Chem.* **2001**, *20*, 3911–3920.
38. Pifferi, G.; Gaviraghi, G.; Pinza, M.; Ventura, P. *J. Heterocycl. Chem.* **1977**, *14*, 1257–1259.
39. Miyano, S.; Sumoto, K.; Satoh, F.; Shima, K.; Hayashimatsu, M.; Morita, M.; Aisaka, K.; Noguchi, T. *J. Med. Chem.* **1985**, *28*, 717–727.

A Convergent General Strategy for the Functionalized 2-Aryl Cycloalkyl-Fused Chromans: Intramolecular Hetero-Diels–Alder Reactions of *ortho*-Quinone Methides

Jumreang Tummatorn,^[a] Somsak Ruchirawat,^[a, b] and Poonsakdi Ploypradith*^[a, b]

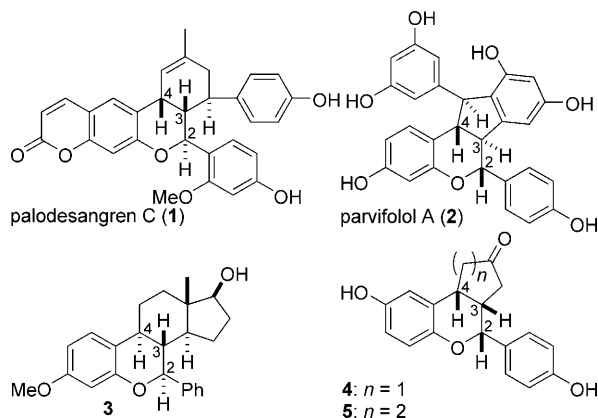
Chroman is a core structure of flavonoids, which have been shown to exhibit a wide array of biological activities.^[1] Palodesangren C (**1**; Scheme 1), a natural Diels–Alder

studied as an estradiol analogue.^[4] Some tricyclic 2-aryl-3,4-cycloalkyl-fused benzopyrans (**4**, **5**; Scheme 1) were synthesized and investigated for their high affinity to and selectivity for the estrogen receptor β over the α .^[5,6]

Some synthetic methods have been developed for chromans by hetero-Diels–Alder (HDA) reactions.^[7] However, despite the presence of the 2-aryl group in some natural products and synthetic compounds, the synthesis of 2-aryl-3,4-cycloalkyl-fused chromans has been relatively unexplored, partly due to the susceptible nature of styrenes to polymerization. To date, the reported syntheses have been largely performed for the 2-alkylcycloalkyl-fused chromans and pyranobenzopyrans.^[8] In addition, modifications on the cycloalkyl-fused rings would be difficult because the cycloalkyl or pyranyl moieties are nonfunctionalized. Moreover, different strategies were required for cyclopentyl- and cyclohexyl-fused compounds (**4**, **5**).^[6] Thus, developing a general synthetic strategy for the tricyclic core of 2-aryl-3,4-cycloalkyl-fused chromans with defined stereocenters (C2, C3, and C4) and functionalizable moieties on the cycloalkyl ring would be pivotal.

Recently, as part of our research in the use of solid-supported reagents in organic synthesis,^[9] our group has reported the successful generation of *o*-QMs and their intermolecular HDA reactions with styrene derivatives under mild conditions mediated by *p*-toluenesulfonic acid (*p*-TsOH) immobilized on silica (PTS-Si) in toluene.^[9d] We now envisioned that PTS-Si could be employed to generate *ortho*-quinone methide (*o*-QM), which, upon reacting intramolecularly with the tethered dienophile (i.e., styrenes), could form the tricyclic 2-aryl-3,4-cycloalkyl-fused chroman.

As shown retrosynthetically in Scheme 2, the precursors for the intramolecular HDA reactions would be derived from aldol condensation between the benzaldehyde derivative (**6**) and ketone (X=H; Y=Me) or the acetophenone derivative (**7**) and the aldehyde (X=Me; Y=H). Synthesis of these cycloalkyl-fused chroman systems would be highly convergent and requires a similar strategy to assemble the precursors for the intramolecular *o*-QM/HDA reactions.



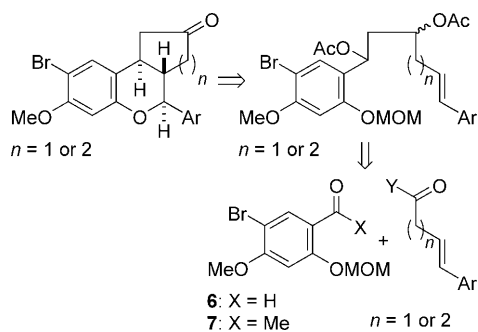
Scheme 1. Examples of 2-arylcycloalkyl-fused chromans (shown with relative stereochemistry).

adduct isolated from *Brosimum rubescens*, showed potent inhibition of the binding of 5 α -dihydrotestosterone (DHT) with the androgen receptor.^[2] Parvifolol A (**2**; Scheme 1), a natural product isolated from *Gnetum parvifolium*, was evaluated for the inhibitory activity in the Maillard reaction (protein glycation) associated with diabetic complications and aging of the skin.^[3] Compound **3** was synthesized and

[a] Dr. J. Tummatorn, Prof. Dr. S. Ruchirawat, Dr. P. Ploypradith
Laboratory of Medicinal Chemistry, Chulabhorn Research Institute
Vipavadee-Rangsit Highway, Bangkok 10210 (Thailand)
Fax: (+662) 574-2027
E-mail: poonsakdi@cri.or.th

[b] Prof. Dr. S. Ruchirawat, Dr. P. Ploypradith
Program in Chemical Biology, Chulabhorn Graduate Institute
Vipavadee-Rangsit Highway, Bangkok 10210 (Thailand)

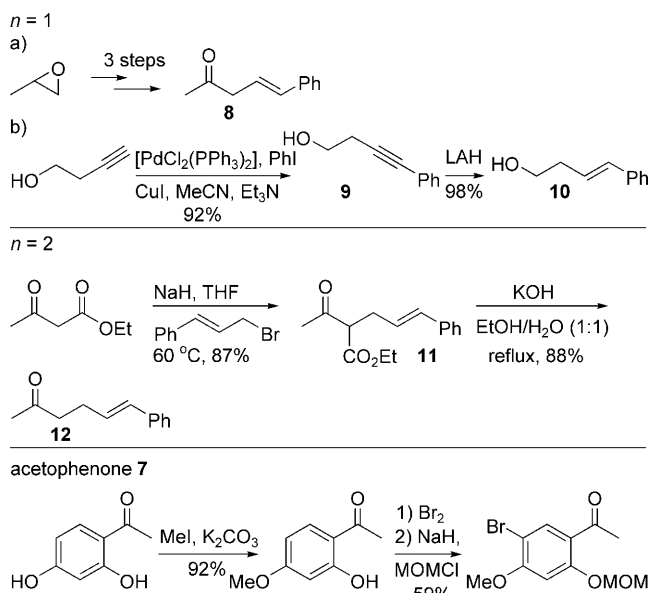
Supporting information for this article is available on the WWW under <http://dx.doi.org/10.1002/chem.200902403>.



Scheme 2. Retrosynthetic analysis for the cycloalkyl-fused chromans. MOM = methoxymethyl.

Our efforts then focused on 1) the syntheses of styrene-containing fragments of different chain length, 2) the aldol condensation, and 3) the *o*-QM/HDA reactions.

As depicted in Scheme 3, the requisite styrene-containing fragments could be easily prepared. For $n = 1$, we first anticipated that ketone **8**^[10] could be used in the aldol condensation.

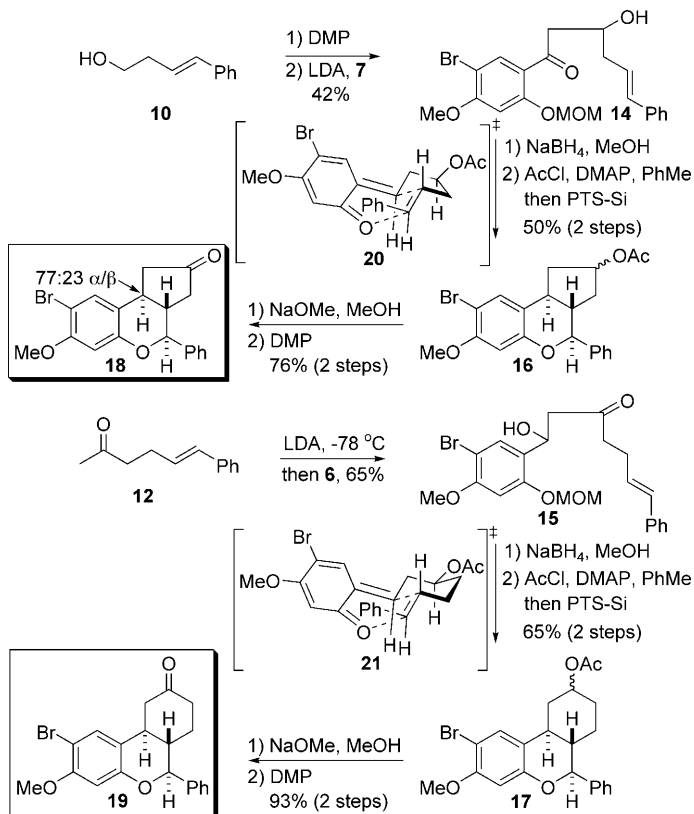


Scheme 3. Synthesis of styrene-containing fragments **12**, **14**, and acetophenone derivative **7**. LAH = lithium aluminum hydride.

tion with benzaldehyde **6**. However, regioselective generation of kinetic enolate of **8** by lithium diisopropylamide (LDA) was difficult. The presence of the styrene moiety rendered the α -methylene protons more acidic and deprotonation of these protons became competitive with that of the α -methyl protons. Thus, an alternative pair for aldol condensation was considered and the target styrene-containing fragment would contain the aldehyde group rather than the ketone. Such a fragment could be synthesized starting from the Sonogashira coupling between iodobenzene and but-3-yn-1-ol, which gave the product **9** in 92% yield. The *trans*-styrene moiety was installed by LAH reduction of the alkyne, giving **10** in 98% yield.

For $n = 2$, alkylation of ethyl acetoacetate with cinnamyl bromide using NaH as base gave **11** in 87% yield, which was subjected to saponification/decarboxylation conditions with KOH to provide **12** in 88% yield. The benzaldehyde **6** could be readily prepared.^[9d] The acetophenone **7** was prepared in three steps from 2,4-dihydroxyacetophenone via **13**.

With both fragments of each cycloalkyl-fused chromans in hand, the aldol condensations of respective pairs were studied (Scheme 4). Alcohol **10** was oxidized to the aldehyde



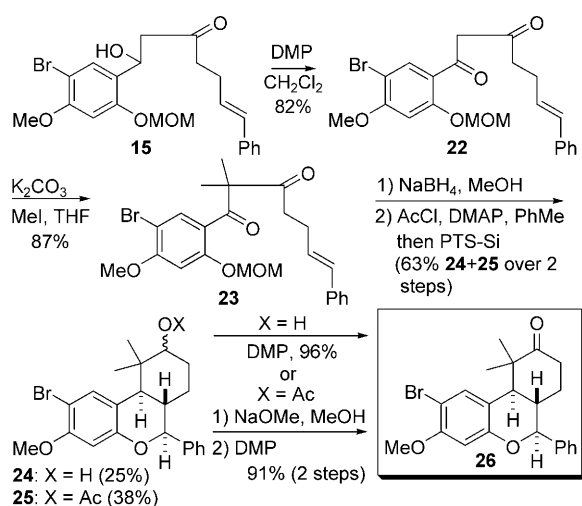
Scheme 4. Aldol condensation/reduction/acetylation/*o*-QM/HDA reactions and proposed *exo* transition states, providing the chromans as racemates (shown with relative stereochemistry). DMAP = 4-dimethylaminopyridine.

using Dess–Martin periodinane (DMP). The crude aldehyde was used directly in the aldol condensation with the enolate of acetophenone **7**, giving **14** in 42% yield. For $n = 2$, aldol condensation of the methyl ketone **12** with benzaldehyde **6** gave **15** in 65% yield.

After some experimentation,^[11] it was found that borohydride reduction of the ketone followed by a one-pot acetylation and PTS-Si-mediated *o*-QM/HDA reaction sequence in toluene occurred smoothly for both substrates, providing the products **16** and **17** in 50 and 65% yields over two steps, respectively. Subsequent base-mediated cleavage of the acetates followed by DMP oxidation furnished the ketones **18** and **19** in 76 and 93% yields over two steps, respectively. Compound **19** was obtained as a single isomer, suggesting that the *o*-QM/HDA reaction occurred with high stereose-

lectivity. Compound **18**, on the other hand, was obtained as a 77:23 (H_α/H_β) mixture of C4-epimers. The C3–C4 *trans* relationship in the major product of **18** and in compound **19** suggested the *exo* transition states **20** and **21**.^[8]

Our new method also allowed easy access to other modifications on the cyclohexyl ring. The β -hydroxy ketone **15** was oxidized by DMP to the 1,3-diketone **22** in 82% yield, which underwent bis-methylation to give the product **23** in 87% yield (Scheme 5). Subsequent borohydride reduction

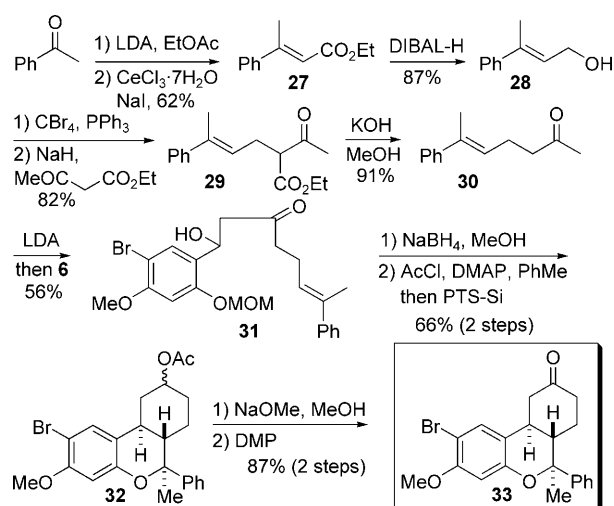


Scheme 5. Synthesis of modified cyclohexyl-fused chroman.

and one-pot acetylation/*o*-QM/HDA reactions provided a mixture of tricyclic alcohol **24** and acetate **25** in 63% combined yields over 2 steps. Treatment of the acetate with NaOMe followed by DMP oxidation gave the ketone **26** as a single isomer in 91% yield over 2 steps. The alcohol **24** was also oxidized to the ketone by DMP in 96% yield.

In addition, modification at C2 as a quaternary center was performed. Aldol condensation between ethyl acetate and acetophenone using LDA followed by $CeCl_3$ –NaI-mediated dehydration^[12] gave the α,β -unsaturated ester **27** in 62% yield (Scheme 6). Subsequent DIBAL-H reduction furnished the alcohol **28** in 87% yield, which was converted to the cinnamyl bromide by using CBR_4 and PPh_3 . Alkylation of the bromide with ethyl acetoacetate, saponification/decarboxylation, and aldol condensation gave ketone **31** via **29** and **30**. Reduction and one-pot acetylation/*o*-QM/HDA reactions provided the tricyclic chroman acetate **32** in 66% yield over 2 steps. Cleavage of the acetate followed by DMP oxidation gave ketone **33** in 87% yield over 2 steps as a single isomer with the C2-methyl group *syn* to the C4-H.

In summary, we have developed a highly efficient and general strategy for the synthesis of cycloalkyl-fused chroman systems by the PTS-Si-mediated *o*-QM/HDA reactions, which proceeded in 50–66% yields in combination with the preceding reduction and acetylation. The generality of this strategy was demonstrated to provide the cyclopentyl- and



Scheme 6. Synthesis of C2-modified cyclohexyl-fused chroman. DIBAL-H = diisobutylaluminum hydride.

cyclohexyl-fused chroman systems. The use of PTS-Si in toluene was critical to suppress styrene polymerization. In addition, all stereocenters at C2, C3, and C4 were installed with good to excellent stereocontrol in a single step. The approach is flexible for a number of modifications and the key steps are compatible with the modified substrates to provide structurally diverse analogues. In addition, the presence of bromine and a methoxy group on the aromatic ring allowed further modifications, such as those required for installing the coumarin moiety in palodesangren C. Applications of this strategy to synthesize other natural products will be reported in due course.

Experimental Section

General procedure for HDA reactions of *o*-QMs: $NaBH_4$ (1.1 equiv) was added to a solution of precursor compounds (**14**, **15**, **23**, **31**) (1 equiv) in MeOH (1 mLmmol^{-1}) at room temperature and then the resulting mixture was stirred for 30 min. After removal of the solvent, H_2O was added to the residue and it was extracted with EtOAc. The combined organic phase was washed with H_2O and brine, dried over Na_2SO_4 , filtered, and concentrated under a vacuum to give a crude alcohol product. This crude product was dissolved in toluene (1 mLmmol^{-1}), followed by the addition of DMAP (2.5 equiv), and the reaction mixture was stirred until completely dissolved. Acetyl chloride (2.5 equiv) was added dropwise to this solution and then the reaction was stirred vigorously overnight. PTS-Si (1.2 equiv) was added to this mixture at room temperature. The reaction mixture was monitored by TLC analysis. After completion, the resulting mixture was filtered and the solid was washed with EtOAc. The combined organic layers were evaporated and the residue was purified by flash chromatography on silica to yield 2-arylcycloalkyl-fused chroman acetates (**16**, **17**, **25**, **32**) and 2-arylcycloalkyl-fused chromanol (**24**).

Acknowledgements

Financial support from the Thailand Research Fund (TRF; BRG5100813 for P.P.) is gratefully acknowledged.

Keywords: chromans • cycloaddition • cyclization • quinone methides • stereoselective reactions

- [1] a) T. P. T. Cushnie, A. J. Lamb, *Int. J. Antimicrob. Agents* **2005**, *26*, 343–356; b) G. Spedding, A. Ratty, E. Middleton, Jr., *Antiviral Res.* **1989**, *12*, 99–110; c) J. P. E. Spencer, *Genes Nutr.* **2007**, *2*, 257–273.
- [2] O. Shirota, K. Takizawa, S. Sekita, M. Satake, *J. Nat. Prod.* **1997**, *60*, 997–1002.
- [3] T. Tanaka, I. Iliya, T. Ito, M. Furusawa, K. Nakaya, M. Iinuma, Y. Shirataki, N. Matsuura, M. Ubukata, J. Murata, F. Simozono, K. Hirai, *Chem. Pharm. Bull.* **2001**, *49*, 858–862. From the isolates of *Gnetum parvifolium*, 2b-hydroxyampelopsin F exhibited the most potent inhibitory activity in the Maillard reaction.
- [4] S. R. Ramadas, A. P. Chaudhuri, *Steroids* **1975**, *26*, 526–536.
- [5] a) J. W. Ullrich, C. P. Miller, *Expert Opin. Ther. Pat.* **2006**, *16*, 559–572; b) O. B. Wallace, T. I. Richardson, J. A. Dodge, *Curr. Top. Med. Chem.* **2003**, *3*, 1663–1680; c) C. P. Miller, *Curr. Pharm. Des.* **2002**, *8*, 2089–2111.
- [6] a) B. H. Norman, J. A. Dodge, T. I. Richardson, P. S. Borrromeo, C. W. Lugar, S. A. Jones, K. Chen, Y. Wang, G. L. Durst, R. J. Barr, C. Montrose-Rafizadeh, H. E. Osborne, R. M. Amos, S. Guo, A. Boodhoo, V. Krishnan, *J. Med. Chem.* **2006**, *49*, 6155–6157; b) T. I. Richardson, J. A. Dodge, Y. Wang, J. D. Durbin, V. Krishnan, B. H. Norman, *Bioorg. Med. Chem. Lett.* **2007**, *17*, 5563–5566.
- [7] a) O. L. Chapman, M. R. Engel, J. P. Springer, J. C. Clardy, *J. Am. Chem. Soc.* **1971**, *93*, 6696–6698; b) M. Fischer, Y. Shi, B. P. Zhao, V. Snieckus, P. Wan, *Can. J. Chem.* **1999**, *77*, 868–874; c) R. W. Van De Water, T. R. R. Pettus, *Tetrahedron* **2002**, *58*, 5367–5405; d) R. M. Jones, C. Selenski, T. R. R. Pettus, *J. Org. Chem.* **2002**, *67*, 6911–6915; e) D. Magdziak, S. J. Meek, T. R. R. Pettus, *Chem. Rev.* **2004**, *104*, 1383–1429; f) C. Selenski, T. R. R. Pettus, *Tetrahedron* **2006**, *62*, 5298–5307; g) C. D. Bray, *Org. Biomol. Chem.* **2008**, *6*, 2815–2819; h) J. P. Lumb, K. C. Choong, D. Trauner, *J. Am. Chem. Soc.* **2008**, *130*, 9230–9231; i) R. Rodriguez, R. M. Adlington, J. E. Moses, A. Cowley, J. E. Baldwin, *Org. Lett.* **2004**, *6*, 3617–3619; j) A. F. Barrero, J. F. Quílez del Moral, M. M. Herrador, P. Arteaga, M. Cortés, J. Benites, A. Rosellón, *Tetrahedron* **2006**, *62*, 6012–6017.
- [8] a) Z. G. Lu, N. Sato, S. Inoue, K. Sato, *Chem. Lett.* **1992**, 1237–1238; b) K. S. Shrestha, K. Honda, M. Asami, S. Inoue, *Bull. Chem. Soc. Jpn.* **1999**, *72*, 73–83; c) H. Miyazaki, K. Honda, M. Asami, S. Inoue, *J. Org. Chem.* **1999**, *64*, 9507–9511; d) H. Miyazaki, Y. Honda, S. Inoue, *Tetrahedron Lett.* **2000**, *41*, 2643–2647; e) Y. R. Lee, Y. M. Kim, S. H. Kim, *Tetrahedron* **2009**, *65*, 101–108.
- [9] a) P. Ploypradith, R. K. Kagan, S. Ruchirawat, *J. Org. Chem.* **2005**, *70*, 5119–5125; b) T. Petchmanee, P. Ploypradith, S. Ruchirawat, *J. Org. Chem.* **2006**, *71*, 2892–2895; c) P. Ploypradith, P. Cheryklin, N. Niyomtham, D. R. Bertoni, S. Ruchirawat, *Org. Lett.* **2007**, *9*, 2637–2640; d) P. Batsomboon, W. Phakhodee, S. Ruchirawat, P. Ploypradith, *J. Org. Chem.* **2009**, *74*, 4009–4012.
- [10] See the Supporting Information for details.
- [11] Direct conversion of the alcohol in compounds **14** and **15** to the acetates for the subsequent *o*-QM/HDA reaction was not successful because of the competing retro-aldol reaction and dehydration among others. Subjecting **15** directly for the *o*-QM/HDA reaction gave **19** in low yield (20%). Treating the 1,3-diol from the borohydride reduction with PTS-Si in toluene or *p*-TsOH in methanol (ref. [8a–d]) gave no desired tricyclic alcohol.
- [12] G. Bartoli, M. C. Bellucci, M. Patrini, E. Marcantoni, L. Sambri, E. Torregiani, *Org. Lett.* **2000**, *2*, 1791–1793.

Received: August 31, 2009
Published online: December 28, 2009

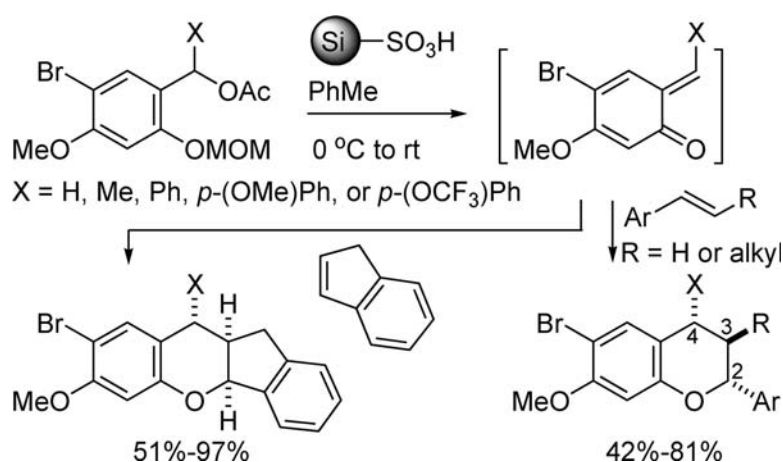
Note

Generation of *ortho*-Quinone Methides by *p*-TsOH on Silica and Their Hetero-Diels-Alder Reactions with Styrenes

Paratchata Batsomboon, Wong Phakhodee, Somsak Ruchirawat, and Poonsakdi Ploypradith

J. Org. Chem., 2009, 74 (10), 4009-4012 • Publication Date (Web): 22 April 2009

Downloaded from <http://pubs.acs.org> on May 8, 2009



More About This Article

Additional resources and features associated with this article are available within the HTML version:

- Supporting Information
- Access to high resolution figures
- Links to articles and content related to this article
- Copyright permission to reproduce figures and/or text from this article

[View the Full Text HTML](#)

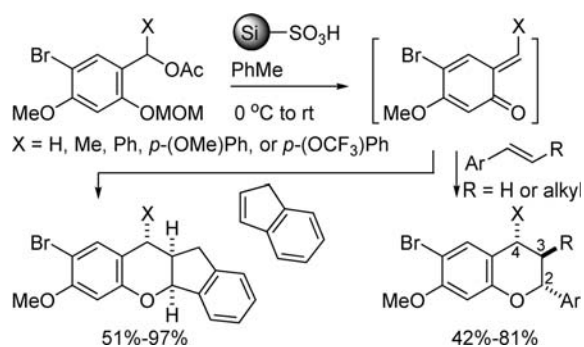
Generation of *ortho*-Quinone Methides by *p*-TsOH on Silica and Their Hetero-Diels–Alder Reactions with Styrenes

Paratchata Batsomboon,[†] Wong Phakhodee,[‡]
Somsak Ruchirawat,^{†,§,§} and Poonsakdi Ploypradith^{*,†,‡}

Laboratory of Medicinal Chemistry, Chulabhorn Research Institute, Program in Chemical Biology, Chulabhorn Graduate Institute, Vipavadee-Rangsit Highway, Bangkok, Thailand 10210, and Program on Research and Development of Synthetic Drugs, Institute of Science and Technology for Research and Development, Mahidol University, Salaya Campus, Nakhon Pathom, Thailand

poonsakdi@cri.or.th

Received March 6, 2009



2-Arylchromans were readily prepared from the hetero-Diels–Alder reactions of styrenes with the *ortho*-quinone methides (*o*-QMs) which, in turn, were generated by treating the MOM-protected benzylacetate derivatives with *p*-TsOH immobilized on silica (PTS-Si) in toluene under mild conditions (0 °C to rt). The corresponding chromans were obtained in moderate to excellent yields (42–97%) and in moderate to excellent diastereoselectivity (up to >99:1).

The chroman, or the benzopyran, can be found as the core structure in a number of natural products such as those in the flavonoid families, which have been shown to exhibit antioxidant, antiallergic, anti-inflammatory, antimicrobial, anticancer,

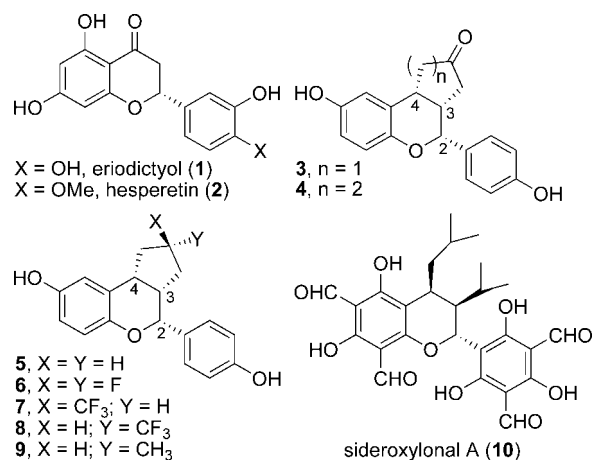


FIGURE 1. Eriodictyol (1), hesperetin (2), selective ER β agonists (3–9), and sideroxylylonal A (10).

anxiolytic, and myorelaxant properties.¹ Eriodictyol (1) and hesperetin (2) are antioxidant 2-arylchromanone natural products (Figure 1). In addition, some synthetic 2-arylchromans (3–9) have been developed as selective estrogen receptor β (ER β) agonists (SERBAs).^{2,3} However, some of the steps in these synthetic routes were low-yielding, and the overall processes involved many chemical steps. Moreover, synthesis of compounds with substituents at the 4-position, such as sideroxylylonal A (10), involved the hetero-Diels–Alder reaction of the *ortho*-quinone methide (*o*-QM).⁴

The hetero-Diels–Alder reactions have been employed in a number of syntheses to construct the heteroatom-containing ring systems.⁵ Reactions between the *o*-QMs as the heterodienes and the properly activated olefins as the dienophiles furnish the benzopyran as well as the spiroketal frameworks.⁶ Among the most commonly used procedures to generate the highly reactive *o*-QMs are thermal and base initiations.⁷ These procedures

(2) (a) Ullrich, J. W.; Miller, C. P. *Expert Opin. Ther. Pat.* **2006**, *16*, 559–572. (b) Wallace, O. B.; Richardson, T. I.; Dodge, J. A. *Curr. Top. Med. Chem.* **2003**, *3*, 1663–1680. (c) Miller, C. P. *Curr. Pharm. Des.* **2002**, *8*, 2089–2111.

(3) (a) Norman, B. H.; Dodge, J. A.; Richardson, T. I.; Borromeo, T. S.; Lugar, C. W.; Jones, S. A.; Chen, K.; Wang, Y.; Durst, G. L.; Barr, R. J.; Montrose-Rafizadeh, C.; Osborne, H. E.; Amos, R. M.; Guo, S.; Boodhoo, A.; Krishnan, V. *J. Med. Chem.* **2006**, *49*, 6155–6157. (b) Richardson, T. I.; Norman, B. H.; Lugar, C. W.; Jones, S. A.; Wang, Y.; Durbin, J. D.; Krishnan, V.; Dodge, J. A. *Bioorg. Med. Chem. Lett.* **2007**, *17*, 3570–3574. (c) Richardson, T. I.; Dodge, J. A.; Durst, G. L.; Pfeifer, L. A.; Shah, J.; Wang, Y.; Durbin, J. D.; Krishnan, V.; Norman, B. H. *Bioorg. Med. Chem. Lett.* **2007**, *17*, 4824–4828. (d) Norman, B. H.; Richardson, T. I.; Dodge, J. A.; Pfeifer, L. A.; Durst, G. L.; Wang, Y.; Durbin, J. D.; Krishnan, V.; Dinn, S. R.; Liu, S.; Reilly, J. E.; Ryter, K. T. *Bioorg. Med. Chem. Lett.* **2007**, *17*, 5082–5085. (e) Richardson, T. I.; Dodge, J. A.; Wang, Y.; Durbin, J. D.; Krishnan, V.; Norman, B. H. *Bioorg. Med. Chem. Lett.* **2007**, *17*, 5563–5566.

(4) Tatsuta, K.; Tamura, T.; Mase, T. *Tetrahedron Lett.* **1999**, *40*, 1925–1928.

(5) (a) Bray, C. D. *Org. Biomol. Chem.* **2008**, *6*, 2815–2819. (b) Kuboki, A.; Yamamoto, T.; Taira, M.; Arishige, T.; Konishi, R.; Hamabata, M.; Shirahama, M.; Hiramatsu, T.; Kuyama, K.; Ohira, S. *Tetrahedron Lett.* **2008**, *49*, 2558–2561.

(6) (a) Pettigrew, J. D.; Bexrud, J. A.; Freeman, R. P.; Wilson, P. D. *Heterocycles* **2004**, *62*, 445–452. (b) Adlington, R. M.; Baldwin, J. E.; Mayweg, A. V. W.; Pritchard, G. J. *Org. Lett.* **2002**, *4*, 3009–3011. (c) Zhou, G.; Zhu, J.; Xie, Z.; Li, Y. *Org. Lett.* **2008**, *10*, 721–724. (d) Marsini, M. A.; Huang, Y.; Lindsey, C. C.; Wu, K.-L.; Pettus, T. R. R. *Org. Lett.* **2008**, *10*, 1477–1480. (e) El Kaim, L.; Grimaud, L.; Oble, J. *Org. Biomol. Chem.* **2006**, *4*, 3410–3413. (f) Rosenau, T.; Netscher, T.; Ebner, G.; Kosma, P. *Synlett* **2005**, 243–246.

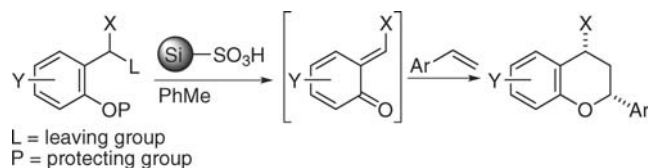
[†] Chulabhorn Graduate Institute.

[‡] Chulabhorn Research Institute.

[§] Mahidol University.

(1) (a) Zaloni, P.; Avallone, R.; Baraldi, M. *Fitoterapia* **2000**, *71*, S117–S123. (b) Welton, A. F.; Tobias, L. D.; Fiedler-Nagy, C.; Anderson, W.; Hope, W.; Meyers, K.; Coffey, J. W. In *Plant Flavonoids in Biology and Medicine*; Cody, V., Middleton, E., Jr., Harborne, J. B., Eds.; Alan R. Liss Inc.: New York, 1986; pp 1–592. (c) Hirano, T.; Oka, K.; Akiba, M. *Res. Commun. Chem. Pathol. Pharmacol.* **1989**, *64*, 69–78. (d) Cassady, J. M.; Baird, W. H.; Chang, C.-J. *J. Nat. Prod.* **1990**, *53*, 23–41. (e) Medina, J. H.; Vioila, H.; Wolfman, C.; Marder, M.; Wasowski, C.; Calvo, D.; Paladini, A. C. *Neurochem. Res.* **1997**, *22*, 419–425.

SCHEME 1. General Structure for the *o*-QM Precursor



provided the products in moderate to excellent yields with good to excellent stereoselectivity. In contrast to the thermal and base initiation procedures, only a limited number of accounts have reported the use of acid to generate the *o*-QMs, mainly due to the low compatibility of acidic conditions with the dienophiles, as well as the low stereoselectivity in the resulting products due to the greater ionic character of the reaction conditions.⁸

In recent years, our research group has investigated and reported the utility of various solid-supported reagents in total synthesis as well as in developing some synthetic methods for selective deprotection of aromatic ethers using solid-supported acids.⁹ Herein, we wish to report the use of *p*-TsOH on silica (PTS-Si) to generate the *o*-QMs and their subsequent intermolecular hetero-Diels–Alder reactions with styrene derivatives, yielding the desired 2-arylchromans.

Our previous investigations in the protecting group chemistry of aromatic ethers indicated that a number of protecting groups could be cleaved under relatively mild conditions using PTS-Si in the nonpolar solvent toluene.^{9b,c} Thus, an appropriate precursor to *o*-QM could assume a structure containing a phenol-protected moiety and a leaving group at the benzylic position (Scheme 1).

As shown in Scheme 2, the *o*-QM precursors were prepared to investigate the effect of substituents on the aromatic ring, protecting group, and leaving group. From the aldehydes **11–13**, the phenol groups were protected as their MOM ethers using standard procedures followed by NaBH₄ reduction of the aldehyde and the conversion of the resulting hydroxy group to the corresponding acetates **14–16**. Bromination of **13** gave the aldehyde **17** in 60% yield. Subsequent phenol protection as Bn, *i*-Pr, or MOM ether, NaBH₄ reduction, and acetylation furnished the corresponding products **18–20** in 62–92% yields. It should be noted that the preparation of these *o*-QM precursors, while not entirely a one-pot procedure, required only one purification by column chromatography in the final step as the crude products from phenol protection and reduction could be used in the subsequent steps without purification.

As summarized in Table 1, the nature of substituents on the aromatic ring played an important role (entries 1–4). If considering the *o*-QM precursor **14** (X = Y = H) as the

SCHEME 2. Synthesis of the *o*-QM Precursors

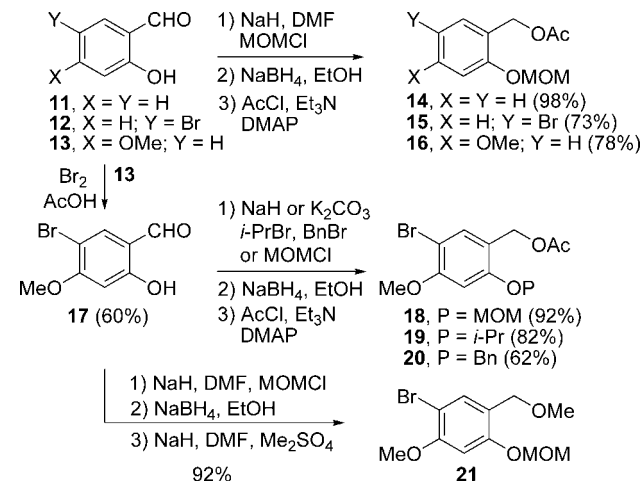


TABLE 1. The Hetero-Diels–Alder Reactions of 14–21^a

entry	compound	X	Y	Z	P	yield (%)
1	14	H	H	OAc	MOM	46
2	15	H	Br	OAc	MOM	48
3 ^b	16	OMe	H	OAc	MOM	0
4	18	OMe	Br	OAc	MOM	81
5 ^{b,c}	19	OMe	Br	OAc	<i>i</i> -Pr	0
6 ^{b,c}	20	OMe	Br	OAc	Bn	0
7	21	OMe	Br	OMe	MOM	61

22, X = Y = H
23, X = H; Y = Br
24, X = OMe; Y = Br

^a Unless otherwise noted, the reactions were performed in toluene at 0 °C to rt. ^b Starting materials were consumed, but complex mixtures were obtained. ^c The protecting groups were cleaved.

reference, substituting bromine (X = H; Y = Br) for proton in **15** showed no effect on the yields of **22** and **23**. Without bromine, but with the methoxy group (X = OMe; Y = H) in **16**, the reaction gave no desired product.¹⁰ The best yield was obtained with **18**, which contained both the methoxy group and bromine (X = OMe; Y = Br).

The effect of the protecting group was then investigated. The reaction of the *o*-QM precursor with the MOM group gave the product in 81% yield (entry 4), while those with the Bn and *i*-Pr groups gave complex mixtures (entries 5 and 6).¹¹ For the leaving group, the best result was obtained with the acetate.¹² Compound **21** with OMe gave **24** in 61% yield.

Various acids were explored for the cycloaddition reactions of the *o*-QM precursor **18** with styrene or styrene derivative **25**

(10) The underlying reasons for the effect of aromatic substituents on the yields of the hetero-Diels–Alder reactions are currently under our investigation. The 0% yield of the corresponding product from compound **16** was presumably due to the formation of competing transient *para*-quinone methide (*p*-QM) from the protonation on the acetate group. The departure of protonated acetate could be assisted by the *p*-OMe group. Subsequent nucleophilic addition of *p*-QM with styrene gave the intermediate which could react further with additional styrene monomer(s) prior to the cleavage of the MOM group. Therefore, the reactions led to the formation of a complex mixture of inseparable product(s). For compound **18**, which gave the corresponding product in 81% yield, the presence of Br on the aromatic ring presumably resulted in the preferential formation of the *o*-QM over the *p*-QM. For the schematic proposed mechanism(s), see Supporting Information.

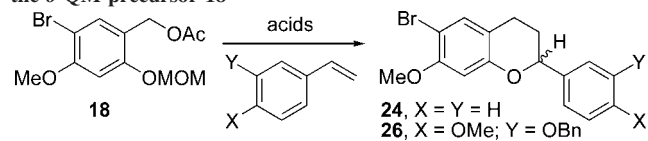
(11) The rate of styrene polymerization in acid might be faster than those of acid-mediated cleavage of the Bn or *i*-Pr groups in compound **19** and **20**, resulting in no cycloaddition product.

(12) Other *o*-QM precursors with the iodide or mesylate decomposed.

(7) (a) Van De Water, R. W.; Pettus, T. R. R. *Tetrahedron* **2002**, *58*, 5367–5405. (b) Sugimoto, H.; Nakamura, S.; Ohwada, T. *J. Org. Chem.* **2007**, *72*, 10088–10095. (c) Crawley, S. L.; Funk, R. L. *Org. Lett.* **2003**, *5*, 3169–3171. (d) Rodríguez, R.; Adlington, R. M.; Moses, J. E.; Cowley, A.; Baldwin, J. E. *Org. Lett.* **2004**, *6*, 3617–3619. (e) Selenski, C.; Pettus, T. R. R. *Tetrahedron* **2006**, *62*, 5298–5307. (f) Jones, R. M.; Selenski, C.; Pettus, T. R. R. *J. Org. Chem.* **2002**, *67*, 6911–6915. (g) Barrero, A. F.; Quílez del Moral, J. F.; Herrador, M. M.; Arteaga, P.; Cortés, M.; Benites, J.; Rosellón, A. *Tetrahedron* **2006**, *62*, 6012–6017. (h) Patel, A.; Netscher, T.; Rosenau, T. *Tetrahedron Lett.* **2008**, *49*, 2442–2445.

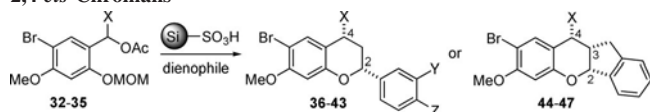
(8) (a) Lu, Z. G.; Sato, N.; Inoue, S.; Sato, K. *Chem. Lett.* **1992**, *21*, 1237–1238. (b) Chiba, K.; Hirano, T.; Kitano, Y.; Tada, M. *Chem. Commun.* **1999**, 691–692. (c) Miyazaki, H.; Honda, K.; Asami, M.; Inoue, S. *J. Org. Chem.* **1999**, *64*, 9507–9511. (d) Miyazaki, H.; Honda, Y.; Honda, K.; Inoue, S. *Tetrahedron Lett.* **2000**, *41*, 2643–2647.

(9) (a) Ploypradith, P.; Kagan, R. K.; Ruchirawat, S. *J. Org. Chem.* **2005**, *70*, 5119–5125. (b) Petchmanee, T.; Ploypradith, P.; Ruchirawat, S. *J. Org. Chem.* **2006**, *71*, 2892–2895. (c) Ploypradith, P.; Cheryklin, P.; Niyomtham, N.; Bertoni, D. R.; Ruchirawat, S. *Org. Lett.* **2007**, *9*, 2637–2640.

TABLE 2. Effect of Acids on the Hetero-Diels–Alder Reactions of the *o*-QM precursor **18**^a


entry	dienophile	acid ^b	X	Y	yield (%)
1		PTS-Si	H	H	81
2 ^c		<i>p</i> -TsOH	H	H	71
3	(10.0 equiv)	TFA	H	H	67
4		HCl	H	H	66
5		PTA	H	H	34
6		PMA	H	H	56
7		TSA	H	H	45
8		PTS-Si	OMe	OBn	73
9 ^c		<i>p</i> -TsOH	OMe	OBn	58
10	25	TFA	OMe	OBn	0
11	(1.1 equiv)	HCl	OMe	OBn	0
12		PTA	OMe	OBn	3
13		PMA	OMe	OBn	4
14		TSA	OMe	OBn	37

^a Unless otherwise noted, the reactions were performed in toluene at 0 °C to rt (normally 4–5 h). ^b TFA = CF₃COOH; PTA = phosphotungstic acid hydrate; PMA = phosphomolybdic acid hydrate; TSA = tungstosilicic acid hydrate. ^c The reactions took 18 h.

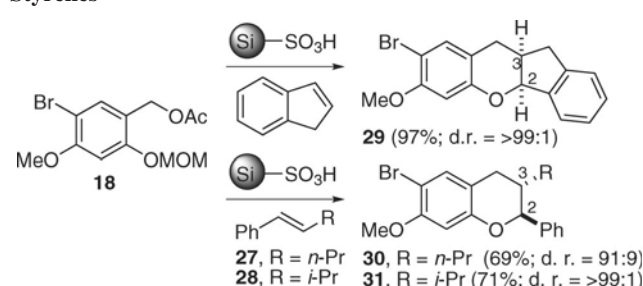
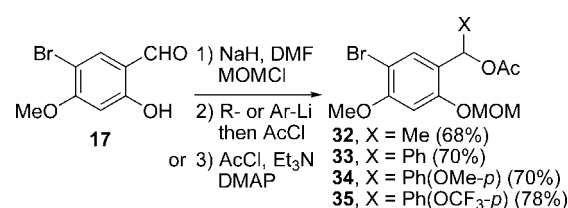
TABLE 3. Diastereoselective Hetero-Diels–Alder Reactions of Benzyl-Substituted *o*-QM Precursors **32–35** to the 2,4-*cis*-Chromans^a


entry	dienophile	<i>o</i> -QM precursor	product	X	Y	Z	yield (%) ^b	d.r. (<i>cis</i> : <i>trans</i>) ^c
1		32	36	Me	H	H	85	76:24
2		33	37	Ph	H	H	66	84:16
3	(10.0 equiv)	34	38	Ph(OMe- <i>p</i>)	H	H	57	86:14
4		35	39	Ph(OCF ₃ - <i>p</i>)	H	H	53	93:7
5		32	40	Me	OBn	OMe	61	77:23
6		33	41	Ph	OBn	OMe	62	75:25
7		34	42	Ph(OMe- <i>p</i>)	OBn	OMe	76	76:24
8	(1.1 equiv)	35	43	Ph(OCF ₃ - <i>p</i>)	OBn	OMe	42	>99:1
9		32	44	Me	-	-	75	85:15
10		33	45	Ph	-	-	90	>99:1
11	(10.0 equiv)	34	46	Ph(OMe- <i>p</i>)	-	-	83	78:22
12		35	47	Ph(OCF ₃ - <i>p</i>)	-	-	51	>99:1

^a Unless otherwise noted, the reactions were performed in toluene at 0 °C to rt (normally 4–5 h). ^b Isolated yields of a mixture of 2,4-*cis* and 2,4-*trans* diastereomers. ^c Diastereomeric ratio between C2 and C4 positions as determined by ¹H NMR.

bearing two electron-donating groups (EDG) on the phenyl ring. The results are summarized in Table 2. Although both *p*-TsOH and PTS-Si gave the product **24** in comparable yields (71–81%, entries 1 and 2), the reaction using PTS-Si proceeded faster perhaps due to the greater surface area of PTS-Si. Interestingly, no desired product was obtained from (+)-camphorsulfonic acid (CSA), albeit bearing an alkyl sulfonic acid functionality, or from other Lewis acids (BF₃·Et₂O, AlCl₃, and SnCl₄). Comparable yields (66–67%, entries 3 and 4) of the product **24** were obtained from the reactions using TFA and HCl, while three heteropolyacids gave the product in lower yields (34–56%, entries 5–7).

In general, the reactions of *o*-QM generated from **18** with the styrene derivative **25** gave the product **26** in poorer yields

SCHEME 3. Reactions of **18** with α,β -Disubstituted Styrenes**SCHEME 4.** Synthesis of Benzyl-Substituted Compounds **32–35**

than those with styrene. Interestingly, only the reactions employing PTS-Si gave both the products **24** and **26** in comparable yields (73–81%), while other acids furnished both **24** (entries 2 and 5–7) and **26** (entries 9 and 12–14) in lower yields. When TFA and HCl were used, only **24** but none of **26** was obtained.

Three α,β -disubstituted styrenes were employed to investigate the diastereoselectivity between the C2–C3 positions. Indene, (*E*)-1-phenylpentene (**27**),¹³ and (*E*)-3-methyl-1-phenylbutene (**28**)¹³ furnished the products **29–31** in 97, 69, and 71% yields, respectively (Scheme 3). Both **29** (C2–C3 *cis*) and **31** (C2–C3 *trans*) were obtained as their single C2–C3 isomers, while **30** was obtained as a 91:9 mixture of diastereomers favoring the *trans* isomer. The observed diastereoselectivity between the C2–C3 positions suggested the concerted cycloaddition for the formation of both products (**29** and **31**).

The *o*-QM precursors **32–35** were prepared (Scheme 4) to study the effects of the substituents at the benzylic position on the diastereoselectivity between C2 and C4. Simple styrene, styrene **25** bearing electron-donating groups, and indene were the dienophiles. The results are summarized in Table 3. In all cases, the styrenes gave the products favoring the *cis* isomer between C2 and C4. The monosubstituted olefins gave the products (**36–43**) favoring the C2–C4 *cis* relationship with the diastereomeric ratios ranging from 75:25 to >99:1. The electronic effect from the *para* position of the aryl substituent was evident. The substrate with an electron-donating *p*-OMe group (**34**) gave the products **38** and **42** in moderate to good yields (57–76%) but only with moderate diastereoselectivity (76:24 to 86:14). On the other hand, the *o*-QM precursor **35** with an electron-withdrawing *p*-OCF₃ group furnished the products **39** and **43** in moderate yields (42–53%) but with excellent diastereoselectivity (93:7 to >99:1). The predominant *cis* relationship between the C2–C4 positions suggested that the hetero-Diels–Alder reactions of these substrates proceeded via the *endo*-type concerted transition state.^{7a}

When indene was employed, only the *cis* diastereomers between C2 and C3 were obtained from **32–35**. Moreover, the

(13) See Supporting Information for preparation and characterization.

cis relationship was also favored between C2 and C4, with moderate to excellent diastereomeric ratios of 78:22 to >99:1. Thus, the products **44–47** all were predominantly C2–C3–C4 *cis* isomers.

In summary, we have developed an efficient means to generate the *o*-QMs using PTS-Si. The hetero-Diels–Alder reactions of the *o*-QMs with the styrene derivatives furnished the 2-arylchroman frameworks in moderate to good yields and moderate to excellent diastereoselectivity.

Experimental Section

General Procedure for the Hetero-Diels–Alder Reactions of 2-Arylchroman Products 22–24, 26, 29–31, 36–47. To a stirred solution of benzyl acetates **14–16**, **18–21**, or **32–35** (1.0 equiv) in toluene (5 mL/mmol of starting material) were added styrene derivatives (10.0 equiv for commercially available styrenes, **27** and **28**, and 1.1 equiv for **25**) at room temperature. The resulting mixture was stirred at 0 °C for 10 min, and then PTS-Si (0.81 mmol/g, 1.1 equiv) was added. The reaction mixture was stirred until all benzyl acetates **14–16**, **18–21**, or **32–35** were consumed as indicated by TLC (typically 4–5 h). At that time, the reaction mixture was filtered to remove the silica, which was washed with excess CH₂Cl₂ (three times). The filtrate was then concentrated under reduced pressure to give a crude product mixture which was further purified by preparative TLC to furnish the desired product.

6-Bromo-7-methoxy-2-phenylchroman (24). Benzyl acetate **18** (0.025 g, 0.078 mmol) in toluene (1 mL) was treated with PTS-Si (0.106 g, 0.086 mmol) and styrene (0.092 mL, 0.78 mmol) according to the general procedure above to give the desired 2-arylchroman product **24** (0.02 g, 0.063 mmol, 81%) as a colorless oil: IR (neat) ν_{\max} 2928, 1610, 1572, 1495, 1485, 1442, 1309, 1266, 1193, 1153, 1053 cm⁻¹; ¹H NMR (200 MHz, CDCl₃) δ 1.97–2.28 (m, 2H), 2.66–2.79 (m, 1H), 2.84–3.01 (m, 1H), 3.85 (s, 3H),

5.05 (dd, $J = 9.4, 3.0$ Hz, 1H), 6.52 (s, 1H), 7.26 (s, 1H), 7.35–7.44 (m, 5H); ¹³C NMR (50 MHz, CDCl₃) δ 24.1, 29.6, 56.2, 78.0, 101.1, 101.8, 115.2, 125.9, 128.0, 128.6, 133.0, 141.1, 154.8, 155.1; LRMS (EI) m/z (rel intensity) 320 (M⁺ + 2, 100), 318 (M⁺, 97), 239 (16), 238 (14); TOF-HRMS calcd for C₁₆H₁₆BrO₂ (M + H⁺) 319.0328, found 319.0327.

6-Bromo-7-methoxy-2-phenyl-3-propylchroman (31). Benzyl acetate **18** (0.024 g, 0.076 mmol) in toluene (1 mL) was treated with PTS-Si (0.102 g, 0.083 mmol) and styrene **28** (0.11 g, 0.76 mmol) according to the general procedure above to give the desired 2-arylchroman product **31** (0.020 g, 0.054 mmol, 71%) as a colorless oil: IR (neat) ν_{\max} 2958, 2926, 1611, 1575, 1496, 1444, 1402, 1310, 1283, 1201, 1157, 1063, 1049 cm⁻¹; ¹H NMR (400 MHz, CDCl₃) δ 0.76 (d, $J = 6.8$ Hz, 3H), 0.88 (d, $J = 6.9$ Hz, 3H), 1.44–1.52 (m, 1H), 1.93–2.00 (m, 1H), 2.53 (dd, $J = 16.2, 5.3$ Hz, 1H), 2.61 (dd, $J = 16.3, 9.6$ Hz, 1H), 3.74 (s, 3H), 3.77 (s, 3H, minor), 4.84 (d, $J = 8.6$ Hz, 1H), 5.34 (d, $J = 3.9$ Hz, 1H, minor), 6.39 (s, 1H), 6.40 (s, 1H, minor), 7.17 (s, 1H), 7.19 (s, 1H, minor), 7.23–7.34 (m, 5H); ¹³C NMR (100 MHz, CDCl₃) δ 16.4, 21.2, 23.4, 26.8, 42.7, 56.2, 81.4, 100.7, 101.7, 115.5, 126.5, 127.0, 128.2, 128.6, 133.2, 139.9, 154.7; LRMS (EI) m/z (rel intensity) 362 (M⁺ + 2, 80), 360 (M⁺, 83), 319 (10), 317 (11), 271 (87), 269 (100), 238 (18), 190 (40), 131 (43); TOF-HRMS calcd for C₁₉H₂₂BrO₂ (M + H⁺) 361.0798, found 361.0800.

Acknowledgment. Financial support from the Thailand Research Fund (TRF; BRG5100813 for P.P.) is gratefully acknowledged.

Supporting Information Available: Experimental procedures and full spectroscopic data for all new compounds. This material is available free of charge via the Internet at <http://pubs.acs.org>.

JO900504Y



Pt(IV)-catalyzed generation and [4+2]-cycloaddition reactions of *o*-quinone methides

Suttipol Radomkit^{a,b}, Pakornwit Sarnpitak^{a,b}, Jumreang Tummatorn^c, Paratchata Batsomboon^c, Somsak Ruchirawat^c, Poonsakdi Ploypradith^{a,b,c,*}

^a Program in Chemical Biology, Chulabhorn Graduate Institute, Vipavadee-Rangsit Highway, Bangkok 10210, Thailand

^b The Center for Environmental Health, Toxicology and Management of Chemicals (ETM), Chulabhorn Graduate Institute, Vipavadee-Rangsit Highway, Bangkok 10210, Thailand

^c Laboratory of Medicinal Chemistry, Chulabhorn Research Institute, Vipavadee-Rangsit Highway, Bangkok 10210, Thailand

ARTICLE INFO

Article history:

Received 16 December 2010

Received in revised form 2 March 2011

Accepted 21 March 2011

Available online 26 March 2011

Keywords:

Cycloaddition

Stereoselective

ortho-Quinone methide

Metal catalysis

Chroman

ABSTRACT

Novel intermolecular and intramolecular generations of *ortho*-quinone methides and their formal [4+2]-cycloaddition reactions with olefins catalyzed by PtCl₄ and AuCl₃ under mild conditions have been developed. Good to excellent yields (up to 99%) and diastereoselectivity (up to >99:1) of the chromans were obtained. PtCl₄ was found to be effective and compatible with various functional groups present in the substrates. A mechanism accounting for its catalytic cycle is proposed and discussed.

© 2011 Elsevier Ltd. All rights reserved.

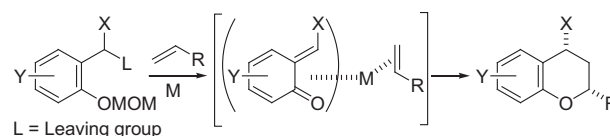
1. Introduction

Metal-catalyzed reactions have revolutionized modern synthetic methodologies and their development has made possible total syntheses of structurally complex natural products. In recent years, platinum and gold salts/complexes have drawn much attention and their use as catalysts for various organic transformations have been developed.¹ The chemistry of Pt(II), Pt(IV), Au(I), and Au(III) and their use in organic synthesis has been studied and reported.^{1f–i} However, chemistry of these metal salts/complexes has largely involved activation of the π -system of the alkyne rather than that of the olefin.^{1e–i}

A number of methods have been developed to generate the transient highly reactive *ortho*-quinone methides (*o*-QMs). In addition to thermal and base initiation, some Lewis acids and transition metal salts/complexes of Os, Rh, Ir, Mn, and Pd were reported to mediate the generation of *o*-QMs.² Recently, our research group has been involved with acid-mediated generation of *o*-QMs and their cycloaddition reactions using *p*-TsOH immobilized on silica (PTS–Si).³ The resulting 2-aryl chromans can be functionalized to provide the core structures of natural and synthetic compounds

* Corresponding author. Tel.: +662 574 0622; fax: +662 574 2027; e-mail address: poonsakdi@cri.or.th (P. Ploypradith).

exhibiting a wide array of biological properties.⁴ Herein, we report, for the first time, a novel Pt(IV)- and Au(III)-catalyzed generation of *o*-QMs and their cycloaddition reactions via Pt(IV)- and Au(III)-activation of olefin and coordination with *o*-QM (Scheme 1).



Scheme 1. Metal-catalyzed generation of *o*-QMs and cycloaddition reactions.

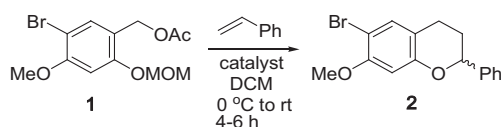
2. Results and discussion

We envisioned that, upon coordination with metal salts/complexes, the *o*-QM may be stabilized for the subsequent cycloaddition reactions to provide the chroman products. One drawback, albeit a minor one, of our previously developed method for the generation of *o*-QM and its cycloaddition reactions using PTS–Si was the required stoichiometric amount of the acid, which may not be compatible with a number of functional groups present on the *o*-QM precursor or the olefin. Taken together, with appropriate metal salts/complexes, a catalytic process may be developed to circumvent the drawback.

2.1. Intermolecular [4+2]-cycloaddition reactions

Our preliminary data using PTS–Si to generate *o*-QMs showed that compound **1** gave the best results and was thus chosen as the *o*-QM precursor for the screening of Lewis acids and transition metal salts/complexes.^{3,5} As summarized in Table 1, it was found that stoichiometric amount of AlCl₃, TiCl₃, TiCl₄, ZrCl₄, FeCl₃, ZnCl₂, AuCl, AuCl₃, InCl₃, PtCl₂, and PtCl₄ gave the desired product **2** in 26–85% yields while catalytic amount (10–30 mol %) of only PtCl₄, AuCl₃, and InCl₃,⁶ furnished the chroman in 62–88% yields. In a larger scale reaction, the required amount of the PtCl₄ could be reduced to 4 mol %, which gave the product in a slightly lower yield (76%). In fact, the reactions using catalytic amount of metal salts proceeded more cleanly than those using stoichiometric amount, giving the product in higher yields (entries 7 and 10). An increase in electrophilicity, rather than the oxidation state, of the metal center (Pt) is an important factor responsible for the successful catalysis of generating *o*-QMs and mediating cycloaddition reactions. Whilst possessing the same oxidation state (Pt(IV)) and ligand (Cl), PtCl₄, but not K₂PtCl₆, is a useful catalyst (entries 10 and 11). Previous work suggested that an increase in oxidation state increases the electrophilicity of the metal center, resulting in increasing the reactivity of the catalyst.^{1h} Thus, successful catalysis of PtCl₄ may be due to its higher Lewis acidity.

Table 1
Screening of the metal salts/complexes for *o*-QMs and cycloaddition reactions with styrene^a



Entry	Catalyst	mol (%)	Yield (%) ^b
1 ^c	AlCl ₃	100	26
2 ^c	TiCl ₃	100	48
3 ^c	TiCl ₄	100	68
4 ^c	ZrCl ₄	100	39
5 ^c	FeCl ₃	100	63
6 ^c	ZnCl ₂	100	83
7 ^d	AuCl	30	84 (75)
8 ^e	AuCl ₃	10	84 (85)
9 ^c	PtCl ₂	100	62
10	PtCl ₄	10	88 (75)
11	K ₂ PtCl ₆	10	0
12	InCl ₃	10	62 (41)
13 ^f	PTS–Si	100	81

^a Unless otherwise noted, all reactions were performed in DCM, using 10 equiv of styrene.

^b Isolated yields. Numbers in parenthesis are yields of **2** when using stoichiometric amount of catalysts.

^c Substoichiometric (30–50 mol %) and catalytic (10–30 mol %) amounts of catalysts resulted in no reaction with recovery of *o*-QM precursor.

^d Compound **2** (91%) was obtained (based on recovered starting materials) if 10 mol % of AuCl was employed.

^e The reaction using 10 mol % AuCl₃ required 36 h to complete.

^f For reference, the reaction using PTS–Si was performed in toluene.

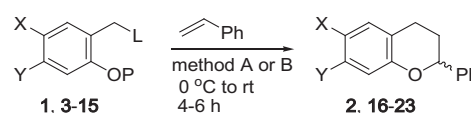
The use of dichloromethane (DCM) as solvent was important.⁷ Toluene, which was the solvent of choice when PTS–Si was employed, gave no desired product with complete recovery of **1** regardless of the metal salts/complexes under current investigation. Because of the higher yield, shorter reaction time, and easier handling, PtCl₄ was chosen as catalyst for the subsequent studies.

The effects of substituents on the aromatic ring as well as those of the leaving group at the benzylic position and the phenol protecting groups were also investigated. As summarized in Table 2, both compound **1** (with the acetate) and **3**⁸ (with the *tert*-butyldimethylsilyloxy (OTBDMS) group) gave better yields (88%) than

compound **4**⁸ containing a hydroxy group (58%) as the leaving group at the benzylic position under similar conditions (entries 1–3). The importance of MOM as a phenol protecting group was evident as compound **5**, with an *i*-Pr group, failed to give any product while compound **6**,⁸ with a MEM group, gave the product only in 49% yield (entries 4 and 5).

Table 2

Effects of the substituents on the aromatic ring, the leaving group, the phenol protecting groups, and the method to generate the *o*-QMs and mediate their cycloaddition reactions^a



Entry	Compound	X	Y	L	P	Product	Method ^b	Yield (%) ^c
1	1	Br	OMe	OAc	MOM	2	A	88
							B	81
2	3	Br	OMe	OTBDMS	MOM	2	A	88
							B	44
3	4	Br	OMe	OH	MOM	2	A	58
							B	46
4	5	Br	OMe	OAc	<i>i</i> -Pr	2	A	0 ^d
							B	0 ^e
5	6	Br	OMe	OAc	MEM	2	A	49
6	7	Br	H	OAc	MOM	16	A	trace ^d
							B	46
7	8	F	OMe	OAc	MOM	17	A	75
							B	66
8	9	OMe	OMe	OAc	MOM	18	A	84
							B	60
9	10	OMe	OMe	OTBDMS	MOM	18	A	56
10	11	OMe	H	OAc	MOM	19	A	46
							B	17
11	12	OMe	Br	OAc	MOM	20	A	91
							B	39
12	13	CO ₂ Me	OMe	OTBDMS	MOM	21	A	88
							B	23
13	14	H	OMe	OAc	MOM	22	A	0 ^d
							B	0 ^d
14	15	H	H	OAc	MOM	23	A	23 ^d
							B	48

^a Unless otherwise noted, all reactions were performed using 10 equiv of styrene.

^b Method A=PtCl₄ (10 mol %) in DCM; method B=PTS–Si (1.1 equiv) in toluene.

^c Isolated yields.

^d The reactions gave complex mixtures of unidentifiable products.

^e Starting material was not consumed.

In order to investigate the effects of the substituents, *o*-QM precursors **7–15** were synthesized⁸ for the cycloaddition reactions leading to the expected chromans **16–23**. In general, PtCl₄ can tolerate a range of substituent X on the aromatic ring with different electronic properties, such as halogens (F and Br), electron-donating group (EDG; OMe), and electron-withdrawing group (EWG; CO₂Me). In case of Y=H, the effects of substituent X on the reactions using PtCl₄ were evident for compounds **7**, **11**, and **15**. If the result of compound **15** (X=Y=H) was considered as a point of reference (23% yield; entry 14), a substrate bearing an EWG (**7**; X=Br; Y=H) gave only trace amounts of the corresponding product **16** and thus had a detrimental effect on the reaction yield (entry 6). Compound **11** (X=OMe; Y=H), on the other hand, with an EDG gave the product **19** in moderate 46% yield (entry 10). Such a trend was not observed for the reactions using PTS–Si as similar yields were obtained for compounds **7** and **15** (46–48%) while a much lower yield was observed for compound **11** (17% yield), suggesting that similar *o*-QMs may be generated by different mechanisms when PtCl₄ or PTS–Si was employed.

The position of an EDG on the aromatic ring appeared crucial for the successful generation of the corresponding *o*-QMs and the subsequent cycloaddition reactions. Compound **14** (X=H; Y=OMe) gave no desired product **22** regardless of whether PTS–Si or PtCl₄

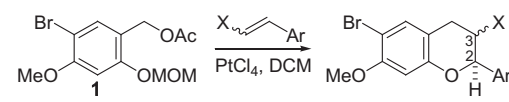
was employed. A mixture of products presumably arising from the displacement of acetate by styrene followed by partial polymerization of the resulting intermediate(s) with other styrene molecule(s) was obtained. In these cases, the presence of OMe *para* to the benzyl acetate rendered the system too reactive. Upon protonation (PTS–Si) or coordination (PtCl₄), the *p*-quinone methide (*p*-QM) might be formed as a result of the departure of acetate before the cleavage of the MOM group to generate the *o*-QM. Subsequently, styrene reacted with the *p*-QM to yield the carbocation-like intermediate, which underwent further reaction(s) with other styrene molecule(s).

When substituents X and Y are not hydrogen, the yields (75–91%) from the reactions using PtCl₄ were largely unaffected by the nature of these substituents (entries 1, 7, 8, 11, and 12). Switching of Br and OMe (**12**, entry 11) does not seem to affect the reactions; the corresponding chroman product **20** was furnished in high yield (91%). Interestingly, a good yield (84%) of the product **18** was obtained from **9**, which contain the methoxy groups as both substituents (entry 8). Replacing Br with F only gave a slightly lower yield of the product (entry 7). Even with a strong EWG in **13**, a good yield (88%) of the product **21** was obtained (entry 12). Thus, it appears that the effects of substituents X and Y should not be considered separately; both substituents may altogether modulate electron density in the aromatic ring for the generation of *o*-QMs as well as in the *o*-QM intermediates for their cycloaddition reactions.

In contrast to the reactions for substrates bearing no hydrogen as substituents X and Y using PtCl₄ as the catalyst, the reactions using PTS–Si gave lower yields of the corresponding products (23–81%). All the changes in substituents X and Y presumably changed the electron density in the aromatic ring. In addition, some side reactions presumably from O–Si cleavage also occurred when PTS–Si was used with compound **3**, resulting in a lower yield (44%; entry 2).

Due to the ease of preparation, the *o*-QM precursor **1** was used as the substrate for the subsequent studies. As summarized in Table 3, moderate to excellent yields (33–99%) and diastereoselectivity of the 2,3-disubstituted chromans **24–28** were obtained. The *trans* olefins gave the products as single diastereomers while the *cis* olefin provided the product as a 1:1⁹ mixture of diastereomers. Cinnamyl benzoate furnished **26** in 99% yield as a single diastereomer.^{10,11} In addition, even with an electron-withdrawing group (CO₂Et) in *trans*-ethyl cinnamate, **27** was obtained in moderate 33% yield;¹² a better yield (76%) of **28**, as a single diastereomer, was obtained with the (*p*-OMe)Ph *trans*-ethyl cinnamate.¹⁰ The CH₂OBz and CO₂Et groups in **26–28** at C3 allow further modifications on the 2-aryl chromans.

Table 3
Stereoselective PtCl₄-catalyzed cycloaddition reactions of *o*-QMs for 2,3-disubstituted chromans^a



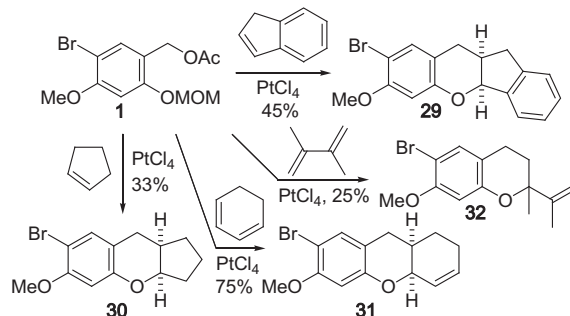
Entry	X	Ar	Olefin	Prod	Yield (%) ^b	dr (trans:cis)
1	<i>n</i> -Pr	Ph	<i>cis</i>	24a	78	1:1
2	<i>n</i> -Pr	Ph	<i>trans</i>	24b	72	>99:1
3	Me	Ph	<i>trans</i>	25	99	>99:1
4	CH ₂ OBz	Ph	<i>trans</i>	26	99	>99:1
5	CO ₂ Et	Ph	<i>trans</i>	27	33	>99:1
6 ^c	CO ₂ Et	Ph(OMe- <i>p</i>)	<i>trans</i>	28	76	>99:1

^a Unless otherwise noted, all reactions were performed using 10 mol % of PtCl₄ and 10 equiv of styrenes.

^b Isolated yields.

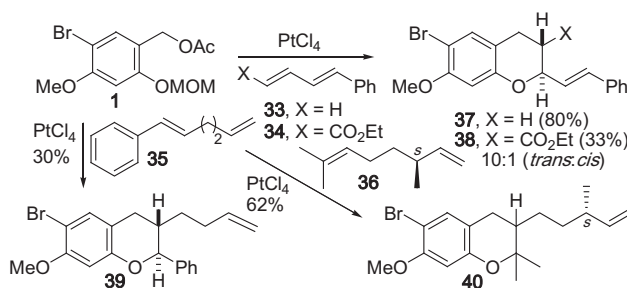
^c Cinnamate (2 equiv) was used.

As shown in Scheme 2, the ring-fused *cis*-styrene (indene) reacted to provide **29** in 45% yield as a single diastereomer.¹² Simple non-conjugated alkene, such as cyclopentene furnished the corresponding product **30** albeit in lower yield.¹³ The addition of *p*-TsOH on silica (PTS–Si) accelerated the reactions but gave only a slightly better yield of the product. Conjugated 1,3-cyclohexadiene gave a better yield of the corresponding product **31** in 75% as a single regioisomer and diastereomer. However, a non-cyclic conjugated 2,3-dimethyl-1,3-butadiene gave **32** only in 25% yield.



Scheme 2. PtCl₄-catalyzed generation and cycloaddition of *o*-QMs with other olefins.

To further investigate the effects of conjugation on the dienophile, dienes **33–36** were employed in the reactions (Scheme 3). Interestingly, both diene **33**⁸ and **34**,⁸ which contain a 1,3-diene system in conjugation with an aryl system, furnished the corresponding products **37** and **38** in 80% and 33% yields, respectively, as single regioisomers. The reactions occurred exclusively on the terminal olefin of the conjugated system. The presence of an EWG at the end of diene **34** had no effect on the regioselectivity of the reaction but dramatically affected the yield (33%) and diastereoselectivity (a 10:1 mixture of diastereomers favoring the C2–C3 *trans* relationship) of the resulting chroman **38**. When a non-conjugated diene **35**⁸ was employed, the product **39** arising solely from the reaction on the styrene moiety was obtained albeit in low yield (30%). Moreover, non-styrene non-conjugated diene **36** furnished the corresponding product **40** as a single isomer (dr>99:1) from the reaction occurring exclusively on the more substituted olefin in moderate 62% yield.¹⁴

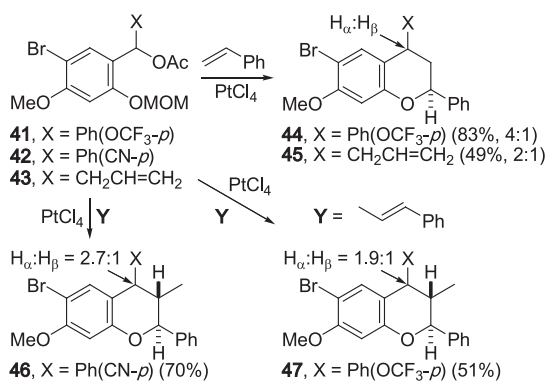


Scheme 3. PtCl₄-catalyzed generation and cycloaddition of *o*-QMs with other olefins.

The precursors **41–43**⁸ furnished the 2,4-disubstituted and 2,3,4-trisubstituted chroman systems **44–47** in moderate to good yields but only in moderate diastereoselectivity favoring the 2,4-*cis* relationship (Scheme 4). For comparison, **44** was previously synthesized from **41** in 51% yield as a single diastereomer.^{3a} Thus, the use of PtCl₄ for the 2,4-disubstituted chromans improved the yield but lowered the diastereoselectivity.

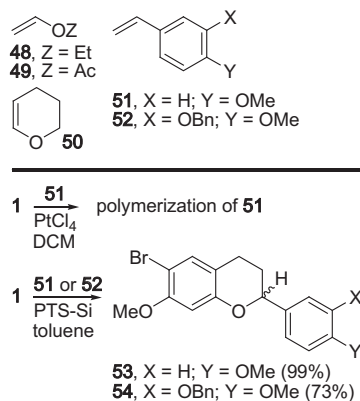
2.2. Scope and limitation of using PtCl₄ as catalyst

Even though the use of a catalytic amount of PtCl₄ in the generation of *o*-QMs and their cycloaddition reactions appears general,



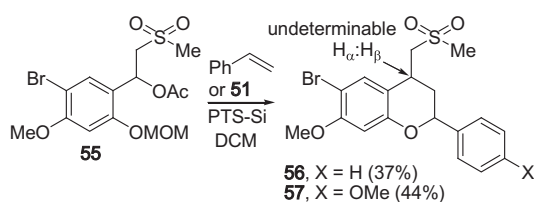
Scheme 4. 2,4-Disubstituted and 2,3,4-trisubstituted chromans from PtCl₄-catalyzed generation and cycloaddition of *o*-QMs with styrenes.

there are a few exceptions. Electron-rich dienophiles (**48–52**, Scheme 5), such as enol ethers and oxygenated aromatic systems did not furnish any chroman products. A ¹H NMR study suggested that *p*-methoxystyrene **51** underwent a facile PtCl₄-mediated polymerization under the reaction condition. It also appeared that polymerization occurred at a faster rate than the generation of the *o*-QM from the precursor. Reactions of precursor **1** with **48–50** using PTS–Si gave similar results. However, the use of PTS–Si, in case of the oxygenated aromatic systems **51** and **52**, gave the desired products **53** and **54**, respectively, in good to excellent yields (73%–99%).



Scheme 5. Electron-rich dienophiles **53–56** and cycloaddition reactions.

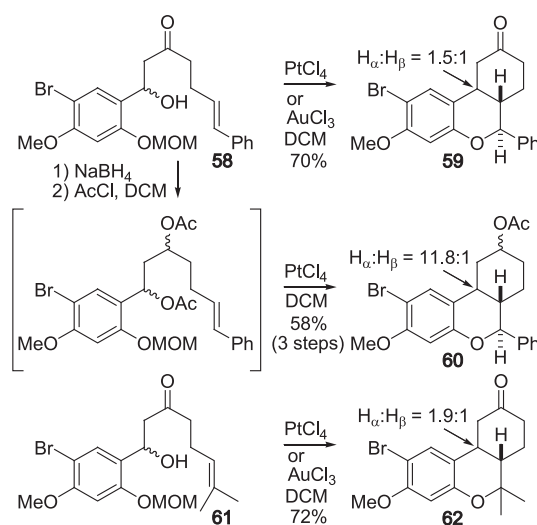
It should be noted also that the presence of sulfone appeared incompatible with PtCl₄. Generation of the *o*-QM from the precursor **55**⁸ containing sulfone and its cycloaddition reaction with styrene using PtCl₄ gave no desired product. However, when similar reactions were performed with styrene or **51** using PTS–Si, the corresponding chromans **56** and **57** were obtained in 37% and 44% yields, respectively (Scheme 6). The stereoselectivity at C2–C4 cannot be determined due to the complex and overlapping ¹H NMR signals.



Scheme 6. Reactions of precursor **55** containing sulfone with styrene derivatives.

2.3. Intramolecular [4+2]-cycloaddition reactions

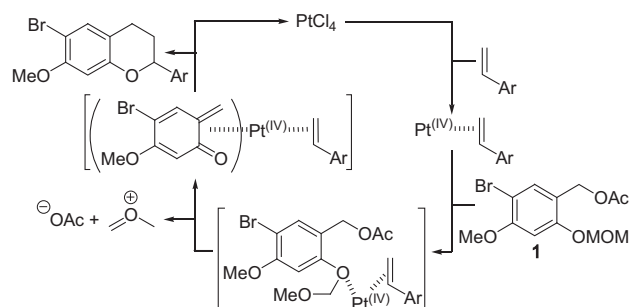
Both PtCl₄ and AuCl₃ effectively catalyzed the intramolecular cycloaddition reactions of the *o*-QM tethered with styrene or simple olefin (Scheme 7).¹⁵ The alcohol **58**^{3b} could be used directly in the reactions to furnish the corresponding tricyclic ketone **59** in one step and 70% yield (as a 1.5:1 mixture of diastereomers). Alternatively, conversion of the β-hydroxyketone to the corresponding bis-acetate intermediate, which upon generating the *o*-QM and the ensuing cycloaddition reaction, gave the chroman **60** in 58% yields over 3 steps (as an 11.8:1 mixture of diastereomers). Thus, the direct use of precursor **58** furnished the tricyclic system in better yield and in fewer chemical steps albeit in lower diastereoselectivity. A similar reaction with precursor **61** containing simple non-styrene olefin gave the corresponding chroman **62** in 72% yield as a 1.9:1 mixture of diastereomers. Thus, the 3,4-*trans* isomers are the major products from these intramolecular reactions.



Scheme 7. Intramolecular PtCl₄- or AuCl₃-catalyzed generation and cycloaddition reactions of *o*-QMs with tethered alkenes.

2.4. Mechanistic studies of the generation of *o*-QMs and [4+2]-cycloaddition reactions via PtCl₄

A plausible mechanism was proposed to involve first the coordination of Pt(IV) to the π-system of olefin (Scheme 8). This Pt(IV)-olefin complex then mediated the generation of *o*-QM from the precursor **1**. In these reactions, it appears that PtCl₄ also serves as a mild Lewis acid, which facilitates the ensuing cycloaddition reaction.¹⁶ The product chroman was produced in concomitant with the regeneration of the catalytic species, completing the catalytic cycle.



Scheme 8. A proposed catalytic cycle of the Pt(IV)-catalyzed generation of *o*-QM and cycloaddition reactions.

Some supporting evidence for this mechanism was as follows. Sequential addition of olefin to the reaction after premixing PtCl_4 with **1** was not successful, giving an unidentifiable mixture of products and signifying the first step of $\text{Pt(IV)}-\pi$ coordination. In addition, in the complete absence of styrene, a similar unidentifiable mixture of products was obtained, suggesting that the *o*-QM was formed from **1** in the presence of PtCl_4 alone.¹⁷ Thus, it is likely that the *o*-QM remains bound to Pt(IV) for the subsequent cycloaddition reaction.¹⁸ The bound state of Pt(IV) to the *o*-QM intermediate might account for the moderate diastereoselectivity for some substrates, presumably due to the steric demand and the positioning of the metal center.¹⁹ The role of PtCl_4 in the cleavage of the MOM group as Lewis acid was evident from the facile cleavage of the MOM ether of salicylaldehyde by PtCl_4 under similar reaction condition to provide salicylaldehyde in 92% yield. Interestingly, no reactions occurred when styrene and PtCl_4 were mixed with nucleophile (phenol) or electrophile (BnOH/BnOAc) or both,²⁰ implying that the reaction proceeded via the intermediacy of *o*-QM rather than a stepwise addition/substitution reaction mechanism.

In order to follow the reactions in more detail, ^1H NMR studies were performed. As shown in Figs. 1 and 2, the NMR studies of the reactions both in the absence and in the presence of styrene with **1** using PtCl_4 as catalyst were conducted. In the absence of styrene, it is evident that the signals of protons belonging to the MOM (singlets at δ 3.45 and 5.19) and the acetate (a singlet at δ 2.03) groups in the precursor **1** slowly disappeared and the new sets of signals could be observed. In particular, the observation of a sharp singlet at δ 9.67 and a broad one at δ 8.25 was remarkable because the increment of these peaks at the beginning of the reaction corresponded with the diminishing height of the sets of peaks of the

MOM and acetate groups. In addition, these peaks started to disappear after $t=30$ min, implying that the nature of the intermediate giving rise to these signals is only transient. Together with the observation that the new sets of signals around δ 2.01–2.15 were likely to correspond to the acetate group(s), these singlets at δ 8.25 and 9.67 were tentatively assigned to an intermediate either (1) resulting from the PtCl_4 -mediated cleavage of the MOM group or (2) possessing a highly unshielded quinone methide-type moiety. Thus, a PtCl_4 -catalyzed cleavage of the MOM group of the MOM ether-containing benzaldehyde (similar structure to compound **1** with the aldehyde moiety in place of the benzyl acetate) was carried out to clarify whether the PtCl_4 -catalyzed MOM cleavage process alone without the possibility of generating any *o*-QM intermediate could generate some species with a signal at δ 9.67 (See Supplementary data for the overlay of the spectra). The cleavage of the MOM group alone by PtCl_4 did not generate any singlets at δ 8.25 or 9.67. However, some similar peaks were observed between the two reactions, especially those new sets of signals around δ 3.30–5.30, suggesting a similar course of reaction for the MOM cleavage. Thus, it is reasonable to postulate that the singlets at 8.25 and 9.67 may come from the Pt(IV) -stabilized *o*-QM intermediate.

In the presence of styrene, to our delight, a similar reaction course occurred. The singlets at δ 8.25 and 9.67 were still observed, suggesting the formation of the Pt(IV) -stabilized *o*-QM intermediate. In addition, the presence of styrene made the overall reaction proceed at a faster rate. Such observation was in good accordance with the role of styrene as dienophile trapping the *o*-QM, thus driving the reaction to completion faster. Taken together, the mechanisms of the reactions both in the absence and in the presence of styrene proceeded via the intermediacy of *o*-QM.

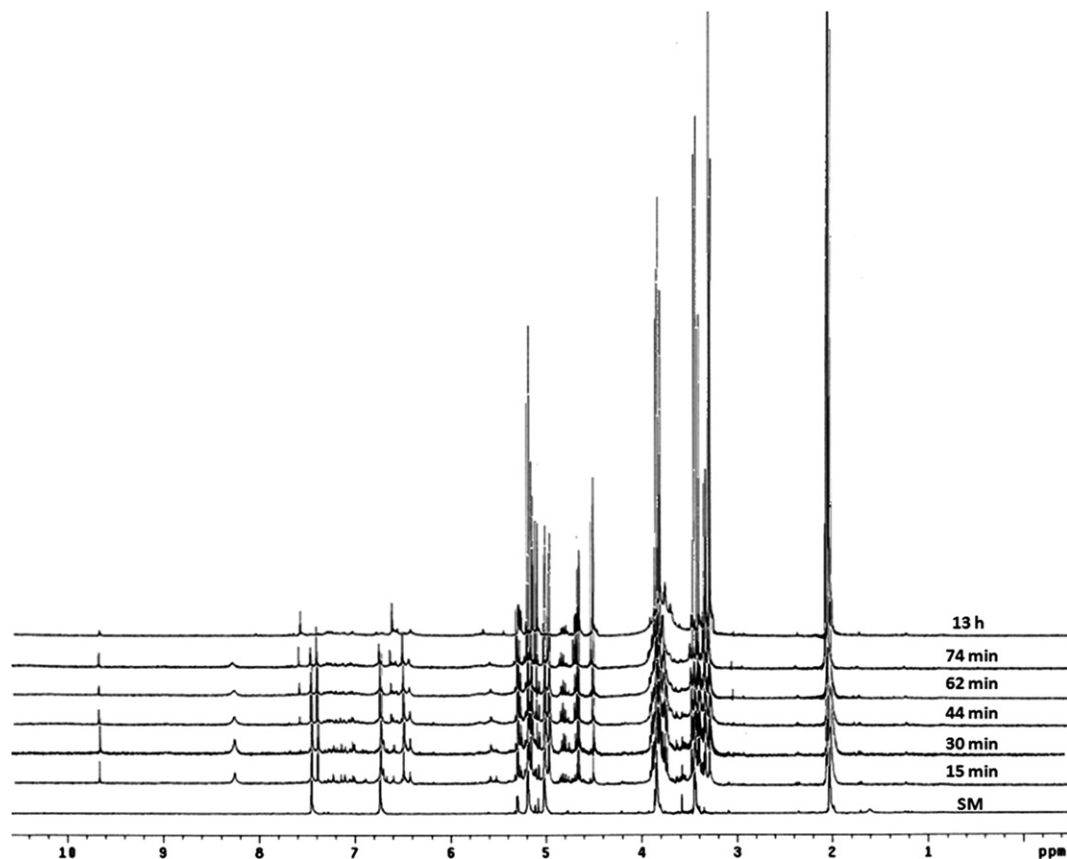


Fig. 1. ^1H NMR study of the reaction between the precursor **1** and PtCl_4 in the absence of styrene in CD_2Cl_2 .

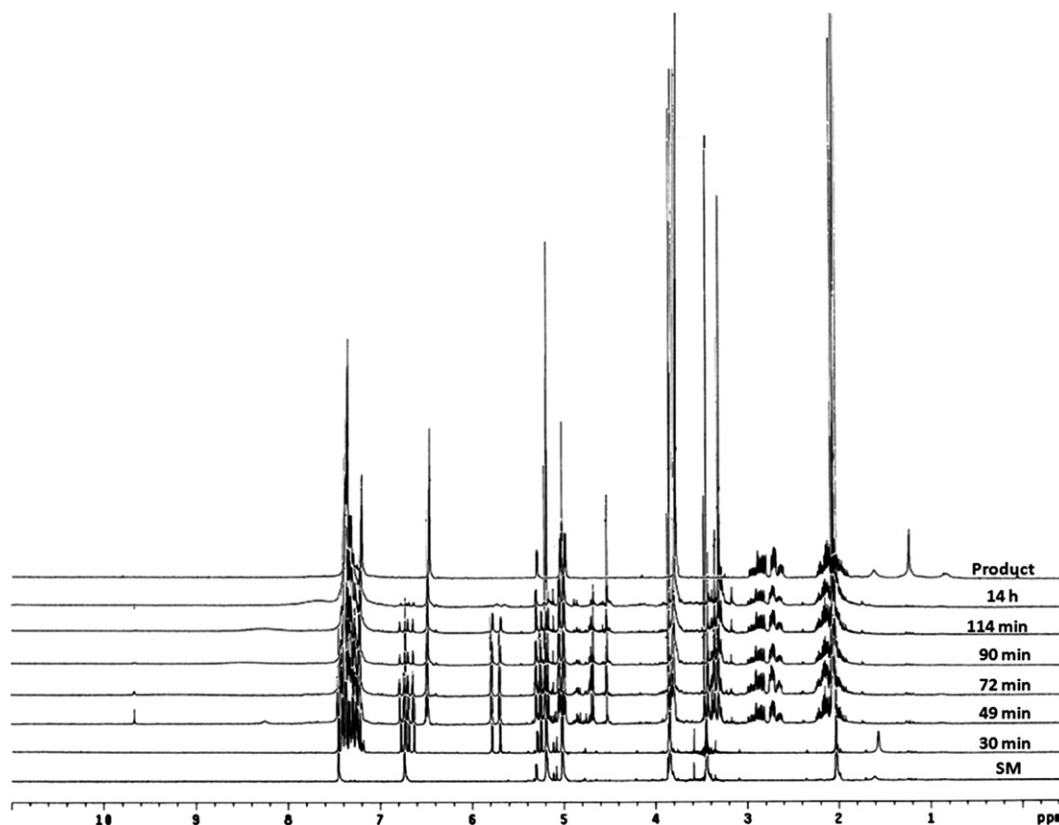


Fig. 2. ^1H NMR study of the reaction between the precursor **1** and PtCl_4 in the presence of styrene in CD_2Cl_2 .

3. Conclusion

In summary, the mild and facile generation of *o*-QMs under the catalysis of PtCl_4 and their formal [4+2]-cycloaddition reactions with styrenes and other activated olefins have been successfully developed. The reactions furnished the 2-alkyl or 2-aryl chromans in moderate to excellent yields and moderate to excellent diastereoselectivity. When compared with our previously reported method using PTS–Si, this novel Pt(IV)-catalyzed process provided some significant advantages of wider range of the substituents on the aromatic ring of the *o*-QM precursors including better functional group compatibility. In addition, most dienophiles, with a few exceptions, gave the products in higher yields when PtCl_4 was employed. However, it should be noted that use of PtCl_4 led to somewhat lower diastereoselectivity at C2–C4. For the intramolecular reactions, the conversion of benzyl alcohol to the corresponding benzyl acetate was not necessary when using PtCl_4 , thus resulting in fewer chemical steps in the synthesis of the desired chroman systems. The intermediacy of *o*-QM in the reactions under the PtCl_4 catalysis was also proposed and the Pt(IV)-stabilized *o*-QM involved in the reactions was detected spectroscopically.

4. Experimental section

4.1. General procedure for the hetero-Diels–Alder reactions of 2-arylchroman products

To a stirred solution of *o*-QM precursors (1.0 equiv) in CH_2Cl_2 (10 mL/mmol of benzyl acetates) were added styrene derivatives (2.0–10.0 equiv) at room temperature. The resulting mixture was stirred at 0°C for 10 min, and then Lewis acids, transition metal salts or complexes (stoichiometric 100 mol %; substoichiometric 30–50 mol %, and catalytic 10–30 mol %) were added. The reaction mixture was stirred until all *o*-QM precursors were consumed as

indicated by TLC (4–6 h). At that time, the reaction mixture was concentrated under reduced pressure to give a crude product mixture, which was further purified by preparative TLC (10–30% EtOAc/hexanes) to furnish the desired products.

4.1.1. 6-Bromo-7-methoxy-2-phenylchroman (2). Following the general procedure and purification by PTLC (30% EtOAc/hexanes), the product was obtained as colorless oil (0.018 g, 0.058 mmol, 88%, using PtCl_4 ; 0.016 g, 0.053 mmol, 81%, using PTS–Si). R_f (30% EtOAc/hexanes) 0.72. ^1H NMR (200 MHz, CDCl_3): δ 1.97–2.28 (m, 2H), 2.66–2.79 (m, 1H), 2.84–3.01 (m, 1H), 3.85 (s, 3H), 5.05 (dd, $J=9.4$, 3.0 Hz, 1H), 6.52 (s, 1H), 7.26 (s, 1H), 7.35–7.44 (m, 5H). ^{13}C NMR (50 MHz, CDCl_3): δ 24.1, 29.6, 56.2, 78.0, 101.1, 101.8, 115.2, 125.9, 128.0, 128.6, 133.0, 141.1, 154.8, 155.1. TOF-HRMS calcd for $\text{C}_{16}\text{H}_{16}\text{BrO}_2$ ($M+H^+$) 319.0328, found 319.0327. These spectroscopic data were identical to those reported previously.^{3a}

4.1.2. 6-Bromo-2-phenylchroman (16). Following the general procedure and purification by PTLC (30% EtOAc/hexanes), the product was obtained as colorless oil (trace, using PtCl_4 ; 0.010 g, 0.035 mmol, 46%, using PTS–Si). R_f (30% EtOAc/hexanes) 0.55. ^1H NMR (200 MHz, CDCl_3): δ 1.94–2.24 (m, 2H), 2.67–2.80 (m, 1H), 2.86–3.03 (m, 1H), 5.02 (dd, $J=9.6$, 2.8 Hz, 1H), 6.78 (d, $J=9.6$ Hz, 1H), 7.20 (m, 2H), 7.27–7.38 (m, 5H). ^{13}C NMR (50 MHz, CDCl_3): δ 24.8, 29.4, 77.8, 112.3, 118.7, 124.0, 125.9, 127.9, 128.5, 130.1, 131.9, 141.1, 154.2. TOF-HRMS calcd for $\text{C}_{15}\text{H}_{12}\text{BrO}$ ($M-H^+$) 287.0063, found 287.0077. These spectroscopic data were identical to those reported previously.^{3a}

4.1.3. 6-Fluoro-7-methoxy-2-phenylchroman (17). Following the general procedure and purification by PTLC (30% EtOAc/hexanes), the product was obtained as colorless oil (0.013 g, 0.048 mmol, 75%, using PtCl_4 ; 0.012 g, 0.046 mmol, 66%, using PTS–Si). R_f (30% EtOAc/hexanes) 0.58. IR (neat): ν_{max} 2928, 1631, 1515, 1446, 1274, 1216, 1195,

1162, 1118 cm^{-1} . ^1H NMR (200 MHz, CDCl_3): δ 1.95–2.23 (m, 1H), 2.62–3.00 (m, 1H), 3.82 (s, 3H), 5.00 (dd, $J=9.8$, 2.8 Hz, 1H), 6.53 (d, $J=7.6$ Hz, 1H), 6.80 (d, $J=11.4$ Hz, 1H), 7.28–7.44 (m, 5H). ^{13}C NMR (50 MHz, CDCl_3): δ 24.4, 29.7, 56.2, 77.9, 102.2, 112.9 (d, $J_{\text{C-F}}=3.2$ Hz), 115.7 (d, $J_{\text{C-F}}=19.2$ Hz), 126.0, 127.9, 128.5, 141, 146.5 (d, $J_{\text{C-F}}=12.8$ Hz), 146.8 (d, $J_{\text{C-F}}=235.9$ Hz), 150.9. LRMS (EI) m/z (rel intensity) 259 ($\text{M}+\text{H}^+$, 17), 258 (M^+ , 100), 227 (20), 167 (30), 154 (28), 104 (73), 91 (33). TOF-HRMS calcd for $\text{C}_{16}\text{H}_{15}\text{FO}_2$ (M^+) 258.1051, found 258.1055.

4.1.4. 6,7-Dimethoxy-2-phenylchroman (18). Following the general procedure and purification by PTLC (30% EtOAc/hexanes), the product was obtained as yellowish oil (0.014 g, 0.052 mmol, 84%, using PtCl_4 ; 0.012 g, 0.045 mmol, 60%, using PTS–Si). R_f (30% EtOAc/hexanes) 0.61. IR (neat): ν_{max} 2929, 2849, 1736, 1619, 1511, 1450, 1413, 1261, 1224, 1193, 1170, 1125, 1018 cm^{-1} . ^1H NMR (200 MHz, CDCl_3): δ 1.98–2.25 (m, 2H), 2.65–3.03 (m, 2H), 3.83 (s, 3H), 3.84 (s, 3H), 4.99 (dd, $J=9.5$, 2.9 Hz, 1H), 6.51 (s, 1H), 6.59 (s, 1H), 7.32–7.45 (m, 5H). ^{13}C NMR (50 MHz, CDCl_3): δ 24.7, 30.1, 55.9, 56.5, 77.8, 101.1, 112.2, 126.0, 127.8, 128.3, 128.5, 141.7, 143.1, 148.3, 148.9. LRMS (EI) m/z (rel intensity) 270 (M^+ , 100), 239 (13), 166 (40), 138 (16), 91 (11). TOF-HRMS calcd for $\text{C}_{17}\text{H}_{19}\text{O}_3$ ($\text{M}+\text{H}^+$) 271.1329, found 271.1325.

4.1.5. 6-Methoxy-2-phenylchroman (19). Following the general procedure and purification by PTLC (30% EtOAc/hexanes), the product was obtained as colorless oil (0.011 g, 0.047 mmol, 46%, using PtCl_4 ; 0.003 g, 0.014 mmol, 17%, using PTS–Si). R_f (30% EtOAc/hexanes) 0.57. IR (neat): ν_{max} 3338, 2927, 2851, 1612, 1494, 1431, 1268, 1220, 1149, 1067, 1048, 1035, 1000 cm^{-1} . ^1H NMR (200 MHz, CDCl_3): δ 1.97–2.25 (m, 2H), 2.71–3.09 (m, 2H), 3.77 (s, 3H), 5.01 (dd, $J=9.6$, 3.0 Hz, 1H), 6.64 (d, $J=3.0$ Hz, 1H), 6.71 (dd, $J=8.8$, 3.0 Hz, 1H), 6.85 (d, $J=8.8$ Hz, 1H), 7.29–7.45 (m, 5H). ^{13}C NMR (50 MHz, CDCl_3): δ 25.5, 30.0, 55.8, 77.6 (superimposed with CDCl_3), 113.4, 114.0, 117.5, 122.3, 126.0, 127.7, 128.5, 141.8, 153.2, 153.3. LRMS (EI) m/z (rel intensity) 240 (M^+ , 100), 149 (41), 136 (89), 108 (31), 91 (25). TOF-HRMS calcd for $\text{C}_{16}\text{H}_{17}\text{O}_2$ ($\text{M}+\text{H}^+$) 241.1223, found 241.1218.

4.1.6. 7-Bromo-6-methoxy-2-phenylchroman (20). Following the general procedure and purification by PTLC (30% EtOAc/hexanes), the product was obtained as colorless oil (0.017 g, 0.052 mmol, 91%, using PtCl_4 ; 0.008 g, 0.024 mmol, 39%, using PTS–Si). R_f (30% EtOAc/hexanes) 0.51. IR (neat): ν_{max} 3027, 2927, 2847, 1603, 1490, 1401, 1312, 1194, 1046, 1006 cm^{-1} . ^1H NMR (200 MHz, CDCl_3): δ 1.96–2.27 (m, 1H), 2.67–3.05 (m, 1H), 3.83 (s, 3H), 5.01 (dd, $J=9.8$, 2.8 Hz, 1H), 6.62 (s, 1H), 7.14 (s, 1H), 7.31–7.41 (m, 5H). ^{13}C NMR (50 MHz, CDCl_3): δ 25.2, 29.6, 56.9, 77.6, 109.6, 112.7, 121.5, 127.6, 127.9, 128.3, 128.5, 141.3, 149.4, 149.8. LRMS (EI) m/z (rel intensity) 320 (M^++2 , 87), 318 (M^+ , 88), 216 (66), 214 (70), 178 (49), 148 (58), 104 (48), 91 (97), 81 (53), 77 (57), 69 (100). TOF-HRMS calcd for $\text{C}_{16}\text{H}_{15}\text{BrO}_2$ (M^+) 318.0250, found 318.0235.

4.1.7. Methyl 7-methoxy-2-phenylchroman-6-carboxylate (21). Following the general procedure and purification by PTLC (30% EtOAc/hexanes), the product was obtained as colorless oil (0.012 g, 0.042 mmol, 88%, using PtCl_4 ; 0.006 g, 0.020 mmol, 23%, using PTS–Si). R_f (30% EtOAc/hexanes) 0.38. IR (neat): ν_{max} 2923, 2853, 1722, 1697, 1619, 1573, 1495, 1434, 1280, 1260, 1193, 1144, 1079 cm^{-1} . ^1H NMR (200 MHz, CDCl_3): δ 1.98–2.30 (m, 2H), 2.68–3.01 (m, 2H), 3.855 (s, 3H), 3.862 (s, 3H), 5.10 (dd, $J=9.9$, 2.5 Hz, 1H), 6.51 (s, 1H), 7.33–7.42 (m, 5H), 7.68 (s, 1H). ^{13}C NMR (50 MHz, CDCl_3): δ 24.0, 29.7, 51.7, 56.0, 78.4, 100.5, 111.8, 113.4, 125.9, 128.0, 128.5, 133.6, 140.8, 159.5, 166.2. LRMS (EI) m/z (rel intensity) 299 ($\text{M}+\text{H}^+$, 19), 298 (M^+ , 93), 239 (89), 179 (43), 178 (61), 149 (52), 104 (51), 91 (52), 71 (68), 57 (100). TOF-HRMS calcd for $\text{C}_{18}\text{H}_{19}\text{O}_4$ ($\text{M}+\text{H}^+$) 299.1278, found 299.1282.

4.1.8. 2-Phenylchroman (23). Following the general procedure and purification by PTLC (30% EtOAc/hexanes), the product was obtained as colorless oil (0.005 g, 0.021 mmol, 23%, using PtCl_4 ;

0.009 g, 0.044 mmol, 48%, using PTS–Si). R_f (30% EtOAc/hexanes) 0.66. ^1H NMR (200 MHz, CDCl_3): δ 2.01–2.32 (m, 2H), 2.75–2.89 (m, 1H), 2.95–3.12 (m, 1H), 5.09 (dd, $J=9.4$, 3.0 Hz, 1H), 6.87–6.96 (m, 2H), 7.10–7.21 (m, 2H), 7.34–7.48 (m, 5H). ^{13}C NMR (50 MHz, CDCl_3): δ 25.1, 29.9, 77.7, 116.9, 120.3, 121.8, 126.0, 127.3, 127.8, 128.5, 129.5, 141.7, 155.1. TOF-HRMS calcd for $\text{C}_{15}\text{H}_{15}\text{O}$ ($\text{M}+\text{H}^+$) 211.1117, found 211.1114. These spectroscopic data were identical to those reported previously.^{3a}

4.1.9. 1:1 Mixture of cis- and trans-6-bromo-7-methoxy-2-phenyl-3-propylchroman (24a). Following the general procedure and purification by PTLC (30% EtOAc/hexanes), the product was obtained as a 1:1 mixture of 2,3-cis and 2,3-trans diastereomers as colorless oil (0.018 g, 0.048 mmol, 78%). R_f (30% EtOAc/hexanes) 0.68. IR (neat): ν_{max} 2957, 2929, 2871, 1610, 1575, 1496, 1443, 1430, 1311, 1282, 1200, 1155, 1058 cm^{-1} . ^1H NMR (400 MHz, CDCl_3): δ 0.77 (t, $J=7.04$ Hz, 3H, trans), 0.81 (t, $J=7.13$ Hz, 3H, cis), 1.01–1.45 (m, 4H), 2.04–2.13 (m, 1H, trans), 2.16–2.22 (m, 1H, cis), 2.48 (dd, $J=16.1$, 9.9 Hz, 1H, trans), 2.61 (dd, $J=16.1$, 4.4 Hz, 1H, cis), 2.81 (dd, $J=16.2$, 5.0 Hz, 1H, trans), 2.97 (dd, $J=16.1$, 5.4 Hz, 1H, cis), 3.81 (s, 3H, trans), 3.85 (s, 3H, cis), 4.71 (d, $J=8.6$ Hz, 1H, trans), 5.22 (d, $J=2.6$ Hz, 1H, cis), 6.47 (s, 1H, trans), 6.52 (s, 1H, cis), 7.23 (s, 1H, trans), 7.24 (s, 1H, cis), 7.28–7.41 (m, 5H). ^{13}C NMR (100 MHz, CDCl_3): δ 14.0, 19.5 (trans), 20.5 (cis), 28.2 (cis), 28.4 (cis), 29.4 (trans), 33.8 (trans), 36.5 (cis), 37.1 (trans), 56.2, 80.2 (cis), 83.2 (trans), 100.7 (trans), 100.8 (cis), 101.8 (cis), 101.9 (trans), 114.5 (cis), 115.2 (trans), 125.9 (cis), 127.0 (trans), 127.3 (cis), 128.1 (cis), 128.2 (trans), 128.5 (trans), 133.0 (trans), 133.5 (cis), 139.6 (cis), 140.0 (trans), 154.8, 154.9. LRMS (EI) m/z (rel intensity) 362 (M^++2 , 43), 360 (M^+ , 44), 271 (60), 269 (63), 190 (100), 117 (97), 115 (40), 104 (38), 91 (42). TOF-HRMS calcd for $\text{C}_{19}\text{H}_{22}\text{BrO}_2$ ($\text{M}+\text{H}^+$) 361.0798, found 361.0798.

4.1.10. trans-6-Bromo-7-methoxy-2-phenyl-3-propylchroman (24b). Following the general procedure and purification by PTLC (30% EtOAc/hexanes), the product was obtained as colorless oil (0.016 g, 0.044 mmol, 72%). R_f (30% EtOAc/hexanes) 0.63. ^1H NMR (400 MHz, CDCl_3): δ 0.81 (t, $J=3.61$ Hz, 3H), 1.01–1.45 (m, 4H), 2.01–2.13 (m, 1H), 2.48 (d, $J=16.1$, 9.9 Hz, 1H), 2.81 (d, $J=16.2$, 5.1 Hz, 1H), 3.82 (s, 3H), 4.71 (d, $J=8.6$ Hz, 1H), 6.47 (s, 1H), 7.23 (s, 1H), 7.33–7.41 (m, 5H). ^{13}C NMR (100 MHz, CDCl_3): δ 14.0, 19.5, 29.4, 33.8, 37.1, 56.2, 83.2, 100.7, 101.8, 115.3, 127.0, 128.2, 128.6, 133.1, 140.1, 154.8, 154.9. TOF-HRMS calcd for $\text{C}_{19}\text{H}_{22}\text{BrO}_2$ ($\text{M}+\text{H}^+$) 361.0798, found 361.0812. These spectroscopic data were identical to those reported previously.^{3a}

4.1.11. trans-6-Bromo-7-methoxy-3-methyl-2-phenylchroman (25). Following the general procedure and purification by PTLC (30% EtOAc/hexanes), the product was obtained as colorless oil (0.020 g, 0.061 mmol, 99%). R_f (30% EtOAc/hexanes) 0.68. IR (neat): ν_{max} 2925, 1611, 1575, 1496, 1443, 1404, 1310, 1281, 1201, 1156, 1051, 1019 cm^{-1} . ^1H NMR (400 MHz, CDCl_3): δ 0.83 (d, $J=6.8$ Hz, 3H), 2.11–2.23 (m, 1H), 2.54 (dd, $J=16.1$, 10.8 Hz, 1H), 2.77 (dd, $J=16.2$, 5.1 Hz, 1H), 3.81 (s, 3H), 4.58 (d, $J=9.3$ Hz, 1H), 6.47 (s, 1H), 7.22 (s, 1H), 7.33–7.41 (m, 5H). ^{13}C NMR (100 MHz, CDCl_3): δ 17.7, 32.6, 32.8, 56.2, 84.4, 100.8, 101.8, 115.4, 127.1, 128.3, 128.5, 132.8, 139.7, 154.8, 155.0. LRMS (EI) m/z (rel intensity) 334 (M^++2 , 37), 332 (M^+ , 38), 162 (33), 118 (42), 117 (100), 115 (34), 91 (73). TOF-HRMS calcd for $\text{C}_{17}\text{H}_{18}\text{BrO}_2$ ($\text{M}+\text{H}^+$) 333.0485, found 333.0475.

4.1.12. trans-(6-Bromo-7-methoxy-2-phenylchroman-3-yl)methyl benzoate (26). Following the general procedure and purification by PTLC (15% EtOAc/hexanes), the product was obtained as colorless oil (0.029 g, 0.063 mmol, 99%). R_f (15% EtOAc/hexanes) 0.34. IR (neat): ν_{max} 2920, 2853, 1718, 1495, 1268, 1109 cm^{-1} . ^1H NMR (200 MHz, CDCl_3): δ 2.75–2.55 (m, 1H), 2.88 (d, $J=7.8$ Hz, 2H), 3.83 (s, 3H), 4.07 (dd, $J=11.4$, 6.0 Hz, 1H), 4.28 (dd, $J=11.3$, 4.7 Hz, 1H),

5.04 (d, $J=8.4$ Hz, 1H), 6.52 (s, 1H), 7.63–7.25 (m, 9H), 8.00–7.92 (m, 2H). ^{13}C NMR (50 MHz, CDCl_3): δ 26.9, 37.7, 56.3, 65.0, 79.9, 100.9, 102.4, 114.2, 126.0, 126.3, 126.4, 126.7, 127.2, 128.4, 128.6, 128.8, 129.5, 129.7, 133.1, 138.9, 154.5, 155.1, 166.2. LRMS (EI) m/z (rel intensity) 454 ($\text{M}^+ + 2$, 15), 452 (M^+ , 13), 332 (30), 330 (24), 251 (21), 115 (26), 105 (90), 91 (22), 77 (100), 51 (43). TOF-HRMS calcd for $\text{C}_{24}\text{H}_{22}\text{BrO}_4$ ($\text{M} + \text{H}^+$) 453.0696, found 453.0706.

4.1.13. trans-Ethyl 6-bromo-7-methoxy-2-phenylchroman-3-carboxylate (27). Following the general procedure and purification by PTLC (15% EtOAc/hexanes), the product was obtained as colorless oil (0.010 g, 0.024 mmol, 33%). R_f (15% EtOAc/hexanes) 0.32. IR (neat): ν_{max} 2925, 1728, 1612, 1442, 1151, 1024 cm^{-1} . ^1H NMR (200 MHz, CDCl_3): δ 0.96 (t, $J=7.2$ Hz, 3H), 3.25–2.83 (m, 3H), 3.82 (s, 3H), 3.94 (q, $J=7.2$ Hz, 2H), 5.07 (d, $J=8.4$ Hz, 1H), 7.27 (s, 1H), 7.40–7.35 (m, 6H). ^{13}C NMR (50 MHz, CDCl_3): δ 13.8, 27.7, 29.7, 45.5, 56.2, 60.8, 79.3, 101.0, 102.7, 113.5, 127.0, 128.5, 128.7, 132.8, 138.3, 154.3, 155.1, 172.1. LRMS (EI) m/z (rel intensity) 392 ($\text{M}^+ + 2$, 99), 390 (M^+ , 100), 346 (81), 344 (84), 265 (96), 238 (60), 237 (56), 131 (55), 91 (93), 77 (66). TOF-HRMS calcd for $\text{C}_{19}\text{H}_{20}\text{BrO}_4$ ($\text{M} + \text{H}^+$) 391.0539, found 391.0532.

4.1.14. trans-Ethyl 6-bromo-7-methoxy-2-(4-methoxyphenyl)chroman-3-carboxylate (28). Following the general procedure and purification PTLC (15% EtOAc/hexanes), the desired product was obtained as colorless oil (0.020 g, 0.048 mmol, 76%). R_f (15% EtOAc/hexanes) 0.21. IR (neat): ν_{max} 2933, 1721, 1612, 1574, 1515, 1447, 1372, 1243, 1201, 1186, 1153, 1032. ^1H NMR (400 MHz, CDCl_3): δ 0.99 (t, $J=7.1$ Hz, 3H), 2.92 (dd, $J=15.6$, 4.9 Hz, 1H), 3.02 (ddd, $J=10.9$, 9.3, 4.9 Hz, 1H), 3.19 (dd, $J=15.5$, 11.0 Hz, 1H), 3.81 (s, 6H), 3.947 (q, $J=7.1$ Hz, 1H), 3.953 (q, $J=7.1$ Hz, 1H), 5.00 (d, $J=9.3$ Hz, 1H), 6.48 (s, 1H), 6.90 (AA'BB', $J=8.7$ Hz, 2H), 7.26 (s, 1H), 7.32 (AA'BB', $J=8.7$ Hz, 2H). ^{13}C NMR (100 MHz, CDCl_3): δ 13.9, 28.0, 45.4, 55.3, 56.2, 60.7, 79.0, 101.0, 102.5, 113.5, 113.9, 128.4, 130.3, 132.8, 154.5, 155.1, 159.9, 172.2. LRMS (EI) m/z (rel intensity) 422 ($\text{M}^+ + 2$, 76), 421 ($\text{M} + \text{H}^+$, 18), 420 (M^+ , 77), 376 (97), 374 (100), 295 (46), 269 (42), 267 (60), 206 (35), 161 (83), 134 (92), 121 (52). TOF-HRMS calcd for $\text{C}_{20}\text{H}_{21}\text{BrO}_5$ (M^+) 420.0572, found 420.0575.

4.1.15. 8-Bromo-7-methoxy-4b,10,10a,11-tetrahydroindeno[1,2-b]chromene (29). Following the general procedure and purification by PTLC (15% EtOAc/hexanes), the desired compound was obtained as colorless oil (0.008 g, 0.024 mmol, 45%). R_f (15% EtOAc/hexanes) 0.51. ^1H NMR (200 MHz, CDCl_3): δ 2.46–2.58 (m, 1H), 2.73–3.13 (m, 4H), 3.79 (s, 3H), 5.48 (d, $J=5.8$ Hz, 1H), 6.45 (s, 1H), 7.19 (s, 1H), 7.23–7.30 (m, 3H), 7.48–7.52 (m, 1H). ^{13}C NMR (50 MHz, CDCl_3): δ 26.7, 36.6, 37.5, 56.1, 81.5, 101.5, 101.7, 116.0, 125.1, 125.2, 126.9, 128.9, 132.5, 142.2, 142.6, 154.7, 155.2. TOF-HRMS calcd for $\text{C}_{17}\text{H}_{16}\text{BrO}_2$ ($\text{M} + \text{H}^+$) 331.0328, found 331.0325. These spectroscopic data were identical to those reported previously.^{3a}

4.1.16. 7-Bromo-6-methoxy-1,2,3,3a,9,9a-hexahydrocyclopenta[b]chromene (30). Following the general procedure and purification by PTLC (15% EtOAc/hexanes), the desired compound was obtained as colorless oil (0.008 g, 0.027 mmol, 33%). R_f (15% EtOAc/hexanes) 0.71. IR (neat): ν_{max} 2941, 1496, 1445, 1200, 1160, 1053 cm^{-1} . ^1H NMR (400 MHz, CDCl_3): δ 1.46–1.35 (m, 2H), 2.00–1.64 (m, 4H), 2.31–2.22 (m, 1H), 2.55 (dd, $J=8.2$, 1.4 Hz, 1H), 2.94 (dd, $J=8.4$, 3.2 Hz, 1H), 3.82 (s, 3H), 4.36 (dt, $J=2.8$, 1.0 Hz, 1H), 6.39 (s, 1H), 7.18 (s, 1H). ^{13}C NMR (100 MHz, CDCl_3): δ 21.8, 25.5, 28.1, 32.9, 37.5, 56.1, 79.6, 101.1, 101.6, 114.3, 133.2, 154.4, 154.6. LRMS (EI) m/z (rel intensity) 284 ($\text{M}^+ + 2$, 100), 282 (M^+ , 99), 217 (36), 215 (33), 203 (17). TOF-HRMS calcd for $\text{C}_{13}\text{H}_{15}\text{BrO}_2$ (M^+) 282.0250, found 282.0244.

4.1.17. 7-Bromo-6-methoxy-2,4a,9,9a-tetrahydro-1H-xanthene (31). Following the general procedure and purification by PTLC

(30% EtOAc/hexanes), the product was obtained as colorless oil (0.011 g, 0.037 mmol, 75%). R_f (30% EtOAc/hexanes) 0.63. IR (neat): ν_{max} 2924, 2853, 1677, 1610, 1576, 1496, 1443, 1476, 1198, 1160, 1051 cm^{-1} . ^1H NMR (200 MHz, CDCl_3): δ 1.53–1.59 (m, 1H), 1.63–1.73 (m, 1H), 2.09–2.26 (m, 4H), 2.50 (dd, $J=16.4$, 3.5 Hz, 1H), 2.96 (dd, $J=16.4$, 6.6 Hz, 1H), 3.81 (s, 3H), 4.48 (t, $J=3.6$ Hz, 1H), 5.92–5.96 (m, 1H), 6.01 (td, $J=10.0$, 3.4 Hz, 1H), 6.41 (s, 1H), 7.18 (s, 1H). ^{13}C NMR (50 MHz, CDCl_3): δ 23.0, 25.0, 28.7, 30.4, 56.1, 70.6, 100.8, 101.6, 113.9, 125.8, 132.9, 133.1, 1153.5, 1154.7. LRMS (EI) m/z (rel intensity) 296 ($\text{M}^+ + 2$, 47), 294 (M^+ , 48), 217 (91), 215 (98), 97 (38), 92 (49), 91 (36), 83 (40), 80 (70), 79 (100). TOF-HRMS calcd for $\text{C}_{14}\text{H}_{16}\text{BrO}_2$ ($\text{M} + \text{H}^+$) 295.0328, found 295.0324.

4.1.18. 6-Bromo-7-methoxy-2-methyl-2-(prop-1-en-2-yl)chroman (32). Following the general procedure and purification by PTLC (30% EtOAc/hexanes), the product was obtained as colorless oil (0.005 g, 0.016 mmol, 25%). R_f (30% EtOAc/hexanes) 0.61. IR (neat): ν_{max} 2924, 2851, 1610, 1574, 1496, 1443, 1200, 1149, 1090, 1051 cm^{-1} . ^1H NMR (200 MHz, CDCl_3): δ 1.46 (s, 3H), 1.77 (s, 3H), 1.68–1.83 (m, 1H), 2.11 (dt, $J=13.6$, 4.9 Hz, 1H), 2.56 (dd, $J=4.8$, 8.0 Hz, 2H), 3.84 (s, 3H), 4.85 (s, 1H), 4.90 (s, 1H), 6.44 (s, 1H), 7.15 (s, 1H). ^{13}C NMR (50 MHz, CDCl_3): δ 35.3, 37.4, 41.0, 43.6, 62.1, 78.9, 94.1, 94.3, 101.7, 104.2, 116.9, 126.5, 132.1, 132.6. LRMS (EI) m/z (rel intensity) 298 ($\text{M}^+ + 2$, 41), 296 (M^+ , 42), 217 (71), 215 (51), 178 (100). TOF-HRMS calcd for $\text{C}_{14}\text{H}_{18}\text{BrO}_2$ ($\text{M} + \text{H}^+$) 297.0485, found 297.0485.

4.1.19. (E)-6-Bromo-7-methoxy-2-styrylchroman (37). Following the general procedure and purification by PTLC (20% EtOAc/hexanes), the desired compound was obtained as colorless oil (0.026 g, 0.074 mmol, 80%). R_f (20% EtOAc/hexanes) 0.50. IR (neat): ν_{max} 3020, 2960, 2925, 2854, 1723, 1610, 1572, 1495, 1443, 1403, 1307, 1261, 1187, 1154, 1047, 1028 cm^{-1} . ^1H NMR (200 MHz, CDCl_3): δ 1.81–2.00 (m, 1H), 2.06–2.17 (m, 1H), 2.73–2.83 (m, 2H), 3.84 (s, 3H), 4.66–4.73 (m, 1H), 6.31 (dd, $J=16.1$, 6.3 Hz, 1H), 6.48 (s, 1H), 6.72 (d, $J=16.0$ Hz, 1H), 7.11–7.44 (m, 6H). ^{13}C NMR (50 MHz, CDCl_3): δ 23.4, 27.8, 56.2, 101.1, 101.9, 115.2, 126.0, 127.9, 128.2, 128.5, 131.9, 133.1, 136.3, 154.5, 154.9. LRMS (EI) m/z (rel intensity) 346 ($\text{M}^+ + 2$, 53), 345 ($\text{M} + \text{H}^+$, 18), 344 (M^+ , 54), 265 (22), 216 (14), 215 (13), 174 (19), 143 (32), 142 (54), 141 (15), 137 (23), 130 (57), 129 (100), 128 (34), 115 (45), 91 (59). TOF-HRMS calcd for $\text{C}_{18}\text{H}_{18}\text{BrO}_2$ ($\text{M} + \text{H}^+$) 345.0485, found 345.0492.

4.1.20. (E)-Ethyl 6-bromo-7-methoxy-2-styrylchroman-3-carboxylate (38). Following the general procedure and purification by PTLC (10% EtOAc/hexanes), the desired compound was obtained as a 10:1 mixture of C2–C3 *trans:cis* diastereomers as colorless oil (0.014 g, 0.034 mmol, 33%). R_f (10% EtOAc/hexanes) 0.29. IR (neat): ν_{max} 2980, 2937, 1729, 1612, 1575, 1496, 1443, 1256, 1200, 1187, 1154, 1018 cm^{-1} . ^1H NMR (200 MHz, CDCl_3): δ 1.17 (t, $J=7.1$ Hz, 3H), 1.27 (t, $J=7.2$ Hz, 3H, minor), 2.79–3.00 (m, 2H), 3.06–3.21 (m, 1H), 3.83 (s, 3H), 3.85 (s, 3H, minor), 4.13 (q, $J=7.1$ Hz, 3H), 4.76 (app t, $J=7.9$ Hz, 1H), 5.21–5.24 (m, 1H, minor), 6.19 (dd, $J=16.0$, 6.6 Hz, 1H, minor), 6.26 (dd, $J=15.8$, 7.4 Hz, 1H), 6.64 (d, $J=16.6$ Hz, 1H, minor), 6.73 (dd, $J=16.0$ Hz, 1H), 7.25–7.43 (m, 6H). ^{13}C NMR (50 MHz, CDCl_3): δ 14.2, 23.5 (minor), 26.9, 42.0 (minor), 44.1, 56.2, 61.1, 75.5 (minor), 77.6 (superimposed with CDCl_3), 100.9, 102.6, 113.4, 125.5, 126.7, 128.2, 128.5, 132.8, 134.2, 135.9, 153.6, 155.1, 172.1. LRMS (EI) m/z (rel intensity) 418 ($\text{M}^+ + 2$, 64), 417 ($\text{M} + \text{H}^+$, 18), 416 (M^+ , 66), 372 (57), 370 (53), 281 (100), 279 (88), 204 (55), 202 (49), 129 (63), 128 (61), 115 (39). TOF-HRMS calcd for $\text{C}_{21}\text{H}_{22}\text{BrO}_4$ ($\text{M} + \text{H}^+$) 417.0696, found 417.0708.

4.1.21. 6-Bromo-3-(but-3-enyl)-7-methoxy-2-phenylchroman (39). Following the general procedure and purification by PTLC (15% EtOAc/hexanes), the desired compound was obtained as colorless oil (0.009 g, 0.023 mmol, 30%). R_f (15% EtOAc/hexanes) 0.52. IR (neat): ν_{max} 2930, 2854, 1611, 1576, 1496, 1444, 1201, 1158, 1053 cm^{-1} . ^1H NMR (400 MHz, CDCl_3): δ 1.13–1.37 (m, 2H),

1.88–2.01 (m, 2H), 2.05–2.17 (m, 2H), 2.49 (dd, 1H, $J=4.9, 8.1$ Hz), 2.82 (dd, 1H, $J=2.2, 8.4$ Hz), 3.82 (s, 3H), 4.73 (d, 1H, $J=4$ Hz), 4.92 (d, 1H, $J=4.4$ Hz), 4.95 (d, 1H, $J=8$ Hz), 5.61–5.72 (m, 1H), 6.47 (s, 1H), 7.23 (s, 1H), 7.30–7.41 (m, 5H). ^{13}C NMR (100 MHz, CDCl_3): δ 29.3, 30.5, 30.8, 36.6, 56.1, 83.0, 100.7, 101.8, 115.0, 115.1, 126.9, 128.3, 128.6, 133.0, 137.9, 139.9, 154.7, 154.9. LRMS (EI) m/z (rel intensity) 374 (M^++1 , 17), 372 (M^+-1 , 17), 241 (14), 239 (17), 217 (24), 215 (24), 178 (51), 161 (30), 149 (30), 117 (100), 91 (53), 71 (46), 69 (88). TOF-HRMS calcd for $\text{C}_{20}\text{H}_{22}\text{BrO}_2$ ($\text{M}+\text{H}^+$) 373.0798, found 373.0793.

4.1.22. 6-Bromo-7-methoxy-2,2-dimethyl-3-((S)-3-methyl pent-4-enyl)chroman (40). Following the general procedure and purification by PTLC (15% EtOAc/hexanes), the desired compound was obtained as colorless oil (0.022 g, 0.062 mmol, 62%). R_f (15% EtOAc/hexanes) 0.60. IR (neat): ν_{max} 2931, 2865, 1610, 1577, 1486, 1497, 1315, 1203, 1161, 1134, 1054 cm^{-1} . ^1H NMR (400 MHz, CDCl_3): δ 1.00 (d, 3H, $J=2.2$ Hz), 1.02 (d, 3H, $J=2.2$ Hz), 1.13 (s, 3H), 1.14 (s, 3H), 1.20–1.72 (m, 2H), 2.06–2.16 (m, 1H), 2.26–2.37 (m, 1H), 2.77 (td, 1H, $J=7.8, 2.5$ Hz), 3.82 (s, 3H), 4.94 (d, 1H, $J=4.6$ Hz), 4.97 (d, 1H, $J=8.3$ Hz), 5.60–5.75 (m, 1H), 6.36 (s, 1H), 7.18 (s, 1H). ^{13}C NMR (100 MHz, CDCl_3): δ 19.9, 20.4, 20.5, 20.7, 27.1, 27.2, 27.5, 27.6, 28.2, 28.3, 34.3, 34.5, 37.8, 37.9, 40.6, 41.0, 56.1, 78.2, 78.3, 101.2, 112.8, 113.1, 115.0, 132.9, 144.1, 144.5, 153.7, 154.9. LRMS (EI) m/z (rel intensity) 354 (M^++2 , 23), 352 (M^+ , 24), 217 (95), 215 (100). TOF-HRMS calcd for $\text{C}_{18}\text{H}_{26}\text{BrO}_2$ ($\text{M}+\text{H}^+$) 353.1111, found 353.1112.

4.1.23. 6-Bromo-7-methoxy-2-phenyl-4-(4-(trifluoromethoxy)phenyl)chroman (44). Following the general procedure and purification by PTLC (30% EtOAc/hexanes), the desired compound was obtained as a 4:1 mixture of C2–C4 *cis:trans* diastereomers as colorless oil (0.019 g, 0.039 mmol, 83%). R_f (30% EtOAc/hexanes) 0.63. ^1H NMR (400 MHz, CDCl_3): δ 2.17 (ddd, $J=11.9, 11.8, 11.8$ Hz, 1H), 2.38 (ddd, $J=13.8, 5.9, 1.8$ Hz, 1H), 2.42–2.48 (m, 1H, minor), 3.85 (s, 3H), 3.89 (s, 3H, minor), 4.17 (dd, $J=5.5, 3.3$ Hz, 1H, minor), 4.31 (dd, $J=12.0, 5.8$ Hz, 1H), 4.98 (dd, $J=10.5, 2.2$ Hz, 1H, minor), 5.17 (dd, $J=11.4, 1.5$ Hz, 1H), 6.54 (s, 1H), 6.60 (s, 1H, minor), 6.89 (s, 1H), 7.12 (s, 1H, minor), 7.14–7.26 (m, 4H), 7.31–7.47 (m, 5H). ^{13}C NMR (100 MHz, CDCl_3): δ 40.5, 42.1, 56.2, 78.4, 101.1, 102.6, 113.6 (minor), 118.5, 121.0 (minor), 121.3, 126.0, 128.3, 128.57 (minor), 128.65, 129.6, 129.8 (minor), 133.1, 134.0 (minor), 140.3, 142.6, 148.1, 155.4, 155.7. TOF-HRMS calcd for $\text{C}_{23}\text{H}_{18}\text{BrF}_3\text{O}_3$ (M^+) 478.0386, found 478.0379. These spectroscopic data were identical to those reported previously.^{3a}

4.1.24. 4-Allyl-6-bromo-7-methoxy-2-phenylchroman (45). Following the general procedure and purification by PTLC (15% EtOAc/hexanes), the desired compound was obtained as colorless oil (0.013 g, 0.033 mmol, 49%). R_f (15% EtOAc/hexanes) 0.52. IR (neat): ν_{max} 2916, 2853, 1609, 1568, 1488, 1443, 1199, 1156, 1052 cm^{-1} . ^1H NMR (400 MHz, CDCl_3): δ 1.98–2.14 (m, 1H), 2.17–2.29 (m, 2H), 2.27–2.44 (m, minor), 2.53–2.61 (m, minor), 2.68–2.475 (m, 1H), 2.80–2.88 (m, minor), 3.07–3.17 (m, 1H), 3.82 (s, 3H), 3.83 (s, minor), 4.98–5.15 (m, 3H), 5.71–5.90 (m, 1H), 6.49 (s, 1H), 6.51 (s, minor), 7.31–7.45 (m, 6H). ^{13}C NMR (100 MHz, CDCl_3): δ 32.8, 33.1, 33.8, 36.4, 38.8, 41.9, 73.9, 78.4, 101.1 (minor), 101.3, 102.3, 117.4 (minor), 117.5, 118.8, 118.9 (minor), 125.9 (minor), 126.0, 128.0 (minor), 128.1, 128.6, 131.1, 133.1, 135.2, 135.9, 141.1, 154.9, 155.5. LRMS (EI) m/z (rel intensity) 360 (M^++2 , 18), 358 (M^+ , 19), 319 (89), 317 (93), 238 (100), 223 (26), 115 (40), 104 (33), 91 (58). TOF-HRMS calcd for $\text{C}_{19}\text{H}_{20}\text{BrO}_2$ ($\text{M}+\text{H}^+$) 359.0641, found 359.0650.

4.1.25. 6-Bromo-7-methoxy-3-methyl-2-phenyl-4-(4-cyanophenyl)chroman (46). Following the general procedure and purification by PTLC (30% EtOAc/hexanes), the desired compound was obtained as

a 2.7:1 mixture of C2–C4 *cis:trans* diastereomers as colorless oil (0.015 g, 0.034 mmol, 70%). R_f (30% EtOAc/hexanes) 0.54. IR (neat): ν_{max} 2960, 2228, 1608, 1574, 1486, 1443, 1399, 1311, 1261, 1197, 1159, 1052, 1020 cm^{-1} . ^1H NMR (400 MHz, CDCl_3): δ 0.54 (d, $J=7.0$ Hz, 3H, minor), 0.58 (d, $J=6.6$ Hz, 3H), 2.17–2.27 (m, 1H), 2.45–2.55 (m, 1H, minor), 3.81 (d, $J=10.8$ Hz, 1H), 3.813 (s, 3H), 3.86 (s, 3H, minor), 4.08 (d, $J=5.4$ Hz, 1H, minor), 4.73 (d, $J=10.1$ Hz, 1H), 4.75 (d, $J=10.0$ Hz, 1H, minor), 6.51 (s, 1H), 6.58 (s, 1H, minor), 6.69 (d, $J=0.8$ Hz, 1H), 7.05 (s, 1H, minor), 7.22–7.42 (m, 5H), 7.62 (AA'BB', $J=8.4$ Hz, 2H), 7.64 (AA'BB', $J=8.3$ Hz, 2H). ^{13}C NMR (100 MHz, CDCl_3): δ 15.2 (minor), 15.4, 36.8 (minor), 40.8, 45.8 (minor), 50.4, 56.2, 79.3 (minor), 84.3, 100.7 (minor), 100.9, 102.7 (minor), 102.8, 110.8 (minor), 111.1, 116.7 (minor), 118.4 (minor), 118.7, 125.5 (minor), 127.1 (minor), 127.4, 128.5, 128.6 (minor), 128.7, 128.8, 130.0, 130.8 (minor), 131.9 (minor), 132.6, 133.3, 133.6 (minor), 138.8, 139.1 (minor), 147.2 (minor), 149.0, 154.8 (minor), 155.4, 155.5, 155.8 (minor). LRMS (EI) m/z (rel intensity) 435 (M^++2 , 98), 433 (M^+ , 100), 344 (40), 342 (42), 317 (46), 316 (88), 315 (43), 314 (72), 263 (46), 118 (74), 117 (74). TOF-HRMS calcd for $\text{C}_{24}\text{H}_{21}\text{BrNO}_2$ ($\text{M}+\text{H}^+$) 434.0750, found 434.0749.

4.1.26. 6-Bromo-7-methoxy-3-methyl-2-phenyl-4-(4-(trifluoromethoxy)phenyl)chroman (47). Following the general procedure and purification by PTLC (30% EtOAc/hexanes), the desired compound was obtained as a 1.9:1 mixture of C2–C4 *cis:trans* diastereomers as colorless oil (0.010 g, 0.020 mmol, 51%). R_f (30% EtOAc/hexanes) 0.62. IR (neat): ν_{max} 2928, 1608, 1572, 1488, 1440, 1399, 1310, 1256, 1195, 1153, 1119, 1053, 1019 cm^{-1} . ^1H NMR (200 MHz, CDCl_3): δ 0.54 (d, $J=7.0$ Hz, 3H, minor), 0.58 (d, $J=6.6$ Hz, 3H), 2.16–2.26 (m, 1H), 2.40–2.50 (m, 1H, minor), 3.75 (d, $J=10.8$ Hz, 1H), 3.81 (s, 3H), 3.85 (s, 3H, minor), 4.03 (d, $J=5.2$ Hz, 1H, minor), 4.73 (d, $J=10.1$ Hz, 1H), 4.79 (d, $J=10.1$ Hz, 1H, minor), 6.50 (s, 1H), 6.57 (s, 1H, minor), 6.77 (d, $J=0.9$ Hz, 1H), 7.09–7.46 (m, 10H). ^{13}C NMR (100 MHz, CDCl_3): δ 15.2 (minor), 15.4, 36.9 (minor), 40.9, 45.1 (minor), 49.6, 56.2, 79.3 (minor), 84.5, 100.6 (minor), 100.8, 102.6, 117.7 (minor), 119.3, 120.5 (minor), 121.1, 125.5 (minor), 127.2, 127.4, 128.4, 128.6 (minor), 128.7, 130.5, 131.3 (minor), 133.5, 133.7 (minor), 139.1, 140.3 (minor), 141.9, 154.8 (minor), 155.2, 155.5. LRMS (EI) m/z (rel intensity) 494 (M^++2 , 19), 492 (M^+ , 19), 277 (27), 278 (33), 277 (100), 117 (57), 91 (26). TOF-HRMS calcd for $\text{C}_{24}\text{H}_{21}\text{BrF}_3\text{O}_3$ ($\text{M}+\text{H}^+$) 493.0621, found 493.0618.

4.1.27. 6-Bromo-7-methoxy-2-(4-methoxyphenyl)chroman (53). Following the general procedure and purification by PTLC (20% EtOAc/hexanes), the desired compound was obtained as colorless oil (0.032 g, 0.092 mmol, 99%). R_f (20% EtOAc/hexanes) 0.56. IR (neat): ν_{max} 3000, 2929, 2852, 1732, 1611, 1573, 1514, 1495, 1443, 1403, 1305, 1246, 1193, 1153, 1034 cm^{-1} . ^1H NMR (200 MHz, CDCl_3): δ 1.92–2.21 (m, 2H), 2.65–3.00 (m, 2H), 3.82 (s, 6H), 4.97 (dd, $J=9.6, 3.0$ Hz, 1H), 6.48 (s, 1H), 6.93 (app. td, $J=8.8, 2.6$ Hz, 2H), 7.24 (s, 1H), 7.34 (app. td, $J=8.8, 1.8$ Hz, 2H). ^{13}C NMR (50 MHz, CDCl_3): δ 29.2, 29.5, 55.3, 56.2, 77.8, 101.3, 102.0, 114.0, 115.3, 127.4, 133.0, 133.5, 155.0, 155.3, 159.5. LRMS (EI) m/z (rel intensity) 351 (M^++3 , 14), 350 (M^++2 , 78), 349 ($\text{M}+\text{H}^+$, 17), 348 (M^+ , 80), 271 (8), 269 (31), 134 (62), 121 (36), 91 (100). TOF-HRMS calcd for $\text{C}_{17}\text{H}_{18}\text{BrO}_3$ ($\text{M}+\text{H}^+$) 349.0434, found 349.0435.

4.1.28. 2-(3-Benzyloxy-4-methoxy)phenyl-6-bromo-7-methoxychroman (54). Following the general procedure and purification by PTLC (20% EtOAc/hexanes), the desired compound was obtained as colorless oil (0.037 g, 0.082 mmol, 73%). R_f (20% EtOAc/hexanes) 0.44. ^1H NMR (200 MHz, CDCl_3): δ 1.92–2.21 (m, 2H), 2.64–2.76 (m, 1H), 2.82–3.04 (m, 1H), 3.86 (s, 3H), 3.93 (s, 3H), 4.96 (dd, $J=9.4, 2.2$ Hz, 1H), 5.20 (s, 2H), 6.50 (s, 1H), 6.92–7.03 (m, 3H), 7.29–7.50 (m, 6H). ^{13}C NMR (50 MHz, CDCl_3): δ 24.0, 29.4, 56.1, 56.2, 71.2, 77.8, 101.1, 101.9, 111.9, 112.4, 115.2, 119.1, 127.4, 127.8, 128.5, 133.0, 133.7,

137.0, 148.3, 149.6, 154.9, 155.1. TOF-HRMS calcd for $C_{24}H_{24}BrO_4$ ($M+H^+$) 455.0852, found 455.0866. These spectroscopic data were identical to those reported previously.^{3a}

4.1.29. 6-Bromo-7-methoxy-4-(methylsulfonylmethyl)-2-phenylchroman (56). Following the general procedure and purification by PTLC (30% EtOAc/hexanes), the desired compound was obtained as colorless oil (0.007 g, 0.018 mmol, 37%). R_f (30% EtOAc/hexanes) 0.22. IR (neat): ν_{max} 2924, 2854, 1609, 1568, 1488, 1443, 1400, 1300, 1197, 1153, 1051 cm^{-1} . 1H NMR (200 MHz, $CDCl_3$): δ 1.9–2.3 (m, 2H), 2.60–2.86 (m, 1H), 3.02 (s, 3H), 3.06–3.16 (m, 1H), 3.35–3.66 (m, 1H), 3.61 (dd, 1H, $J=3.0, 13.6$ Hz), 3.85 (s, 3H), 5.07 (ddd, 1H, $J=15.6, 11.3, 1.7$ Hz), 6.52 (s, 1H), 7.30–7.48 (m, 6H). ^{13}C NMR (50 MHz, $CDCl_3$): δ 33.4, 36.8, 42.3, 42.5, 56.3, 59.8, 60.0, 73.7, 101.4, 101.8, 102.9, 115.3, 126.0, 126.1, 128.3, 128.4, 128.7, 130.9, 132.7, 140.0, 155.7, 155.8. LRMS (EI) m/z (rel intensity) 412 (20, M^++2), 410 (19, M^+), 330 (77), 332 (74), 315 (97), 317 (100), 148 (84), 104 (86), 91 (84), 77 (74). TOF-HRMS calcd for $C_{18}H_{20}BrO_4S$ ($M+H^+$) 411.0260, found 411.0262.

4.1.30. 6-Bromo-7-methoxy-2-(4-methoxyphenyl)-4-(methylsulfonylmethyl)chroman (57). Following the general procedure and purification by PTLC (30% EtOAc/hexanes), the desired compound was obtained as colorless oil (0.013 g, 0.029 mmol, 44%). R_f (30% EtOAc/hexanes) 0.20. IR (neat): ν_{max} 2926, 2846, 1610, 1514, 1489, 1300, 1247, 1197, 1154, 1051, 1030 cm^{-1} . 1H NMR (200 MHz, $CDCl_3$): δ 1.93–2.34 (m, 1H), 2.55–2.84 (m, 1H), 3.02 (s, 3H), 3.07–3.70 (m, 2H), 3.83 (s, 6H), 5.02 (dd, 1H, $J=11.4, 15.0$ Hz), 6.50 (s, 1H), 6.93 (d, 2H, $J=8.8$ Hz), 7.34 (s, 1H), 7.35 (d, 2H, $J=8.8$ Hz). ^{13}C NMR (50 MHz, $CDCl_3$): δ 33.2, 36.6, 44.2, 42.5, 55.4, 56.3, 59.9, 60.2, 73.4, 77.4, 101.4, 101.8, 102.8, 112.1, 115.3, 115.6, 127.4, 127.5, 130.8, 132.1, 132.7, 155.2, 155.6, 156.0, 159.6. LRMS (EI) m/z (rel intensity) 442 (M^++2 , 10), 440 (M^+ , 10), 362 (26), 360 (27), 347 (34), 345 (32), 134 (100), 119 (39), 91 (38), 77 (20). TOF-HRMS calcd for $C_{19}H_{22}BrO_5S$ ($M+H^+$) 441.0366, found 441.0376.

4.1.31. 2-Bromo-3-methoxy-6-phenyl-7,8,10,10a-tetrahydro-6H-benzo[c]chromen-9(6aH)-one (59). Following the general procedure and purification by PTLC (20% EtOAc/hexanes), the C3-C4 *trans* isomer was obtained as a white solid (0.042 g, 0.11 mmol, 42%, using $PtCl_4$; 0.035 g, 0.09 mmol, 44%, using $AuCl_3$). R_f (20% EtOAc/hexanes) 0.29. IR (neat): ν_{max} 2953, 1713, 1609, 1488, 1443, 1202, 1052 cm^{-1} . 1H NMR (400 MHz, $CDCl_3$): δ 1.40 (ddd, $J=25.7, 13.4, 4.8$ Hz, 1H), 1.57–1.63 (m, 1H), 2.13–2.04 (m, 1H), 2.25–2.35 (m, 2H), 2.45 (dq, $J=15.1, 2.4$ Hz, 1H), 2.98–3.04 (m, 1H), 3.06 (ddd, $J=13.3, 4.3, 2.0$ Hz, 1H), 3.82 (s, 3H), 4.79 (d, $J=10.0$ Hz, 1H), 6.50 (s, 1H), 7.24 (s, 1H), 7.46–7.38 (m, 5H). ^{13}C NMR (100 MHz, $CDCl_3$): δ 27.6, 39.1, 40.3, 42.0, 44.9, 56.2, 83.0, 100.9, 102.4, 117.4, 127.2, 128.8, 128.9, 129.5, 138.7, 154.6, 155.5, 208.8. LRMS (EI) m/z (rel intensity) 388 (M^++2 , 93), 386 (M^+ , 100), 307 (37), 293 (25), 291 (26), 230 (25), 228 (25), 216 (26), 117 (16), 115 (20), 91 (13), 77 (4). TOF-HRMS calcd for $C_{20}H_{20}BrO_3$ ($M+H^+$) 387.0596, found 387.0591.

The C3–C4 *cis* isomer was obtained as colorless oil (0.028 g, 0.072 mmol, 28%, using $PtCl_4$; 0.022 g, 0.057 mmol, 27%, using $AuCl_3$). R_f (20% EtOAc/hexanes) 0.23. IR (neat): ν_{max} 2945, 2099, 1715, 1609, 1488, 1443, 1199, 1158, 1053 cm^{-1} . 1H NMR (400 MHz, $CDCl_3$): δ 1.66–1.74 (m, 1H), 1.87–1.96 (m, 1H), 2.27–2.40 (m, 2H), 2.48–2.54 (m, 1H), 2.62–2.75 (m, 2H), 3.18–3.23 (m, 1H), 3.82 (s, 3H), 5.22 (d, $J=8.6$ Hz, 1H), 6.50 (s, 1H), 7.24 (s, 1H), 7.36–7.44 (m, 5H). ^{13}C NMR (100 MHz, $CDCl_3$): δ 25.7, 35.0, 36.7, 37.6, 45.6, 56.2, 77.8, 101.0, 102.6, 117.3, 126.5, 128.6, 128.8, 132.0, 139.2, 153.9, 155.5, 209.1. LRMS (EI) m/z (rel intensity) 388 (M^++2 , 100), 386 (M^+ , 97), 307 (28), 230 (32), 228 (37), 216 (41), 178 (29), 149 (49), 117 (33), 91 (25). TOF-HRMS calcd for $C_{20}H_{20}BrO_3$ ($M+H^+$) 387.0596, found 387.0588.

4.1.32. 2-Bromo-3-methoxy-6-phenyl-6a,7,8,9,10,10a-hexahydro-6H-benzo[c]chromen-9-yl acetate (60). To a solution of compound **58** (0.067 g, 0.15 mmol) in MeOH (3 mL) was added $NaBH_4$ (0.0060 g, 0.16 mmol) at room temperature and then stirred for 30 min. After removal of solvent, the residue was added with H_2O and extracted with EtOAc (2×10 mL). The combined organic phases were washed with H_2O and brine, dried over Na_2SO_4 , filtered, and concentrated under a vacuum to give an alcohol crude product. This crude product was dissolved in CH_2Cl_2 (0.15 mL), followed by addition of DMAP (0.045 g, 0.37 mmol), and the reaction mixture was stirred until completely dissolved. Acetyl chloride (0.03 mL, 0.37 mmol) was added dropwise into this solution and then the reaction was stirred vigorously overnight. To this mixture was added $PtCl_4$ (0.0050 g, 0.01 mmol) and the resulting mixture was stirred at room temperature for 5 h. Following concentration under reduced pressure, the residue was purified by flash chromatography on silica gel to yield compound **60** as a white solid (0.037 g, 0.085 mmol, 58%). R_f (20% EtOAc/hexanes) 0.48. IR (neat): ν_{max} 2944, 1732, 1610, 1444, 1243 cm^{-1} . 1H NMR (400 MHz, $CDCl_3$): δ 1.05–1.71 (m, 6H), 1.96–2.06 (m, 1H), 2.07 (s, 3H), 2.10 (s, 3H, minor), 2.60–2.68 (m, 1H), 2.88–3.02 (m, 1H, minor), 3.82 (s, 3H), 4.74 (d, $J=10.0$ Hz, 1H), 4.80 (d, $J=10.6$ Hz, 1H, minor), 4.84–4.95 (m, 1H), 5.22–5.26 (m, 1H, minor), 6.47 (s, 1H), 7.30–7.42 (m, 6H). ^{13}C NMR (100 MHz, $CDCl_3$): δ 21.35, 21.44, 22.6, 26.1, 29.0, 30.8, 33.7, 35.0, 37.4, 42.5, 42.8, 56.2, 68.8, 72.2, 83.4, 100.8, 101.8, 101.9, 118.0, 118.6, 127.17, 127.23, 128.6, 129.5, 139.1, 154.6, 154.8, 155.0, 155.1, 170.4, 170.6. LRMS (EI) m/z (rel intensity) 432 (M^++2 , 91), 430 (M^+ , 100), 372 (31), 370 (37), 291 (30), 281 (56), 279 (65), 200 (20). TOF-HRMS calcd for $C_{22}H_{24}BrO_4$ ($M+H^+$) 431.0852 found 431.0859.

4.1.33. 1-(5-Bromo-4-methoxy-2-(methoxymethoxy)phenyl)-1-hydroxy-7-methyloct-6-en-3-one (61). To a stirred solution of LDA prepared by treating a solution of *i*- Pr_2NH (0.59 mL, 4.22 mmol) in THF (20 mL) and *n*-BuLi (2.06 M in hexane, 2.05 mL, 4.22 mmol) at 0 °C was added 6-methylhept-5-en-2-one (0.50 mL, 3.38 mmol) dropwise at –78 °C. After 1 h, a solution of 5-bromo-4-methoxy-2-(methoxymethoxy)benzaldehyde (0.76 g, 2.81 mmol) in THF (3 mL) was added, and the resulting mixture was stirred for 1 h at –78 °C. The reaction was quenched with H_2O at –78 °C, and then the mixture was extracted with EtOAc, washed with H_2O and brine, dried over $MgSO_4$, filtered, and concentrated at reduced pressure. The residue was purified by flash chromatography on silica gel (30% EtOAc/hexanes) to give compound **61** (0.97 g, 2.42 mmol, 86%) as colorless oil. R_f (30% EtOAc/hexanes) 0.30. IR (neat): ν_{max} 3486, 2960, 1706, 1603, 1492, 1287, 1142 cm^{-1} . 1H NMR (400 MHz, $CDCl_3$): δ 1.59 (s, 3H), 1.66 (s, 3H), 2.16–2.30 (m, 2H), 2.41–2.49 (m, 2H), 2.68 (B of ABX, $J_{BA}=17.6$ Hz, $J_{BX}=8.8$ Hz, 1H), 2.82 (A of ABX, $J_{AB}=17.2$ Hz, $J_{AX}=3.4$ Hz, 1H), 3.46 (s, 3H), 3.48 (d, $J=3.8$ Hz, 1H), 3.84 (s, 3H), 4.99–5.06 (m, 1H), 5.17 (s, 2H), 5.35 (app dt, $J=8.8, 3.4$ Hz, 1H), 6.70 (s, 1H), 7.59 (s, 1H). ^{13}C NMR (100 MHz, $CDCl_3$): δ 17.6, 22.1, 25.6, 43.4, 49.5, 56.1, 56.2, 64.1, 94.7, 99.3, 103.5, 122.4, 125.2, 130.4, 132.9, 153.5, 155.6, 211.4. TOF-HRMS calcd for $C_{18}H_{25}BrNaO_5$ ($M+Na^+$) 423.0778, found 423.0787.

4.1.34. 2-Bromo-3-methoxy-6,6-dimethyl-7,8,10,10a-tetrahydro-6H-benzo[c]chromen-9(6aH)-one (62). Following the general procedure, the C3–C4 *trans* isomer was obtained as a white solid (0.052 g, 0.15 mmol, 47%, using $PtCl_4$; 0.047 g, 0.14 mmol, 44%, using $AuCl_3$). R_f (30% EtOAc/hexanes) 0.39. IR (neat): ν_{max} 2926, 2860, 1716, 1609, 1488, 1199, 1055 cm^{-1} . 1H NMR (400 MHz, $CDCl_3$): δ 1.15 (s, 3H), 1.48 (s, 3H), 1.53–1.42 (m, 1H), 1.84 (td, $J=12.1, 3.0$ Hz, 1H), 2.15 (qt, $J=6.5, 2.6$ Hz, 1H), 2.25 (t, $J=13.6$ Hz, 1H), 2.41 (td, $J=14.4, 6.5$ Hz, 1H), 2.54 (dm, $J=14.8$ Hz, 1H), 2.78 (td, $J=12.1, 4.3$ Hz, 1H), 3.01 (ddd, $J=14.2, 4.3, 2.0$ Hz, 1H), 3.82 (s, 3H), 6.38 (s, 1H), 7.19 (d, $J=0.7$ Hz, 1H). ^{13}C NMR (100 MHz, $CDCl_3$): δ 19.8, 27.0, 27.9, 35.3, 40.6, 45.5, 45.8, 56.1, 77.8, 101.3, 101.9, 117.0, 129.8, 153.3, 155.4,

209.0. LRMS (EI) m/z (rel intensity) 340 ($M^+ + 2$, 97), 338 (M^+ , 100), 257 (36), 254 (46), 230 (31), 228 (32). TOF-HRMS calcd for $C_{16}H_{20}BrO_3$ ($M + H^+$) 339.0590, found 339.0594.

The C3–C4 *cis* isomer was obtained as a white solid (0.028 g, 0.083 mmol, 25%, using $PtCl_4$; 0.025 g, 0.073 mmol, 23%, using $AuCl_3$). R_f (30% EtOAc/hexanes) 0.34. IR (neat): ν_{max} 2893, 1717, 1607, 1489, 1443, 1166, 1150, 1054 cm^{-1} . 1H NMR (400 MHz, $CDCl_3$): δ 1.34 (s, 3H), 1.45 (s, 3H), 1.67–1.56 (m, 1H), 2.07–2.02 (m, 1H), 2.17–2.10 (m, 1H), 2.27 (dm, $J=14.6$ Hz, 1H), 2.37 (td, $J=13.9$, 6.4 Hz, 1H), 2.72 (dd, $J=14.9$, 6.0 Hz, 1H), 2.98 (dt, $J=14.9$, 2.5 Hz, 1H), 3.63 (br s, 1H), 3.81 (s, 3H), 6.36 (s, 1H), 7.36 (d, $J=0.9$ Hz, 1H). ^{13}C NMR (100 MHz, $CDCl_3$): δ 22.9, 26.3, 26.6, 34.0, 39.6, 39.9, 42.7, 56.1, 101.3, 102.3, 114.0, 131.2, 153.3, 155.5, 209.4. LRMS (EI) m/z (rel intensity) 340 ($M^+ + 2$, 100), 338 (M^+ , 99.6), 270 (14), 250 (34), 230 (30), 228 (31). TOF-HRMS calcd for $C_{16}H_{20}BrO_3$ ($M + H^+$) 339.0590, found 339.0585.

Acknowledgements

Financial support from the Thailand Research Fund (BRG5180013 for P.P.) is gratefully acknowledged.

Supplementary data

General methods, detailed characterization and copies of 1H and ^{13}C NMR of all new compounds as well as the overlay of 1H NMR (not shown in the manuscript). Supplementary data related to this article can be found online at doi:10.1016/j.tet.2011.03.059. These data include MOL files and InChIKeys of the most important compounds described in this article.

References and notes

- (a) Li, Z.; Brouwer, C.; He, C. *Chem. Rev.* **2008**, *108*, 3239–3265; (b) Gorin, D. J.; Sherry, B. D.; Toste, F. D. *Chem. Rev.* **2008**, *108*, 3351–3378; (c) Arcadi, A. *Chem. Rev.* **2008**, *108*, 3266–3325; (d) Hashmi, A. S. K. *Chem. Rev.* **2007**, *107*, 3180–3211; (e) Fürstner, A.; Davies, P. W. *Angew. Chem., Int. Ed.* **2007**, *46*, 3410–3449; (f) Hiroya, K.; Matsumoto, S.; Ashikawa, M.; Ogiwara, K.; Sakamoto, T. *Org. Lett.* **2006**, *8*, 5349–5352; (g) Kobayashi, S.; Kakumoto, K.; Sugiura, M. *Org. Lett.* **2002**, *4*, 1319–1322; (h) Pastine, S. J.; Youn, S. W.; Sames, D. *Org. Lett.* **2003**, *5*, 1055–1058; (i) Xia, Y.; Huang, G. *J. Org. Chem.* **2010**, *75*, 7842–7854.
- For review, see: (a) Van De Water, R. W.; Pettus, T. R. *Tetrahedron* **2002**, *58*, 5367–5405; (b) Tang, Y.; Oppenheimer, J.; Song, Z.; You, L.; Zhang, X.; Hsung, R. P. *Tetrahedron* **2006**, *62*, 10785–10813; (c) Ferreira, S. B.; da Silva, F. d. C.; Pinto, A. C.; Gonzaga, D. T. G.; Ferreira, V. F. *J. Heterocycl. Chem.* **2009**, *46*, 1080–1097; For transition metal-complexed *o*-QMs, see: (d) Poverenov, E.; Milstein, D. In *Quinone Methides*; Rokita, S. E., Ed.; Wiley: New Jersey, 2009; pp 69–88; For thermal and base initiation, see: (e) Bray, C. D. *Org. Biomol. Chem.* **2008**, *6*, 2815–2819; (f) Rodriguez, R.; Adlington, R. M.; Moses, J. E.; Cowley, A.; Baldwin, J. E. *Org. Lett.* **2004**, *6*, 3617–3619; (g) Selenski, C.; Pettus, T. R. *Tetrahedron* **2006**, *62*, 5298–5307; (h) Jones, R. M.; Selenski, C.; Pettus, T. R. *J. Org. Chem.* **2002**, *67*, 6911–6915; (i) Barrero, A. F.; Quílez del Moral, J. F.; Herrador, M. M.; Arteaga, P.; Cortés, M.; Benites, J.; Rosellón, A. *Tetrahedron* **2006**, *62*, 6012–6017 For acid initiation, see: (j) Chiba, K.; Hirano, T.; Kitano, Y.; Tada, M. *Chem. Commun.* **1999**, 691–692; (k) Miyazaki, H.; Honda, K.; Asami, M.; Inoue, S. *J. Org. Chem.* **1999**, *64*, 9507–9511; (l) Miyazaki, H.; Honda, Y.; Honda, K.; Inoue, S. *Tetrahedron Lett.* **2000**, *41*, 2643–2647 For catalytic enantioselective cycloaddition reactions of *o*-QMs, see: (m) Alden-Danforth, E.; Scerba, M. T.; Lectka, T. *Org. Lett.* **2008**, *10*, 4951–4953.
- (a) Batsomboon, P.; Phakhodee, W.; Ruchirawat, S.; Ploypradith, P. *J. Org. Chem.* **2009**, *74*, 4009–4012; (b) Tummatorn, J.; Ruchirawat, S.; Ploypradith, P. *Chem.—Eur. J.* **2010**, *16*, 1445–1448.
- (a) Ullrich, J. W.; Miller, C. P. *Expert Opin. Ther. Pat.* **2006**, *16*, 559–572; (b) Wallace, O. B.; Richardson, T. I.; Dodge, J. A. *Curr. Top. Med. Chem.* **2003**, *3*, 1663–1680.
- These Lewis acids or transition metal salts/complexes did not give any product: $BF_3 \cdot Et_2O$, $SnCl_4$, $CoCl_2$, Ag_2O , $NiCl_2$, $YbCl_3 \cdot 6H_2O$, $Pd(OAc)_2$, K_2PdCl_6 , $Pd(PPh_3)_2Cl_2$, $(NH_4)_4Ce(SO_4)_4 \cdot 2H_2O$, $Ti(O-i-Pr)_3Cl$, $Y(C_5H_7O_2)_3$, $[(COD)Ir(PCy_3)Py]PF_6$, and $Mg(ClO_4)_2$. For comparison, Nafion® NR50 and montmorillonite K 10, the proton source, gave the product **2** in low yields (25% and 30%, respectively).
- $InCl_3$ -catalyzed aqueous Diels–Alder reactions, in which $InCl_3$ served as Lewis acid, have been reported. See: (a) Loh, T.-P.; Pei, J.; Lin, M. *Chem. Commun.* **1996**, 2315–2316; (b) Fringuelli, F.; Piermatti, O.; Pizzo, F.; Vaccaro, L. *Eur. J. Org. Chem.* **2001**, 439–455.
- Except for MeOH, which gave no product, use of THF, $CHCl_3$, and $(CH_2Cl)_2$ furnished the product in 22%, 26%, and 83% yields, respectively, but the reactions took 18 h. In MeCN, the reaction required 72 h to complete, giving the product in moderate 46% yield. Thus, solubility does not seem to be an important contributing factor, which accounts for the difference in yields. In addition, toluene gave no product regardless of the Lewis acids or transition metal salts/complexes under investigation.
- See the Supplementary data for the detailed preparation of **3**, **4**, **6–15**, **33–35**, **41–43**, **55**, and **58**.
- In contrast to the proposed [4+2]-cycloaddition of the reaction using *trans* olefin, the 1:1 mixture of diastereomeric **2a** from the reaction using *cis* olefin may suggest a stepwise mechanism. In a separate experiment, it was found that the *cis* olefin did not isomerize to the *trans* olefin under the reaction condition. Thus, the *trans* product is likely to arise from the stepwise nature of the reaction.
- Cinnamyl acetate and methyl cinnamyl ether gave no product under similar reaction conditions using $PtCl_4$.
- Under acid-mediated conditions (Ref. 3), cinnamyl benzoate, cinnamyl acetate, and methyl cinnamyl ether as well as both *trans*-ethyl cinnamates gave no desired products.
- In addition to the products **27** and **29**, only the baseline unidentified materials were obtained.
- Better yields were obtained with $SnCl_4$ when employed with other systems. See: Schmidt, R. R. *Tetrahedron* **1969**, *10*, 5279–5282.
- The structure of chroman **40** contains a known 's' stereocenter on the sidechain at C3. However, the relative as well as absolute configuration at C3 has not been determined. Compound **40** exhibited optical activity ($[\alpha]_D^{25.3} -4.22$ (c 1.43, $CHCl_3$)). The compound was obtained as a single diastereomer ($dr > 99:1$). Determination of the absolute configuration is underway in our laboratory.
- Similar yields and stereoselectivity were obtained with $AuCl_3$.
- The role of Pt(IV) as a mild Lewis acid in the cycloaddition may be similar to that of $InCl_3$ in the Diels–Alder reactions (see Ref. 6).
- Under other acid-mediated conditions (Ref. 3) to generate *o*-QMs, it is known that, once generated in the reactions without the appropriate dienophiles (olefins), the *o*-QMs similar to those in the current study are not stable and decompose very rapidly.
- The exact position of Pt(IV) coordination on the *o*-QM has not been fully determined and is currently under our investigation.
- In the bound state of *o*-QM with Pt(IV), the metal may position itself between the *o*-QM and dienophile to disfavor the otherwise favorable *endo* transition state. See Supplementary data for more details.
- Both phenol and $BnOH/BnOAc$ are the functional groups similar to those present in the reactions under $PtCl_4$ catalysis.